This corrected Title-Index page with prices inserted is to replace the present printed Title-Index page now in the Journal of Research of National Bureau of Standards. March 1950 issue. Vol. 44, No. 3.

U. S. DEPARTMENT OF COMMERCE
Charles Sawyer, Secretary
NATIONAL BUREAU OF STANDARDS
E. U. Condon, Director

MARCH 1950
VOLUME • 44
NUMBER 3

JOURNAL OF RESEARCH

of the

NATIONAL BUREAU OF STANDARDS

Contents

RP		Page
2072	Introduction of measured liquid samples into the mass spectrometer. C. Edward Wise, Robert M. Reese, Vernon H. Dibeler, and Fred L. Mohler. (Price 10 cents)	215
2073	Heats of polymerization. A summary of published values and their relation to structure. Donald E. Roberts. (Price 10 cents)	221
2074	Stress corrosion of wrought magnesium base alloys. Hugh L. Logan and Harold Hessing. (Price 10 cents)	233
2075	Preliminary list of levels and g-values for Ta II. C. C. Kiess, G. R. Harrison, and W. J. Hitchcock. (Price 5 cents)	245
2076	Electrode function (pH response), hygroscopicity, and chemical durability of Na_2O-CaO-SiO_2 glasses. Donald Hubbard, Given W. Cleek, and Gerald F. Rynders. (Price 10 cents)	247
2077	Soil-corrosion studies, 1946 and 1948: Copper alloys, lead, and zinc. Irving A. Denison and Melvin Romanoff. (Price 20 cents)	259
2078	Mass spectra of nonanes. Fred L. Mohler, Laura Williamson, C. Edward Wise, Edmund J. Wells, Helen M. Dean, and Evelyn G. Bloom. (Price 10 cents)	291
2079	Syntheses and properties of two olefins, six paraffins, and their intermediates. Thomas W. Mears, Abraham Fookson, Philip Pomerantz, Edwin H. Rich, Cecil S. Dussinger, and Frank L. Howard. (Price 10 cents)	299
2080	Effect of deuteration, oxidation, and hydrogen bonding on the infrared spectrum of cellulose. John W. Rowen and Earle K. Plyler. (Price 10 cents)	313
2081	Vapor pressure and fixed points of oxygen and heat capacity in the critical region. Harold J. Hoge. (Price 15 cents)	321

For sale by the Superintendent of Documents, U. S. Government Printing Office, Washington 25, D. C. - Price 75 cents a copy
Subscription price per year—$4.50, domestic; $5.50, foreign

UNITED STATES GOVERNMENT PRINTING OFFICE, WASHINGTON : 1950

S. Department of Commerce
tional Bureau of Standards

Research Paper RP2072
Volume 44, March 1950

Part of the Journal of Research of the National Bureau of Standards

ntroduction of Measured Liquid Samples Into the Mass Spectrometer

By C. Edward Wise, Robert M. Reese, Vernon H. Dibeler, and Fred L. Mohler

Several methods of introducing measured amounts of liquid samples of neohexane and of styrene into a mass spectrometer are compared by measuring the sensitivity (ion current per unit pressure) on mass peaks 71 and 104. A precision microburet and pipet made of thermometer tubing were used to introduce samples of about 0.0015 milliliter. A reproductibility of about 2 percent is obtained with the microburet and of 5 to 8 percent with the pipet. Sensitivities obtained by either method are lower than the sensitivity obtained by a direct pressure measurement using a micromanometer. They are low by 13 percent for neohexane and by 30 percent for styrene. Styrene is retained on the glass walls and in the stopcock grease, and after pumping out 20 minutes some styrene is gradually evolved.

I. Introduction

The conventional method of introducing measd gas samples into the mass spectrometer is at of measuring the pressure of the gas in a small lume of a few milliliters and then expanding e gas one thousand fold into a reservoir. For uid samples of low vapor pressure, the method comes very inaccurate because nearly saturated por does not expand as a perfect gas. The use multiplying manometers[1] to read pressures re accurately before expansion of the gas does remove the difficulty. For this reason, thods of introducing known volumes of liquid the large reservoir have been investigated th here and in other laboratories.[2] Micromanomters have also been developed for measuring ectly the pressure in the large reservoir.[3] In this per we present comparative data on sensitivities neohexane, boiling at approximately 49° C, d styrene, boiling at 146° C, as examples of uid samples differing considerably in physical perties. Several methods of introducing the uids are used, and the measured sensitivities compared with values obtained with a micromanometer. The research includes the adaptation of a precision ultra-microburet[4] available through the Emil Greiner Co. of New York, N. Y., to the use of introducing measured volumes of liquid directly into the reservoir of the mass spectrometer.

II. Experimental Details

The microburet, figure 1, consists of a capillary delivery tube, *E*, attached to a capillary reservoir, *C*. The amount of mercury in the delivery tube is controlled by displacement of mercury from *C* by the stainless steel rod, *B*. The movement of the rod is controlled by the screw, *F*, and is indicated by the micrometer dial, *A*. The dial is graduated in one hundred divisions and can be read directly to 0.0001 ml for a buret of 0.1 ml total volume or to 0.00001 ml for a buret of 0.01 ml total volume. The liquid sample was introduced by close contact of the tip of the capillary with the surface of a Corning "fine" fritted glass disk (see footnote 2) as shown in figure 1. The disk was sealed with a layer of clean mercury.

For these experiments it was found convenient to mount the buret on a rack and pinion device (not shown in fig. 1), which permitted controlled vertical movement as well as rotation of 360° about the vertical. Careful control of the posi-

[1] For a complete discussion of pressure measuring devices, see Experimental methods in gas reactions by A. Farkas and H. W. Melville (Macmillan and Co. Ltd., London, 1939).

[2] R. C. Taylor and W. S. Young, Ind. Eng. Chem., Anal. Ed. **17**, 811 (1945).
W. S. Young and R. C. Taylor, Anal. Chem. **19**, 133 (1947).

[4] R. Gilmont, Anal. Chem. **20**, 1109 (1948).

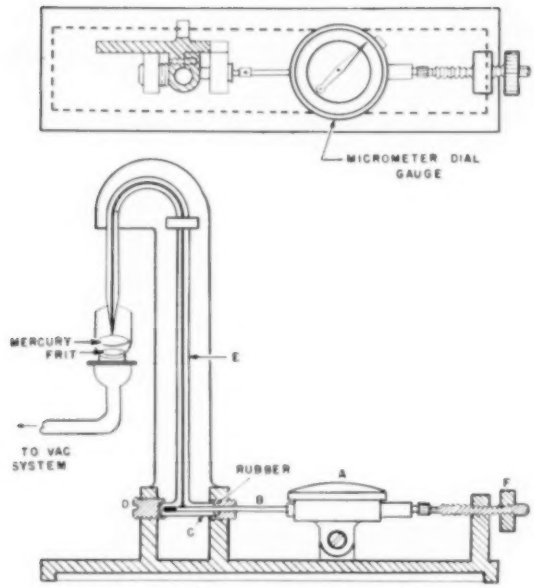

FIGURE 1. *Microburet assembly.*

tion of the buret by means of the rack and pinion was necessary because of the possibility of chipping the capillary tip on the porous disk.

The buret is charged with sample in the following manner: The mercury is forced into the capillary, *E*, by turning the control knob until a drop begins to form at the tip. Then with the tip below the surface of the sample, a portion is drawn into the capillary by rotating the screw in the reverse direction. When sufficient liquid has been drawn into the capillary, the buret tip is removed from the liquid and is carefully wiped with a piece of filter paper. The buret is then brought into position above the porous disk and very cautiously lowered by means of the rack and pinion until the tip is below the surface of the mercury and makes contact with the porous surface of the fritted disk. An appropriate quantity of sample, measured by the difference between two readings of the micrometer dial, is then introduced into the vacuum manifold by forcing the mercury forward into the capillary, *E*.

Figure 2 shows a calibration curve of the volume of liquid delivered in milliliters times 100 as a function of the number of divisions read on the dial of the micrometer gauge. The calibration was done by weighing the mercury delivered from the buret.

When the desired amount of liquid has be drawn through the porous disk into the evac manifold, the tip and porous disk are immediat separated to prevent evaporation of additio sample into the manifold. The tip, however, left below the surface of the mercury in order prevent loss by evaporation from the capillary contamination of the sample. The samples co be introduced into the mass spectrometer reserv directly through a porous disk attached to t reservoir, or condensed with liquid nitrogen i lengths of 3-mm tubing, sealed off and sto until it was convenient to introduce them into t mass spectrometer through an appropriate brea off device. Most of the samples in this work we introduced in the latter fashion. The samp manifold, containing the porous disk and 3-m sample tubing, was pumped out for 5 min betwe the introduction of successive samples through t disk. The time allowed for the sample to conde in the 3-mm tube was from 5 to 8 min, depend on the size of the sample taken.

The 3-mm tubing containing the sample w waxed into a break-off stopcock of the ma spectrometer by using accepted procedures a after evacuation of the stopcock, the end of t tubing was broken off and the liquid samp allowed to evaporate directly into the reservo Four minutes were allowed to establish equilibriu between the adsorbed vapor and the expand

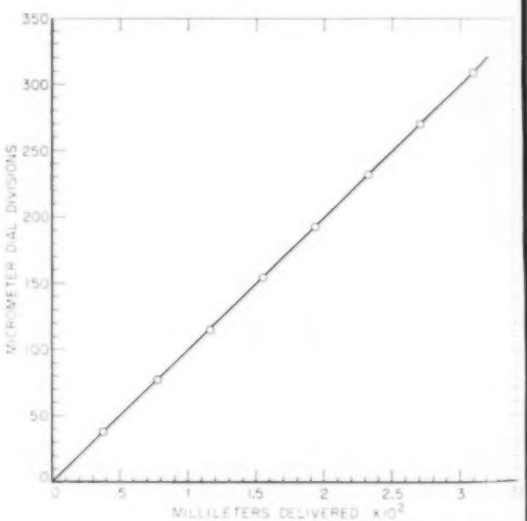

FIGURE 2. *Volume calibration of the microburet.*

vapor in the 2-liter reservoir. An additional 4 min were allowed after opening the reservoir to the leak before scanning over a range of $m/e=65$ to 75 for neohexane and 100 to 108 for styrene. The time allowed for evacuation between successive runs of neohexane was 10 min; for styrene, 15 to 20 min. The spectrogram was recorded in the conventional manner with a Consolidated Mass Spectrometer. Constant magnetic field was used with varying ion accelerating voltage. The energy of the electrons was nominally 50 electron volts. The magnet current was 0.675 amp. The 71 peak of neohexane was in focus at approximately 800 v, while the 104 peak of styrene was collected at approximately 600-v ion accelerating voltage.

The neohexane was Phillips "pure" grade. The purity as stated by the manufacturer was not less than 99 mole percent.

The styrene was obtained from the University of Akron and had no detectable impurities of over 0.1 mole percent as determined by the mass spectrometer.

III. Experimental Results

1. Neohexane

Maximum deflections were obtained with neohexane when 0.0015 ml was expanded into the 2.2-liter reservoir. Table 1 lists the results obtained for a number of samples measured and introduced as described above. The first column gives the number of divisions indicated by micrometer dial of the buret. The second column gives the ion intensity of the $m/e=71$ ion as scale divisions of the spectrogram. The third column gives the sensitivity or the number of scale divisions per micron of sample pressure in the reservoir. The sample pressure is calculated from the following relation:

$$p=7.6\times10^5\, k\left(\frac{vd}{M}\right),$$

where p=pressure in microns;

k=ratio of molar volume of the vapor to the volume of the reservoir;

v=volume of sample in milliliters;

d=density of liquid sample;

M=molecular weight of compound.

TABLE 1. *Sensitivity of neohexane using microburet and 2.2-liter reservoir*

Microburet divisions	Ion intensity	Sensitivity divisions/micron	Mean sensitivity	Percentage deviation
15	1870	19.73		−1.8
15	1917	20.23		+0.6
15	1914	20.20		+.5
15	1870	19.73		−1.8
15	1921	20.27		+0.8
15	1870	19.73		−1.8
16	2047	20.25		+0.7
16	2016	19.95		−.8
16	2067	20.45		+1.7
17	2201	20.50		+2.0
17	2153	20.05	20.10± .23	−0.3

The fifth column gives the percentage deviation from the mean sensitivity.

In several experiments the pressure in the reservoirs was measured with a diaphragm-type micromanometer, to be described in a later publication. The reproducibility of the pressure readings was usually better than ±1 percent of the value when calibrated with *n*-butane, using the mass spectrometer as the calibrating instrument.

Table 2 lists the data obtained by pipetting a number of samples of neohexane directly into the mass spectrometer reservoir and into the 3-mm

TABLE 2. *Sensitivity of neohexane*

Pipet	Divisions	Ion intensity	Sensivity (div-micron)	Percentage deviation from mean
Calibrated thermometer pipet and porous disk with 2.2-liter mass spectrometer reservoir.	39.3	865	18.3	−5.2
Do	19.9	473	19.8	−2.6
Do	24.4	594	20.3	+5.2
Do	49.6	1119	18.8	−2.6
Mean sensitivity (pipet)			19.3	
Mean sensitivity (micromanometer)			23.1	
Calibrated thermometer pipet and porous disk with 3-mm gas-sampling manifold.	70	1682	20.9	−3.7
Do	77	3024	22.9	+5.5
Do	137	* 3140	20.0	−7.8
Do	138	* 3626	22.9	+5.5
Mean sensitivity (pipet)			21.7	

* Calculated from the 57+ peak.

sampling manifold through a porous disk using a length of calibrated thermometer tubing. Column one gives the number of scalar divisions of the thermometer tubing; other columns are similar to those of table 1.

Five minutes of evacuation removed 99.9 percent of the neohexane from the reservoir as indicated by measurement of the 71^+ peak. If the reservoir were then isolated from the pumps, the background of the 71^+ ion did not increase during thirty minutes.

2. Styrene

Approximately 0.0015 ml of liquid expanded into a 4.2-liter reservoir was found to be suitable for mass spectrometric measurements of the 104 peak of styrene. Table 3 summarizes the data for the 2.2- and 4.2-liter volumes. Column two gives the volume of liquid in terms of divisions of the micrometer dial of the buret. Column three gives the ion intensity of the 104 peak in scale divisions. Column four gives the sensitivity as the number of scale divisions per micron of sample pressure in the reservoir. The calculations are similar to those for neohexane. The fifth and sixth columns give the mean sensitivity, and percentage deviations, respectively.

Table 4 gives the sensitivity data of styrene obtained by pipetting the liquid from a calibrated thermometer tubing directly into the reservoir and into the 3-mm gas sampling manifold through a porous disk.

TABLE 3. *Sensitivity of styrene using the microburet and 2.2- and 4.2-liter reservoirs*

Reservoir volume	Microburet divisions	Ion intensity	Sensitivity	Mean sensitivity	Percentage deviation
Liters					
2.2	7	1494	29.48	.....	+2.25
2.2	7	1482	29.24	.....	+1.42
2.2	7	1482	29.24	.....	+1.42
2.2	7	1458	28.77	.....	−0.21
2.2	7	1389	27.41	28.83	−4.93
4.2	15	1584	27.85	.....	−4.16
4.2	15	1665	29.27	.....	+0.72
4.2	15	1665	29.27	.....	+.72
4.2	15	1650	29.01	.....	−.17
4.2	15	1653	29.06	.....	.00
4.2	15	1641	28.85	.....	−0.72
4.2	15	1683	29.59	.....	+1.82
4.2	15	1668	29.32	.....	+0.89
4.2	15	1668	29.32	29.06	+.89

TABLE 4. *Sensitivity of styrene*

Pipet	Divisions	104^+ Ion intensity	Sensitivity (div/micron)	Percentage deviation from mean
Calibrated thermometer pipet and porous disk with 2.2-liter mass spectrometer reservoir.	24.2	1104	33.1	+4.4
Do	45.5	2037	32.5	+2.5
Do	43.4	1686	28.2	−11.0
Do	45.5	2073	32.9	+3.8
Mean sensitivity (pipet)			31.7	
Mean sensitivity (micromanometer)			40.9	
Calibrated thermometer pipet and porous disk with 3-mm gas sampling manifold.	46	2529	30.7	+13.7
Do	56	2916	29.1	+7.8
Do	61	2924	26.8	−0.7
Do	69	[a] 3292	24.9	−7.8
Do	71	[a] 3114	23.6	−12.6
Mean sensitivity (pipet)			27.0	

[a] Calculated from the 103^+ peak.

A sample of styrene stored in the reservoirs for less than ½ hr, decreased to about 0.1 percent of the original sample, (in terms of peak height) in 5 min of pumping and to 0.05 percent in 20 min. If the reservoir were then isolated from the pumps, the background peak of the 104^+ ion increased to about 3 percent of the original peak height in 1 hr, as indicated in figure 3. In a similar experiment, a sample of styrene was stored in the reservoirs for 16 hr, during which time no decrease in pressure was observed. At the end of that time, a pump-out curve was obtained that was quite similar to that shown in figure 3 with an increase of the 104^+ peak (after isolation of the reservoirs from the pumps) of approximately 3 percent of the original peak height in 1 hr. Thus the amount of styrene desorbed is nearly independent of the length of time it is stored in the reservoirs.

TABLE 5. *Summary of results*

Experimental method	Sensitivity (div./micron)	
	Neohexane	Styrene
Buret into 2.2-liter reservoir	20.1 ±0.23	28.83 ±0.59
Buret into 4.2-liter reservoir	.....	29.1 ±0.44
Pipet into reservoir	19.3 ±0.75	31.7 ±1.7
Pipet into sample manifold	21.7 ±1.25	27.0 ±2.3
Micromanometer	23.1 ±0.4	40.9 ±0.8

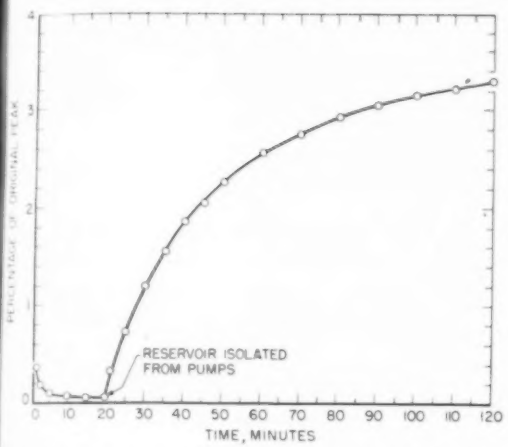

FIGURE 3. *Styrene desorption in reservoir after pumping for 20 minutes.*

A summary of the results obtained is given in table 5. Column 1 gives the experimental method of introducing samples, columns 2 and 3 give the average sensitivities for neohexane and styrene, respectively. The average deviation from the mean is given in each case.

With no special precautions, a reproducibility usually better than 2 percent has been attained for introducing pure neohexane or pure styrene through a porous disk by means of a microburet with a capillary diameter of 0.8 mm.

No significant difference in results was obtained between direct introduction of the sample into the reservoir of the mass spectrometer or condensing and sealing in a separate capsule, which later was opened into the inlet system of the mass spectrometer. This suggests that known amounts of liquid samples can be prepared and stored for future use if the usual precautions are taken to prevent polymerization or decomposition.

Some decrease in precision occurs when liquid volumes less than 0.0015 ml are introduced with the buret or pipet. This is not a function of the uncertainty of reading the buret or pipet scale alone since the use of a microburet with a capillary diameter of 0.3 mm and about 10 times the linear scale for the same interval as the larger buret, resulted in a 3-fold decrease in precision The increased ratio of surface of the buret walls to volume of liquid delivered provides greater opportunity for variation in the amount of sample retained by the buret or pipet. The elliptical cross-sectional area of the thermometer tubing was estimated as slightly less than that of the smaller buret. It is interesting therefore to note that the precision of the pipet is considerably lower than that of the 0.8 mm buret and generally lower than the value given above for the 0.3 mm buret.

Although errors are probably introduced as the result of varying amounts of liquid retained by the pipet or buret walls, a more serious source of error is the sorption of vapor in the reservoir. This is suggested by the larger difference between the sensitivities of styrene and neohexane calculated when the pipet and the micromanometer were used. Apparently styrene is strongly adsorbed in the reservoir, both on the walls and in the lubricant, and this causes a lower sensitivity when computed from the amount of liquid introduced. The micromanometer of course measures only the vaporized fraction and should give the true sensitivity. The large adsorption of styrene is substantiated by the pump-out behavior since, even after 20 min of pumping, there is still sorbed material equivalent to at least 3 percent of the original amount of sample introduced. Although a similar experiment on neohexane shows a negligible amount remaining in the reservoir after 5 min of pumping, some sorption probably occurred since there is a small but apparently real difference between the sensitivities computed from the buret and micromanometer reading. The pump-out behavior of styrene indicates that in comparing sensitivities of successive samples of styrene and similar compounds, sufficient pump-out time must be allowed between the introduction of successive samples to prevent accumulation of the sample in the reservoirs. It is not sufficient simply to pump until a low pressure is indicated.

If it is assumed that the difference between the sensitivity for styrene as measured by the microburet and by the micromanometer comes from adsorption on the walls alone, then from table 5 a fraction of about 0.3 of the liquid sample is adsorbed. It happens that this amount of styrene is nearly equal to the amount in a monomolecular layer over the surface of the reservoir. This is probably fortuitous, as the amount sorbed increases with the pressure as shown in table 4. A liquid neohexane sample gives a sensitivity 13 percent less than a gas sample. In this case it is not certain whether there is some

adsorption or whether there is some loss of liquid because of wetting of the walls of the pipet or buret. Further research is planned in the effort to determine the nature of the sorption on the walls and in the lubricant in this region of the inlet system of the mass spectrometer.

Obviously mixtures of styrene and less strongly adsorbed compounds will change composition in an unpredictable manner depending on the relative amounts and characteristics of the components of the mixture when introduced into the reservoir, unless the walls have been exactly pretreated with similar mixtures immediately beforehand.

Other laboratories have reported use of heated inlet systems at temperatures in the neighborhood of 150° C. This undoubtedly will decrease the effects noted above but will make difficult the u of a micromanometer of the type described b Young and Taylor or the one used in the prese research. In addition, problems of increased ra of polymerization of compounds such as styre are posed by higher temperatures.

The authors gladly acknowledge indebtedne to valuable discussions on liquid sample introdu tion contributed by different members of vario laboratories at the Chicago and New York mee ings of Consolidated mass spectrometer users.

We also wish to express our thanks to Leo A Wall for occasional advice and help.

WASHINGTON, August 8, 1949.

U. S. Department of Commerce
National Bureau of Standards

Research Paper RP2073
Volume 44, March 1950

Part of the Journal of Research of the National Bureau of Standards

Heats of Polymerization. A Summary of Published Values and Their Relation to Structure

By Donald E. Roberts

This paper contains a table showing values of heats of polymerization assembled from a survey of the literature. There are 42 substituted vinyl compounds arranged as follows: vinyl alkyls, vinyl aryls, other vinyls, vinyl acids and esters, dienes and copolymers. Values reported by different authors are given for each compound, with corresponding states of monomers and ploymers and a notation on the methods used in obtaining the values. A second table gives structural formulas of monomers.

Some values of heats of polymerization to hypothetical polymers having no steric hindrance are calculated from published values of heats of formation of hydrocarbons, making certain assumptions regarding branch groups. The method of calculation is explained. Heat of polymerization is arbitrarily assigned to four energy effects: (1) the reaction $\begin{matrix} | & | \\ C{=}C & \end{matrix} \longrightarrow \begin{matrix} | & | \\ -C-C- & \end{matrix}$; (2) the effect of side groups on bond energies when there is no interaction between the groups; (3) the effect of steric hindrance between side groups; and (4) the "end effect" arising from the nearness of the double bond to the end of the monomer molecule.

Values of heats of polymerization are compared, and their relation to structure is examined, with particular emphasis on the effect of steric hindrance. Etyhlene has the highest and alpha-methylstyrene the lowest heat of polymerization; isobutene and the methacrylates also are low. Disubstitution on the same vinyl carbon is a frequent cause of steric interference, with consequent reduction in heat of polymerization. Large branched substituents may cause steric interference. The substitution of chlorine on the aromatic ring of styrene has little effect on heat of polymerization. Steric interference may prevent polymerization above the dimer. The heat of copolymerization of butadiene and styrene lies between the values for the separate monomers. Heat of copolymerization of other monomer pairs may be higher or lower than the value for the separate components. Heat of polymerization depends somewhat on the ratio of 1,2- and 1,4-addition, and on the amount of crystallinity of the polymers.

I. Introduction

Values of the heats of polymerization of various materials are recorded in many journal articles, but there is no recent systematic compilation and comparison of these values. Flory [1] [1] calculated a number of values in 1937 before there were many experimental observations available, and Roth and Rist-Schumacher [2] published in 1942 a summary of values almost entirely obtained from German sources. Since then a large number of experimental observations have been made, and many interesting comparisons are now possible. This paper has been written to collect the scattered data and list them in a convenient form for reference so that useful values of heats of polymerization can readily be obtained without extensive searching. A second purpose is to permit comparison of the data for different compounds, so that systematic trends and anomalies can be recognized. The discussion that follows calls attention to some of the relations between the

[1] Figures in brackets indicate the literature references at the end of this paper.

871926—50——2

heats of polymerization and the structures of the monomers and polymers. The reader may wish to make further comparisons of the types illustrated.

II. Description and Use of Tables

The table of values of heats of polymerization (table 1) is arranged for convenience according to substituent groups as follows: vinyl alkyls, vi aryls, other vinyls, and vinyl acids and est these are followed by dienes and copolym Within each class, the compounds are arran according to increasing size and molecular weig of the monomer. The values reported by several authors are arranged chronologically each compound.

TABLE 1. *Heats of polymerization*

Compound	$-\Delta Hp$ [a]	States of monomer and polymer	Experimental (E) or Calculated (C) [b]	Method and comment
VINYL ALKYLS				
Ethylene [b]	*kcal/mole of monomer*			*Polymer is 55 to75% crystalline* [36, 37].
Flory [1] (1937)	23.1	gas→gas	C	Heats of formation.
Jessup [15] (1948)	[c] 12.4	do	C	Do.
Do	[d] 22.3	do	C	Limit value for ∞ chain, no steric hindrance between side groups. $\Delta He=2.4$, $\Delta Hm=1.2$.
Do	24.7	Gas→liquid	C	
Do	25.9	Gas→solid	C	
Jessup (Roberts) [15] (1948), Prosen & Rossini [8] (1946)	25.4	do	E	Heats of combustion.
Propylene				
Flory [1] (1937)	22.8	Gas→gas	C	Heats of formation.
Roberts [e] (1949)	20.5	do	C	Do.
Fontana & Kidder [42] (1948)	16.5 (−74.5°C)	Liquid→solid	E	Equilibrium constants.
1-Butene				
Flory [1] (1937)	23.4	Gas→gas	C	Heats of formation.
Roberts [e] (1949)	20.9	do	C	Do.
Isobutene				
Flory [1] (1937)	23.0	do	C	Do.
Roberts [e] (1949)	19.2	do	C	Do.
Thomas, et al [43] (1940)	10 (−78°C)	Liquid→solid [e]	E	
Kazanskii & Rozengart [44] (1942)	10.2° (130° to 295°C)	Gas→gas [e]	E	Equilibrium constants; dimerized with catalyst, product is mixed isomers
Evans & Polanyi [3] (1943)	12.8	Solution in hexane	E	Calorimetric.
Evans & Tyrrall [4] (1947)	9.9	Gas→gas	C	Heats of formation; dimer is 2,4,4-trimethyl-1-pentene.
Do	19.2 (20.3)	do	C	Heats of formation, head-tail, no steric hindrance between side groups.
Do	12.6	Liquid→liquid	E	Heats of formation and combustion, with steric hindrance.
cis-2-Butene				
Flory [1] (1937)	23.2	Gas→gas	C	Heats of formation.
Roberts [e] (1949)	19.4	do	C	Do.
trans-2-Butene				
Flory [1] (1937)	22.3	do	C	Do.
Roberts [e] (1949)	18.4	do	C	Do.
2-Methyl-1-butene				
Flory [1] (1937)	23.6	do	C	Do.
Roberts [e] (1949)	18.7	do	C	Do.
cis-2-Pentene				
Flory [1] (1937)	23.1	do	C	Do.
Roberts [e] (1949)	19.2	do	C	Do.
trans-2-Pentene				
Flory [1] (1937)	23.1	do	C	Do.
Roberts [e] (1949)	18.1	do	C	Do.

See footnotes at end of table.

TABLE 1. *Heats of polymerization*—Continued

Compound	$-\Delta Hp$ [a]	States of monomer and polymer	Experimental (E) or Calculated (C) [b]	Method and comment
VINYL ALKYLS—Continued				
	kcal/mole of monomer			
2,3-Dimethyl-1-butene				
Flory [1] (1937)	23.1	Gas→gas	C	Heats of formation.
Roberts [c] (1949)	18.4	do	C	Do.
1-Heptene				
Flory [1] (1937)	23.6	do	C	Do.
Roberts [c] (1949)	20.5	do	C	Do.
VINYL ARYLS				
Styrene				
Flory [1] (1937)	20	Gas→gas	C	Heats of formation.
Roberts [c] (1949)	19	do	C	Three kcal less than for ethylene [1].
Luschinsky [45] (1938)	13.8	Liquid→solid	E	Heats of combustion, fractionated polymer.
Roth & Rist-Schumacher [2] (1942)	20.2*	Liquid→liquid	E	Heats of combustion. Perhaps the value is per mole of dimer.
Votinov, et al [46] (1942)	21.9	Liquid→solid [e]	E	Heats of combustion.
Goldfinger, et al [47] (1943)	15.0 (70° to 140° C)	Liquid→solution (35 to 85%) in monomer.	E	Adiabatic calorimeter.
Ferguson, et al [48] (1945)	17.2	Liquid→solution (12%) in monomer.	E	Do.
Tong & Kenyon [49] (1947)	16.3 to 18.0 (76.8° C)	Liquid→solid	E	Isothermal calorimeter.
Do	16.1 (76.8° C)	do	E	Extrapolated to zero catalyst.
Roberts, et al [50] (1947)	16.7	do	E	Heats of combustion.
Do	17.5	Liquid→solution (7%) in monomer.	E	Heat of solution ($-\Delta Hs$=0.86).
Indene				
Roth & Rist-Schumacher [2] (1942)	16.9*	Liquid→solid	E	Heats of combustion. Perhaps the value is per mole of dimer.
alpha-Methylstyrene				
Roberts & Jessup [17] (1948)	8.8 to 10.1	do	E	Heats of combustion; fractionated polymer, average D. P. 15 to 7.5, respectively.
para-Ethylstyrene				
Tong & Kenyon [49] (1947)	16.4 to 16.9 (76.8° C)	do	E	Isothermal calorimeter.
Do	16.3 (76.8° C)	do	E	Extrapolated to zero catalyst.
ortho-Chlorostyrene				
Tong & Kenyon [49] (1947)	16.5 to 17.6 (76.8° C)	do	E	Isothermal calorimeter.
Do	16.4 (76.8° C)	do	E	Extrapolated to zero catalyst.
para-Chlorostyrene				
Tong & Kenyon [49] (1947)	16.2 to 17.5 (76.8° C)	do	E	Isothermal calorimeter.
Do	16.0 (76.8° C)	do	E	Extrapolated to zero catalyst.
2,5-Dichlorostyrene				
Tong & Kenyon [49] (1947)	16.8 to 18.0 (76.8° C)	do	E	Isothermal calorimeter.
Do	16.5 (76.8° C)	do	E	Extrapolated to zero catalyst.
Anethole				
Staudinger & Schläpfer [51] (1939)	13.8	do [e]	E	Heats of combustion.
OTHER VINYLS				
Ethylene oxide [b]				*Polymer may be crystalline.*
Staudinger & Schläpfer [51] (1939)	22.6	Liquid→solid	E	Heats of combustion. *Polymer may be crystalline.*
Acrylonitrile [b]				
Tong & Kenyon [41] (1947)	17.3 (76.8° C)	do	E	Isothermal calorimeter; extrapolated to zero catalyst.
Vinyl acetate				
Tong & Kenyon [41] (1947)	21.3 (76.8° C)	do	E	Isothermal calorimeter; not dependent on catalyst concentration.

See footnotes at end of table.

TABLE 1. *Heats of polymerization*—Continued

Compound	$-\Delta Hp$ [a]	States of monomer and polymer	Experimental (E) or Calculated (C) [b]	Method and comment
OTHER VINYLS—Continued				
Vinylidene chloride [h]	*kcal/mole of monomer*			*Polymer is largely crystalline* [39, 40].
Tong & Kenyon [41] (1947)	14.4 (76.8° C)	Liquid→solid	E	Isothermal calorimeter; extrapolated to zero catalyst.
Vinyl butyl ether [h]				
Shostakovskii & Bogdanov [52] (1942)	14.4 (40° to 60° C)	Liquid→liquid [d]	E	Polymerized with alcoholic $FeCl_3$.
VINYL ACIDS AND ESTERS				
Acrylic acid				
Staudinger & Schläpfer [51] (1939)	15.0	Liquid→solid [d]	E	Heats of combustion.
Evans & Tyrrall [4] (1947)	18.5	Solution 5 ml in 100 ml H_2O.	E	Calorimetric.
Methacrylic acid				
Evans & Tyrrall [4] (1947)	15.8	Solution 10 ml in 100 ml H_2O.	E	Do.
Methyl acrylate				
Evans & Tyrrall [4] (1947)	20.2	Solution 50 ml in 50 ml EtOH.	E	Do.
Tong & Kenyon [41] (1947)	18.7 (76.8° C)	Liquid→solid	E	Isothermal calorimeter; not corrected for unreacted monomer; 0.01% benzoyl peroxide.
Methyl methacrylate				
Iwai [53] (1946)	16.3	do [d]	E	Heats of combustion.
Tong & Kenyon [54, 55] (1945–46)	13.0 (76.8° to 110° C)	do	E	Isothermal calorimeter.
Tong & Kenyon [54] (1945)	13.1 (76.8° C)	Solution (51%) in CCl_4	E	Do.
Do	13.6 (76.8° C)	Solution 26 to 32% H_2O, 26 to 32% MeOH.	E	Isothermal calorimeter; polymer insoluble in MeOH–H_2O.
Kunst & Magat [56] (1947)	10 to 13		E	
Evans & Tyrall [4] (1947)	12.9	Emulsion 25 ml in 100 ml H_2O.	E	Calorimetric.
Do	20	Gas→gas	C	Estimated from isobutene, head-tail, no steric hindrance between side groups.
Ethyl methacrylate				
Iwai [53] (1946)	14.1	Liquid→solid [d]	E	Heats of combustion.
normal-Butyl methacrylate				
Tong & Kenyon [55] (1946)	13.5 (76.8° C)	do	E	Isothermal calorimeter.
Phenyl methacrylate				
Tong & Kenyon [55] (1946)	12.3 (76.8° C)	do	E	Do.
Cyclohexyl methacrylate				
Tong & Kenyon [55] (1946)	12.2 (76.8° C)	do	E	Do.
Benzyl methacrylate				
Tong & Kenyon [55] (1946)	13.4 (76.8° C)	do	E	Do.
DIENES				
1,3-Butadiene				
Lebedev, et al [51] (1935)	18.1 to 38.4	Gas→solid	E	Heats of combustion; several polymers, formed in different ways.
Do	12.2 to 32.5	Liquid→solid		
Flory [1] (1937)	19.9	Gas→gas	C	Heats of formation, 1,2-polymerization.
Roberts [e] (1949)	17.4	do	C	Heats of formation, 1,2-polymerization.
Flory [1] (1937)	20.4	do	C	Heats of formation, 1,4-polymerization.
Roberts [e] (1949)	18.7	do	C	Heats of formation, 1,4-polymerization.
Roberts & Jessup [57] (1948); Prosen & Rossini [5] (1947)	23 (preliminary)	Gas→solid	E	Heats of combustion.
Do	18 (preliminary)	Liquid→solid	E	Do.
1,3-Cyclopentadiene				
Baur & Frater [58] (1941)	8.7[e] (149° to 185° C)	Gas→gas [d]	E	Equilibrium constant, dissociation at constant volume. Cyclic dimer.
1,4-Pentadiene				
Flory [1] (1937)	24.1	do	C	Heats of formation, 1,2-polymerization.
Roberts [e] (1949)	20.7	do	C	Heats of formation, 1,2-polymerization.

See footnotes at end of table.

TABLE 1. *Heats of polymerization*—Continued

Compound	$-\Delta Hp$ [a]	States of monomer and polymer	Experimental (E) or Calculated (C) [b]	Method and comment
		DIENES—Continued		
Isoprene	*kcal/mole of monomer*			
Jessup [59] (1938)	24.1	Gas→solid	E	Heats of combustion; polymer is purified natural rubber.
Do	17.9	Liquid→solid	E	
Staudinger & Schläpfer [51] (1939)	21.6	do [c]	E	Heats of combustion.
Evans & Tyrrall [4] (1947)	16.1 (16.9)	Gas→gas	C	Heats of formation, no steric hindrance between side groups.
Roberts [f] (1949)	16.9 (17.7)	do	C	Heats of formation, no steric hindrance between side groups.
		COPOLYMERS		
Butadiene-styrene				
Jessup [60] (1944)	17 to 18	Liquid, liquid→solid	E	Heats of combustion, 23% (wt) styrene.
Roberts & Jessup [50,61] (1947, 1944); Prosen & Rossini [5] (1945)	17.9	do	E	Heats of combustion, 25.5% (wt) styrene.
Vinyl acetate-maleic anhydride				
Tong & Kenyon [29] (1948)	20.2 (76.8° C)	Solution of monomers→solid	E	Isothermal calorimeter; 1:1 copolymer insoluble in the system.
Isopropenyl acetate-maleic anhydride				
Tong & Kenyon [29] (1948)	17.8 (76.8° C)	do	E	Isothermal calorimeter; 1:1 copolymer insoluble in system.
Vinyl acetate-diethyl maleate				
Tong & Kenyon [29] (1948)	20.0 (76.8° C)	do	E	Isothermal calorimeter; 1:1 copolymer.
Vinyl acetate-diethyl fumarate				
Tong & Kenyon [29] (1948)	18.6 (76.8° C)	do	E	Isothermal calorimeter; 1:1 copolymer.

[a] At or near 25° C unless otherwise indicated.

[b] The calculated values (except those for ethylene and dimerization if isobutene) are not the actual heats of polymerization which would be obtained experimentally, but apply only to hypothetical ploymers that are free from steric interference between substituent groups attached to the polymer chain.

[c] *denotes heat of dimerization.

[d] Recalculation of Flory's values by the author was done in the same manner and gives this same value.

[e] Recalculated by the author following Flory [1] (see Section III).

[f] Reference [62] gives a value for the heat of formation of isoprene, supposed to be the "best value" to date. It was obtained by applying certain corrections to the data of Jessup [59] (which was used unchanged by Evans and Tyrrall), and combining this result with calculations by Prosen and Rossini. Using this value for isoprene, calculations like those of Evans and Tyrrall give the values shown for $-\Delta Hp$.

[g] Probable states.

[h] See comments in last column.

A table of structural formulas (table 2) is included so that the reader can readily compare the structural features of the polymers. The arrangement of this table is the same as that of table 1. The monomers are shown with the vinyl or diolefin group as the principal portion with substituent groups to the side. The polymer chain would be formed by joining these vinyl or diolefin groups. Since the diagrams in table 2 represent only one view of the molecule, they do not show the zig-zag nature of the polymer chain, which is shown here in idealized form:

Polyethylene

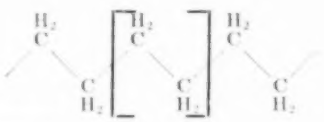

Polybutadiene (*cis*-1,4-polymerization)

TABLE 2. *Formulas and molecular weights*

Ethylene		28.052
Propylene		42.078
1-Butene		56.104
Isobutene		56.104
cis-2-Butene	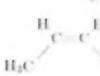	56.104
trans-2-Butene		56.104
2-Methyl-1-butene		70.130
cis-2-Pentene		70.130
trans-2-Pentene		70.130
2, 3 - Dimethyl-1-butene		84.156
1-Heptene		98.182
Styrene		104.144
Indene		116.154
alpha-Methylstyrene		118.170
para-Ethylstyrene	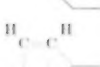	132.196
ortho - Chlorostyrene		138.593
para-Chlorostyrene		138.593
2,5-Dichlorostyrene		173.037
Anethole		148.198
Ethylene oxide		44.052
Acrylonitrile		53.062
Vinyl acetate		86.088
Vinylidene chloride		96.950
Vinyl butyl ether		100.156
Acrylic acid		72.062
Methacrylic acid		86.088
Methyl acrylate		86.088
Methyl methacrylate		100.114
Ethyl methacrylate		114.140

TABLE 2. *Formulas and molecular weights*—Continued

normal-Butyl methacrylate	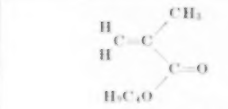	142.192
Phenyl methacrylate	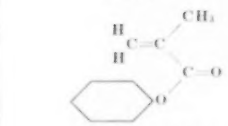	162.180
Cyclohexyl methacrylate	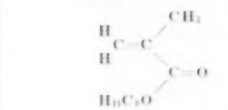	168.228
Benzyl methacrylate	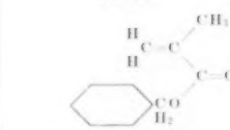	176.206
1,3-Butadiene	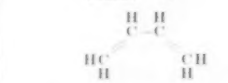	54.088
1,3-Cyclopentadiene		66.098
1,4-Pentadiene (1,2-polymerization)	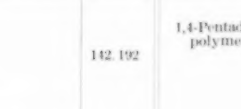	68.114
Isoprene		68.114
Maleic anhydride		98.056
Isopropenyl acetate	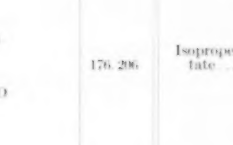	100.114
Diethyl maleate	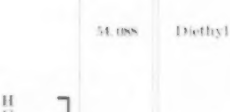	172.176
Diethyl fumarate		172.176

Some values of heat of polymerization that can be found in the literature have not been included in the table for one of three reasons: (1) the compounds are not closely related to those listed here (e. g., tricyano compounds) and involve a different type of reaction; condensation reactions also are excluded; (2) the values reported appear to be in serious error, e. g., because of oxidation of the material; (3) values have been superseded by later values by the same authors. Early values reported by other authors have been included for completeness, although some of these values may be regarded as obsolete. Heats of polymerization can be calculated not only from heats of combustion and formation, but also from activation energies and equilibrium constants. There are many data in the literature other than those listed in this paper, from which heats of polymerization could be calculated if desired, although in some cases the uncertainty of such values will be large.

The states of monomer and polymer and the corresponding values of heats of polymerization given in table 1 are those reported by the several authors, and no corrections have been applied. The values have been rounded to the nearest 0.1 kcal in some cases, since uncertainties in general may amount to the order of 0.5 kcal. Values of heat capacities, and of heats of fusion, vaporization, and solution are known only for a few monomers and polymers, so it is not often possible to convert values of heats of polymerization to correspond to temperatures and states other than those in which the measurements were made. It can sometimes be assumed [3, 4] that the heats of fusion, vaporization and solution for the polymer are not very different from those for the monomer because of the chemical similarity with the monomer.

In making comparisons of heats of polymerization, values for equivalent states should be used, otherwise the included heats of vaporization, fusion, and solution may result in misleading values, especially if these heats are unusually large, as in styrene [5]. For polymers that are noncrystalline or have a second-order transition with no heat of fusion, as in polystyrene [6], the solid

state is equivalent to the liquid state for purposes of comparison. Strictly, comparisons of heats of polymerization should be made only when the monomers and polymers are all referred to the same state. In converting values of heats of polymerization to other states, heats of vaporization, fusion, and solution should be used which are for the same temperature as that which applies to the heat of polymerization. The possibility of dependence of heat of solution upon concentration should also be considered.

III. Recalculation of Flory's Values

The author of this paper has recalculated the values given by Flory [1] for heats of ploymerization to hypothetical head-to-tail polymers having no steric hindrance between branch groups attached to the polymer chain. The method of calculation was essentially the same as Flory's except that a later expression for heats of formation of hydrocarbons [7] was used in calculating heats of formation of polymers, and the heats of formation of the monomers were obtained directly from [8], or for 1,4-pentadiene from [9], instead of calculating them. The estimated corrections for branching in the polymer were obtained by comparing the heats of formation of the octanes [7] (see also [4]). These were chosen from the available data as being more likely than shorter molecules to give the best approximations.

The recalculated values are 1 to 5 kcal lower than those given by Flory, varying between 18 and 21 kcal/mole of monomer; there are also greater differences among the recalculated values. The calculated values for the diolefins are not appreciably lower than those for the monolefins. Hypothetical polymers without steric hindrance having double-branch structures have lower heats of polymerization (18.1 to 19.4 kcal/mole of monomer) than do those with single-branch structures (20.5 to 20.9); polymers with *trans* structure have heats of polymerization about 1 kcal less than those with *cis* structure. The calculated value for 1,2-polymerization of 1,3-butadiene (17.4) is much lower than that for 1,4-pentadiene (20.7). The hypothetical value for polymerization of styrene (19 kcal), obtained by use of the calculations of Kharasch [10] as was done by Flory, falls about 1.5 kcal lower than that for the single-branch structures.

The above relations are due partly to the assumption of certain values for branch corrections and apply to polymers having no steric interference between side groups. The calculations were performed as follows:

The expression for heat of formation per mole of a long normal saturated hydrocarbon, C_nH_{2n+2} ($n>5$,gas) [7] is:

$$\Delta Hf°_{298} = -10.408 - 4.926n \text{ kcal/mole},$$

$$= -4.926n \text{ as } n \text{ approaches } \infty.$$

If the chain is sufficiently long, any part of it will have a heat of formation proportional to the length of that part. The heat of formation of a structural unit of the hypothetical polymer is then $\Delta Hf°(\text{unit}) = -4.926n + \Delta_b$ kcal/unit where Δ_b is the correction for the bond effect of branches on the unit. The heat of polymerization is obtained by taking the difference in heats of formation in the gas state of the polymer unit and the monomer, $\Delta Hf°(m)$ [8,9]: $\Delta Hp° = -4.926 + \Delta_b - \Delta Hf°(m)$ kcal/mole of monomer. The unsaturated group at the end of the polymer chain is neglected. Since the above calculations apply to saturated polymers, a correction must be applied for diolefins in which an unsaturated group remains. The same values of heats of hydrogenation may be used as in Flory's calculations: +29.95 kcal for $-HC=CH_2$ and +27.80 kcal for $-HC=CH-$. These values were obtained as the mean of those given in [11,12] for mono- and 1,2-di-substituted ethylenes and reduced to 298° C by the correction −0.25 kcal.

In calculating corrections for branching, the heat of formation [7] of *n*-octane was compared with that of 4-methylheptane for the correction where there is a single branch per polymer unit, 3,3-dimethylhexane where there are two branches on one of the carbons of the polymer unit, and 3,4-dimethylhexane where there are adjacent single branches in the polymer unit. The following assumptions were made in applying the branch corrections for hypothetical polymers:

1. Length of a normal alkyl substituent makes little difference in bond effect. (This is supported by data of Kistiakowsky and coworkers [12] on heats of hydrogenation.)

2. Branches in the octanes mentioned are far enough removed from the end carbon atoms to

avoid end effects, so that a suitable value for the branch effect is obtained by comparing these octanes.

3. The application of branch corrections to the hypothetical polymer unit is appropriate when those corrections were obtained from correspondingly branched octanes. This neglects the small bond effect of having substituents on nearby C atoms of the polymer chain, which are not present in the octanes. Although certain objections can be raised to the use of these branching corrections, it is felt that they afford a better approximation than those available at the time of Flory's calculations, and they were obtained from the best data available at the present time.

IV. Comparison of Values and Steric Effects

The heat of polymerization of vinyl compounds can be arbitrarily assigned to four energy effects, which are not entirely separable, the second and third being negative with respect to the first and fourth. These energy effects are: (1) the reaction $\text{C=C} \longrightarrow \text{—C—C—}$; (2) the effect of side groups on bond energies when such side groups are so spaced that there is no interaction between them; (3) the effect of steric hindrance between side groups attached to the polymer chain; (4) the "end effect" arising from the nearness of the double bond to the end of the monomer molecule [13].

The first and fourth effects are represented by the polymerization of ethylene, whose polymer has no side groups and therefore no bond effect nor steric hindrance from such groups. The second effect arises from the fact that the bonds to the substituents and the chain bonds in the monomer have different effects on each other from those they exert in the polymer. The value of the third effect can be obtained by the difference between the calculated values of heats of polymerization, which include effects (1), (2), and (4), for the hypothetical polymers, and the experimental values, which include all effects. Both calculated and experimental values are available in only a few cases; isobutene may be used as an example. The difference between 19.2 calculated and 12.8 observed is −6.4 kcal/mole of monomer, attributable to steric hindrance between side groups.

The end effect will be different for each monomer and can generally be neglected in polymers. The value of this effect is given by the deviations from linearity with number of carbon atoms of the heats of formation of the lower members of the homologous series and is known at present for only a few monomers, as follows [14]:

Ethylene	+2.76 kcal,
Propylene	0.7,
1-Butene	0.39,
1-Heptene	0.00.

For the others, it is estimated to be of the order of 0.5 kcal or less. This effect will make a small difference in the values obtained in comparison of heats of polymerization, depending on the difference in the end effects of the monomers to be compared. The true value of effect (1) above is 19.59 kcal, obtained by deducting the end effect in ethylene from the value 22.35 kcal [15].

Substituent groups of larger sizes may cause greater amounts of steric interference, resulting in lower experimental heats of polymerization. Length of the *n*-alkyl substituents makes little difference, although branched substituents may cause steric hindrance [12]. The substitution of chlorine on the aromatic ring of styrene has little effect on the heat of polymerization, since the substituent is well removed from the polymerizing bonds and is not likely to interfere with other branch groups. In ethylene whose polymer has no steric hindrance between side groups, the experimental and calculated values of heat of polymerization agree within experimental error (the calculated values for ethylene were derived from experimental data on hydrocarbons), whereas isobutene, alpha-methylstyrene, and the methacrylates have values of heat of polymerization about two-thirds of what would be expected if there were no steric hindrance between side groups. Ethylene has the highest and alpha-methylstyrene the lowest heat of polymerization among the compounds listed.

A frequent cause of steric interference between side groups is the presence of two substituents on the same vinyl carbon atom, especially if one or more of the substituents is a methyl group. This

can be seen by comparing the experimental values of heat of polymerization for styrene (16.7 kcal) and alpha-methylstyrene (8.8 to 10.1 kcal). If the latter values are increased by an allowance of 2.2 kcal for the bond effect of the methyl group, they become 11.0 to 12.3 kcal, respectively. (The value 2.2 kcal is obtained by taking the difference between the calculated values for 1-butene and 2-methyl-1-butene in table 1.) Effect (4) above cancels in this comparison. A substituent phenyl group may be able to rotate so that its plane is perpendicular to the direction of the polymer chain thus making the steric interference less than might be expected [3]. Another example of the effect of disubstitution can be seen by comparing methyl acrylate (18.7 kcal) and methyl methacrylate (13.0+2.2=15.2 kcal).

Steric hindrance becomes so great in some molecules that polymerization becomes impossible, although in some cases a dimer may be formed [3, 16]. There is generally no steric interference between side groups in dimers, but it becomes noticeable in the trimers and higher polymers in those polymers that show that property [4]. For actual polymers, in the absence of steric hindrance between side groups, heat of polymerization per mole of monomer should increase as the polymer chain becomes longer, because of the factor $(1-1/n)$, which takes account of the fact that there is one less bond reacting than there are monomer units, as shown in Jessup's calculations for ethylene [15]. (The expression for heat of polymerization of ethylene [13, 14, 15] may be written $\Delta Hp°=-19.59\ (1-1/n)-\delta$, where δ is the end effect in ethylene, 2.76 kcal.) If steric hindrance occurs in the polymer, its effect should increase rapidly at first as more units are added to the chain, and after the first three units the heat of polymerization per monomer unit should either increase more slowly or decrease, and the steric energy per unit added should approach a constant value as the chain lengthens. The data for alpha-methylstyrene [17] show some of these effects; here the heat of polymerization per mole of monomer decreases as the molecular weight increases.

Ethylene oxide appears to be a somewhat different monomer from the others listed. The reaction, which differs from vinyl polymerization in being a stepwise addition process rather than a free radical mechanism [18, 19, 20] involves the net difference of the breaking of one C—O bond and the forming of another C—O bond in the chain:

This simple C—O bond rearrangement in itself can not account for the heat of polymerization. The chain is terminated by —OH groups: HO—H_2C—O—$(CH_2)_n$$CH_2$—OH, but if the average molecular weight is large, the contribution to the heat of polymerization from the addition of H—OH would then be very small. The explanation for the heat of polymerization is to be found in the following consideration. The three-membered ring of ethylene oxide has been regarded as a strained structure [21] but Walsh [22, 23] (see also [24, 25, 26, 27]) believes it advantageous to translate much of the old idea of strain in ethylene, cyclopropane, ethylene oxide, and other similar molecules into terms of hybridization. He has suggested that ethylene oxide contains overlapping orbitals and carbon atoms that are more nearly trigonal (ethylenic) than tetrahedral. When this molecule is converted to a straight-chain polymer structure containing ordinary tetrahedral C atoms, energy will be evolved, as with ethylene.

The effect of the esterification of the acrylic acids is confusing. In the case of acrylic acid, esterification increases the heat of polymerization, whereas the opposite effect occurs with methacrylic acid.

The heat of copolymerization of the butadiene-styrene mixture lies between the values for the separate monomers. Copolymers having different monomer ratios from those given will of course have different heats of polymerization. The heats of copolymerization of vinyl acetate with maleic anhydride, diethyl maleate, and diethyl fumarate are lower than the heat of polymerization of vinyl acetate alone. In some cases, however, the effect of steric hindrance between side groups in copolymers may be diminished by 1:1 alternation of the units. Tong and Kenyon [28] have observed that with methyl acrylate and methyl methacrylate the heat of copolymerization is higher than the sum of the heats of polymerization of the components alone. These authors [29] point out that with the diethyl fumarate and maleate copolymers with vinyl acetate, the difference in their heats of copolymerization is less

than half of the heat of isomerization of maleic to fumaric esters, suggesting that different stereoisomers are produced. A discussion of heat of copolymerization appears in reference [30].

Polymers having different structure, although derived from the same monomer (see butadiene [31]) may have different heats of polymerization. In a polymer or copolymer containing a diene, there is the possibility that there will be present a mixture of 1,2- and 1,4-addition (or 3,4- in isoprene), and the value of heat of polymerization will vary according to the ratio [32, 33, 34, 35]. The 1,2-addition may lead to cross-linking. The 1,4-polymers may be partly *cis* and partly *trans* structure.

Ethylene [36, 37, 38] and vinylidene chloride [39, 40] both form polymers that are rather highly crystalline. The polymers of ethylene oxide and acrylonitrile also are probably crystalline. The apparent heat of polymerization to solid polymer must then include a small quantity representing the heat of crystallization, depending on the percentage of crystallinity. If we use the value for heat of fusion of polyvinylidene chloride (0.3 kcal) given by Reinhardt [39], then the heat of polymerization in the liquid states would be reduced from 14.4 [41] to 14.1 kcal/mole of monomer at 76.8° C.

The author expresses his appreciation for helpful comments offered by Raymond F. Boyer, D. R. Stull, L. K. J. Tong and W. O. Kenyon, Ralph S. Jessup, Edward J. Prosen, and Leo A. Wall.

It has been brought to our attention that there is no reported value for the heat of polymerization of vinyl chloride. An estimate of the value can be made by considering its structure and comparing with other values in the table. Not enough data are available for an accurate prediction, but at least a rough idea can be obtained. Assuming that the end effects are negligible in all cases, and that the heats of vaporization are the same for the monomers as for their polymers, vinyl chloride should be between ethylene (19.6 kcal/mole, no end effect, gas-gas) and vinylidene chloride (at 25°, about 14.0 kcal/mole, liquid-liquid), and somewhere near propylene since the bond and steric effects of Cl are similar to those for CH_3. To obtain an estimate from the data of Fontana and Kidder for propylene, their value may be adapted by subtracting 0.7 kcal for heat of fusion of the polypropylene (same as for the monomer), and adding a few tenths of a kilocalorie for raising the temperature from —75° to 25° C. The value then becomes about 16 kcal/mole for liquid-liquid at 25° C. The second estimate, obtained from ethylene and vinylidene chloride, should be somewhat above the midpoint of the difference between 19.6 and 14.0, since substitution of a second chlorine causes a greater steric effect than that of the first. The final estimate for vinyl chloride might then be placed at about 17 kcal/mole (liquid-liquid or gas-gas, 25° C).

References

[1] P. J. Flory, J. Am. Chem. Soc. **59,** 241 (1937).
[2] W. A. Roth and E. Rist-Schumacher, Kautschuk **18,** 137 (1942).
[3] A. G. Evans and M. Polanyi, Nature **152,** 738 (1943).
[4] A. G. Evans and E. Tyrrall, J. Polymer Sci. **2,** 387 (1947).
[5] E. J. Prosen and F. D. Rossini, J. Research NBS **34,** 59 (1945) RP1628.
[6] R. F. Boyer and R. S. Spencer, J. Applied Phys. **15,** 398 (1944).
[7] E. J. Prosen and F. D. Rossini, J. Research NBS **34,** 263 (1945) RP1642.
[8] E. J. Prosen and F. D. Rossini, J. Research NBS **36,** 269 (1946) RP1702.
[9] Selected Values of Properties of Hydrocarbons. Table 11p (Part 1). National Bureau of Standards, Washington 25, D. C. (February 28, 1949).
[10] M. S. Kharasch, BS J. Research **2,** 359 (1929) RP41.
[11] G. B. Kistiakowsky, J. R. Ruhoff, H. A. Smith, and W. E. Vaughan, J. Am. Chem. Soc. **57,** 876 (1935).
[12] G. B. Kistiakowsky, J. R. Ruhoff, H. A. Smith, and W. E. Vaughan, J. Am. Chem. Soc. **58,** 137 (1936).
[13] E. J. Prosen, private communication.
[14] E. J. Prosen, W. H. Johnson, and F. D. Rossini, J. Research NBS **37,** 51 (1946) RP1728.
[15] R. S. Jessup, J. Chem. Phys. **16,** 661 (1948).
[16] V. V. Korshak and K. K. Samplanskaya, Doklady Akad. Nauk SSSR **59,** 497 (1948). (Chem. Abstracts **42,** 6203 (1948)).
[17] D. E. Roberts and R. S. Jessup, 1948, to be published.
[18] H. Moureu and M. Dode, Bul. soc. chim. [5] **4,** 637 (1937).
[19] P. J. Flory, J. Am. Chem. Soc. **62,** 1561 (1940).
[20] S. Perry and H. Hibbert, J. Am. Chem. Soc. **62,** 2599 (1940).
[21] H. de V. Robles, Recueil des Travaux Chimiques des Pays-Bas **59,** 184 (1940).
[22] A. D. Walsh, Nature **159,** 165 and 712 (1947).
[23] A. D. Walsh, Trans. Faraday Soc. **45,** 179 (1949).
[24] T. M. Sugden, Nature **160,** 367 (1947).
[25] P. Karrer, Helv. Chim. Acta. **30,** 1780 (1947).

[26] C. L. Arcus, Chem. and Ind. **1947,** 646.
[27] C. A. Coulson and W. E. Moffitt, Phil. Mag. **40,** 1 (1949).
[28] L. K. J. Tong and W. O. Kenyon, unpublished, private comunication.
[29] L. K. J. Tong and W. O. Kenyon, J. Am. Chem. Soc. **71,** 1925 (1949).
[30] T. Alfrey, Jr., and C. Lewis, J. Polymer Sci. **4,** 221 (1949).
[31] S. V. Lebedev, G. G. Koblyanskiĭ, M. A. Khokhlovkin, N. I. Kulbina, and M. M. Gol'dman, Trudy Gosudarst. Opyt. Zavoda Sintet. Kauchuka Litera B. IV. Synthetic Rubber **1935,** 46. (Chem. Abstracts **31,** 6958 (1937)).
[32] A. Saffer and B. L. Johnson, Ind. Eng. Chem. **40,** 538 (1948).
[33] H. L. Dinsmore and D. C. Smith, Anal. Chem. **20,** 11 (1948).
[34] A. W. Meyer, Ind. Eng. Chem. **41,** 1570 (1949). See also E. J Hart and A. W. Meyer, J. Am. Chem. Soc. **71,** 1980 (1949).
[35] I. M. Kolthoff, T. S. Lee, and M. A. Mairs, J. Polymer Sci. **2,** 220 (1947).
[36] E. Hunter and W. G. Oakes, Trans. Faraday Soc. **41,** 49 (1945).
[37] H. C. Raine, R. B. Richards, and H. Ryder, Trans. Faraday Soc. **41,** 56 (1945).
[38] G. S. Parks and J. R. Mosley, J. Chem. Phys. **17,** 691 (1949).
[39] R. C. Reinhardt, Ind. Eng. Chem. **35,** 422 (1943).
[40] W. C. Goggin and R. D. Lowry, Ind. Eng. Chem. **34,** 327 (1942).
[41] L. K. J. Tong and W. O. Kenyon, J. Am. Chem. Soc. **69,** 2245 (1947).
[42] C. M. Fontana and G. A. Kidder, J. Am. Chem. Soc. **70,** 3745 (1948).
[43] R. M. Thomas, W. J. Sparks, P. K. Frolich, M. Otto, and M. Mueller-Cunradi, J. Am. Chem. Soc. **62,** 276 (1940).
[44] B. A. Kazanskiĭ and M. I. Rozengart, J. Gen. Chem. (USSR) **12,** 246 (1942). (Chem. Abstracts **37,** 3045) (1943)).
[45] W. von Luschinsky, Z. physik. Chem. **A182,** (1938).
[46] A. Votinov, P. Kobeko, and F. Marei, J. Phys. Ch (USSR) **16,** 106 (1942). Chem. Abstracts **37,** (1943).
[47] G. Goldfinger, D. Josefowitz, and H. Mark, J. Chem. Soc. **65,** 1432 (1943).
[48] W. J. Ferguson, I. C. Schoonover, and F. G. Bo wedde, National Bureau of Standards 1945, published.
[49] L. K. J. Tong and W. O. Kenyon, J. Am. Ch Soc. **69,** 1402 (1947).
[50] D. E. Roberts, W. W. Walton, and R. S. Jess J. Research NBS, **38,** 627 (1947) RP1801. J. Polymer Sci. **2,** 420 (1947).
[51] H. Staudinger and P. Schläpfer, unpublished da quoted in chapter by G. V. Schulz in Chemie Technologie der Kunststoffe, edited by R. H wink, Vol. 1, p. 60, Table 5, Leipzig, (1942 (one vol.) p. 79, Table 6, Leipzig (1939).
[52] M. F. Shostakovskiĭ and I. F. Bogdanov, J. Appl Chem. (USSR) **15,** 249 (1942). (Chem. Abstr **37,** 2486 (1943)).
[53] S. Iwai, J. Soc. Chem. Ind. (Japan) **49,** 185 (19 (Chem. Abstracts **42,** 6161 (1948)).
[54] L. K. J. Tong and W. O. Keynon, J. Am. Chem. S **67,** 1278 (1945).
[55] L. K. J. Tong and W. O. Kenyon, J. Am Chem. S **68,** 1355 (1946).
[56 E. Kunst and M. Magat, Compt. rend. **225,** (1947).
[57] D. E. Roberts and R. S. Jessup, 1948, to be publish
[58] E. Baur and S. Frater, Helv. Chim. Acta. **24,** (1941).
[59] R. S. Jessup, J. Research, NBS **20,** 589 (19 RP1093.
[60] R. S. Jessup, Preliminary Report, 1944, unpublish
[61] D. E. Roberts, R. S. Jessup, 1944, unpublished.
[62] J. E. Kilpatrick, C. W. Beckett, E. J. Prosen, K. Pitzer, and F. D. Rossini, J. Research NBS 225 (1949) RP1964.

Washington, October 6, 1949.

U. S. Department of Commerce
National Bureau of Standards

Research Paper RP2074
Volume 44, March 1950

Part of the Journal of Research of the National Bureau of Standards

Stress Corrosion of Wrought Magnesium Base Alloys

By Hugh L. Logan and Harold Hessing

The rates of corrosion of many metals and alloys are increased by the presence of tensile stresses in the materials. In order to determine the effect of tensile stress on the behavior of magnesium alloys exposed to corrosive media, stress-corrosion tests were made on several magnesium base alloys at two weather exposure sites, and in the laboratory by continuous immersion in a $NaCl+K_2CrO_4$ solution and by intermittent immersion in a dilute NaCl solution.

The periods of time to failure of specimens exposed under tensile stress in the atmosphere at the National Bureau of Standards were less than those for the same materials exposed in a marine atmosphere at Hampton Roads, Va.

The M1 clad AZ31X-h sheet alloy proved more resistant to stress corrosion than bare AZ31X-h, AZ51X, or AZ61X sheet alloys and AZ80X extruded alloys.

Predictions of relative susceptibility of materials to stress corrosion from intermittent immersion laboratory tests in a 0.01-percent NaCl solution were in good agreement with the results obtained from weather exposure tests at this Bureau.

I. Introduction

Early in World War II a number of welded airplane booms, constructed of AZ61X magnesium alloy sheet and extrusions were subjected to static loading until buckling occurred and were then stored in the open exposed to the weather. Subsequent examination revealed stress corrosion in the buckled areas.

Inasmuch as the Bureau of Aeronautics, Navy Department, was interested in the possibilities of the use of magnesium alloys in aircraft structures, it gave financial support to the National Bureau of Standards to study the resistance of various commercial wrought alloys to stress corrosion. The investigation was carried out with the specific purpose of determining the relative susceptibility of various alloys to stress corrosion, and whether a correlation could be established between the results of various laboratory tests and those of weather exposure tests.

II. Materials and Methods of Test

1. Materials

Seven wrought magnesium alloys were studied in this investigation. Four of these materials, the M1, AZ31, AZ61, and AZ80 alloys had been used in this country in structural applications prior to the war. An AZ31 alloy clad with thin layers of the M1 alloy; an alloy designated as AZ51 and a zinc, zirconium alloy, designated by Dow as ZK60, all developed by the Dow Chemical Co. during the war, were also included in the study. The materials were supplied by the American Magnesium Corp. and the Dow Chemical Co. The ASTM and manufacturers' designations, and the nominal chemical compositions are given in table 1.

Materials received from the Dow Chemical Co. generally had an oiled finish. After the sheet or extruded material had been machined into specimens the thickness was reduced approximately 0.002 in. by immersion in an aqueous solution containing 30 ml of concentrated HNO_3, and 10 ml of concentrated H_2SO_4 per liter.

Materials received from the American Magnesium Corp. had a chrome-pickled finish. They were machined into tensile specimens, and the chrome-pickle film was then removed by immersion in an aqueous solution containing 22.5 g of Na_2CO_3, and 15 g of NaOH per liter.

TABLE 1. *ASTM and manufacturers' designations, and nominal compositions [a] of the magnesium base alloys investigated*

Designation			Chemical composition Mg=remainder			
ASTM	American Magnesium Corp.	Dow Chemical Co.	Al	Zn	Mn	Zr
			%	%	%	%
M1	AM38	M			1.5	
AZ31X	AM–C528	FS–1	3.0	1.0	0.3	
AZ51X		JS–1	5.0	1.0		
AZ61X	AM–C578	J–1	6.5	0.7	.2	
AZ80X	AM–C588	O–1	8.5	.5	.2	
		[b] ZK–60		5.7	.07	0.6
MIClad AZ31X		MClad FS–1				
AZ31X		Core	3.0	1.00	0.3	
M1		Cladding			1.5	

[a] Nominal compositions given are those prevailing at the time the materials were received for test. Analyses furnished by the manufacturers did not differ significantly from the above values.

[b] Composition determined by chemical and spectrochemical means at this Bureau.

After the treatment to remove the chrome-pickle film or the outer layers of material, all of the specimens except the clad AZ31X–h material, whose thin cladding would have been seriously affected, were ground parallel to the long axes of the specimens, prior to testing, using number 400 Aloxite belts on a rubber backed wheel. The chemical and grinding treatments were used to obtain uniform surface conditions on specimens before exposure.

In general, the alloys supplied in sheet form were tested in each of two tempers, annealed (—a) and hardened by rolling (—h), and also in two thicknesses 0.064 and 0.125 in. The extruded material (except the ZK–60 alloy) was supplied in two rectangular cross sections. The heat-treatable extruded alloy AZ80X was supplied both in the as-extruded and in the extruded, heat-treated and aged (HTA) conditions. The tensile properties of the sheet materials as received are given in tables 2, 3, and 4. The sheet material was rolled by the usual manufacturing process except that two lots of material (see table 4) were rolled by a special process developed by M. A. Hunter of Rensselaer Polytechnic Institute. The cross-sectional dimensions and tensile properties of the extruded materials are given in table 5.

TABLE 2. *Tensile properties of the AZ61X and M1 magnesium base sheet alloys and threshold stresses (as determined in the $NaCl + K_2CrO_4$ solution) of the AZ61X alloy*

Alloy and condition [a]	Supplier [b]	Nominal thickness	Specimen orientation [c]	Tensile properties of uncorroded material [d]			Threshold stress	
				Yield strength	Ultimate tensile strength	Elongation in 2 in.	Average	Percentage of yield strength
		in.		*lb/in.²*	*lb/in.²*	*Percent*	*lb/in.²*	*Percent*
AZ61X–a	Dow	0.064	L	24,300	42,700	20	21,500	88
Do	do	.064	T	27,800	39,800	7	23,500	85
Do	Am. Mg. Corp	.064	L	23,100	41,300	19	22,500	97
Do	do	.064	T	27,200	41,000	17	24,000	89
AZ61X–a	Dow	.125	L	23,600	37,800	7	22,500	95
Do	Am. Mg. Corp	.125	L	23,200	39,400	9	21,000	90
Do	do	.125	T	26,500	40,000	7	23,000	87
AZ61X–h	Dow	.064	L	35,600	46,200	6	28,000	79
Do	do	.064	T	37,800	50,400	14	31,000	82
Do	Am. Mg. Corp	.064	L	39,300	47,100	5	28,500	72
Do	do	.064	T	41,200	51,600	8	28,000	69
AZ61X–h	Dow	.125	L	33,300	43,800	10	29,000	87
Do	do	.125	T	35,700	47,500	7	31,500	88
Do	Am. Mg. Corp	.125	L	37,500	45,700	5	29,000	77
Do	do	.125	T	36,400	48,200	7	31,000	85
M1–h	Dow	.064	L	29,300	34,800	3		
Do	do	.064	T	22,400	34,300	13		
Do	Am. Mg. Corp	.064	L	30,700	35,700	4		

[a] "a" indicates annealed material; "h" material hardened by rolling.

[b] Dow indicates Dow Chemical Co.; Am. Mg. Corp. indicates American Magnesium Corp.

[c] L and T designate, respectively, longitudinal and transverse specimens.

[d] Each value is the average of 5 or more determinations.

TABLE 3. *Tensile properties and threshold stresses (as determined in the $NaCl+K_2CrO_4$ solution) of AZ31X magnesium base sheet alloy*

Alloy and condition [a]	Supplier	Nominal thickness	Specimen orientation [b]	Tensile properties of uncorroded material [c]			Threshold stress	
				Yield strength	Ultimate tensile strength	Elongation in 2 in.	Average	Percentage of yield strength
		in.		*lb/in.²*	*lb/in.²*	*Percent*	*lb/in.²*	*Percent*
AZ31X-a	Dow	0.064	L	22,500	37,200	17	20,000	90
Do	do	.064	T	22,900	37,200	20	21,000	92
Do	Am. Mg. Corp	.064	L	20,000	36,100	19	18,500	93
Do	do	.064	T	19,300	36,200	22	18,000	93
AZ31X-a	Dow	.125	L	21,500	36,600	22	19,500	90
Do	do	.125	T	22,900	37,200	20	20,000	88
Do	Am. Mg. Corp	.125	L	20,200	35,900	21	19,000	94
Do	do	.125	T	19,500	35,800	22	18,000	92
AZ31X-h	Dow	.064	L	33,400	42,800	10	30,000	89
Do	do	.064	T	32,500	42,700	11	29,500	90
Do	Am. Mg. Corp	.064	L	35,500	41,800	7	29,500	84
Do	do	.064	T	30,600	43,300	16	28,500	94
AZ31X-h	Dow	.125	L	31,800	41,400	12	29,000	92
Do	do	.125	T	32,400	43,400	17	29,500	91
Do	Am. Mg. Corp	.125	L	36,200	42,600	8	29,500	81
Do	do	.125	T	33,000	45,000	15	28,500	86

[a] "a" indicates annealed material; "h" material hardened by rolling.
[b] L and T designate, respectively, longitudinal and transverse specimens.
[c] Each value is the average of 5 or more determinations.

TABLE 4. *Tensile properties and threshold stresses (as determined in the $NaCl+K_2CrO_4$ solution) of the AZ51X-h and the AZ31X-h magnesium base sheet alloys 0.064 in. thick, rolled by two processes and supplied by the Dow Chemical Co.*

Alloy and condition	Specimen orientation [a]	Tensile properties of uncorroded material [b]			Threshold stress	
		Yield strength	Ultimate tensile strength	Elongation in 2 in.	Average value	Percentage of yield strength
ROLLED BY THE STANDARD DOW PROCESS						
		lb/in.²	*lb/in.²*	*Percent*	*lb/in.²*	*Percent*
AZ51X-h	L	34,800	47,000	11	34,000	98
AZ51X-h	T	40,600	50,600	15	37,000	91
AZ31X-h	L	32,900	43,100	10	29,000	88
AZ31X-h	T	34,800	44,700	12	29,000	83
ROLLED BY THE HUNTER PROCESS						
AZ51X-h	L	34,300	46,000	11	33,000	96
AZ51X-h	T	39,200	49,300	12	36,500	93
AZ31X-h	L	32,700	42,600	11	29,500	90
AZ31X-h	T	34,200	44,000	18	31,500	92

[a] L and T designate, respectively, longitudinal and transverse specimens
[b] Each value is the average of 5 or more determinations.

TABLE 5. *Tensile properties and threshold stresses (as determined in the $NaCl+K_2CrO_4$ solution) of the 5.7-percent zinc, 0.6-percent zirconium (Dow ZK–60), the AZ61X, and the AZ80X magnesium base alloy extrusions*

Alloy and condition	Supplier	Nominal dimensions		Tensile properties of uncorroded material [a]			Threshold stress	
		Thickness	Width	Yield strength	Ultimate tensile strength	Elongation in 2 in.	Average	Percentage of yield strength
TESTED AS EXTRUDED								
		in.	*in.*	*lb/in.²*	*lb/in.²*	*Percent*	*lb/in.²*	*Percent*
ZK–60	Dow	1/16	1	39,500	50,000	13	33,000	84
AZ61X	Dow	1/16	3/4	25,800	43,900	12	23,500	91
Do	Am. Mg. Corp	1/16	1	29,500	42,900	16	27,500	87
Do	Dow	1/8	1 1/4	26,900	44,800	17	23,500	87
Do	Am. Mg. Corp	1/8	1 1/4	31,800	43,600	16	25,500	81
AZ80X	Dow	1/16	3/4	28,900	47,200	12	26,500	92
Do	Am. Mg. Corp	1/16	1	29,900	46,800	17	25,000	84
Do	Dow	1/8	1 1/4	31,000	48,400	12	26,500	85
Do	Am. Mg. Corp	1/8	1 1/4	34,500	48,500	19	27,000	78
EXTRUDED, HEAT TREATED, AND AGED								
AZ80X–HTA	Dow	1/16	3/4	34,200	49,000	7	32,500	95
Do	Am. Mg. Corp	1/16	1	29,000	49,200	13	27,500	95
Do	Dow	1/8	1 1/4	37,200	49,600	4	32,000	86
Do	Am. Mg. Corp	1/8	1 1/4	35,100	50,600	10	31,500	90

[a] Each value is the average of 5 or more determinations.

2. Preparation of Specimens

Tests were made with ½-in. reduced-section standard ASTM tension specimens for sheet metals, except that the grip ends were 1 or 1¼ in. wide, when possible, instead of the standard ¾ in.,[1] to minimize the failure of specimens as the result of stress corrosion around the bolt holes. Specimens of the sheet material machined with their long axes in and at right angles to the direction of rolling of the sheet, are designated hereafter as longitudinal (L) and transverse (T) specimens, respectively.

3. Methods of Test

Exposure tests were made on stressed specimens on the roof of the Northwest Building at this Bureau and in a marine atmosphere at Hampton Roads, Va. The stress-corrosion racks at Hampton Roads have been described in an earlier paper.[2] Those at this Bureau are shown in figure 1, and the method of supporting the specimens, using flexure plates, is shown in figure 2. The ends of the specimens were gripped between two pieces of 61S–T6 aluminum alloy bar by means of ⅜-in. bolts of 17S–T4 aluminum alloy.

A stress-corrosion crack that developed in the reduced section of one of the specimens exposed in the weather is shown in figure 3. Loose[3] has suggested that a specimen should be considered to have failed when a stress-corrosion crack first appears. It was not possible with the personnel available to make the necessary inspections, at

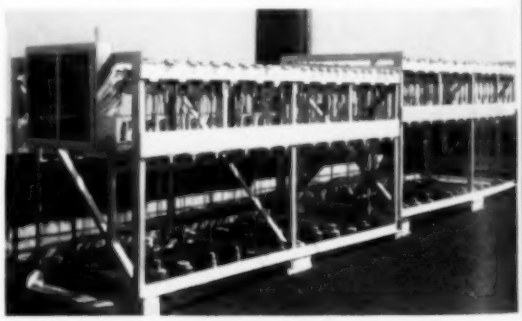

FIGURE 1. *Stress-corrosion racks on the roof of the Northwest Building at the National Bureau of Standards.*

Box at extreme left houses electric solenoid counters to determine exposure period of specimens to failure.

[1] One set of extrusions supplied by the Dow Chemical Co. had a rectangular cross section ¾ by 1/16 in.

[2] H. L. Logan and H. Hessing, J. Research NBS **41**, 69 (1948) RP1905.

[3] W. S. Loose, private communication, Dow Chemical Co., Midland, Mich.

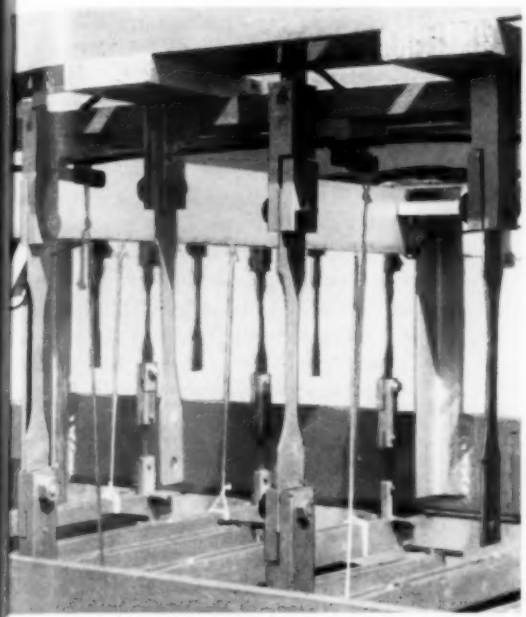

FIGURE 2. *Method of supporting stress-corrosion specimens in rack shown in figure 1, using flexure plates above and below stressed specimens.*

Fixtures were 618–T6 aluminum alloy; bolts, 178–T4 aluminum alloy. Knife switches were connected in series with solenoid counters shown in figure 1. Unstressed specimens were mounted adjacent to stressed specimens.

either weather exposure site, to determine when stress-corrosion cracks first appeared. Accordingly, the period to failure for the various specimens was determined as the interval between insertion and actual failure as recorded with electric solenoid counters that have been described in an earlier paper (see footnote 2).

At the time this investigation was begun other workers in the field were advocating the testing of sheet magnesium alloys in the laboratory by continuous immersion, under stress, in a sodium chloride-potassium chromate solution. "Threshold" stresses, defined as the maximum stresses that materials can withstand without failure for a fixed period of time when immersed in the corroding medium, were determined as a measure of the resistance of the alloys to stress corrosion.

The specimens tested in corroding solutions at this Bureau were immersed in glass cells and stressed by means of lever systems. The apparatus used in an earlier investigation (see footnote 2) was modified for these tests by the insertion, in the supports, of flexure plates (made of stainless steel sheet 1 inch wide by 0.020 inch thick), which are modifications of those used by Loose and Barbian (see footnote 3). The corrosive medium, a solution containing 3.5-percent NaCl and 2.0-percent K_2CrO_4 was suggested by R. H. Brown and G. F. Sager.[4]

Preliminary work in this laboratory and results obtained by other workers indicated that different values for the threshold stress were obtained depending on whether the specimens were loaded in tension before or after the solution was added. Work hardening of the specimens following loading and prior to adding the solution gave threshold stresses considerably higher than those obtained if the solution was added prior to the application of the major part of the load. Therefore all succeeding tests were made by loading the specimens after the solution was added to the cells.

In order to supplement and possibly replace the continuous immersion test in the NaCl+

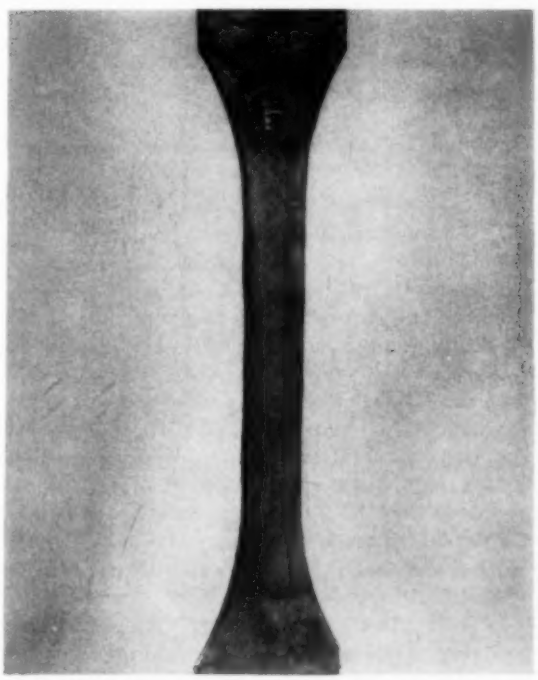

FIGURE 3. *Stress-corrosion crack in specimen exposed to weather at the National Bureau of Standards.*

[4] R. H. Brown, private communication (Aluminium Research Laboratories, New Kensington, Pa.)

FIGURE 4. *Specimens mounted for intermittent immersion tests in the laboratory.*

Flexure plates were used in the supports above and below specimens, corrodent was raised from flasks (see lower right) to cells by means of compressed air.

K_2CrO_4 solution, intermittent immersion tests were made in various corrosive media at a constant temperature of 95° F (35° C). Specimens were mounted in cells as shown in figure 4, and the corroding solution was raised into the cells by means of compressed air, wetting the specimens four times per hour. They were immersed for approximately 1 min and were permitted to dry for 14 min in each cycle. Intermittent immersion tests in a 3.5-percent sodium chloride solution produced such severe pitting of the specimens that stress-corrosion effects were obscured. Intermittent immersion in a 0.01-percent NaCl solution or in a 0.01 normal $NaHCO_3$ solution produced stress corrosion in magnesium alloys without producing general or pitting corrosion. Exposure periods to failure for a given alloy were approximately the same in either of these dilute solutions. However, the 0.01-percent NaCl solution was used for the balance of the intermittent immersion tests.

III. Results and discussion of Stress-Corrosion Tests

1. Weather Exposure Tests

The results of weather exposure tests on the various magnesium alloys are shown graphically in figures 5 to 9, inclusive, and are given for the AZ31X–h material in table 6. The plotted values in figure 5 generally represent the averages of three or more specimens exposed at a given stress. The results for individual M1–Clad specimens (exposed in the marine atmosphere), however, are shown as separate points in the figure. All the specimens exposed at a given stress, and duplicate specimens stressed differently were not necessarily exposed concurrently.

The data indicate that the M1–clad AZ31X-h material was more resistant to stress corrosion at high stresses than any of the other materials studied. Specimens of this material may be expected to have a life in a marine atmosphere of at least 500 days at a stress of 30,000 lb/in.^{2} The bare (unclad) material, exposed in a marine

TABLE 6. *Results of stress-corrosion tests on the AZ31X-h magnesium base alloy, 0.064 in. thick, exposed in [illegible] weather at the NBS, Washington, D. C. and at Hampton Roads, Va.*

Average stress	Specimens exposed at NBS, Washington, D. C.			Specimens exposed at Hampton Roads, Va.		
	Number of specimens	Period to failure		Number of specimens	Period to failure	
		Average	Range		Average	Range
lb/in.^{2}		*Days*	*Days*		*Days*	*Days*
32,000				7	13.5	8.3 to 20
31,000				8	14.3	10.8 to 20
30,000				15	22.1	0.5 to [illegible]
29,000	4	14	10 to 23	13	21.2	11.5 to [illegible]
28,000	6	17.3	1 to 47	24	37.3	12.5 to 8[illegible]
27,000	23	13.2	5 to 35	15	36.5	16.0 to [illegible]
26,000	4	26.5	17 to 45	9	55.0	33.0 to 1[illegible]
25,000	13	23.8	4 to 39	8	41.9	27.5 to [illegible]
24,000	[a] 12	26.8	13 to 53	12	76.1	39.0 to 1[illegible]
24,000	[b] 3	27.3	20 to 45			
23,000	8	26.8	16 to 45			
22,000				7	127	5.6 to 1[illegible]
21,000	[a] 41	95.2	11 to 280			
21,000	[c] 9	132	61 to 273	[c] 9	214	76 to 32[illegible]
20,000	[b] 6	184	144 to 280			
20,000	[d] 3	69	64 to 72			
20,000	[e] 3	37	37 to 37.5			
18,000	[a] 37	97.4	32 to 255			
18,000	[c] 3	89	74 to 104			
16,000	[a] 14	151	26 to 248			
16,000	[c] 6	131	26 to 248			

[a] Total number specimens tested under designated stress.
[b] Tested simultaneously with 0.125-in. thick material.
[c] Tested simultaneously.
[d] Tested simultaneously with AZ51X and AZ61X material.
[e] Tested simultaneously with annealed material.

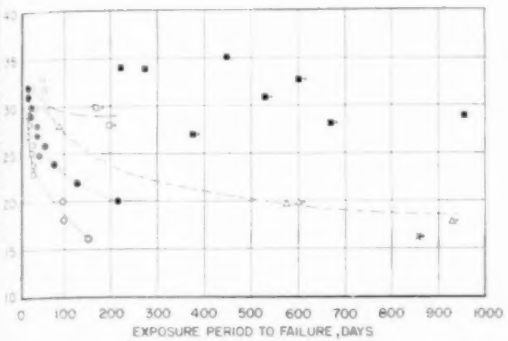

FIGURE 5. *Stress-exposure period to failure curves for magnesium alloys exposed to the weather.*

□, M1 clad AZ31X–h sheet exposed at NBS; ■, M1 clad AZ31X–h sheet exposed at Hampton Roads; △, ZK60 extrusions exposed at NBS; ○, AZ31X–h sheet exposed at NBS; ●, AZ31X–h sheet exposed at Hampton Roads; X, M1–h sheet exposed at NBS; →, specimen had not failed.

atmosphere, fractured under stresses of 20,000 lb/in.² in an average period of 214 days. The clad specimen thickness was 0.080 in. compared to 0.064 in. for the bare alloy. This difference in thickness of the two materials would not be expected to produce more than a small difference in the expected life of specimens of the same material. The results, therefore, showed that the clad material was definitely more resistant to stress corrosion than the bare material.

Data shown in figure 5 and given in table 6 indicate that the exposure period to failure was generally shorter for specimens exposed under a given stress at the National Bureau of Standards site than for the same material exposed under the same stress in a marine atmosphere at Hampton Roads, Va. As a further check, 18 specimens were machined from the same sheet of the AZ-31X–h alloy and were exposed to the weather on the same date and at the same stress, 20,000 lb/in.², one group at this Bureau, the other at Hampton Roads. The average period to failure for specimens exposed at the National Bureau of Standards was 152 days and at Hampton Roads, 214 days; ranges were 61 to 263 days and 76 to 323 days, respectively. No analysis of the atmosphere in the vicinity of the racks at this Bureau was made, but the smoke stack on an adjacent building, shown in figure 1, in all probability increased the corrosiveness of the atmosphere in the neighborhood of the stress-corrosion racks.

The results shown in figure 5 also indicate that the M1 sheet and the ZK–60 extruded materials (exposed at the National Bureau of Standards site) were relatively more resistant to stress-corrosion at moderate stresses than other bare materials studied. The M1 alloy specimens stressed at 16,000 lb/in.² at the National Bureau of Standards site had not failed in 857 days. Specimens of the AZ31X–h alloy placed under test on the same date at the same stress failed after an average exposure period of 131 days (range 26 to 248 days). Two ZK–60 specimens exposed under stresses of 20,000 lb/in.² failed after 555 and 596 days exposure. Three specimens

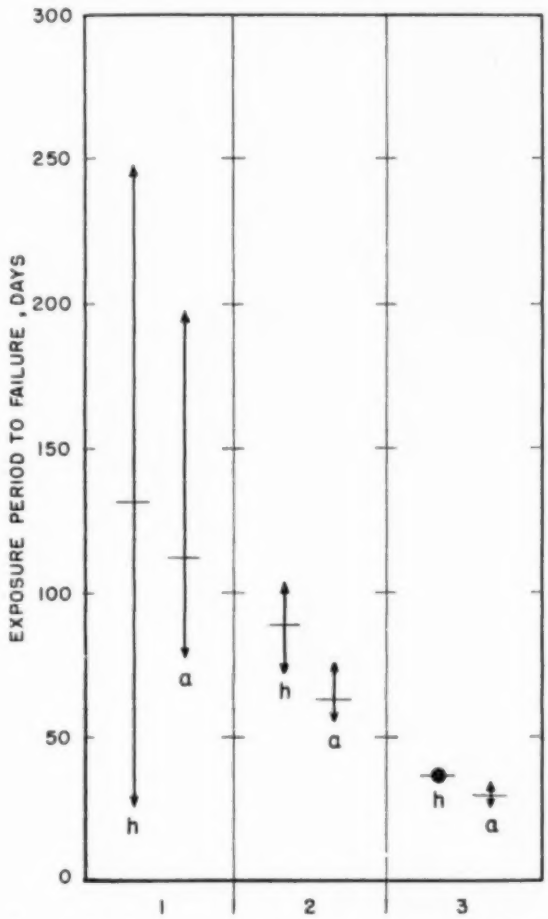

FIGURE 6. *Resistance to stress corrosion of hardened* (h) *and annealed* (a) *AZ31X sheet materials exposed to the weather at the National Bureau of Standards site at three different stresses.*

1, Stress, 16,000 lb/in.²; 2, stress, 18,000 lb/in.²; 3, stress, 20,000 lb/in.²; +, average value; ⟷, range.

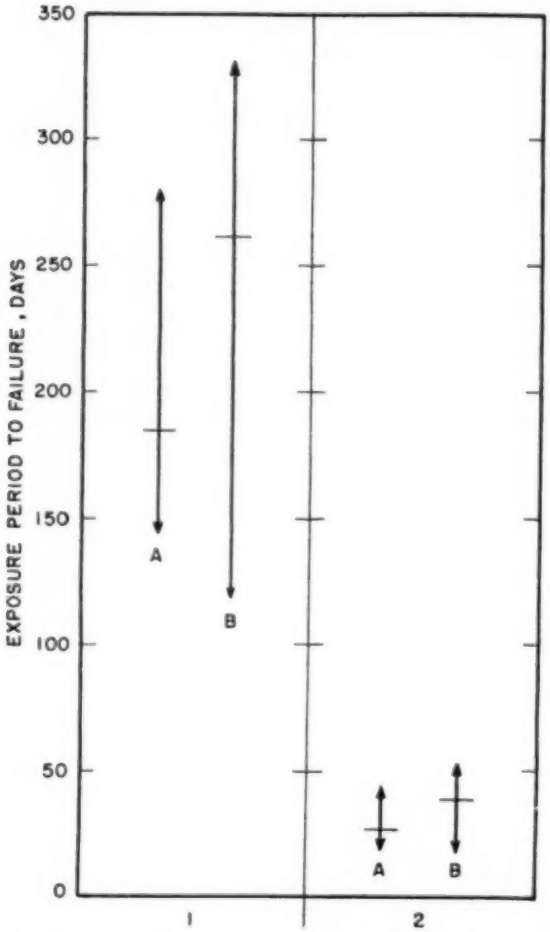

FIGURE 7. *Effect of specimen thickness on the resistance of the AZ31X-h material to stress corrosion.*

1, Stress 20,000 lb/in.²; 2, stress, 24,000 lb/in.²; +, average value; ←→, range. A, 0.064-in. material; B, 0.125-in. material.

exposed at the same stress had not failed in 600 days.

It was noted that, although an occasional specimen failed during a period of dry weather, most failures occurred during the drying period after the specimens had been wet by rain. This fact is believed to account, at least in part, for the wide variations in exposure periods required for failure, for specimens subjected to the same stress, seen in table 6 and shown graphically in figures 6 to 9 inclusive. Because of the increased number of failures occuring after rain had fallen, direct comparisons of weather exposure results, shown in figures 6 to 9, inclusive, were made o specimens inserted in the racks on the same dat under the same stresses.

Results obtained on the AZ31X alloy in th annealed and rolled conditions (see fig. 6) indicate that for stresses of 18,000 and 20,000 lb/in.² th hardened material was more resistant to stress corrosion than the annealed material. Dat obtained at 16,000 lb/in.² are not so conclusiv because of the small difference between the average values and the large scatter in the observed values.

The effect of specimen thickness on the resist ance of the AZ31X-h material to stress corrosion s shown in figure 7. The average period to failur for the 0.125-in. thick material was greater tha that for the 0.064-in. thick material. However the scatter was such that it is not possible to say that any particular 0.064-in. specimen would fa

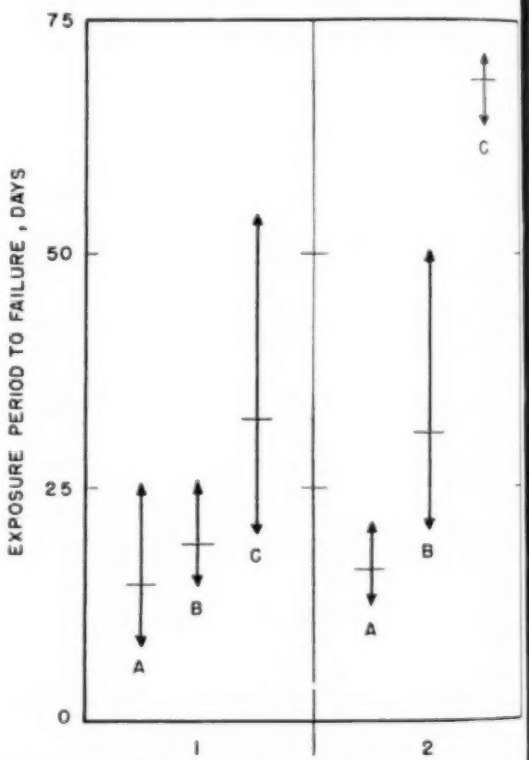

FIGURE 8. *Effect of aluminum content on the stress corrosion behavior of three magnesium alloys.*

AZ61X contained 6.5% Al; AZ51X, 5.0% Al; AZ31X, 3.0% Al. 1, Intermittent immersion in 0.01% NaCl solution; A, AZ61X-h; B, AZ51X-h; C, AZ31X-h. 2, Weather exposure NBS; A, AZ61X-h; B, AZ51X-h; C, AZ31X-h. Stress=20,000 lb/in.²; +, average value; ←→, range.

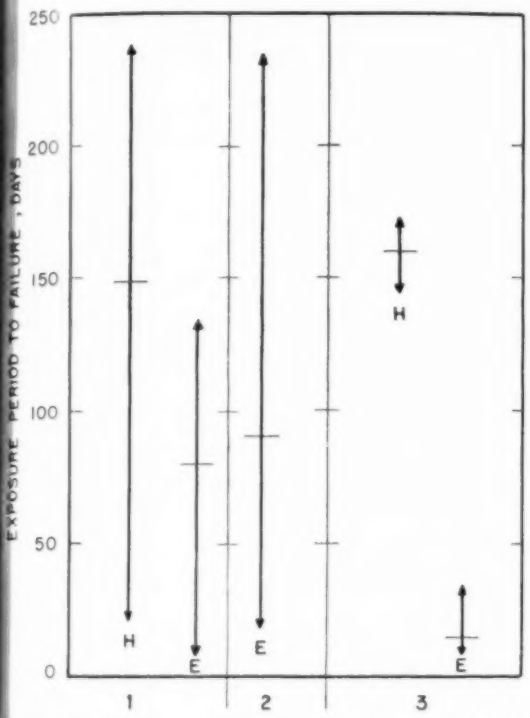

FIGURE 9. *Resistance to stress corrosion of two extruded magnesium alloys under stress of 20,000 lb/in².*

1, AZ80X. 2, AZ61X; weather exposure. 3, AZ80X, intermittent immersion. —•—, average value; ⟷, range. H=heat treated and aged; E=as extruded.

in a shorter period of time than a given 0.125-in. thick specimen.

The results discussed above for the M1-h and AZ31X-h material and the results of tests on the AZ31X-h, AZ51X-h, and AZ61X-h alloys, shown at the right in figure 8 indicate that at moderate stresses the resistance of the wrought magnesium alloys to stress-corrosion decreased with increased aluminum content up to about 6.5 percent of aluminum.

Although it was badly discolored, the ZK–60 extruded alloy, as indicated above, was the most resistant to stress corrosion of any of the extruded materials studied. The average periods to failure and the ranges for the AZ80X alloy exposed as extruded and after heat treatment and aging, and for the AZ61X extruded alloy (4 to 6 specimens of each alloy) all exposed in the weather at this Bureau under stress of 20,000 lb/in.² are shown graphically in figure 9. It can be seen that the average period to failure of the heat-treated and aged AZ80X material was greater than the maximum value for the material as extruded. Because of the scatter obtained with both materials, it was difficult to say whether the AZ61X was more susceptible to stress-corrosion than the AZ80X-HTA alloy.

Ultimate tensile strengths of the bare AZ31X-h, the ZK–60, and the AZ80X alloys, determined after specimens had been exposed unstressed in the weather at this Bureau for periods of 750 to 800 days, were at least 94 percent of those of the unexposed material. Changes in ductility (measured in percentage elongation in 2 in.) varied with the different alloys; values for the exposed ZK–60 and AZ31X-h materials were 85 percent or more of those of the unexposed materials. No elongation data were obtained on the AZ80X material.

The decrease in the ultimate tensile strength of M1-clad AZ31X-h material exposed unstressed for periods up to 960 days in a marine atmosphere was small; the tensile strength was 95 percent or more of that of the original material. Elongations, however, were reduced to 25 to 50 percent of those of the unexposed material.

The maximum exposure periods for the AZ61X-h and AZ51X-h materials, exposed unstressed at this Bureau, were 50 days and 22 days, respectively. Ultimate tensile strengths were 94 percent or more of those of the unexposed materials; elongations of the AZ61X-h and AZ51X-h materials were 70 percent or more and 85 percent or more, respectively, of those of the unexposed materials.

The data indicate that: (1) the M1-clad AZ31X-h alloy is relatively immune to stress corrosion at stresses of about 30,000 lb/in.² (2) The ZK–60 and the M1-h alloys are relatively immune to stress corrosion at stresses below 20,000 and 16,000 lb/in.², respectively. The tensile properties of the M1 alloy were lower than those of other alloys studied. Hence it was exposed only at a stress of 16,000 lb/in.² on longitudinal specimens. The AZ51X, AZ61X, and AZ80X alloys were all susceptible to stress corrosion in the weather when subjected to stresses of 20,000 lb/in.² These alloys were not exposed in the weather at lower stresses. (3) The AZ31X-h alloy was susceptible to stress-corrosion in the weather at stresses of 16,000 or more lb/in.²

2. Continuous Immersion Tests in the $NaCl+K_2CrO_4$ Solution

The curve in figure 10 shows the relationship between the stress and the exposure period to failure for specimens of annealed AZ31X material. The stresses that the materials would withstand for 24 hr or longer in the $NaCl+K_2CrO_4$ solution, as determined from curves of this type, are defined as the threshold stresses. It was suggested that such a test could be used as an accelerated test to evaluate the resistance of magnesium alloys to stress corrosion, if a relationship could be established between the threshold values and the ultimate tensile strengths or yield strengths of the material or the long-time stress-corrosion data.

Threshold stresses for the various sheet and extruded alloys, given in tables 2 to 5, inclusive, show that with the exception of 0.064-in. thick AZ61X-h sheet material supplied by the American Magnesium Corp. the threshold stresses were greater than 75 percent of the yield strength of the material. The threshold stresses (in terms of yield strengths) of the annealed AZ61X alloy were generally higher than those of the hardened (rolled) material. The threshold stresses of other materials studied, in percentages of the yield strength, were generally approximately the same whether the material was in the annealed or rolled conditions.

The threshold stresses obtained in the $NaCl+K_2CrO_4$ solution do not indicate the minimum stresses at which the material will fail by stress-corrosion cracking in the weather. Furthermore, the relative susceptibilities of some of the alloys, as determined from threshold stresses given in tables 2 to 5 do not agree with weather exposure data shown in figures 8 and 9.

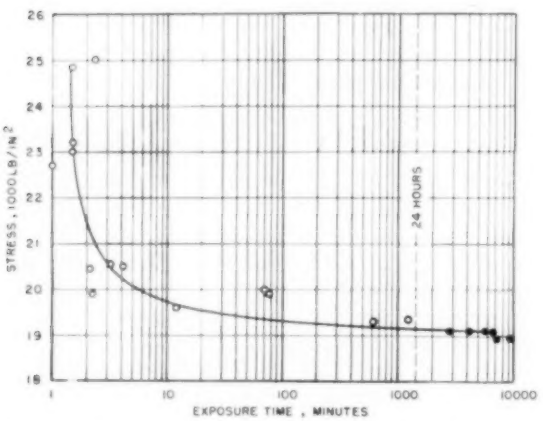

FIGURE 10. *Stress-exposure behavior of AZ31X-a specimens, immersed continuously in a* $NaCl+K_2CrO_4$ *solution.*

○, Specimen failed; ●, specimen did not fail.

3. Intermittent Immersion Tests in the 0.01-Percent NaCl Solution

The results of intermittent immersion stress-corrosion tests on the AZ61X, AZ51X, and AZ31X alloys (all in the rolled condition) are shown graphically in figure 8 (left). For comparison, results of weather exposure tests on these alloys are shown at the right in figure 8. The resistance to stress corrosion of the three materials was in the same order in the intermittent immersion tests in the 0.01-percent NaCl solution as in the weather exposure tests.

The results of intermittent immersion tests in the 0.01-percent NaCl solution for the AZ80X alloy after heat treatment and aging and for the alloy as extruded are shown graphically in figure 9. The results are in qualitative agreement with those obtained in weather exposure tests for this alloy in the two conditions.

There were insufficient data from intermittent immersion tests on the other materials studied to determine whether these results show close correlation with weather exposure data.

4. Discussion of Laboratory Accelerated Tests

It was pointed out in section III, 2, that continuous immersion tests in the $NaCl+K_2CrO_4$ solution have two drawbacks. First, threshold stresses (stresses below which stress-corrosion fractures did not occur in the $NaCl+K_2CrO_4$ solution) were much higher than those obtained for the same alloy in the weather. Second and more important, the correlation was poor between predictions of relative susceptibilities of various magnesium alloys, made from the results of this test and the results of weather exposure data.

There was general agreement between the results of intermittent immersion and weather exposure tests on the AZ31X-h, AZ51X-h, and AZ61X-h alloys as was indicated in section III, 3. These results, and the limited results obtained on other materials, indicate that intermittent immersion tests in a dilute chloride solution are a better

boratory means of predicting the relative susptibilities of magnesium alloys to stress corrosion the atmosphere than is continuous immersion in odium chloride-potassium chromate solution.

IV. Summary

1. Stress-corrosion tests were made on M1, bare d clad AZ31X, AZ51X, AZ61X, AZ80X, and K–60 wrought magnesium base alloys. Stressposure period to failure results were obtained th in weather exposure and in two types of boratory tests.

2. The decrease in tensile properties of unressed specimens exposed at the National Bureau Standards site was small.

3. The M1-clad AZ31X–h alloy was resistant stress corrosion in a marine atmosphere at resses up to 30,000 lb/in.^{2}

4. The bare AZ31X alloy was susceptible to ress corrosion in the weather at stresses of 16,000 in.^{2} or more.

5. The sheet M1 and the extruded Dow ZK–60 loys were resistant to stress corrosion in weather posure tests at stresses up to 16,000 and 20,000 in.^{2}, respectively.

6. The AZ51X, AZ61X, and AZ80X alloys were all susceptible to stress corrosion in the weather when subjected to stresses of 20,000 lb/in.^{2} These alloys were not tested at lower stresses.

7. The susceptibility of magnesium base alloys to stress corrosion increased with the aluminum content up to approximately 6.5-percent aluminum.

8. Results of intermittent immersion laboratory tests, using a 0.01-percent NaCl solution as a corrodent, were in better agreement with those obtained in weather exposure than were those obtained by continuous immersion in a 3.5-percent NaCl+2.0-percent K_2CrO_4 solution.

The cooperation of Fred M. Reinhart and the late Willard H. Mutchler of the National Bureau of Standards, and of Lieutenants C. A. Snavely and M. Franklin, of the Naval Air Station, Hampton Roads, Va., in securing the weather exposure data at Hampton Roads is appreciated. Houston Babb and Thomas P. Royston, Jr., assisted in obtaining the data at the National Bureau of Standards.

Washington, September 22, 1949.

U. S. Department of Commerce
National Bureau of Standards

Research Paper RP2075
Volume 44, March 1950

Part of the Journal of Research of the National Bureau of Standards

Preliminary List of Levels and g-Values for Ta II

By C. C. Kiess, G. R. Harrison,[1] and W. J. Hitchcock [1]

A new description of the spectrum emitted by singly ionized tantalum atoms has been compiled from observations made at this Bureau. The list of wavelengths contains about 2,500 lines between 5300 and 2000 A. About a third of these lines, including most of the strong ones, have been classified as transitions among energy levels that were identified with the help of well-resolved Zeeman patterns. The low and metastable levels arise from the electron-configurations $5d^2\,6s^2$, $5d^3\,6s$, and $5d^4$. The higher levels with which the low ones combine arise from the excited configurations $5d^2\,6s\,6p$ and $5d^3\,6p$. The presence of the $d^2\,s^2$ configurations in ionized tantalum, almost equal in stability with $d^3\,s$, is noteworthy because it is unknown in the homologous vanadium and columbium ions.

At various times during the past 25 years, the spectra of tantalum have been under investigation, at the National Bureau of Standards, not only to set up standard descriptions of them but also to analyze their structure. A description of the spectrum of the neutral tantalum atom and a preliminary list of levels for Ta I have already been published.[2 3] An analogous description of the spectrum emitted by singly ionized tantalum atoms has been completed and has, in part, been classified. The levels are communicated in the tables of this note. A revision and extension of the Ta I levels will follow in due course.

The spectrograms on which the descriptions of the spectra are based were obtained with the prism and grating spectrographs of this Bureau and cover the wavelength range from 2000 A, in the ultraviolet, to beyond 12,000 A in the infrared. The light sources were arcs and condensed sparks between electrodes of pure tantalum metal. They were operated in enclosures in which the air pressure was maintained at half an atmosphere or less so as to reduce the intensity of the background of continuous radiation that always accompanies tantalum arcs and sparks in air at normal pressure.

The clues to the term-structure of Ta I and Ta II were furnished by the Zeeman effect. So far as is known the first observations of the splitting of tantalum lines in magnetic fields were made especially for this investigation, in 1924, at the Brace Laboratory of Physics of the University of Nebraska, by the late Professor B. E. Moore. These earliest observations, measured and reduced at the National Bureau of Standards, exhibited some well-resolved, complex patterns for the stronger lines and gave the first insight into the structure of the tantalum spectra. Although McLenan and Durnford [4] published some Zeeman effects for tantalum lines, in 1928, their observations refer, apparently, only to unresolved patterns and were not used in this investigation.

Following Professor Moore's untimely death, further work on the Zeeman effect of tantalum was carried on at this Bureau. In 1932, a set of observations was made with the water-cooled Weiss magnet for which the light-source was a spark discharge between tantalum electrodes in air. In a second set of observations, made 11 years later, the light-source was a Ta arc operated in a Back Lamp [5] in which the air pressure was reduced to about ¼ atm. In the meantime, however, observations of tantalum were included in the Zeeman-effect program with the powerful magnet at the Massachusetts Institute of Tech-

[1] Spectroscopy Laboratory, Massachusetts Institute of Technology.
[2] C. C. Kiess and E. Z. Stowell, J. Research, NBS **12**, 459 (1934) RP671.
[3] C. C. Kiess and H. K. Kiess, J. Research, NBS **11**, 277 (1933) RP589.
[4] J. C. McLennan and A. M. I. A. W. Durnford, Proc. Roy. Soc. [A] **120**, 502 (1928).
[5] E. Back, Ann. Physik. (IV) **70**, 333 (1923).

871926—50——3

nology. These have been particularly valuable in resolving close patterns that were unresolved with the weaker fields.

The data acquired at both laboratories have led to the levels and g-values presented in the following tables. Table 1 contains the low and metastable even levels from the electron configurations $5d^2\,6s^2$, $5d^3\,6s$, and $5d^4$. Table 2 contains the odd levels from the configurations $5d^2\,6s\,6p$ and $5d^3\,6p$ resulting from excitation of an s or d electron out of the low configurations. The permissible transitions between these sets of levels give the classifications of more than a third of the known lines of Ta II, including most of the strongest ones.

Except for the levels of the lowest ^{5}F term the g-values do not agree strictly with those required for LS-coupling. However, the most plausible designation of the levels seems to be the term-symbols entered in the last column of table 1. Inspection of the table shows that intermingled with the components of ^{5}F and lying above them are triplet and probably singlet levels, apparently from the $d^2\,s^2$ configuration. It is rather striking that in singly ionized tantalum the configuration $d^2\,s^2$ is almost equal in stability to $d^3\,s$, whereas there is no evidence of its occurrence in singly ionized vanadium and columbium.

Details of the analysis of Ta I and Ta II will be presented in subsequent papers.

TABLE 1. *Even levels of* Ta II

Level	J	g	Designation	Level	J	g	Designation
0.00	1	0.000	$^5F_1$	13560.25	2	1.111	
1031.33	2	1.008	$^5F_2$	14494.90	2	1.472	$^3D_2$
2642.19	3	1.250	$^5F_3$	14581.00	3	1.004	
3180.04	2	0.750	$^3F_2$	14627.75	1	0.850	
4124.77	0	0.0	$^3P_0$	15726.06	3	1.476	$^3D_3$
4415.70	4	1.350	$^5F_4$	16424.36	2	1.405	
5330.66	1	1.550	$^3P_1$	17168.50	2	1.211	
5658.00	2	1.340	$^3P_2$	17231.22	4	1.23	$^1D_4$?
6186.72	5	1.33	$^5F_5$	17375.11	1	1.171	
6831.35	3	1.098	$^3F_3$	18500.60	2	1.462	
9690.46	2	1.063	$^1D_2$	22928.62	2	0.700	$^3F_2$
9746.33	4	1.225	$^3F_4$	23082.70	4	1.026	
10713.30	1	2.374	$^3P_1$	23294.72	3	1.120	
11767.14	3	0.915	$^3G_3$	23381.19	0	0.0	
11875.46	2	1.48	$^3P_2$?	23620.36	3	1.076	$^3F_3$
12435.85	3	1.614	$^3P_3$	24432.77	4	0.978	
12600.87	0	0.0	$^1D_0$	24869.61	3	0.995	
12705.32	4	1.021	$^3G_4$	25413.95	5	1.052	
12830.94	5	1.280	$^3G_5$	26829.09	3	0.855	
13475.40	1	1.510	$^1D_1$				

TABLE 2. *Odd levels of* Ta II

Level	J	g	Level	J	g
29256.87	2	0.522	46387.28	2	
33706.50	1	.291	46645.81	4	1.210
33715.15	2	.800	46831.39	3	1.204
36112.97	3		46850.69	2	1.097
36177.12	2	.947	47169.18	3	1.060
36763.73	3	1.169	47280.92	4	1.198
36987.73	1	0.685	47514.61	2	1.292
37230.80	2	.64	47596.02	1	
38515.55	2	1.026	47800.95	0	
38535.26	1	0.472	47825.41	3	1.198
38962.38	3	1.001	48064.50	0	
39265.83	3	1.140	48166.44	2	
39743.64	4	1.222	48223.11	2	1.148
40023.76	0		48470.35	4	1.268
40233.53	2	1.158	48666.55	2	1.137
40304.78	1	1.232	48776.36	1	0.750
41145.00	2	1.161	48962.66	3	1.273
41355.06	1	1.893	49080.44	2	1.33
41554.52	3	1.204	49536.28	3	1.318
41775.29	4	0.72	49592.90	2	1.61
42122.91	4	1.265	49646.60	3	1.045
42153.32	2	1.210	49887.03	1	2.023
42959.59	3	1.117	49937.82	4	
43064.95	2	1.061	51073.88	3	1.156
43544.44	3	1.086	51197.32	2	1.363
43553.87	1	1.50	51326.37	1	1.052
44005.16	4		51534.21	2	1.317
44206.19	1	0.255	52121.22	4	1.088
44259.20	2	1.251	52155.76	1	1.618
44430.38	3	0.950	52580.41	3	1.403
44434.70	0		52824.53	1	0.930
44585.33	5	1.245	53465.72	3	1.226
44626.00	4	1.264	53644.82	2	1.339
44835.23	3	1.34	54533.76	2	1.035
45233.85	1	1.461	54648.81	3	0.935
45446.91	2	1.150	55128.36	3	1.250
46174.63	1	1.361	56018.75	2	0.991
46286.97	4	1.405	56142.49	4	1.26

WASHINGTON, October 20, 1949.

U. S. Department of Commerce
National Bureau of Standards

Research Paper RP2076
Volume 44, March 1950

Part of the Journal of Research of the National Bureau of Standards

Electrode Function (pH Response), Hygroscopicity, and Chemical Durability of Na_2O-CaO-SiO_2 Glasses

By Donald Hubbard, Given W. Cleek, and Gerald F. Rynders

The hydrogen electrode function (pH response), hygroscopicity (water sorbing property), and chemical durability (surface alteration in solutions of various hydrogen ion concentrations) were measured for a series of Na_2O-CaO-SiO_2 glasses. The resulting data both confirmed and extended the previous conclusion that glasses having inadequate hygroscopicity and poor chemical durability are incapable of producing satisfactory electrodes for pH measurements. Each family of glasses having equal SiO_2 content and varying Na_2O:CaO ratios was found to have a limited composition range that gave electrodes that approached the theoretical voltage. However, low hygroscopicity, poor chemical durability and devitrification limit the number of useful glasses to a small area from which the eutectic composition, 22 percent Na_2O, 6 percent CaO, 72 percent SiO_2 (Corning 015), is already known to be superior for its pH response. For the series of 70 percent SiO_2 content, the pH response and chemical durability curves appear to indicate the compositions at which changes in the primary phase are indicated by the phase diagram of the system.

I. Introduction

That the water content plays an important role in determining the suitability of glasses as indicators of the hydrogen ion activity of aqueous solutions was recognized by the early investigators of the glass electrode [1, 2, 3, 4, 5, 6, 7].[1] However, only recently have simple, semiquantitative techniques been available for readily comparing and classifying glasses for their water sorbing capacities [8, 9, 10, 11, 12, 13, 14]. Such hygroscopicity data upon comparison with the accompanying pH responses have shown in all cases investigated that glasses of very low hygroscopicity fail to develop the theoretical voltage of 59 mv per pH at 25° C predicted from the simplified Nernst equation, $\Delta E = 0.000198\ T\ \Delta pH$ [15].

Other conspicuous departures of the glass electrode from the straight-line relation of the Nernst equation appear in solutions that cause detectable changes in the chemical durability of the glass, such as hydrofluoric acid and various strong alkaline solutions [7, 16, 17, 18]. Voltage departures (errors) also occur in the "super acid" region, in nonaqueous solutions, and other solutions of a dehydrating nature [4, 18, 19, 20].

As the composition, hygroscopicity, pH response, voltage departure, and chemical durability of glasses seem to be so intimately associated, each of these properties was investigated for a series of Na_2O–CaO–SiO_2 glasses covering as great a range of compositions as the nature of the glasses and the limitations of the available glass-making equipment would permit.

II. Experimental Procedures

The procedure employed for determining hygroscopicity was that reported in previous publications [10, 11, 12], which consisted of weighing the water "sorbed" [21] upon exposing approximately 1.5 g of powdered glass that passed a 150 mesh Tyler standard sieve, to the high (approximately 98%) humidity maintained by a saturated solution of $CaSO_4 \cdot 2H_2O$. To insure speed in obtaining equilibrium and uniformity throughout the humidity chamber, the walls were lined with a blotter wick, while the atmosphere of the closed system

[1] Figures in brackets indicate the literature references at the end of this paper.

was circulated continuously. All glasses were exposed for 1- and 2-hr. periods at 25° C and the results reported as milligrams of water sorbed per cubic centimeter of sample.

The experimental electrodes were blown from tubes drawn from the melts at the time the glasses were poured. These electrodes were filled with mercury for the inner electrical connection [22], and were examined for voltage characteristics using a well-conditioned Beckman glass electrode as a reference standard. The voltage and pH observations were made at room temperature with a Beckman pH meter, model G. The pH response values (mv per pH) were calculated from the emf readings at pH 4.1 and pH 8.1. The voltage difference between the reference and experimental electrodes obtained in the buffer of pH 2 was taken as the zero voltage departure.

The durability measurements were obtained by the interferometer procedure [16, 18, 23, 24, 25] on optically flat specimens exposed to Britton-Robinson universal buffer solutions at 80° C ±0.2° C. All attack data are reported as change in thickness in fringes for 6-hr exposures, although some of the glasses were exposed for as short a period as 15 min in order to keep the attacks within the range limitations of the interferometer. Dimensional changes greater than three to five fringes are difficult to read, and the large values of swelling would be unobservable after 6 hr because of sloughing off of the swollen surface leaving a rough pitted area. As many of the glasses exhibited swelling in acid buffers, it was necessary to plot these data as "negative attack".

Throughout the paper, the glasses are identified by their composition (computed from the batch) given in weight percentage in the ratio of Na_2O:CaO:SiO_2.

III. Results and Discussion

Table 1 gives the characteristic voltage departures exhibited by electrodes prepared from typical Na_2O-CaO-SiO_2 glasses. In the same table also appear the hygroscopicity and chemical durability data for this series of glasses.

Figure 1, in which the pH response (mv per pH between pH 4.1 and 8.1 is plotted against the hygroscopicity (water sorbed for 1-hr. exposure to 98% relative humidity), probably gives the most understandable picture of the electrode performance of this series of glasses. Electrodes prepared from glasses below a certain hygroscopicity (group A, fig. 1) failed to develop the theoretical 59 mv per pH at 25° C,[2] while those electrodes prepared from glasses that sorbed water between the approximate limits 30 to 75 mg per cm³ (group B, fig. 1

[2] Whether or not the failure of electrodes prepared from glasses of low hygroscopicity to indicate the theoretical voltage can be attributed to the limited sensitivity of the indicating instrument or to an actual failure of the glass to respond to H^+ ions is not yet certain.

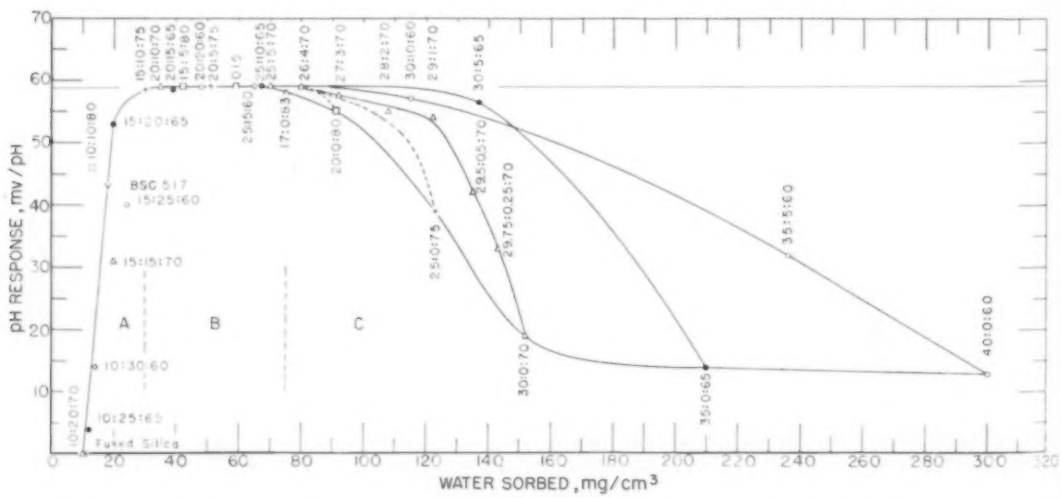

FIGURE 1. *Variation in* pH *response with increasing hygroscopicity for a series of* Na_2O-CaO-SiO_2 *glasses.*

Corning 015 electrode glass and BSC 517 optical glass are included for comparison.

TABLE 1. *Comparison of the hygroscopicity (water sorbed), pH response and chemical durability of some* Na_2O-CaO-SiO_2 *glasses*

No.	Glasses			Water sorbed after—		Voltage departure at pH—						pH response, pH 4.1 to pH 8.1	Chemical durability (attack) at pH					
	Na_2O	CaO	SiO_2	1 hr	2 hr	2.0	4.1	6.1	8.1	9.9	11.9		2.0	4.1	6.1	8.1	9.9	11.9
	%	%	%	mg/cm²	mg/cm²	mv	mv	mv	mv	mv	mv	mv/pH	*Fringes*	*Fringes*	*Fringes*	*Fringes*	*Fringes*	*Fringes*
1	10	30	60	14	20	0	57	.....	238	.....	486	14	1/10 swell	D swell [a]	D	1 1/2+	2 1/4	16 1/2.
2	15	25	60	24	35	0	−21	−2	53	126	234	40	D	D swell	1/4	<0.2	3	19 1/2.
3	20	20	60	48	88	0	6	1	6	47	77	59	D swell	D swell	1/10+	2 1/4	4 1/2	24.
4	25	15	60	65	134	0	−10	−10	−10	14	55	59	D swell	D	3/10−	3/10 SC [b]	4 1/2	27.
5	30	10	60	115	275	0	1	4	7	18	35	57	1/4 swell	1/4+ swell	1/10 SC	SC	5 1/2	14 1/2.
6	35	5	60	236	568	0	−22	15	86	152	269	32	36 swell	40 swell	45 swell	36 swell	SC swell	18.
7	40	0	60	300	.....	0	95	187	280	360	462	13	(c)	(c)	(c)	(c)	(c)	(c)
8	10	25	65	12	24	0	85	205	307	420	533	4	D D swell	D swell	D	2 1/2	6 1/4	10.
9	15	20	65	20	38	0	6	12	30	119	205	53	swell	D swell	D swell	1 1/4	7 1/2	10 1/2.
10	20	15	65	39	85	0	0	0	2	9	14	58.5	D swell	D swell	D	3 SC, 1 attack	4 1/2	10.
11	25	10	65	67	139	0	0	0	0	2	−7	59	D swell	1/10 swell	D swell	1 1/4	3 1/4	10.
12	30	5	65	137	270	0	−3	−3	3	17	68	57	3 1/2 swell	4 swell	4 1/2 swell	3 3/4	6 3/4	12.
13	35	0	65	210	.....	0	70	162	250	312	391	14	(c)	(c)	(c)	(c)	(c)	(c)
14	10	20	70	10	21	0	68	190	304	418	498	0	ND	ND	D	D SC	1/2	4 1/2.
15	15	15	70	20	36	0	19	84	130	184	218	31	ND	ND	ND	D SC	1/2+	6.
16	20	10	70	35	88	0	0	0	0	0	−5	59	ND	ND	D	D SC	1/2	7.
17	25	5	70	70	160	0	0	0	0	2	9	59	1/2+swell	1/2+swell	3/4 swell	1/2 swell	1/2+	7.
18	26	4	70	80	185	0	0	1	1	4	10	59−	2 swell	3 swell	3 swell	2 swell	D attack	7 attack.
19	27	3	70	92	219	0	1	5	9	14	19	57	6 swell	6 swell	7 swell	6 swell	4 swell	10 attack.
20	28	2	70	108	249	0	−2	4	14	26	34	55	18 swell	18 swell	18 swell	16 swell	6 swell	12 attack.
21	29	1	70	122	290	0	5	8	24	61	102	54	30 swell	30 swell	30 swell	30 swell	15 swell	70 attack.
22	29.5	0.5	70	135	314	0	2	15	72	136	210	42	75 swell	70 swell	70 swell	65 swell	40 swell	144 attack.
23	29.75	0.25	70	143	360	0	6	27	113	187	260	33	120 swell	108 swell	108 swell	108 swell	72 swell	288 attack.
24	30	0	70	152	379	0	45	112	205	299	400	19	60 attack [d]	70 attack [d]	.....	Pitted	Pitted	Pitted.
25	15	10	75	30	59	0	0	0	1	0	−6	58.7	ND	ND	ND	D	1/2+	3.
26	20	5	75	51	113	0	0	0	0	0	−1	59	1/10 swell	D swell	D swell	D swell	3/10	3−.
27	25	0	75	123	296	0	40	84	120	191	256	39	Pitted	15	15	17	.....	38.
28	10	10	80	13	32	0	25	44	75	101	155	46	ND	ND	ND	ND	D	23/4.
29	15	5	80	42	99	0	0	0	0	4	−7	59	ND	ND	ND	SC D	1/4+	3−.
30	20	0	80	91	223	0	10	22	26	30	55	55	1 1/2 swell	2 swell	2+swell	2 swell	1 swell	3 attack.
31	17	0	83	75	200	0	7	10	10	11	4	58	1/2+swell	1/2+swell	1/2swell	?	1 1/2	3 3/4.
32	10	0	90	50	97	(e)	(e)	(e)	(e)	(e)	(e)	.....	D swell	D swell	D swell	D	.....	1 1/2−.
33	Fused silica			11	12	(f)	(f)	(f)	(f)	(f)	(f)	0	ND	ND	ND	ND	ND	1/2.
34	Corning 015			59	138	0	0	0	0	0	3	59	3/16−swell	3/16−swell	3/10−swell	3/10 SC D	1/4+	2−.
35	BSC 517 [9]			18	33	.....	.....	.....	.....	.....	.....	43	1/10	D	D	1/4+	3/4	13/4.

[a] D, Detectable; ND, not detectable.
[b] SC, Surface cut.
[c] Failed to maintain polish.
[d] Durability data for this glass were calculated from the attack for 15 min at 80° C; however, it is not definitely known if the glass does or does not exhibit swelling during the earliest stages of exposure to the acid buffers.
[e] No tube.
[f] No definite pH response.

UNIVERSITY OF MICHIGAN LIBRARIES

approximated the theoretical voltage over the pH range chosen for comparison. For the glasses of higher hygroscopicity (group C, fig. 1) the pH response again falls off, but, not as sharply as is the case for the glasses of very low hygroscopicity. This decrease in pH response at the higher hygroscopicities is associated with a progressive decrease in the chemical durability of successive members of the series.

It is evident from figure 1 that the previous suggestion that a low pH response might be used as a satisfactory indicator of the serviceability [3] of optical glasses [9] must be accepted with reservations. For example, a low pH response at the left end of the curve is accompanied by low hygroscopicity and satisfactory serviceability, while at the other end of the same curve a low pH response is accompanied by high hygroscopicity, poor chemical durability, and unsatisfactory serviceability.

It is interesting to note that the Na_2O–SiO_2 glasses 20:0:80, 25:0:75, 30:0:70, 35:0:65, and 40:0:60 fall into a family distinct from the Na_2O–CaO–SiO_2 glasses. Figure 2 shows how remarkably some of these glasses, chosen from the boundaries of group C, figure 1, differ among themselves in chemical durability.[4] Glasses 30:10:60, 35:5:60, and 30:5:65 containing CaO demonstrated pronounced swelling in the acid pH range while the Na_2O–SiO_2 glasses 30:0:70 and 25:0:75 were vigorously dissolved [12]. On the other hand, glass 20:0:80, which gave a much smaller voltage departure, showed swelling. A comparison of the voltage departure curves and the chemical durability curves for these six glasses shows the expected qualitative correlation. The voltage departures for electrodes from the glasses 30:0:70, 25:0:75, and 20:0:80 are in the same relative order as the durability curves for these glasses. The voltage departure curves for electrodes from the glasses containing CaO that exhibit swelling in the acid pH range also follow a durability sequence, although glass 30:5:65 possibly should not be compared with 30:10:60 and 35:5:60, as the latter are in a different family with respect to SiO_2 content. It is obvious that each series of glasses having a fixed percentage of SiO_2 falls into a distinct family (fig. 1). These

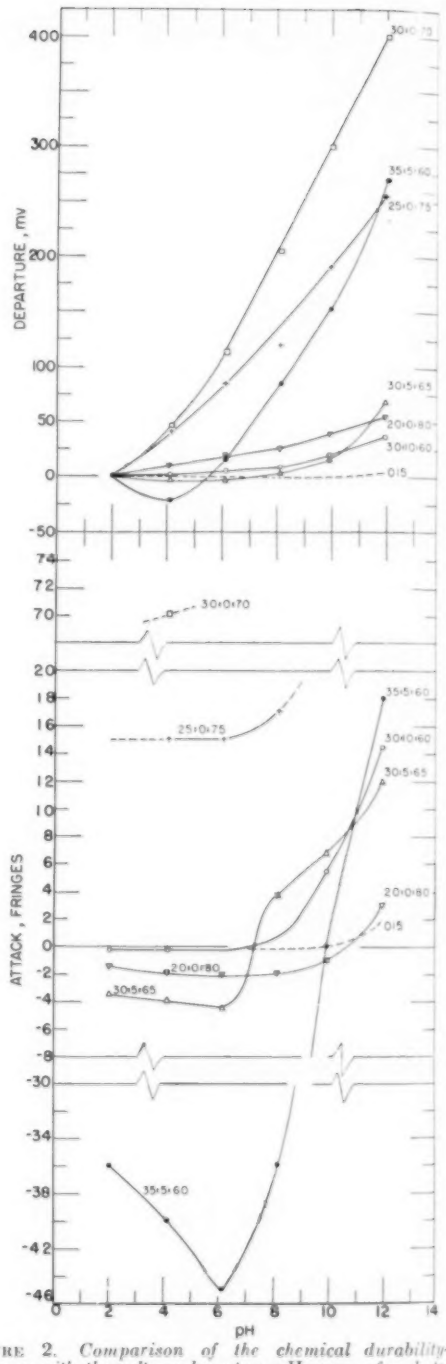

FIGURE 2. *Comparison of the chemical durability-[illegible] curves with the voltage departure-*pH *curves for electrod[illegible] prepared from typical* Na_2O-CaO-SiO_2 *glasses of hi[illegible] hygroscopicity and poor chemical durability.*
Corning 015 electrode glass is included for comparison.

[3] Ability to maintain a clear surface upon exposure to the atmosphere.
[4] Durability values on the Na_2O–SiO_2 glasses 40:0:60 and 35:0:65 were not obtained because the specimens did not maintain polished surfaces.

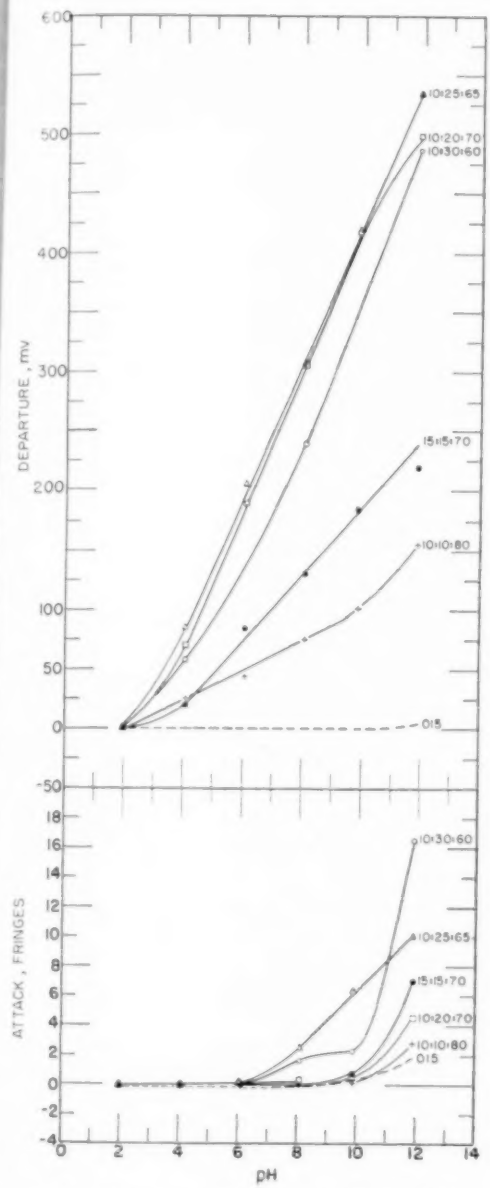

FIGURE 3. *Comparison of the chemical durability-*pH *curves with the voltage departure-*pH *curves for electrodes prepared from typical* Na_2O-CaO-SiO_2 *glasses of low hygroscopicity.*

Corning 015 electrode glass is included for comparison.

families coincide in their pH response only for those members that have adequate hygroscopicity and possess uniform chemical durability over the pH range chosen for comparison. For convenience in observing the trends within each family the pH response values in table 1 have been separated into groups. To obtain a qualitative picture of the inter-relationships between voltage departure, composition, pH response, hygroscopicity, and chemical durability of such a family of glasses (70% SiO_2) see figures 1, 6, 7, 8, and 9.

Electrodes from glasses of low hygroscopicity, group A of figure 1, show large voltage departures (fig. 3). In general the property of very low hygroscopicity seems to obscure any additional voltage departure attributable to chemical durability shifts in the alkaline range. Figure 4 shows that there are two apparent exceptions to this, viz. glasses 15:25:60 and 15:20:65. However, these two glasses are obviously not exceptions, inasmuch as their hygroscopicity is nearly adequate to yield the correct pH response, provided they possessed desirable durability characteristics.

The glasses in group B of figure 1 (i. e. those having adequate hygroscopicity and uniform chemical durability over an extended pH range and with reduced attack in the alkaline range) produced electrodes with very much decreased voltage departures (fig. 5). Also, these voltage departures are confined to the alkaline pH range of decreased chemical durability. The difference in performance of some of these electrodes in the alkaline range can possibly be rationalized. For instance, glasses 20:10:70 and 25:5:70 exhibit voltage departures in the opposite directions. Although the attack for the two glasses was the same at pH 11.9, such is not the case in the acid range. Glass 20:10:70 had no detectable attack at pH 4.1, so it is conceivable that going from no attack to an appreciable attack is not altering the surface of the glass nearly so radically as for glass 25:5:70, which passed from a swollen condition in the acid range to an over-all solution in the alkaline buffers. However it is also possible that accidental variations in blowing the electrode bulbs were responsible for such reversals.

In order to obtain some indication of the com-

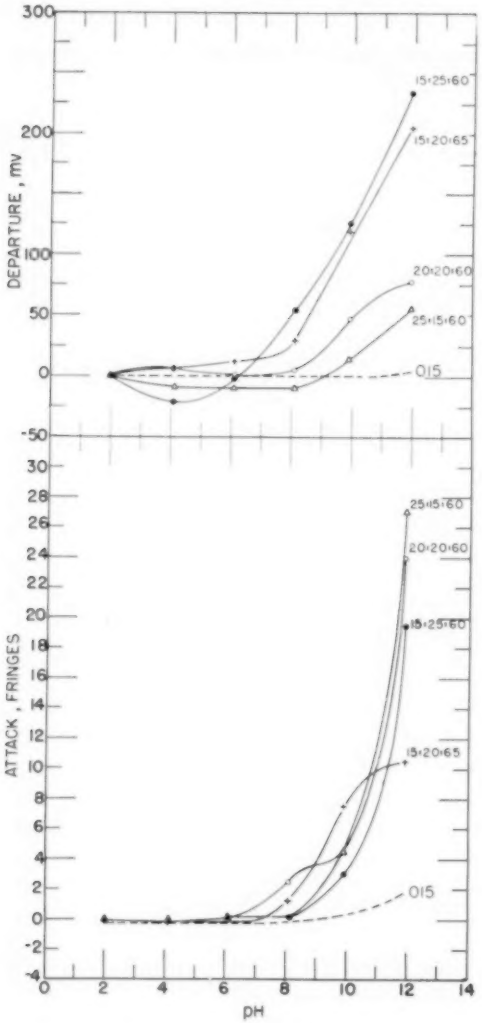

FIGURE 4. *Comparison of the chemical durability*-pH *curves with the voltage departure*-pH *curves for electrodes prepared from typical* Na_2O-CaO-SiO_2 *glasses having poor chemical durability in the alkaline range with large voltage departures appearing in this same* pH *region.*

Corning 015 electrode glass is included for comparison.

position limits within which electrodes approximating the theoretical pH response can be made, figure 6 was prepared showing composition lines of equal hygroscopicity.[5] The compositions of the experimental glasses are represented by small open circles. Those that produced electrodes that approximated the theoretical 59 mv per pH are inclosed in small hexagons, while the interpolated compositions are located as heavy dots. The lines of equal hygroscopicity (iso-sorbs) are identified by their sorption values inscribed in circles.

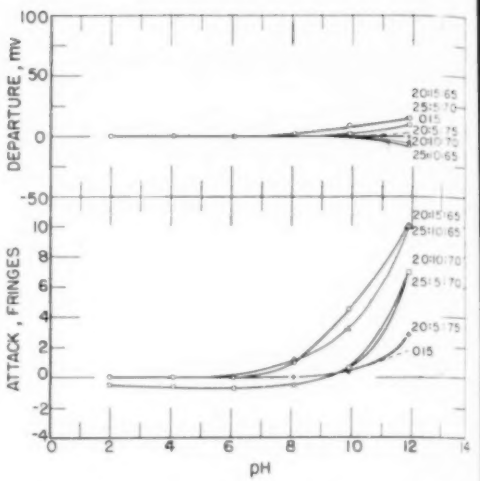

FIGURE 5. *Comparison of the chemical durability-p curves with the voltage departure-*pH *curves for electro prepared from typical* Na_2O-CaO-SiO_2 *glasses of adeq hygroscopicity for* pH *determination.*

The resulting figure reveals that the area of promising compositions (shaded) is bounded by two hygroscopicity barriers, the one of decreasing Na_2O content, which is too "dry" and the other of increasing Na_2O, which is too "wet". The latter area is also a region of poor chemical durability. Thus figure 6 indicates the same three groupings A, B, and C that are shown in figure 1.

The glasses included in the shaded area of figure 6 are not all equally satisfactory for pH measurements. Glasses 20:20:60 and 25:15:60 (table 1) devitrified so rapidly upon reheating that it was almost impossible to obtain unpunctured electrodes. Successful electrodes, when obtained, deteriorated so very rapidly because of the poor durability of the glasses that the erratic voltage readings obtained must be considered as superficial. Electrodes prepared from glasses 20:15:65 and 25:10:65 also deteriorated rapidly

[5] The position of these iso-hygroscopicity lines for the 1-hr exposures was determined by plotting the interpolated values obtained from the hygroscopicity composition data drawn as smooth curves. No effort was made to establish a correspondence between the apparent breaks in the hygroscopicity-composition curves and the critical compositions of the phase equilibrium diagram, partly because of the paucity of data, partly because of the limited capacity of the humidity chamber which necessitated the spacing of data, but more particularly because the compositions of the glasses were known only from the batch compositions.

It is obvious that these four glasses do not rightfully deserve the favorable position assigned them in figures 1 and 6. Thus the useful range of the shaded area in figure 6 is greatly reduced from left to right. The area shaded with broken lines is unexplored and is possibly too broad.

The glass compositions of optimum pH performance, (i. e. those that offer a compromise between adequate hygroscopicity and acceptable chemical durability) would probably appear in figure 6 as a line rather than an area. With all other factors involved taken into consideration, including the liquidus temperatures, the difficulty of melting, fining, drawing tubes, and tendency toward devitrification upon reworking, it is conceivable that but one composition makes the most satisfactory compromise of all these factors. The glass having the composition, 22 percent Na_2O, 6 percent CaO, 72 percent SiO_2, near the eutectic having the lowest melting temperature for this three component system [2, 3, 7], seems to be a worthy candidate for this honor for pH measurements at room temperatures. For use at elevated temperatures a glass of much better chemical durability is desirable. As the electrical resistance of glass electrodes decreases greatly with increasing temperatures [26, 27], glasses of lower hygroscopicity and much improved chemical durability can be used for pH determinations at elevated temperatures.

Concerning the possibility of any glasses of the Na_2O-CaO-SiO_2 system possessing better performance in the high pH range than does this eutectic glass, a few of the experimental electrodes gave small negative departures in the buffer solution at pH 11.9. As the reference electrode was also a glass electrode normally showing a small positive departure in the alkaline range, these negative departures reported for the experimental electrodes indicate that some improvement for determinations of high pH values might be expected. Electrodes from glasses 20:10:70, 15:10:

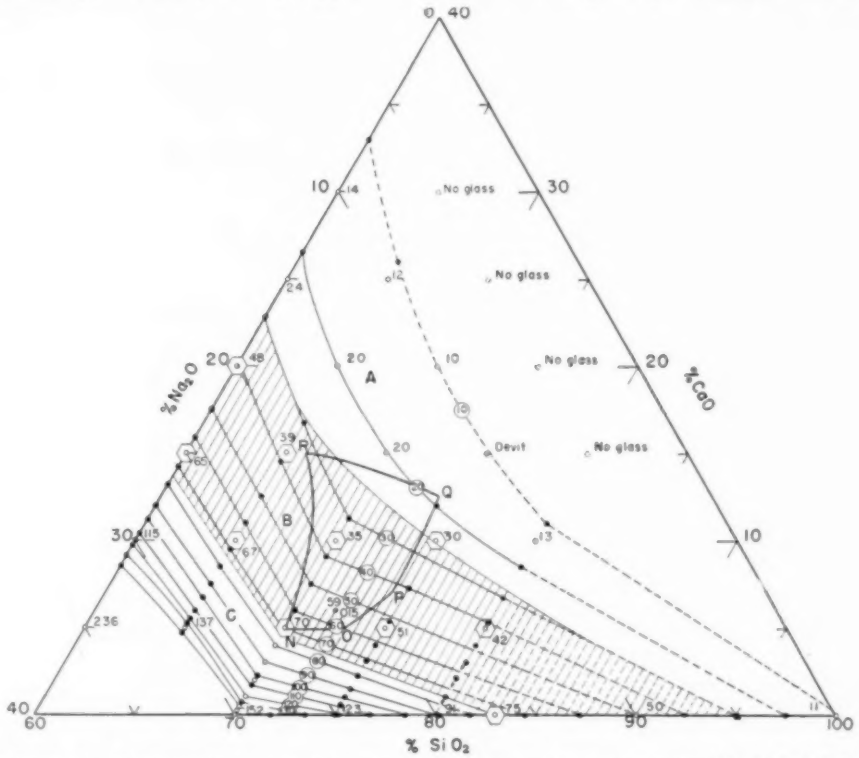

FIGURE 6. *Hygroscopicity-composition relation for glasses of the ternary system* Na_2O-CaO-SiO_2.

Shaded area indicates composition range over which electrodes were prepared approximating the theoretical pH response of 59 mv per pH.

871926—50——4

75, and 20:5:75 (table 1) are typical examples of compositions showing this negative departure at pH 11.9.

If the region N O P Q R of the Na_2O-CaO-SiO_2 phase diagram, which includes the compositions of the best commercial glasses obtainable from this ternary system [29], is superimposed upon figure 6, most of the factors controlling the practical composition limitations for glass electrode use can be seen at a glance. This area includes the composition range in which devitrite (Na_2O·3CaO·6SiO_2) is the primary phase. Glasses near the boundary RN are too readily attacked by water and buffer solutions except near R where devitrification causes trouble. Below the boundary NO, excessive hygroscopicity and poor chemical durability limit the usefulness of the glasses. Above RQ, devitrification, low hygroscopicity, and high melting temperatures interfere. To the right of O P Q, the area of adequate hygroscopicity is limited by devitrification and high melting temperatures.

A fairly comprehensive picture of the nature of the Na_2O-CaO-SiO_2 glasses can be obtained by plotting the voltage departure-hygroscopicity curve for 70 percent SiO_2, and comparing it with the accompanying chemical durability-hygroscopicity curve, figure 7. The resulting two curves illustrate the subtle relationship between glass electrode performance, hygroscopicity, chemical durability and composition. For instance, voltage departures appear for electrodes from glasses of low hygroscopicity and for electrodes from glasses of high hygroscopicity and poor chemical durability. The over-all picture also suggests that these voltage departures appear at the compositions at which the phase diagram indicates a shift in the primary phase [28, 29, 30]. To emphasize this point, the approximate positions at which the primary phases CaO·SiO_2, Na_2O·3CaO·6SiO_2, and Na_2O-2SiO_2 appear, are indicated on the graph. Perhaps the most interesting feature illustrated in figure 7 is the effect of small additions of CaO to the parent Na_2O-SiO_2 glass. The reversal from rapid solution to an even more rapid rate of swelling brought about by the addition of as little as 0.25 percent CaO suggests pertinent experiments concerning the effect of network-modifiers. [14, 27]. Any other families of glasses of constant SiO_2 content would give curves quantitatively different from, but qualitatively similar to figure 7. This is easy to visualize upon inspection of figure 1.

The performance (voltage departure), over an extended pH range of typical electrodes prepared from members of 70 percent SiO_2 series of glasses and the chemical durability of the individual glasses over the same pH range are plotted in figure 8. One point of interest in the electrode

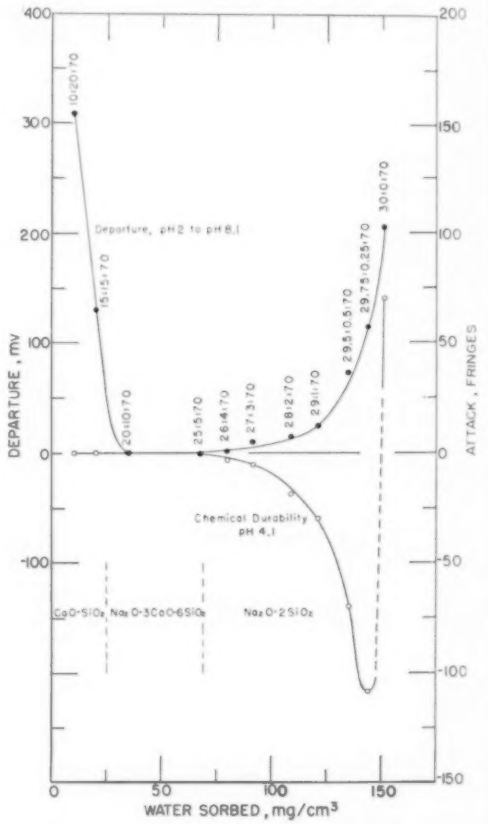

FIGURE 7. *Comparison of the chemical durability-hygroscopicity curve of* Na_2O-CaO-SiO_2 *glasses of 70% SiO_2 content.*

●, Voltage departure; ○, chemical durability.

performance is the steady improvement with increasing percentages of CaO to near 10 percent, followed by a sharp reversal for percentages above this value.

The voltage departure curves for these glasses of low hydroscopicity are plotted in figure 8 as broken lines to distinguish them from the curves of glasses having poor chemical durability. The

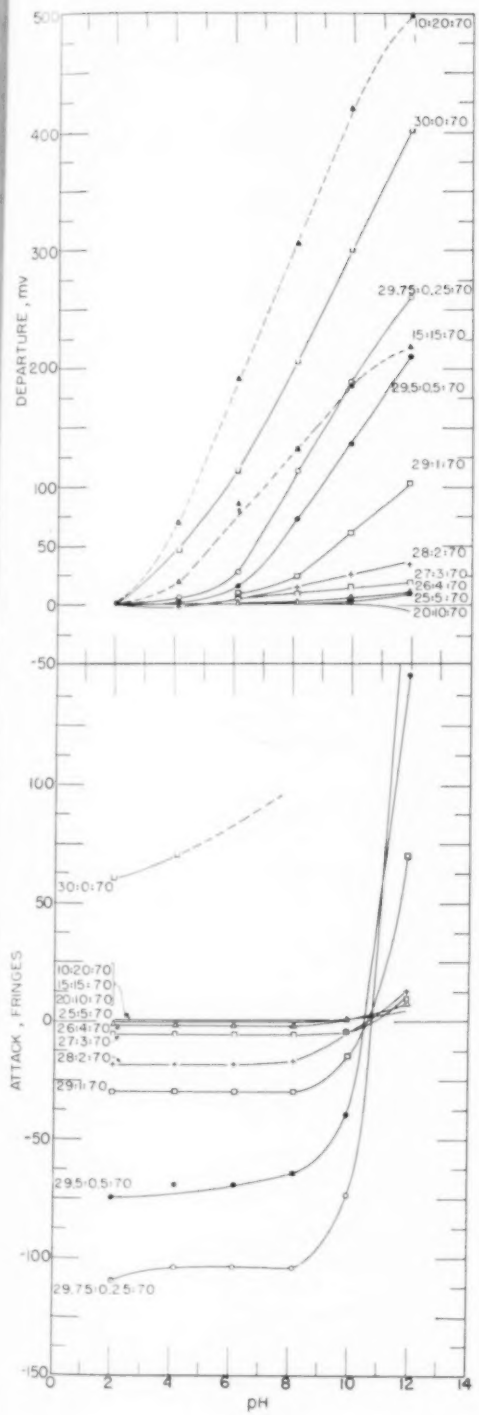

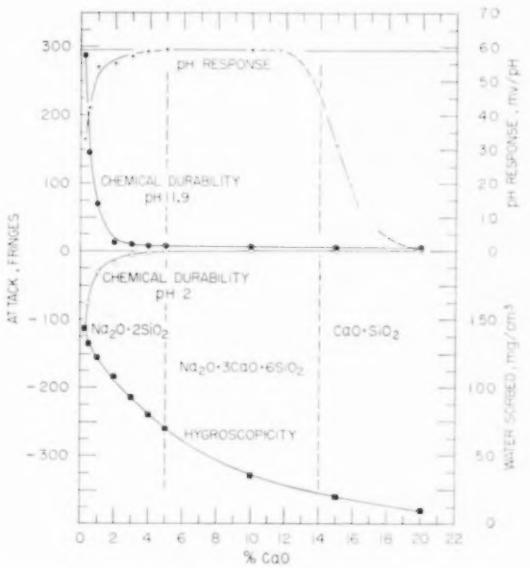

FIGURE 9. *Comparison of the* pH *response, the hygroscopicity, and chemical durability at* pH *2 and 11.9 of a series of* Na_2O-CaO-SiO_2 *glasses containing 70%* SiO_2.

The compositions at which a new primary phase appears in the equilibrium diagram are indicated by vertical dashed lines.

durability curves are of interest because of the exaggerated swelling in the acid range exhibited by members having low percentages of CaO.

The question always arises whether the chemical or physical properties of a series of glasses reflect any of the critical points of the corresponding phase equilibrium diagram [31]. To determine what evidence the present data offer on this subject, the properties of pH response, chemical durability at pH 2 and 11.9 and, hygroscopicity were plotted against the percentage of CaO for the glasses of the 70 percent SiO_2 series (fig. 9). The chemical durabilities at pH 2 and 11.9 were chosen because these curves departed in opposite directions, thereby emphasizing the composition at which a marked durability shift occurred. These chemical durability curves and the pH response curve superficially suggest the composition at which the primary phase changes from $Na_2O \cdot 2SiO_2$ to $Na_2O \cdot 3CaO \cdot 6SiO_2$. The evidence is

FIGURE 8. *Comparison of the chemical durability-*pH *curves with the voltage departure-*pH *curves for electrodes prepared from* Na_2O-CaO-SiO_2 *glasses containing 70%* SiO_2 *with the* Na_2O *progressively replaced by* CaO.

less convincing although not entirely lacking for the other boundary of the devitrite field at which $CaO \cdot SiO_2$ appears as the primary phase. The hygroscopicity curve cannot be offered as evidence, because of the experimental limitations imposed in obtaining the data.

IV. Summary

The pH response, hygroscopicity, and chemical durability of a series of Na_2O-CaO-SiO_2 glasses have been investigated. The results obtained re-emphasize the fact that glasses of inadequate hygroscopicity fail to yield electrodes that perform satisfactorily as indicators of the hydrogen ion activity of aqueous solutions at room temperatures. Many of the glasses exhibited swelling in the acid buffers, and all of them showed the usual attack in the alkaline range. For any family of glasses of constant percentage of SiO_2 the extent of swelling in the acid pH range decreased progressively with the replacement of Na_2O by CaO. For such glasses the chemical durability in alkaline solutions also improved.

The glasses of the Na_2O-CaO-SiO_2 series, which produced electrodes that most nearly approximated the theoretical straight-line relation of the Nernst equation, were those whose hygroscopicity and chemical durability characteristics most nearly approached the corresponding properties of the glass of the eutectic composition, 22 percent Na_2O, 6 percent CaO, 72 percent SiO_2 (Corning 015). In accordance with previous experience, all glasses of poor chemical durability failed to yield satisfactory electrodes for pH measurements.

V. References

[1] F. Haber and Z. Klemensiewicz, On electrical interfacial potentials, Z. physik. Chem. **67,** 385 (1909).

[2] W. S. Hughes, On Haber's glass cell, J. Chem. Soc. 491 (1928).

[3] D. A. MacInnes and M. Dole, The behavior of glass electrodes of different compositions, J. Am. Chem. Soc. **52,** 29 (1930).

[4] D. A. MacInnes and D. Belcher, Further studies on the glass electrode, J. Am. Chem. Soc. **53,** 3315 (1931).

[5] Malcolm Dole, The relation between the acitivity of the water and the potentials of the glass electrode, J. Am. Chem. Soc. **54,** 2120 (1932).

[6] Malcolm Dole, The theory of the glass electrode. II The glass as a water electrode, J. Am. Chem. Soc. **54,** 3095 (1936).

[7] Malcolm Dole, The glass electrode (John Wiley & Sons, Inc., New York, N. Y., 1941).

[8] Donald Hubbard, Hygroscopicity of optical glass as an indicator of serviceablility, J. Research NBS **36,** 365 (1946) RP1706.

[9] Donald Hubbard, Hygroscopicity and electrode function (pH response) of glasses as a measure of serviceability, J. Research NBS **36,** 511 (1946) RP17

[10] Donald Hubbard, Electrode function (pH response of potash-silica glasses, J. Research NBS **37,** (1946) RP1743.

[11] Donald Hubbard and Gerald F. Rynders, Effect annealing and other heat treatment on the response of the glass electrode, J. Research NB **40,** 105 (1948) RP1859.

[12] Gerald F. Rynders, Oscar Grauer, and Donald H bard, Electrode function (pH response) of the so silica glasses, J. Research NBS **41,** 273 (19 RP1923.

[13] Frederick R. Matson, The hygroscopicity of so lime-silica container glasses, J. Am. Ceram. S **32,** 121 (1949).

[14] M. K. Roman, E. C. Marboe, and W. A. Weyl, T influence of heavy metal ions on the hygroscopic of a glass surface, J. Soc. Glass Tech. **32,** 260 (19

[15] W. Nernst, Die elektromotorische Wirksamkeit Ionen, Z. physik. Chem. **4,** 129 (1889).

[16] Donald Hubbard, Edgar H. Hamilton, and Alfred Finn, Effect of the solubility of glass on the beha of the glass electrode, J. Research NBS **22,** (1939) RP1187.

[17] Malcolm Dole, R. M. Roberts, and C. E. Holley, Jr The theory of the glass electrode. V. The influe of negative ions, J. Am. Chem. Soc. **63,** 725 (19

[18] Donald Hubbard and Gerald F. Rynders, Volta anomalies of the glass electrode and the chemi durability of the glass, J. Research NBS **39,** (1947) RP1848.

[19] G. Buchböck, A property of the glass electrode, physik. Chem. **156-A,** 232 (1931).

[20] M. Dole, The theory of the glass electrode, J. A Chem. Soc. **53,** 4260 (1931).

[21] James W. McBain, The mechanism of the adsorp ("sorption") of hydrogen on carbon, Phil. Mag. **18,** 916 (1909); Z. physik. Chem. **68,** 471 (1909

[22] M. R. Thompson, A metal-connected glass electr BS J. Research **9,** 833 (1932) RP511.

[23] Relative durability of optical glass, NBS Tech. N Bul. **221,** 88 (Sept. 1935).

[24] E. Berger, Grundsätzliches über die chemis Angreifbarkeit von Glasen I, Glastech. Ber. **14,** 351 (1936).

[25] Donald Hubbard and Edgar H. Hamilton, Studies the chemical durability of glass by an interferome method, J. Research NBS **27,** 143 (1941) RP140

[26] Henry H. Carey and Warren P. Baxter, National Technical Laboratories, U. S. 2,383,709 (Aug. 1945).
[27] W. A. Weyl, Some practical aspects of the surface chemistry of glass. Glass Science (Pennsylvania State College, State College, Pa.).
[28] George W. Morey, The properties of glass, Am. Chem. Soc. Monograph No. 77 (Reinhold Publishing Corp., New York, N. Y., 1938).
[29] G. W. Morey and N. L. Bowen, The Ternary System Sodium Metasilicate-Calcium Metasilicate-Silica, J. Soc. Glass Tech. **9,** 232 (1925).
[30] F. P. Hall and Herbert Insley, Phase diagrams for ceramists, J. Am. Ceram. Soc. **30,** 11, Part II, p. 47 (1947).
[31] Norman J. Kreidl, Problems relating to glass structure, Ceramic Age **52** [5], 255 (1948).

Washington, October 4, 1949.

U. S. Department of Commerce
National Bureau of Standards

Research Paper RP2077
Volume 44, March 1950

Part of the Journal of Research of the National Bureau of Standards

Soil-Corrosion Studies, 1946 and 1948: Copper Alloys, Lead, and Zinc

By Irving A. Denison and Melvin Romanoff

This report contains the results of measurements of the corrosion of copper, lead and zinc, and certain alloys of these metals after exposure to different soil conditions for a maximum of 14 years. The soils to which the materials were exposed range from well-aerated soils deficient in soluble salts to very poorly aerated soils containing high concentrations of water-soluble materials. The magnitude and progress of corrosion with respect to weight loss and pitting are interpreted in relation to the composition of the materials and the properties of the soils at the test sites. Comparative data are given for the corrosion of plain iron and steel, copper, lead, and zinc in typical soil environments.

I. Introduction

The results of the first series of soil corrosion field tests conducted by this Bureau indicated that underground structures of cast iron, wrought iron, and steel could not be expected to withstand for long periods the corrosive action of many of the soils of the United States. Although certain types of installations, such as large-diameter pipe lines, can be protected from corrosion by bituminous coatings supplemented where necessary by cathodic protection, corrosion of certain other underground installations, such as distribution systems of small-diameter pipe, is more readily combatted by metals and alloys that are inherently resistant to corrosion. In order to obtain information on the corrosion resistance of materials otherwise suitable for underground construction, specimens of a variety of metals and alloys were installed at 14 test sites in 1932.

Sufficient specimens were buried to provide for removal of two specimens of each material after each of five periods of exposure. Accordingly, specimens were removed in 1934, 1937, 1939, 1941, and 1946, and returned to the laboratory for measurement of weight loss and maximum depth of pits. At the time of the removals in 1937 and in 1941, specimens of several alloys of lead and of zinc, and in 1939, specimens of arsenical brass, were buried at the same sites and at one additional site. Specimens of the latter materials were removed from each site at the subsequent removal dates and also in 1948. In this paper results are reported for exposures up to 14 yr for specimens of copper and copper alloys, for exposures up to 11 yr for specimens of lead and zinc, and for exposures up to 9 yr for specimens of arsenical brass. Corrosion data for the removals prior to 1946 have been published in a series of reports that were summarized by K. H. Logan [1],[1] by whom this investigation was initiated.

The results of corrosion tests of ferrous materials were described in the first report of this series [2]. Succeeding reports will deal with specimens of asbestos-cement, and those with metallic and nonmetallic protective coatings.

II. Properties of the Soils at the Test Sites

The test sites were selected not only to represent a wide range of corrosiveness, but also wide differences in the physical and chemical properties of soils. For example, the hydrogen-ion concentration of the soils ranges (table 1) from pH 2.6 to 9.4, and the resistivity from 62 to 17,800 ohm-cm. Differences in the composition of the water soluble material of the soils are also indicated in table 1. The salts contained in soil 64, Docas clay, for example, are seen to consist of sodium and

[1] Figures in brackets indicate the literature reference at the end of this paper

TABLE 1. *Properties of the soils at the test sites*

Soil		Location	Aeration [a]	Moisture equivalent	Apparent specific gravity	Resistivity at 60° F (15.6° C)	pH	Total acidity [b] (milligram equivalents per 100 g of soil)	Sulfide content [c]	Composition of water extract-milligram equivalent per 100 g of soil						
No.	Type									Na+K as Na	Ca	Mg	CO_3	HCO_3	Cl	SO_4
				Percent		*Ohm-cm*										
51	Acadia clay	Spindletop, Tex.	P	47.1	2.07	190	6.2	13.2	+	10.27	15.55	5.03	0.00	0.56	5.75	22.0
53	Cecil clay loam	Atlanta, Ga.	G	33.7	1.60	17,800	4.8	5.1	−							
55	Hagerstown loam	Loch Raven, Md.	G	32.0	1.49	5,210	5.8	10.9	−							
56	Lake Charles clay	El Vista, Tex.	VP	28.7	2.03	406	7.1	5.1	+	3.12	0.69	0.47	.00	.80	1.59	3.9
58	Muck	New Orleans, La.	P	57.8	1.43	712	4.8	15.0	++	2.03	2.23	1.29	.00	.00	0.47	2.3
59	Carlisle muck	Kalamazoo, Mich.	VP	43.6	....	1,660	5.6	12.6	+++	1.03	3.08	2.70	.00	.00	3.47	1.9
60	Rifle peat	Plymouth, Ohio	P	43.4	1.28	218	2.6	297.4	+++	2.91	10.95	2.86	.00	.00	0.00	56.7
61	Sharkey clay	New Orleans, La.	P	30.8	1.78	943	6.8	4.9	+	0.73	0.68	0.33	.00	.71	.10	0.6
62	Susquehanna clay	Meridian, Miss.	F	34.6	1.79	6,920	4.5	12.0	−							
63	Tidal marsh	Charleston, S. C.	VP	46.7	1.47	84	6.9	14.6	+++	33.60	6.85	4.00	.00	.00	12.70	36.9
64	Docas clay	Cholame, Calif.	P	41.1	1.88	62	7.5	A	−	28.10	2.29	0.76	.00	.80	28.80	0.2
65	Chino silt loam	Wilmington, Calif.	G	26.4	1.41	148	8.0	A	−	7.65	12.40	2.20	.00	1.30	6.05	16.9
66	Mohave fine gravelly loam.	Phoenix, Ariz.	F	16.5	1.79	232	8.0	A	−	6.55	0.51	0.18	.00	0.73	2.77	2.0
67	Cinders	Milwaukee, Wis.	VP	....	....	455	7.6	A	++	0.77	3.03	.53	.00	.55	0.08	2.8
70	Merced silt loam	Buttonwillow Calif.	F	24.7	1.69	278	9.4	A	−	8.38	0.38	.22	.02	1.87	1.12	5.2

[a] Aeration of soils: G, good; F, fair; P, poor; VP, very poor.
[b] A indicates absence of acidity because of alkaline reaction.
[c] −, Sulfides absent; +, sulfides present in low concentration; ++, sulfides present in moderate concentration: +++, sulfides present in high concentra

potassium chlorides; whereas, the salts in soil 60, Rifle peat, are sulfates of the alkalies and of the alkaline earth metals.

The retentiveness of the soils for moisture is indicated by values for the moisture equivalent, i. e., the quantity of water retained by a previously saturated soil subjected to a centrifugal force of 1,000 times the force of gravity.

Values for apparent specific gravity are presented as relative measures of the porosity of the soils. Because the real specific gravity of the mineral portion of soils varies within narrow limits, the apparent specific gravity indicates the compactness and, hence, porosity of soils that are primarily inorganic in nature.

III. Description of the Materials

The form, dimensions, and composition of the specimens of copper and copper alloys are given in table 2. Specimens of some materials were in the form of pipe, others of plate. The ends of the pipe specimens were closed by caps to exclude moisture, thereby preventing corrosion of the interior. An additional precaution was taken to prevent internal corrosion by coating the interna surface of the pipe specimens with a heavy grease. The exposed area of most of the specimens was approximately 0.3 ft.^{2} Microphotographs of the copper and copper alloys studied are shown in figures 1 and 2.

The compositions of the zinc and lead specimens are given in table 3. The composition of materia Z corresponds approximately to that of "high-grade" zinc slab. The die-casting zinc alloy C is substantially the same as ASTM alloy XXV The lead alloys contained copper, antimony, tellurium, or tin in various amounts to produce greater hardness and better mechanical properties than ordinary lead.

TABLE 2. *Composition of copper and copper alloys*

Material	Identification	Year buried	Form	External width or diameter	Length	Wall thickness	Density	Cu	Zn	Sn	Pb	Ni	Fe	Si	Mn	P	As
				in.	*in.*	*in.*	*lb/ft*³	%	%	%	%	%	%	%	%	%	%
Tough-pitch copper	*C*	1932	Pipe	1.7	12	0.145	555	99.9	....	....	....	....	....	....	....	....	....
Deoxidized copper	*A*	1932	do	1.7	13	.144	558	99.94	....	....	....	....	....	....	....	0.18	....
Copper with soldered fittings	*M*	1932	do	1.5	12	.062	....	....	....	....	....	....	....	....	....	....	....
Red brass	*F*	1932	do	1.7	12	.143	546	85.18	14.80	....	....	....	0.01	....	....	....	....
Admiralty metal	*H*	1932	do	1.7	12	.143	532	71.28	27.59	1.30	0.01	....	.02	....	....	....	....
Leaded-silicon brass	*K*	1932	do	1.7	12	.08	532	67.08	31.07	....	.84	....	Trace	1.01	....	....	....
Yellow brass	*J*	1932	do	1.7	13	.145	529	66.50	33.06	....	42	....	0.02	....	....	....	....
Muntz metal	*L*	1932	do	1.7	12	.08	524	60.06	39.58	....	.36	....	Trace	....	....	....	....
Muntz metal with arsenic	*B*	1939	Plate	2.5	12	.25	524	62.37	37.54	....	.005	....	0.007	....	....	....	0.08
Copper-silicon alloy	*E*	1932	Pipe	1.7	12	.141	548	97.15	....	1.80	....	....	.01	1.01	....	....	....
Do	*N*	1932	do	1.7	12	.145	546	98.11	....	0.14	....	0.01	.11	1.49	0.18	....	....
Do	*D*	1932	do	1.7	12	.143	532	95.46	....	....	....	.08	.21	3.19	1.06	....	....
Copper-nickel-zinc alloy	*G*	1932	do	1.7	12	.145	553	74.45	4.93	....	....	20.04	....	....	0.52	....	....

TABLE 3. *Composition of zinc and lead alloys*

Material	Identification	Year buried	Form	Nominal diameter or width	Length	Thickness	Density	Zn	Al	Cu	Fe	Pb	Sn	Bi	Sb	Cd	Te	Ca	Mg
								ZINC											
				in.	*in.*	*in.*	*lb/ft*³	%	%	%	%	%	%	%	%	%	%	%	%
Rolled zinc	Z	1937	plate	2.3	12	0.15	449	[a] 99.89	....	....	0.009	0.095	.....	.....	.....	0.0038	.....	.....	.....
Die-casting zinc	CZ	1937	do	4.4	6.8	.125	418	[a] 94.9	4.09	1.05	.018	< .003	<0.001	.....	.....	< .003	.....	.....	0.02 to .05
								LEAD											
Chemical lead	O	1937	pipe	1.5	12	0.177	709	.....	.....	0.056	.....	>99.94	None	0.002	0.0011	.....	.....	.....	.....
Tellurium lead	T	1937	do	1.5	12	.177	709	.....	.....	.082	.....	>99.87	None	None	.0011	.....	0.043	.....	.....
Antimonial lead	B	1937	do	1.5	12	.177	687	.....	.....	.036	.....	>94.64	None	0.016	5.31	.....	.....	.....	.....
Special lead alloy	[b] M	1941	do	1.25	15	.172	709	.....	.....	.....	.....	>99.7	0.25	....	.....	.....	....	0.02	0.02

[a] By difference.

[b] This material also contains the usual impurities found in lead.

IV. Copper and Copper-Silicon Alloys

1. Loss in Weight and Depth of Pitting

Prior to examination, the corroded specimens were cleaned by methods that have been previously described [1]. The extent of corrosion was measured by the loss in weight after exposure and by the depths of the deepest pits. These data are recorded in table 4. Unless indicated otherwise, each value is the average of measurements made on two specimens. Except as noted in table 4, the exposure periods at the different test sites did not differ by more than 5 percent.

The condition of specimens of tough pi copper after exposure at 14 test sites for 14 is illustrated in figure 3. Because of the shallo ness of many of the pits, the appearance of t specimens is somewhat deceptive in giving t impression that copper tends to corrode un formly. Actually, as will be seen later, copp exposed to soils shows the same general tende toward localized corrosion as is shown by ca iron, wrought iron, and steel.

The progress of corrosion with time for toug pitch copper C, deoxidized copper A, and copp silicon alloys D, E, and N is shown in figure 4

TABLE 4. *Loss in weight and depth of maximum penetration of copper and copper-silicon alloys*

(Average of two specimens)

Identification	Material	Average exposure	Test site number and soil type: 51 Acadia clay	53 Cecil clay loam	55 Hagerstown loam	56 Lake Charles clay	58 Muck	59 Carlisle muck	60 Riffle peat	61 Sharkey clay	62 Susquehanna clay	63 Tidal marsh	64 Docas clay	65 Chino silt loam	66 Mohave fine gravelly loam	67 Cinder
			LOSS IN WEIGHT (OUNCES PER SQUARE FOOT) [a]													
		Years														
		2.0	0.40	0.12	0.14	0.10	0.16	.....	1.47	[b] 0.06	0.16	1.13	1.41	1.71	0.28	3.98
		5.4	1.01	.15	.14	.51	1.56	0.12	3.82	.35	.26	2.45	2.22	[c] 1.02	[c] .75	9.33
A	Deoxidized copper	7.4	0.40	.20	.15	.80	1.72	[c] .11	1.10	.38	.38	4.25	3.00	[c] 2.37	[c] 1.32	4.89
		9.3	.....	.22	.18	.78	2.10	.11	5.01	.35	.48	4.22	5.32	0.24	[c] 0.62	11.30
		14.3	[d] .60	.24	.16	.89	2.39	[d] .21	11.97	.66	.52	6.57	5.17	1.07	.54	13.77
		2.0	.42	.12	[e] .14	.12	0.13	.....	1.37	[b] .09	.15	1.31	0.67	0.50	.11	3.13
		5.4	.91	.16	.19	.34	1.40	.13	4.68	.34	.26	2.99	.96	.47	.16	8.04
C	Tough-pitch copper	7.4	.35	.23	.17	.60	1.66	[c] .09	1.03	.37	.33	4.33	1.56	.55	.32	1.42
		9.3	.....	.24	.20	.71	1.95	.12	7.26	.33	.36	4.46	2.80	.26	.45	9.81
		14.3	[d] .46	.23	.16	.61	1.98	[d] .19	[c] 14.66	.58	.49	8.31	1.04	.47	.27	6.71
		2.0	.35	.19	.14	.16	0.11	.....	1.57	[b] .14	.25	1.45	1.32	1.03	.22	5.37
		5.4	1.02	.24	.28	.32	1.36	.22	4.13	.42	.40	4.37	2.10	0.53	[c] .67	15.51
N	Copper-silicon alloy	7.4	0.48	.38	.23	.40	1.70	[c] .14	1.06	.38	.42	4.57	1.74	2.42	.55	1.99
		9.3	.....	.30	.30	.62	1.97	[c] .24	[c] 3.96	.48	.57	6.96	4.87	0.62	[c] .51	22.31
		14.3	.53	.51	.38	.60	2.80	[d] .26	10.65	.77	.54	8.30	4.59	.66	.53	9.46
		2.0	.....	.....	.....	.14	.....	.....	0.79	[b] .12	.15	1.98	1.48	1.23	.14	5.90
		5.4	.....	.21	.....	.....	.....	.26	.....	.24	.....	.....	1.38	.....	.....	.....
[f] N_1	Copper-silicon alloy	7.4	.....	.25	.....	.....	1.56	.....	.....	.....	.....	.....	.....	2.74	.....	.....
		9.3	.....	.....	.....	.....	.....	.....	1.82	.....	.....	.....	.....	.....	.34	23.17
		14.3	.....	.....	.29	.55	.....	.20	.....	.....	.44	6.84	.....	.....	.....	.....
		2.0	.51	.24	.29	.23	0.19	.....	1.61	[b] .19	.33	1.16	0.79	0.48	.38	3.25
		5.4	1.04	.28	.29	.48	1.64	.28	3.76	.51	.61	1.93	1.26	.72	.51	5.63
E	Copper-silicon alloy	7.4	0.97	.38	.24	.60	1.67	[c] .23	1.03	.65	.52	3.53	1.44	1.17	1.22	1.47
		9.3	.....	.37	.35	.76	2.11	.17	[c] 3.22	.61	.69	[c] 4.38	2.30	0.96	[c] 1.53	8.76
		14.3	[d] 1.40	.45	.26	.70	2.73	[d] .31	9.32	.87	.70	4.84	2.82	1.42	1.82	8.49
		2.0	0.45	.18	.15	.10	0.11	.....	1.33	[b] .13	.24	1.23	0.67	1.10	0.21	4.23
		5.4	1.07	.25	.20	.35	1.70	.10	3.32	.52	.42	2.64	1.14	[c] 0.62	[c] .53	20.95
D	Copper-silicon alloy	7.4	0.41	.39	.28	.52	1.75	[c] .18	0.72	.61	.50	4.86	1.43	[c] 1.28	.40	2.69
		9.3	.....	.36	.28	.63	2.12	.15	4.46	.52	.60	5.32	2.88	0.48	.55	13.47
		14.3	[d] .55	.48	.24	.77	2.49	[d] .21	9.74	.88	.66	5.16	2.81	1.24	.45	17.34

See footnotes at end of table.

TABLE 4. *Loss in weight and depth of maximum penetration of copper and copper-silicon alloys*—Continued

(Average of two specimens)

Identification	Material	Average exposure	Test site number and soil type													
			51	53	55	56	58	59	60	61	62	63	64	65	66	67
			Acadia clay	Ceeil clay loam	Hagerstown loam	Lake Charles clay	Muck	Carlisle muck	Rifle peat	Sharkey clay	Susquehanna clay	Tidal marsh	Docas clay	Chino silt loam	Mohave fine gravelly loam	Cinders
			MAXIMUM PENETRATION (MILS)													
		Years														
A	Deoxidized copper	2.0	[a] M	<6	<6	M	M	.....	7	[b] <6	<6	M	<6	<6	6	38
		5.4	<6	7	<6	<6	12	<6	28	[c] 23	9	M	9	10	7	54
		7.4	<6	10	<6	<6	10	<6	8	8	14	8	<6	18	8	44
		9.3	.....	<6	<6	<6	[c] 14	<6	38	8	8	10	[c] 16	<6	10	88
		14.3	[d] <6	8	<6	<6	19	[d] 6	48	24	10	10	10	9	10	64
C	Tough-pitch copper	2.0	M	M	[a] <6	M	<6	.....	<6	[b] <6	<6	<6	7	<6	<6	26
		5.4	<6	<6	6	<6	12	6	33	[c] 15	6	<6	8	9	<6	56
		7.4	<6	11	7	8	14	6	9	16	6	7	14	20	<6	24
		9.3	.....	6	8	<6	10	<6	40	8	8	6	[c] 14	10	<6	51
		14.3	[d] <6	6	<6	<6	16	[d] 6	46	20	10	14	14	12	<6	42
N	Copper-silicon alloy	2.0	M	<6	<6	<6	M	.....	7	[b] <6	<6	<6	10	6	15	46
		5.4	<6	6	8	<6	7	<6	17	11	<6	<6	10	16	[a] 18	80
		7.4	<6	<6	6	<6	9	<6	<6	11	6	6	12	20	14	31
		9.3	.....	<6	<6	<6	12	M	10	10	<6	12	21	20	13	[b] 145+
		14.3	[d] <6	6	7	<6	15	[d] <6	24	17	6	16	16	12	10	42
[e] N_1	Copper-silicon alloy	2.0	.....	.....	.....	<6	.....	.....	7	[b] <6	<6	<6	10	15	M	40
		5.4	.....	<6	.....	.....	.....	<6	.....	<6	.....	.....	12	.....	.....	.....
		7.4	.....	9	.....	.....	16	.....	.....	.....	.....	.....	.....	24	.....	.....
		9.3	.....	.....	.....	.....	.....	.....	8	.....	.....	.....	.....	.....	<6	90
		14.3	.....	.....	7	<6	.....	11	.....	.....	8	11	.....	.....	.....	.....
E	Copper-silicon alloy	2.0	<6	12	13	12	11	.....	24	[b] <6	14	16	20	23	12	38
		5.4	8	14	16	9	33	11	22	26	15	<6	19	21	16	49
		7.4	6	14	15	12	33	6	12	35	<6	14	12	33	15	33
		9.3	.....	12	20	12	53	20	18	[c] 37	22	10	34	22	22	102
		14.3	[d] 15	20	20	12	54	[d] 16	35	42	23	11	22	23	21	78
D	Copper-silicon alloy	2.0	M	<6	7	M	M	.....	<6	[b] M	6	<6	19	<6	<6	34
		5.4	11	10	10	M	8	M	15	7	10	<6	11	11	[c] 12	90
		7.4	<6	<6	10	7	12	<6	<6	6	12	13	12	14	16	28
		9.3	.....	8	8	M	12	<6	21	<6	6	9	[c] 16	11	9	80
		14.3	[d] <6	8	10	<6	16	[d] <6	28	13	10	10	24	13	10	74

[a] Each ounce per square foot corresponds to an average penetration of 0.0014 inch.

[b] Exposed for 1.0 yr only.

[c] Data for the individual specimens differed from the average by more than 50%.

[d] Data for 4 specimens.

[e] Data for only 1 specimen—the other specimen was missing.

[f] These specimens had welded joints—data for only 1 specimen.

[g] M, shallow metal attack, roughening of the surface, but no definite pitting.

[h] +, both specimens contained holes because of corrosion.

In preparing the curves shown in this figure, values for average penetration, calculated from the data for weight loss given in table 4,[2] and for maximum penetration were plotted against the corresponding periods of exposure.

The curves for average penetration indicate that except in soils 60 and 63, which are high in sulfides, and occasionally in other soils, the deoxidized copper A and the copper-silicon alloys D, E, and N, corroded at somewhat higher rates than the tough-pitch copper C.

Unlike the curves for average penetration, the pit depth-time curves for a number of the soils indicate that the deoxidized copper A and the copper-silicon alloys D and N did not pit any deeper than the tough-pitch copper C. In fact, only in soil 66 was tough-pitch copper significantly

[2] Average penetration (mils) = weight loss $\frac{(\text{oz/ft}^2)\times 750}{\text{density (lb/ft}^3)}$.
See tables 2 and 3 for the densities of the materials.

more resistant to pitting than the other materials. In all soils except 60 and 63, the copper-silicon alloy E pitted considerably more than tough pitch copper.

V. Copper-Zinc and Copper-Nickel-Zinc Alloys

1. Loss in Weight and Depth of Pitting

The results of the corrosion tests of the copper-zinc alloys and of a single copper-nickel-zinc alloy are given in table 5. Materials H, J, K, and L were corroded in part by dezincification in certain of the soils, and some of the values for weight loss of these materials necessarily include some loss from this form of corrosion. However, as the corrosion product of spongy copper was not removed in measuring pits on dezincified areas the values of maximum penetration given in the table are not affected by dezincification.

TABLE 5. *Loss in weight and depth of maximum penetration of copper-zinc alloys and copper-nickel-zinc alloy*

[Average of two specimens]

Identification	Material	Average exposure	Test site number and soil type														
			51	53	55	56	58	59	60	61	62	63	64	65	66	67	70
			Acadia clay	Cecil clay loam	Hagerstown loam	Lake Charles clay	Muck	Carlisle muck	Rifle peat	Sharkey clay	Susquehanna clay	Tidal marsh	Docas clay	Chino silt loam	Mohave fine gravelly loam	Cinders	Merced silt loam
			LOSS IN WEIGHT (OUNCES PER SQUARE FOOT) [a]														
		Years															
		2.0	0.42	0.12	0.14	0.12	0.13	.....	1.37	[b] 0.09	0.15	1.31	0.67	0.50	0.11	3.15	.....
		5.4	.91	.16	.19	.34	1.40	0.13	4.68	.34	.26	2.99	.96	.47	.16	8.04	.....
C	Tough-pitch copper	7.4	.35	.23	.17	.60	1.66	[c] .09	1.03	.37	.33	4.33	1.56	.55	.32	1.42	.....
		9.3	.....	.24	.20	.71	1.95	.12	7.26	.33	.36	4.46	2.80	.26	.45	9.84	.....
		14.3	[d] .46	.23	.16	.61	1.98	[d] .19	[e] 14.66	.58	.49	8.31	1.04	.47	.27	6.71	.....
		2.0	.33	.12	.13	.11	0.12	.....	1.47	.11	.15	0.55	0.33	.52	.18	3.36	.....
		5.4	.97	.16	.22	.34	1.44	.17	4.11	.38	.27	.54	.33	.27	.32	12.95	.....
F	Red brass	7.4	.45	.25	.16	.64	1.43	[c] .12	0.80	.49	.39	1.10	.52	.58	.48	2.37	.....
		9.3	.....	.25	.25	.70	2.06	.12	3.55	.41	.43	0.75	[c] 1.12	.28	.77	8.46	.....
		14.3	[d] .61	.28	.18	.65	2.46	[d] .24	[e] 13.04	.69	.43	[c] 1.88	0.78	.60	.63	18.73	.....
		2.0	.28	.12	.12	.07	0.15	.....	1.38	[b] .12	.18	0.64	.08	.17	.20	2.08	.....
		5.4	.88	.14	.20	.33	[c] 1.35	.14	3.64	.33	.31	2.89	.10	.29	.37	2.87	.....
G	Copper-nickel-zinc alloy	7.4	.45	.29	.15	.56	1.22	[c] .08	0.92	.69	.44	2.85	.27	.43	.38	1.25	.....
		9.3	.....	.27	.20	.78	1.40	.09	3.61	.43	.47	3.55	[c] .74	.44	[c] .60	6.28	.....
		14.3	[d] .58	.39	.18	.68	1.70	[d] .17	10.23	.94	.60	5.61	.59	.54	.54	3.55	.....
		2.0	.32	.14	.15	.08	0.19	.....	1.13	[b] .17	.20	0.25	.02	.31	.23	5.55	.....
		5.4	1.07	.21	.25	.29	2.16	.10	3.56	.60	.36	.11	.24	.34	.43	14.71	.....
H	Admiralty metal	7.4	0.57	.29	.23	.46	1.87	.10	1.16	.77	.43	.18	.40	.87	.44	2.96	.....
		9.3	.....	.29	.25	.57	2.09	.09	[c] 2.85	.51	.53	.18	.98	.58	.80	8.27	.....
		14.3	[d] .73	.35	.24	.64	2.91	[d] .16	[c] 8.98	1.18	.62	.22	.73	.78	.79	17.15	.....
		2.0	.17	.25	.20	.16	0.25	.....	1.14	[b] 0.11	.29	.47	.24	.14	.25	6.85	.....
		5.4	.36	.33	.25	.32	1.10	.15	2.97	.56	.55	.15	.21	[c] 1.00	[c] .82	[f] D	.....
K	Leaded silicon brass	7.4	.59	.48	.27	.48	1.59	[c] .10	0.85	.61	.55	.35	.80	1.03	[c] 1.24	D	.....
		9.3	.....	.47	.36	.89	[c] 1.66	.20	[c] 3.22	.87	.71	[c] .52	[c] 1.07	1.39	0.95	D	.....
		14.3	[d] .48	.58	.37	.76	3.76	[d] .24	[c] 12.30	1.89	.71	.51	0.68	1.50	.84	D	.....
		2.0	.33	.10	.18	.08	0.21	.....	1.71	[b] 0.11	.22	.04	.57	1.37	.35	16.56	.....
		5.4	1.41	.22	.34	.38	1.52	.01	5.14	1.00	.55	.02	1.31	1.17	.92	D	.....
J	Yellow brass	7.4	0.79	.42	.37	.74	2.20	.01	1.52	1.35	.51	.07	2.11	3.10	.88	D	.....
		9.3	.....	.41	.30	.94	3.33	.03	[c] 4.21	1.22	.94	.08	1.94	1.60	[c] 1.16	D	.....
		14.3	[d] 1.23	.51	.39	.91	3.98	[d] .02	[c] 27.30	2.42	.75	.08	1.66	2.52	0.96	D	.....
		2.0	0.68	.19	.19	.14	0.20	.....	1.73	[b] 0.16	.33	.14	4.02	2.43	.63	D	.....
		5.4	1.45	.30	[c] .58	.46	3.47	.02	4.42	1.75	1.20	.06	6.91	1.56	1.68	D	.....
L	Muntz metal	7.4	1.04	.61	.66	.71	4.61	.02	1.43	2.97	1.08	.09	9.79	3.38	1.50	D	.....
		9.3	.....	.52	.77	1.21	5.25	.03	[c] 4.56	2.58	1.79	.10	11.53	1.45	1.41	D	.....
		14.3	[d] 1.19	.62	.65	1.43	4.83	[d] .03	[c] 20.43	4.21	1.10	.09	15.38	1.73	2.06	D	.....

See footnotes at end of table.

TABLE 5. *Loss in weight and depth of maximum penetration of copper-zinc alloys and copper-nickel-zinc alloy*—Continued

(Average of two specimens)

Identification	Material	Average exposure	Test site number and soil type														
			51	53	55	56	58	59	60	61	62	63	64	65	66	67	70
			Acadia clay	Cecil clay loam	Hagerstown loam	Lake Charles clay	Muck	Carlisle muck	Rifle peat	Sharkey clay	Susquehanna clay	Tidal marsh	Docas clay	Chino silt loam	Mohave fine gravelly loam	Cinders	Merced silt loam
			LOSS OF WEIGHT (OUNCES PER SQUARE FOOT)—Continued														
B	Muntz metal with arsenic.	*Years*															
		2.1	.....	0.18	0.16	0.55	0.54	0.30	1.87	0.40	0.32	0.04	0.47	0.21	0.30	15.2	0.28
		7.0	[a] 0.77	.75	.32	1.12	1.55	1.09	3.46	1.61	.96	.06	.46	.69	.38	26.3	.23
		9.0	.....	.74	.42	0.74	1.38	1.32	4.89	[a] 0.82	.92	.05	1.11	.46	.39	16.54	.42
			MAXIMUM PENETRATION (Mils)														
C	Tough pitch copper	2.0	[b] M	M	<6	M	<6	.....	<6	[b] <6	<6	<6	7	<6	<6	26	.....
		5.0	<6	<6	6	<6	12	6	33	[a] 15	6	6	8	9	<6	56	.....
		7.4	<6	11	7	8	14	6	9	16	6	7	14	20	<6	24	.....
		9.3	.....	6	8	<6	10	<6	40	8	8	6	[c] 14	10	<6	51	.....
		14.3	[d] <6	6	<6	<6	16	[d] 6	46	20	10	14	14	12	<6	42	.....
F	Red brass	2.0	M	6	11	M	M	.....	9	[b] <6	8	<6	13	6	<6	29	.....
		5.4	8	8	11	<6	9	<6	24	[c] 17	17	<6	<6	13	8	56	.....
		7.4	<6	12	11	<6	<6	8	6	20	12	10	8	12	14	32	.....
		9.3	.....	10	7	<6	10	M	34	7	14	6	[c] 26	<6	<6	[c] 54	.....
		14.3	[d] <6	15	8	<6	9	[d] 6	42	32	12	[a] 18	18	16	<6	62	.....
G	Copper-nickel zinc alloy	2.0	M	<6	6	M	[a] 8	.....	10	[b] <6	<6	<6	<6	<6	M	24	.....
		5.4	<6	<6	9	M	9	<6	32	[c] 14	15	11	6	<6	8	29	.....
		7.4	<6	<6	<6	<6	8	<6	11	21	12	<6	13	10	<6	26	.....
		9.3	.....	8	6	<6	<6	<6	32	<6	12	<6	18	<6	<6	36	.....
		14.3	[d] <6	10	6	<6	7	[d] <6	44	18	15	10	11	<6	10	34	.....
H	Admiralty metal	2.0	M	8	20	M	<6	.....	6	[d] 6	15	M	14	30	M	50	.....
		5.4	<6	13	35	M	29	M	25	32	19	<6	6	9	25	88	.....
		7.4	8	21	20	<6	37	8	14	36	26	<6	<6	31	[c] 56	47	.....
		9.3	.....	20	20	<6	26	<6	16	[c] 35	24	<6	[c] 46	13	<6	68	.....
		14.3	[d] <6	17	17	<6	35	[d] <6	34	48	26	<6	26	12	31	86	.....
K	Leaded silicon brass	2.0	M	M	M	M	M	.....	<6	[b] <6	<6	M	M	M	M	41	.....
		5.4	7	<6	<6	M	<6	M	15	<6	9	<6	<6	8	<6	D	.....
		7.4	<6	<6	6	<6	12	6	<6	<6	12	<6	10	6	7	D	.....
		9.3	.....	<6	7	<6	[c] <6	<6	[c] 12	6	<6	<6	[c] 15	<6	<6	D	.....
		14.3	[d] <6	<6	7	<6	<6	[d] <6	32	6	<6	<6	18	8	6	D	.....
J	Yellow brass	2.0	M	6	10	M	M	.....	14	[b] 6	<6	<6	<6	M	M	D	.....
		5.4	12	11	10	<6	<6	<6	35	16	15	<6	17	16	9	D	.....
		7.4	9	9	8	6	13	<6	14	9	14	<6	24	20	18	D	.....
		9.3	.....	6	10	<6	8	M	[c] 33	6	13	M	20	18	8	D	.....
		14.3	[d] 8	<6	6	<6	7	[d] <6	[c] 104	22	<7	<6	10	10	8	D	.....
L	Muntz metal	2.0	M	<6	6	M	<6	.....	9	[b] <6	<6	M	<6	M	<6	D	.....
		5.4	7	6	<6	M	10	<6	34	13	8	<6	16	M	8	D	.....
		7.4	<6	6	6	<6	8	<6	8	20	6	<6	6	12	6	D	.....
		9.3	.....	6	6	<6	6	<6	[c] 27	12	<6	<6	6	<6	<6	D	.....
		14.3	[d] <6	8	<6	10	<6	[d] <6	55+	20	<6	<6	6	7	9	D	.....
B	Muntz metalwith arsenic	2.1	.....	<6	<6	12	6	<6	13	<6	<6	<6	<6	<6	8	122	12
		7.0	[a] 8	7	6	6	6	6	20	8	6	6	13	10	6	150	6
		9.0	.....	6	6	8	<6	<6	8	[a] 8	9	<6	19	<6	8	120	6

[a] Each ounce per square foot corresponds to an average penetration of 0.0014 in.
[b] Exposed for 1.0 yr only.
[c] Data for the individual specimens differed from the average by more than 50%.
[d] Data for 4 specimens.
[e] Data for only 1 specimen. The other specimen was missing.
[f] D, specimens destroyed by dezincification.
[g] Data for 10 specimens.
[h] M, shallow metal attack, roughening of the surface, but no definite pitting.

Because the porous deposit produced by dezincification is the product of one process of corrosion, complete evaluation of the condition of a corroded specimen in terms of weight loss and pitting necessarily entails removal of the dezincified corrosion product.[3] However, in the present study, it was desired to distinguish between weight loss and pitting due to dezincification, and that resulting from other corrosion processes. Consequently, in order to exclude from present consideration the corrosion that resulted from dezincification, weight loss data for materials appreciably affected by dezincification were not used in plotting the average penetration-time curves shown in figure 5. For comparison with the corrosion of copper, the corrosion-time curves for tough-pitch copper C are included in the figure.

A progressive increase in average penetration with increasing zinc content is indicated by the curves, except for the soils high in sulfides. In those sulfide soils (59 and 63), which are continuously saturated throughout the year, the average penetration tends to increase inversely with the zinc content. This tendency is also indicated by the data for soil 60; but because of seasonal drying and consequent oxidation of sulfides to sulfates, this trend is not so pronounced. The relatively high resistance of the high-zinc brasses to corrosion by sulfur compounds in other environments has been previously observed [3]. It should be noted that the high values for materials J and L for the final period, which indicate a departure from the inverse order, are unaffected by dezincification. As will be seen later, this form of corrosion was not observed in any of the soils high in sulfides.

The pit depth-time curves shown in figure 5 do not indicate any correlation between maximum penetration and zinc content. Instead of showing greater resistance to pitting than any of the copper-zinc alloys, as might have been predicted from the average penetration-time curves, tough-pitch copper C and red brass F occupy an intermediate position in all soils with the exception of soils 51, 56, and 66, in which they are as resistant as any of the other materials. It is surprising that the alloys that showed the maximum and minimum tendency toward pitting, namely material H (67.08% of Cu, 31.07% of Zn, 1.01% of Si, and 0.84% of Pb) and material K (71.28% of Cu, 27.39% of Zn, and 1.30% of Sn) should differ so little in composition.

[3] Methods for removal of products of dezincification without loss of uncorroded metal are currently under investigation.

2. Dezincification

Although the extent of dezincification of the materials subject to this form of corrosion was indicated qualitatively in earlier progress reports, measurements of dezincification have not previously been made in the course of this investigation. In the present study, the depth of dezincification was measured in the following manner. The specimens were first cut longitudinally and examined for evidence of dezincification. They were then cut into transverse sections so that the areas having the maximum depth of dezincification could be located. Measurements of the depth of dezincification were made independently by two observers with the aid of magnifying lenses and were recorded as percentage of the wall thickness, after which the measurements were converted into mils. In order to check the accuracy of this procedure, the depth of dezincification was measured directly on photographs of transverse sections enlarged 15 magnifications. Agreement between the two methods was excellent.

The form and depth of dezincification on materials B, H, K, J, and L are shown in table 6. The specimens of red brass F, and copper-nickel-zinc alloy G did not dezincify in any of the soils. A tranverse section of a typical dezincified area of a Muntz metal specimen removed from Sharkey clay (soil 61) is shown in figure 6.

The microstructures of a partially dezincified section of a leaded silicon brass specimen removed from the same soil is shown in figure 7.

From the extent of dezincification indicated by the data of table 6, it is evident that the values of weight loss and maximum penetration given in table 5 may be entirely misleading as measures of the extent of deterioration of these materials. On the basis of the values for weight loss and maximum penetration, one might conclude that a certain low-copper alloy is highly resistant to corrosion; whereas data for dezincification might indicate actual failure. If, for example, only the values for average and maximum penetration tabulated below are considered, one would conclude that

TABLE 6. *Maximum depth of dezincification on brasses exposed for 14 years* [a]

+, one or both specimens dezincified through wall thickness of pipe.
P, plug type of dezincification.
U, uniform type of dezincification.

Soil No.	Admiralty metal		Leaded silicon brass		Yellow brass		Muntz metal		Muntz metal with arsenic	
	71.28% Cu 27.39% Zn 1.30% Sn		67.09% Cu 31.07% Zn 0.84% Pb 1.01% Si		66.50% Cu 33.06% Zn 0.42% Pb		60.09% Cu 39.58% Zn 0.30% Pb		62.37% Cu 37.54% Zn 0.08% As	
	H		K		J		L		B [b]	
	Maximum depth	Type	Maximum depth	Type	Maximum depth	Type	Maximum depth	Type	Maximum depth	Type
			Mils		*Mils*		*Mils*		*Mils*	
51	0	.....	[c] 60+	U	38	P	73+	U	0	.....
53	0	.....	6	U	18	U	0	.....	0	.....
55	0	.....	[d] 10	U	0	.....	0	.....	0	.....
56	0	.....	0	.....	[d] 14	P	68	U	0	.....
58	0	.....	48+	U	66	U	80+	U	0	.....
59	0	.....	0	.....	0	.....	0	.....	0	.....
60	0	.....	0	.....	0	.....	0	.....	0	.....
61	0	.....	80+	U	80	P	32	U	0	.....
62	0	.....	28	U	22	P	4	U	0	.....
63	0	.....	0	.....	0	.....	0	.....	0	.....
64	[d] 22	U	28	P	80	U	80+	U	0	.....
65	7	P	80+	U	76	U	80+	U	0	.....
66	[d] 72+	P	[d] 40+	U	26	U	72+	U	0	.....
67	0	.....	80+	U	145+	U	80+	U	[e] 0	.....
70	.....	.....	.....	.....	.....	.....	.....	.....	0	.....

[a] Average for 2 specimens except in soils 51 and 59, which represent the average for 4 specimens.
[b] The arsenical Muntz metal specimens (B) were exposed for 9 yr.
[c] Average of 3 specimens. The other specimen was unaffected by dezincification.
[d] Only one specimen affected by dezincification. The other specimen was unaffected.
[e] Intergranular corrosion.

materials H and K are equally resistant to corrosion in soil 51. However, when dezincification is

Material	Penetration		Depth of dezincification
	Average	Maximum	
	Mils	*Mils*	*Mils*
H	1.0	6	0
K	0.7	6	60+
J	1.7	8	38
L	1.7	6	73+

considered, it is evident that the values for penetration define accurately the condition of material H only, because material K has been entirely dezincified. Similarly, the condition of materials J and L is indicated more accurately by the data for dezincification than for penetration.

Dezincification of the two-phase copper-zinc alloys, K and L, and the single-phase copper-zinc alloy, J, was fairly general, the specimens of these alloys being dezincified to some extent in most of the soils (table 6). The much greater dezincification of these alloys than of the single-phase alloy, H, was, of course, to be expected. Although the surface of the specimens of the arsenic bearing 60–40 brass B, showed incipient dezincification after exposure for 2 yr, careful examination of the specimens of this material exposed for 7 and for 9 yr indicated that this effect was entirely superficial.

Arsenical brasses normally exhibit good resistance to dezincification, but occasionally they undergo intergranular corrosion in environments other than soils [3]. Specimens of arsenic-bearing brass B were carefully examined after exposure, and only in those that had been exposed to cinders at site 67 was intergranular corrosion observed (fig. 8).

Superficial dezincification of arsenical brass B, red brass F, and of the copper-zinc-nickel alloy G

was reported in an earlier publication [1] to have been observed on specimens of these materials from all of the soils except 59 and 63. However, as the surfaces so affected have shown no tendency to increase in depth with time, it is questionable whether the term dezincification should be applied to what is, in effect, mere surface discoloration.

It is evident that dezincification of brasses in soils is influenced not only by alloy composition, but by the nature of the environment as well. The occurrence and intensity of dezincification appear to be largely independent of the corrosiveness of the soils as measured by weight loss and depth of pits. For example, in the corrosive Rifle peat, soil 60, materials H, K, J, and L showed no evidence of dezincification. The fact that dezincification did not occur in this and in other soils high in sulfides, 59 and 63, shows that sulfides in high concentration act as inhibitors of dezincification.

VI. Soldered and Welded Joints in Copper

Because lead-tin solders are anodic to copper, it is necessary to consider the possibility of galvanic corrosion of the solder when soldered joints are used in underground construction. Hiers [4] has reported that serious galvanic action between lead-tin solders and copper pipe may take place in sea water. During the soldering operation a copper-tin alloy cathodic to copper may be formed, providing thereby a source of galvanic corrosion of the copper [5].

For study of the galvanic action between copper and solder in soils, short sections of copper tubing were connected by means of standard sweated joints and soldered with 50–50 lead-tin solder. The joint consisted of two 6-in. sections of tubing 1¼ in. in diameter joined by a coupling 2¼ in. in length. Streamlined caps were used to close the exposed ends. The solder was applied to the sweat fittings through one hole in each cap and two holes in the coupling.

Inspection of the soldered specimens from the 14 test sites after exposure for periods ranging up to 14 yr showed no indication of galvanic corrosion of the solder. Neither was there evidence that corrosion had penetrated into the solder to an appreciable extent. In practically all of the soils to which the specimens were exposed, a dense hard coating or film of white corrosion products covered the entire surface of the exposed solder, which was thereby protected from further corrosion. These results are in agreement with those reported by Crampton [3] of tests of sweated joints made with various commercial solders when exposed for 2 yr to a saline solution maintained at 60° C. The results also agree with those obtained by Tracy [6] in 6-yr tests to determine the effect of hot circulating water, with and without carbon dioxide, on solders of different compositions.

An additional source of galvanic corrosion of copper arises from the possibility that oxides formed in welding operations may impart to the weld a potential that is cathodic to a pickled copper surface. Specimens for study of the effect of welds on corrosion were prepared by joining two 6-in. lengths of copper pipe, 1.5 in. in diameter, by means of a circumferential arc weld. The welding rod was of the same nominal composition as the pipe. Neither the depths of the maximum pits nor the distribution of corrosion on the welded specimens after exposure for 14 yr (material N, table 4) gave any indication of accelerated corrosion in the vicinity of the weld.

VII. Effect of Environment on the Corrosion of Copper

The corrosion-time curves for copper and for the copper-silicon alloys that were used to study the effect of alloy composition on corrosion (fig. 4) indicate wide differences not only in the corrosiveness of the soils, but also in the progress of corrosion with time. The corrosion rates of tough pitch copper C in soils 55 and 56 for example, differ widely; but it is also noteworthy that in soil 55, corrosion practically ceased after a short period of exposure, whereas in soil 56, it proceeded nearly in proportion to the duration of exposure.

For study of the effect of environment on the corrosion of copper, tough-pitch copper C, deoxidized copper A, and the copper-silicon alloys D and N were considered as behaving essentially alike. By combining weight losses, expressed as average penetration, for two specimens of each of these four materials, average values of eight measurements were obtained for each soil for each of five periods of exposure. In the same manner, average values of maximum penetration were obtained for the different exposure periods and soils.

In order to study the effect of environment in somewhat greater detail an equation of the form

$$y = ax^n, \tag{1}$$

was employed for expressing the relation between corrosion and time.

Taking logarithms of both sides,

$$\log y = \log a + n \log x. \tag{2}$$

Expressing the logarithm of the pit depth as log P, the logarithm of the time as log T, and the y-intercept as log k:

$$\log P_{max} = \log k + n \log T. \tag{3}$$

By similar substitutions, a linear equation expressing the relation between average penetration and time was obtained:

$$\log P_{avg} = \log k' + u \log T. \tag{4}$$

The slopes of these equations are given by the constants n and u. The y-intercepts, log k and log k', signify the logarithm of the maximum and average penetration at 1 yr, respectively. These equations were derived originally by Logan, Ewing, and Denison [7] and by Martin [8] to express, respectively, the progress with time of the pitting and weight loss of ferrous materials in soils. The equations have recently been employed in studying the effect of environment on the corrosion of ferrous metals in soils and in comparing the corrodibility of different ferrous metals and alloys [2]. Typical average penetration- and maximum penetration-time curves for copper on logarithmic coordinates are shown in figure 9.

In table 7 are shown values for maximum and average penetration at 14 yr, computed by eq 3 and 4, and for the respective constants. The standard errors of these constants computed according to the method of Ezekiel [9] are also given. The arrangement of the data is in the order of increasing values of the constant u.

In rating the soils in the order of corrosiveness, it is obviously necessary to consider not only the values of average and maximum penetration at 14 yr, but also the progress of corrosion with time as measured by the values of the constants u and n. For example, although the average and maximum penetration of copper at 14 yr in soils 58 and 64 is roughly the same, the values of the constants

TABLE 7. *Corrosion of copper at 14 years and constants of equations connecting average and maximum penetration with duration of exposure* [a]

Soil		Aeration	Penetration												Pitting factor [b]	
			Average						Maximum							
No.	Type		P_T=14 yr	±P_T=14 yr	k'	±k'	u	±u	P_T=14 yr	±P_T=14 yr	k	±k	n	±n	Copper	Plain iron and steel
			Mils	*Mils*	*Mils*	*Mils*			*Mils*	*Mils*	*Mils*	*Mils*				
65	Chino silt loam	Good	1.0	0.4	1.59	1.35	−0.18	0.40	16.0	4.3	3.51	1.8	0.57	0.26	16.0	5.3
51	Acadia clay	Poor	0.8	.3	0.63	0.45	.10	.36	4.7	0.7	1.73	0.46	.38	.14	5.9	.....
55	Hagerstown loam	Good	.3	.02	.17	.02	.26	.04	7.2	.8	4.74	.96	.16	.10	24.0	15.8
59	Carlisle muck	Very poor	.3	.05	.11	.07	.36	.28	5.0	.5	2.35	.97	.28	.17	16.7	5.7
53	Cecil clay loam	Good	.5	.03	.15	.02	.45	.06	7.8	.9	2.69	.60	.40	.11	15.6	11.8
66	Mohave fine gravelly loam.	Fair	.9	.2	.26	.12	.45	.22	10.1	.9	7.43	1.6	.12	.11	11.2	4.5
67	Cinders	Very poor	15.1	8.6	4.40	5.4	.47	.52	64.7	21	31.7	21.0	.27	.32	4.3	.....
62	Susquehanna clay	Fair	0.8	0.03	0.19	0.02	.54	.04	9.6	2.8	4.04	1.00	.33	.12	12.0	7.8
64	Docas clay	do	4.7	.9	.84	.29	.67	.17	15.1	7.1	7.04	2.0	.29	.14	3.2	1.6
61	Sharkey clay	Poor	1.0	.2	.14	.04	.69	.07	15.4	3.1	3.60	1.08	.55	.15	15.4	6.4
60	Rifle peat	do	8.6	5.8	.88	1.30	.86	.60	31.2	14.6	3.00	2.86	.89	.43	3.6	2.0
63	Tidal marsh	Very poor	9.9	.03	.95	0.05	.88	.03	11.2	2.6	1.81	0.88	.68	.23	1.1	6.8
56	Lake Charles clay	Poor	1.2	.2	.10	.03	.96	.16	4.9	1.0	1.88	.72	.37	.19	4.1	4.1
58	Muck	do	4.9	1.6	.09	.06	1.52	.31	19.0	3.0	1.28	.40	1.02	.16	3.9	6.0

[a] $P=kT^n$(s), where P=average or maximum penetration at the time, T.

[b] Pitting factor = $\frac{\text{maximum penetration}}{\text{average penetration}}$.

u and n for soil 64, namely 0.67 and 0.29, respectively, indicate decreasing rates of corrosion with time; whereas the corresponding values of these constants for soil 58, namely, 1.52 and 1.02, respectively, indicate rates of corrosion at least proportional to time. On the basis of inherent corrosivity, as indicated by values of average and maximum penetration at 1 yr (k'=0.09 mils, k=1.28 mils), soil 58 would be considered the least corrosive of any of the soils with respect to both weight loss and pitting. However, because the rate of corrosion in this soil was continuously maintained over the period of the test the total corrosion at the end of 14 yr was exceeded by only three soils, 60, 63, and 67.

Comparison of the values of the constant u with the aeration of the soils indicates that the rate of average penetration tended to decrease most rapidly in the better aerated soils. However, the fact that the values of u are small in two poorly aerated soils, 51 and 59, indicates that abundance of oxygen is not the sole factor that tends to diminish the rate of average penetration of copper in soils. Deposits of difficultly soluble salts on copper would be expected to have a similar effect.

The conditions that have the most corrosive action on copper are cinders (soil 67) sulfides (soils 60 and 63), and those factors that prevent the formation of protective films, such as carbon dioxide in excess, and high concentrations of hydrogen ions (soils 58 and 60). High concentrations of chloride are also corrosive to copper (soil 64).

It was previously stated that the smooth appearance of the specimens from many of the soils gave the impression that copper, unlike iron and steel, tended to corrode uniformly (fig. 3). However, the values of the ratios of the maximum to the average penetration (pitting factor) recorded in table 7 indicate an even greater tendency for copper to corrode locally in certain soils than plain irons and steels.

VIII. Zinc

The corrosion of zinc is illustrated by photographs of specimens of rolled zinc exposed at the test sites for 11 yr (fig. 10). Weight losses and maximum depths of pitting of both rolled and die-casting zinc are recorded in table 8. Measured in terms of loss in weight, there is no significant difference in the corrosion of the two varieties of zinc. However, maximum penetration of rolled zinc was definitely less than die-casting zinc except in soil 65, and in those soils in which both materials failed or in which the differences are too small to be considered significant.

For study of the effect of soil properties on the corrosion of zinc, values for average and maximum penetration of rolled zinc at 11 yr were calculated by means of the equation previously used in studying the corrosion of copper. The constants of the equation, which is linear on logarithmic coordinates, were computed by the method of least squares. Values of the constants $k'(k)$ and $u(n)$ representing the y-intercept and the slope, respectively, are recorded in table 9. The arrangement is in the order of decreasing average penetration at 11 yr. Because of the severe corrosion of the zinc specimens in cinders, values for soil 67 could not be computed.

The poorly and very poorly aerated soils are, as a class, corrosive to zinc, although high average penetration is not necessarily associated with deep pitting, as in soil 51. Soils of fair to good aeration containing high concentrations of chlorides and sulfates induce relatively deep pitting (64, 63, and 66). A probable explanation for this accelerated pitting is that soluble salts diminish anodic polarization. The rather severe corrosion in soil 70 is to be attributed to the highly alkaline reaction of this soil (pH 9.4) as well as to its content of soluble salts. The effect of soil reaction on the corrosion of zinc is further indicated by the very large values for average and maximum penetration in soil 60 (pH=2.6).

The values of the constants u and n, which range between approximately zero and unity, indicate that corrosion of zinc may vary between a linear rate and complete cessation. However, as there is no correlation between the constants $k'(k)$ and $u(n)$, a linear rate of corrosion will not result in severe corrosion unless the initial rate of corrosion is also high. No consistent variation of the constants with soil properties is indicated by the data.

TABLE 8. *Loss in weight and maximum penetration of zinc* [a]

Identification	Material [b]	Average exposure	Test site number and soil type: 51 Acadia clay	53 Cecil clay loam	55 Hagerstown loam	56 Lake Charles clay	58 Muck	59 Carlisle muck	60 Riffle peat	61 Sharkey clay	62 Susquehanna clay	63 Tidal marsh	64 Docas clay	65 Chino silt loam	66 Mohave fine gravelly loam	67 Cinders	70 Merced silt loam
LOSS IN WEIGHT (OUNCES PER SQUARE FOOT)																	
		Years															
Z	Rolled zinc	2.1	1.97	0.24	0.39	1.09	3.30	0.69	4.62	0.49	0.56	1.15	0.70	0.54	1.69	[c] 4.59	1.71
		4.0	....	.62	.60	3.42	5.09	1.70	10.36	.96	1.24	[d] 2.30	.57	.76	[d] 2.61	[c] 12.16	[c] 1.62
		9.0	4.83	1.11	.70	4.47	7.42	4.60	[f] D	1.06	1.25	[c] 2.04	1.37	1.43	0.91	D	3.62
		11.2	....	1.61	1.32	6.63	7.61	3.93	D	2.07	1.29	3.78	1.60	1.06	[d] 4.37	12.04	D
		2.1	2.61	0.27	0.40	2.25	3.67	0.91	7.50	[d] 0.47	0.43	0.90	1.34	1.24	3.63	10.6	2.05
		4.0	....	.54	.61	4.96	6.33	1.64	14.98	1.12	.60	1.43	2.53	0.76	4.74	13.08	[c] 2.19
CZ	Die-cast zinc	9.0	4.99	.97	.81	6.27	7.35	[c] 3.89	D	1.22	.75	3.06	2.52	2.00	1.42	D	1.72
		11.2	....	1.48	1.05	6.73	9.68	3.86	D	[d] 2.70	.97	3.89	[c] 3.95	2.11	3.77	17.02	16.29
MAXIMUM PENETRATION (MILS)																	
		2.1	30	10	13	10	38	<6	53	12	9	26	16	30	25	[c] 107+	36
		4.0	....	10	8	[d] 26	66	10	100	8	9	34	18	36	[d] 28	118+	[c] 102+
Z	Rolled zinc	9.0	28	13	8	29	58	22	150+	14	12	[c] 25	79	56	44	150+	84
		11.2	....	16	10	42	75	28	150+	17	11	30	35	40	56	78	150+
		2.1	33	15	21	25	108+	12	74	[d] 14	[d] 12	12	18	22	95	57	34
		4.0	....	22	20	30	125+	36	125+	28	16	24	20	16	124+	125+	[d] 80+
CZ	Die-cast zinc	9.0	52	26	30	56	125+	[c] 96	125+	36	19	34	45	33	36	125+	38
		11.2	....	22	20	71	125+	86	123+	28	27	36	[c] 46	32	86+	48	125+

[a] Average loss in weight or depth of maximum penetration for 2 specimens except when indicated otherwise.
[b] See table 3 for composition of materials.
[c] Data for 1 specimen only. The other specimen was destroyed by corrosion.
[d] Data for the individual specimens differs from the average by more than 50%.
[e] Data for 1 specimen only. The other specimen was missing.
[f] D, both specimens destroyed by corrosion.
[g] +, one or both specimens contained holes due to corrosion

TABLE 9. *Corrosion of rolled zinc at 11 years and constants of equations connecting average and maximum penetration with duration of exposure* [a]

Soil: No.	Soil: Type	Aeration	Penetration: Average: $P_{T=11\ yr}$	Average: k'	Average: n	Maximum: $P_{T=11\ yr}$	Maximum: k	Maximum: n
			Mils	*Mils*		*Mils*	*Mils*	
60	Riffle peat	Poor	61.4	3.05	1.25	271	25.5	0.99
58	Muck	do	13.3	3.96	0.50	72	34.1	.31
56	Lake Charles clay	Very poor	10.8	1.07	.97	40	7.0	.73
51	Acadia clay	Poor	9.1	2.08	.62	28	31.1	−.05
59	Carlisle muck	Very poor	7.7	0.56	1.09	27	2.9	.92
70	Merced silt loam	Fair	6.0	1.67	0.54	89	45.5	.28
63	Tidal marsh	Very poor	5.3	1.42	.54	29	28.4	.003
66	Mohave fine gravelly loam	Fair	3.8	2.66	.15	49	15.5	.50
61	Sharkey clay	Poor	3.1	0.51	.71	15	8.0	.26
53	Cecil clay loam	Good	2.6	.20	1.08	15	7.6	.27
64	Docas clay	Fair	2.4	.61	0.58	53	7.9	.79
62	Susquehanna clay	do	2.4	.82	.44	11	7.7	.17
65	Chino silt loam	Good	2.1	.63	.51	52	23.8	.30
55	Hagerstown loam	do	1.7	.45	.57	8	12.5	−.16

[a] $P=k(k')^{T^n(n)}$

IX. Lead

Photographs of specimens of lead after exposure for 11 yr are shown in figure 11. The losses in weight and depths of maximum pitting of four varieties of lead are given in table 10. These data show fairly conclusively that neither the common impurities of lead, namely, copper and bismuth, nor the hardening agents, antimony and tellurium, have had any effect on its corrosion. The conclusion that these impurities and alloying constituents are without significant effect in the corrosion of lead in soils was drawn previously by Burns [10] from the results of field tests of a wi variety of lead alloys in five typical soils of Indian The results of the present series of field tests mu be considered to extend considerably the range soil conditions to which the conclusions of Burn apply.

Because of the similarity in behavior of le alloys O, T, and B, corrosion data for a total six specimens were averaged in obtaining th values recorded in table 11. The values fo average and maximum penetration at 11 yr, an the constants k', k, u, and n were computed described in the section on copper.

TABLE 10. *Loss in weight and maximum penetration of lead alloys* [a]

Identification	Material [b]	Average exposure	Test site number and soil type														
			51	53	55	56	58	59	60	61	62	63	64	65	66	67	70
			Acadia clay	Cecil clay loam	Hagerstown loam	Lake Charles clay	Muck	Carlisle muck	Rifle peat	Sharkey clay	Susquehanna clay	Tidal marsh	Docas clay	Chino silt loam	Mohave fine gravelly loam	Cinders	Merced silt loam
LOSS IN WEIGHT (OUNCES PER SQUARE FOOT)																	
		Years															
		2.1	0.62	0.22	0.37	0.21	1.56	0.36	0.18	1.46	0.30	0.05	0.20	0.14	0.10	3.67	0.00
		4.0	.....	.21	.20	.45	2.41	.81	.28	2.21	.93	.02	.19	.13	.10	12.21	.12
O	Chemical lead	9.0	3.06	.53	.37	2.02	2.49	1.76	.54	1.22	.67	.10	.46	.45	.34	11.21	.26
		11.2	.....	.64	.41	3.49	2.82	2.06	.75	3.03	.94	.02	.60	.35	.18	3.06	.19
		2.1	1.21	.25	.34	0.38	1.68	0.23	.15	1.21	.36	.06	.25	.17	.25	3.35	.00
		4.0	.....	.31	.28	.82	2.80	1.08	.20	1.75	.64	[c].02	.18	.16	.12	13.22	.15
T	Tellurium lead	9.0	3.82	.73	.54	2.30	2.60	2.09	.57	1.44	1.37	.13	.48	.59	.58	11.28	.32
		11.2	.....	.67	.57	4.60	3.47	1.77	.84	3.40	1.00	.02	.88	.40	.36	3.42	.28
		2.1	1.05	.25	.19	0.31	1.45	0.20	.10	0.94	0.27	.04	.12	.17	.06	3.14	.10
		4.0	.....	.22	.15	.50	2.12	1.04	.22	1.75	1.03	.01	.19	.21	.12	4.21	.14
B	Antimonial lead	9.0	3.09	.62	.30	1.65	2.24	1.97	.54	1.16	0.77	[c].05	.47	.51	.28	12.27	.20
		11.2	.....	.70	.35	4.54	3.02	1.09	.79	3.78	1.24	.01	.96	.35	.20	4.28	.16
		5.0	.....	.43	.17	0.52	0.54	1.23	.74	0.82	0.69	.18	.50	.42	.24	1.18	.33
M	Special lead alloy	7.2	.....	[d].46	.27	4.98	.70	0.82	[d].61	[d].63	[d].64	.20	.40	.38	.39	2.23	.18
MAXIMUM PENETRATION (MILS)																	
		2.1	40	18	24	38	34	21	18	35	32	14	24	40	44	79	48
		4.0	.....	12	26	37	28	15	15	39	29	18	16	24	34	104	34
O	Chemical lead	9.0	68	26	19	86	46	14	16	31	26	29	25	32	36	135	24
		11.2	.....	18	31	100	52	20	33	70	34	12	25	15	24	85	24
		2.1	54	12	26	30	55	8	29	33	19	10	21	22	23	71	16
		4.0	.....	20	26	48	56	12	10	30	31	[c]12	11	16	41	94	27
T	Tellurium lead	9.0	66	18	26	110	33	18	36	43	25	32	20	21	30	104	37
		11.2	.....	16	30	107	53	21	23	73	40	8	17	20	23	61	16
		2.1	56	10	26	39	50	9	6	31	12	<6	12	6	12	56	11
		4.0	.....	10	18	52	58	7	<6	42	30	16	12	15	15	90	12
B	Antimonial lead	9.0	63	14	15	74	66	20	20	62	26	[c]44	10	26	24	125	20
		11.2	.....	9	16	104	51	12	28	89	14	6	19	7	16	46	9
		5.0	.....	12	15	30	18	25	13	24	18	36	21	19	34	26	28
M	Special lead alloy	7.2	.....	[d]13	8	58	8	8	[d]8	[d]18	[d]10	8	10	12	18	15	10

[a] Average loss in weight or depth of maximum penetration for 2 specimens except when indicated otherwise.
[b] See table 3 for composition of materials.
[c] Data for 1 specimen only. The other specimen was missing.
[d] Data for 3 specimens.

TABLE 11. *Corrosion of lead of 11 years and constants of equations connecting average and maximum penetration with duration of exposure* [a]

Soil No.	Soil Type	Aeration	Penetration [b]					
			Average			Maximum		
			$P_{T=11\ yr}$	k'	n	$P_{T=11\ yr}$	k	n
			mils	*mils*		*mils*	*mils*	
67	Cinders	Very poor	7.54	4.64	0.20	89	74.3	0.08
51	Acadia clay	Poor	[c] 4.21	0.55	.85	[c] 69	43.4	.19
56	Lake Charles Clay	Very poor	3.52	.09	1.54	101	20.6	.66
58	Muck	Poor	3.07	1.64	0.26	50	43.7	.06
59	Carlisle muck	Very poor	2.56	0.18	1.11	17	9.7	.24
61	Sharkey clay	Poor	2.47	1.00	0.38	61	23.3	.42
62	Susquehanna clay	Fair	1.23	0.26	.66	29	20.9	.14
60	Riffle peat	Poor	0.76	.07	1.02	24	10.1	.36
53	Cecil clay loam	Good	.70	.14	0.69	20	12.0	.13
54	Docas clay	Fair	.67	.08	.86	18	14.9	.09
65	Chino silt loam	Good	.47	.09	.68	18	23.7	−.11
55	Hagerstown loam	do	.43	.22	.28	23	24.8	−.04
66	Mohave fine gravelly loam	Fair	.32	.08	.58	26	28.8	−.05
70	Merced silt loam	do	.27	.05	.73	20	24.3	−.09
63	Tidal marsh	Very poor	.04	.04	−.03	18	9.8	.24

[a] $P=k(T)^n$ $T=80$.
[b] Average of 3 lead alloys (see text).
[c] Data for 9 yr only.

The tendency for maximum penetration to decrease with increasing aeration of the soil, which has been seen to apply to plain irons and steels [2], and in the present paper to copper and zinc, is also to be observed in table 11. In fact, a fairly definite tendency for maximum penetration also to decrease with increasing aeration is indicated by the data. The exceptions to this trend, namely, the low corrosion rates for soils 60 and 63, can be readily explained as being due to the inhibitive effect of sulfates in high concentration. The fact that severe corrosion of lead occurred in soil 51, likewise high in sulfates, does not necessarily weaken this explanation, because ions present in concentrations less than that required for passivation tend to accelerate the corrosion of lead [10]. The partially inhibitive effect of bicarbonate, chloride, and sulfate ions is indicated by the data for the group of alkaline soils of fair to good aeration, 64, 65, 66, and 70. In spite of their high contents of soluble salts these soils as a class are actually less corrosive than soils of similar aeration, which are low in soluble salts, namely, soils 53, 55, and 62.

Comparison of the values of the constants n and n indicates that in general the rate of pitting of lead decreases considerably more rapidly than the rate of average penetration. In fact, except for several of the poorly aerated soils, the values of n indicate virtually complete cessation of pitting during the 11-yr exposure period. It is reasonable to attribute this marked reduction in the rate of pitting to anodic polarization, which resulted from the deposition of difficult soluble corrosion products in close proximity to the anodic areas.

X. Comparison of the Corrosion of Ferrous and Nonferrous Metals

Because copper, zinc, and lead, together with iron and steel are the metals most commonly used for underground construction, a comparison of the corrosion resistances of these metals forms a basis for selecting materials according to their suitability for specific environmental conditions. Although zinc is not ordinarily considered to be a material of construction, it is desirable to include it in the present study because of the extensive use of zinc underground as a protective coating for iron and steel and as an anode for cathodic protection.

For the purpose of comparing the corrosion resistances of the four metals, the soils were grouped into four environments, as follows: (1) well aerated, acid soils low in soluble salts, 53, 55, 62; (2) poorly aerated soils (51, 56, 58, 61); (3)

alkaline soils high in soluble salts (64, 65, 66, 70) and (4) soils high in sulfides (59, 60, 63). In figure 12, corrosion time curves for soils typical of these environments are shown.

For study of the comparative behavior of copper, lead and zinc in the 14 soils, the average and maximum penetration of each metal were plotted against the duration of exposure (fig. 12). Each point in the curves for copper is the average of a total of eight measurements, made on specimens of four varieties of copper and copper-silicon alloys. For zinc, each point is the average of two measurements made on the specimen of rolled zinc, and for lead, each point is the average of a total of six measurements, made on three varieties of lead. For each soil, corrosion-time curves are also shown to illustrate the average behavior of steel and other wrought ferrous metals that corroded at the same rate as steel in these soils. Each point on these curves is the average of a total of eight measurements made on specimens of carbon steel, mechanically puddled wrought iron, hand-puddled wrought iron, and copper molybdenum open-hearth iron. Data on the corrosion of these ferrous materials were given in a previous paper [2].

In all of the soils represented in figure 12, except Rifle peat (soil 60), the ferrous materials are seen to be corroded at considerably higher rates than any of the other metals. However, because of its poor aeration, high acidity (pH 2.6), high content of soluble salts (resistivity 218 ohm-cm), and because of the presence of sulfides, none of the materials under consideration with the exception of lead would be expected to withstand for a long period the corrosive action of this soil. Even a heavy zinc coating on steel would probably protect for a short period only because of corrosion of the zinc by local action. The inhibitive effect of high concentrations of sulfates on the corrosion of lead, indicated in the curves for soil 60, has been previously referred to.

The curves for soil 64 illustrate the corrosive effect of high concentrations of chlorides on iron, copper, and zinc, and the passifying action of chlorides on lead.

The curves for soils 53 and 56 indicate in a general way the progress of corrosion in well aerated soils low in soluble salts and in poorly aerated soils. With longer periods of exposure, the rates of average and maximum penetration for iron and steel decrease rapidly with time in the well aerated soil (53), but in the poorly aerated soil (56) average and maximum penetration were proportional to the length of exposure. Similarly, the curves for maximum penetration of the other materials show a much greater tendency to decrease with time in the well aerated soil. Under such conditions, ordinary wrought ferrous metals of reasonable thickness would be expected to provide long service.

XI. Summary

This report contains the results of measurements of corrosion made on specimens of copper, lead, and zinc, and of alloys of these metals exposed to different soil conditions for periods up to 14 years. With respect to weight loss, tough pitch copper was generally more resistant than deoxidized copper and the copper-silicon alloys, except in soils high in sulfides. However, in a number of the soils, the maximum depths of pits on tough-pitch copper were greater than those on one or more of these materials.

The loss in weight of the copper-zinc and copper-nickel-zinc alloys was approximately in the order of increasing zinc content, except in soils high in sulfides in which the reverse order was followed. Admiralty metal (70% of Cu, 29% of Zn, 1% of Sn) showed the greatest tendency toward localized corrosion of any of the copper-zinc alloys. Although a two-phase leaded silicon brass (67% of Cu, 31% of Zn, 1% of Si, and 0.8% of Pb) showed the least tendency to develop deep pits, this alloy was dezincified in many of the soils. All two-phase copper-zinc alloys were dezincified to some extent in most of the soils, except a 60–40 brass containing 0.08 percent of arsenic, which showed only superficial discoloration. The presence of arsenic did, however, induce intergranular corrosion in the specimens exposed to cinders.

No differences were observed in the corrosion of chemical lead, antimonial lead, and tellurium lead.

A die-casting zinc alloy had greater maximum pit depths than rolled zinc, but there was no significant difference in weight loss.

In general, copper, zinc, and lead, and alloys of these metals were corroded most severely in poorly aerated soils, particularly, in soils that were highly acid or that contained high concentrations of soluble salts. Copper was corroded in soils high

sulfides. Lead was passivated by soils containing high concentrations of sulfates and chlorides.

The field tests in this paper were initiated and installed, and until 1946 were conducted, under the supervision of K. H. Logan. The measurements of corrosion were made chiefly by Warren F. Dettmers, who also assisted in other capacities.

XII. References

[1] K. H. Logan, NBS Circular C450, Underground corrosion (1945).

[2] I. A. Denison and M. Romanoff, J. Research NBS **44**, 47 (1950) RP2057.

[3] D. K. Crampton, Ind. Eng. Chem. **28**, 1397 (1936).

[4] G. O. Hiers, Corrosion handbook (John Wiley and Sons, New York, N. Y., 1948).

[5] P. D. Merica, Chem. Met. Eng. **16**, 657 (1917).

[6] A. W. Tracy, Heating, Piping, Air Conditioning **14**, 538 (1942).

[7] K. H. Logan, S. P. Ewing, and I. A. Denison, Symposium on corrosion testing procedures, ASTM (Philadelphia, Pa., 1937).

[8] L. M. Martin, NBS Soil corrosion conference, unpublished (1937).

[9] Mordecai Ezekiel, Methods of correlation analysis (John Wiley and Sons Inc., New York, N. Y., 1930).

[10] R. M. Burns, Bell Syst. Tech. J. **15**, 603 (1936).

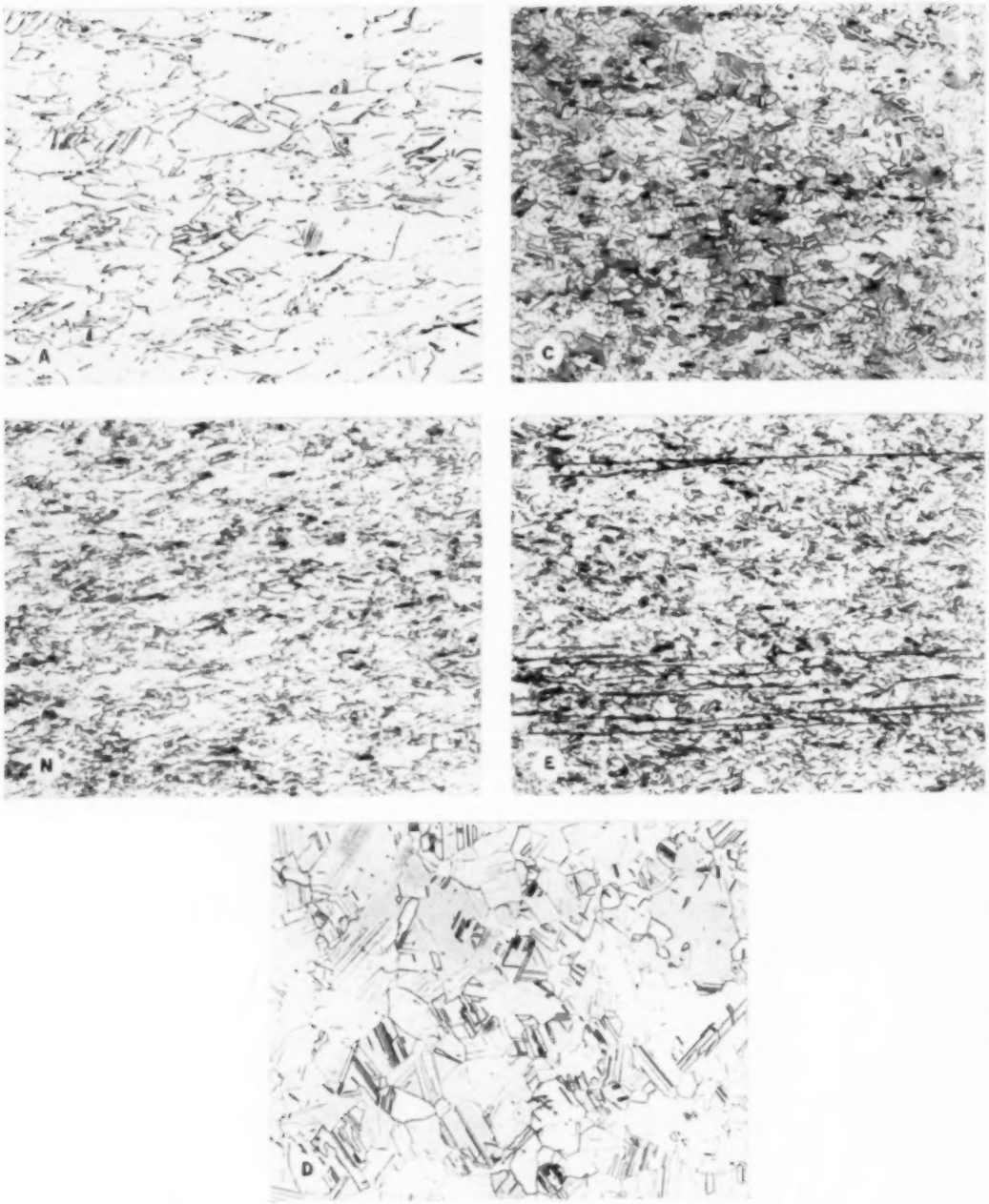

FIGURE 1. *Structures of specimens of copper and copper-silicon alloys,* $\times 100$.

A, Deoxidized copper; C, tough pitch copper; N, copper-silicon alloy; E, copper-silicon alloy; D, copper-silicon alloy. See table 2 for composition of material. Etching solutions: A, $FeCl_3$ and swabbed with CrO_3; C, $(NH_4)_2S_2O_8$; N, E, and D, $K_2Cr_2O_7+FeCl_3$.

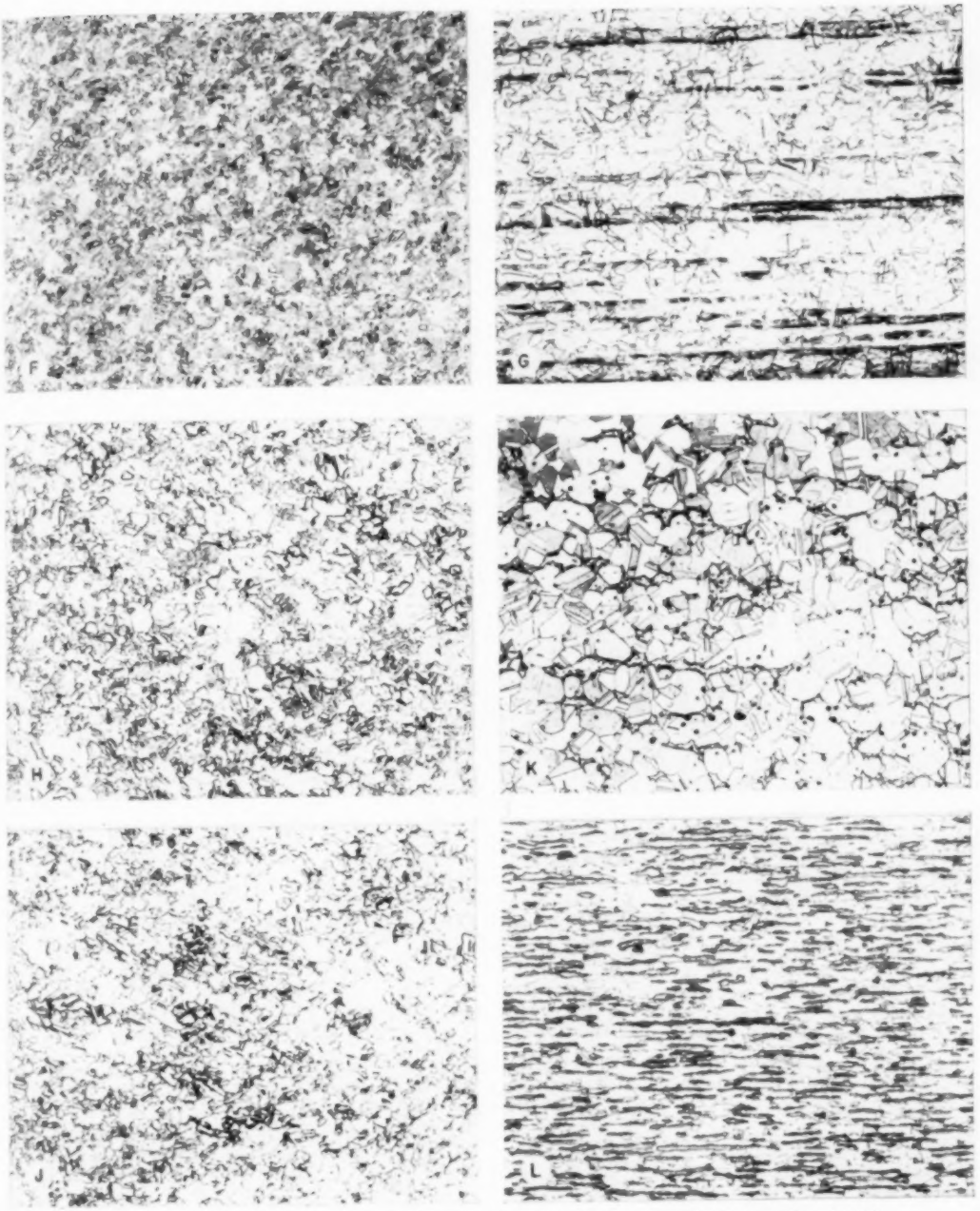

FIGURE 2. *Structures of specimens of copper-zinc alloys and copper-nickel-zinc alloy,* $\times 100$.

F, Red brass; G, copper-nickel-zinc alloy; H, Admiralty metal; K, leaded-silicon brass; J, yellow brass; L, Muntz metal. See table 2 for composition of materials. Etching solutions: F, $(NH_4)_2S_2O_8$; G, H, K, and J, $K_2Cr_2O_7$+FeCl$_3$; L, FeCl$_3$+$K_2Cr_2O_7$+Cr_2O_3.

571926—50——5

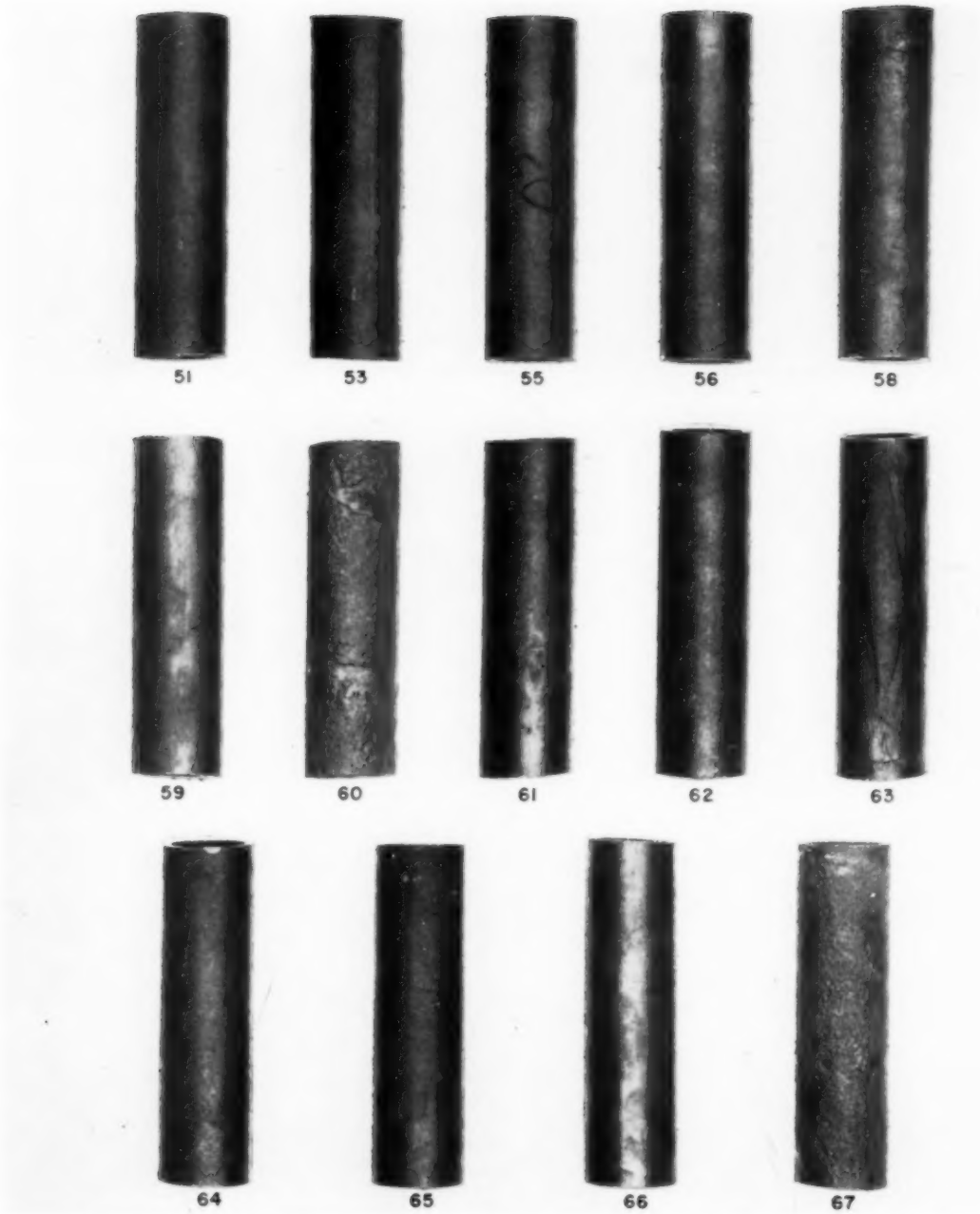

FIGURE 3. *Condition of specimens of tough pitch copper removed after exposure for 14 years to 14 soils.*

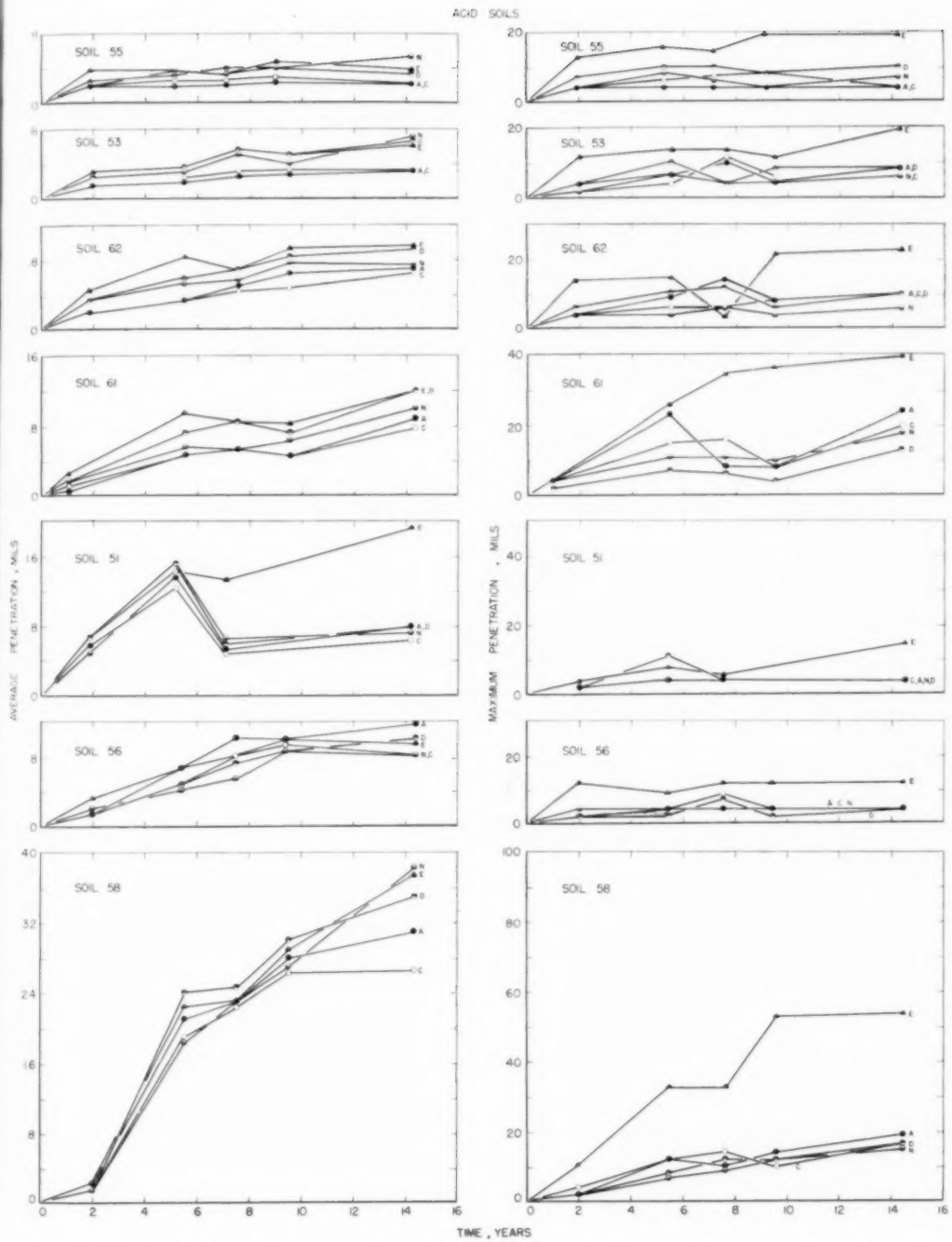

FIGURE 4. *Average and maximum penetration-time curves of copper and copper-silicon alloys.*

Each point is the average of 2 specimens. ○, C, tough-pitch copper, 99.9% Cu. ●, A, deoxidized copper, 99.94% Cu, 0.018% P. ◓, D, copper-silicon alloy, 3.07% Cu, 3.19% Si. ◒, N, copper-silicon alloy, 98.11% Cu, 1.49% Si. ▲, E, bronze, 97.15% Cu, 1.04% Si, 1.80% Sn.

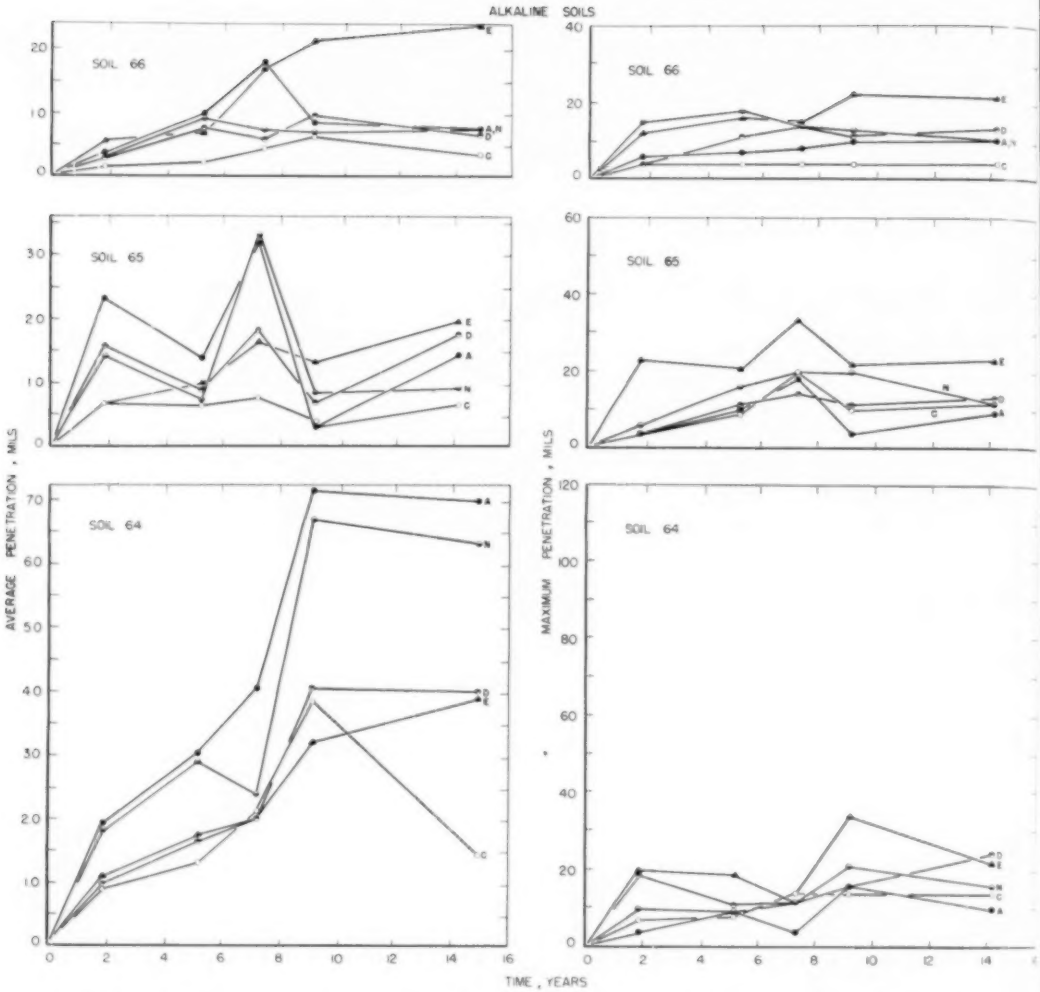

FIGURE 4—Continued. *Average and maximum penetration-time curves of copper and copper-silicon alloys.*

Each point is the average of 2 specimens. ○, C, tough-pitch copper, 99.9% Cu. ●, A, deoxidized copper, 99.94% Cu, 0.018% P. ◓, D, copper-silicon alloy, 95.46% Cu, 3.19% Si. ◒, N, copper-silicon alloy, 98.11% Cu, 1.49% Si. ▲, E, bronze, 97.15% Cu, 1.04% Si, 1.80% Sn.

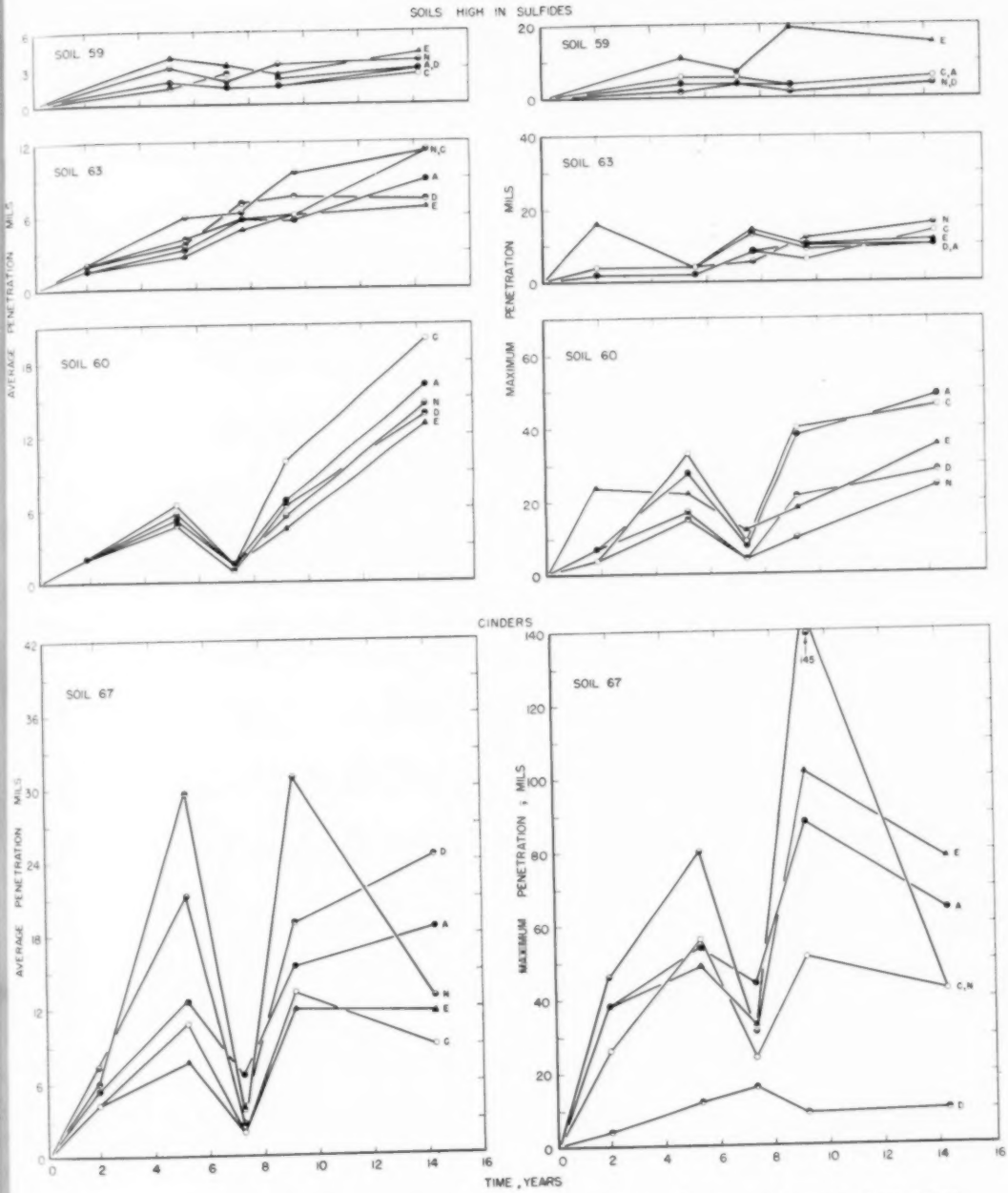

FIGURE 4—Continued. *Average and maximum penetration-time curves of copper and copper-silicon alloys.*

Each point is the average of 2 specimens. ○, C, tough-pitch copper, 99.9% Cu. ●, A, deoxidized copper, 99.94% Cu, 0.018% P. ◒, D, copper-silicon alloy, 96.46% Cu, 3.19% Si. ◒, N, copper-silicon alloy, 98.11% Cu, 1.49% Si. ▲, E, bronze, 97.15% Cu, 1.04% Si, 1.80% Sn.

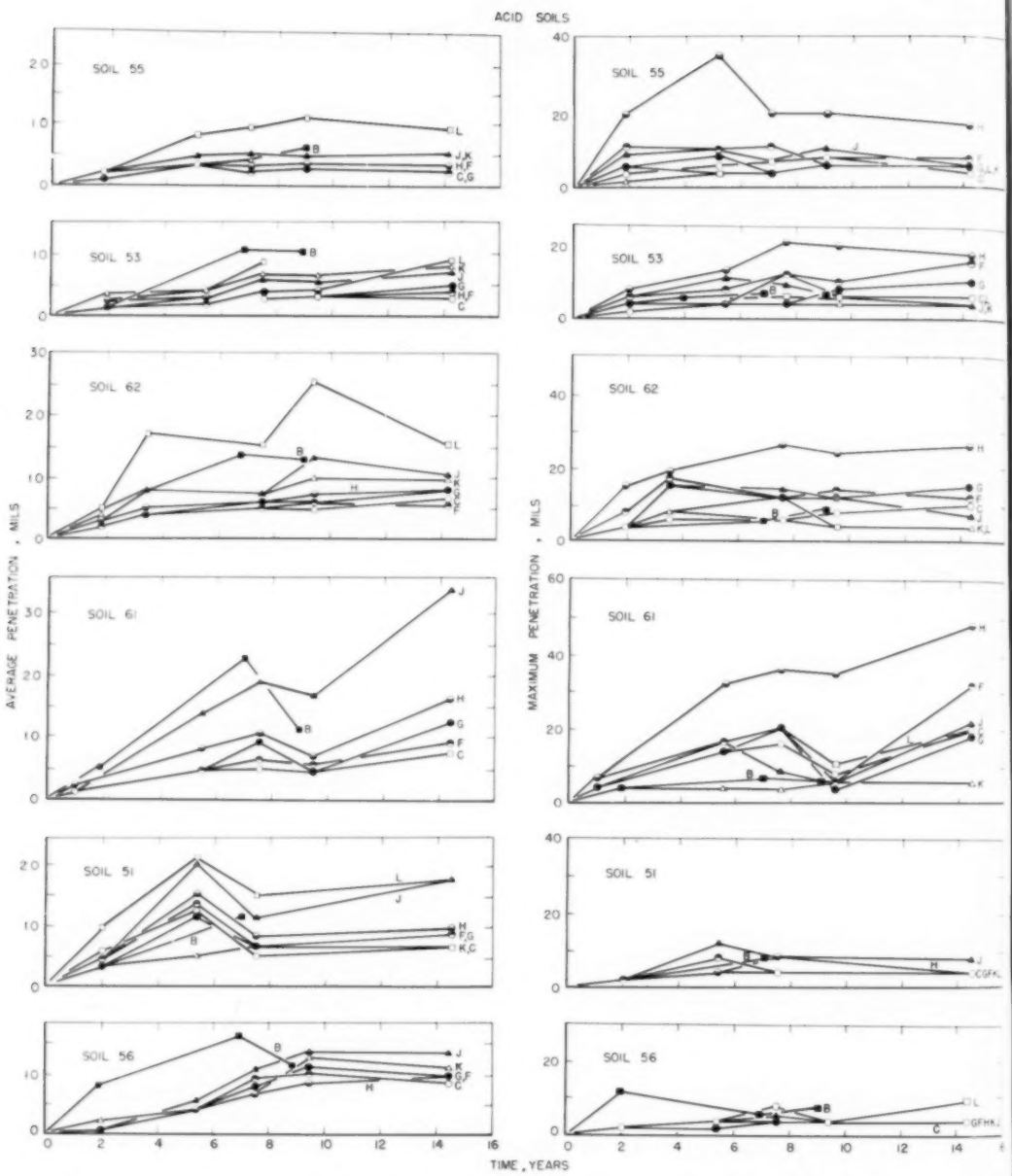

FIGURE 5. *Average and maximum penetration-time curves of copper-zinc alloys and copper-nickel-zinc.*

Each point is the average of 2 specimens. The average penetration-time curves for the specimens whose weight loss was appreciably affected by dep cation were not plotted (see text). ○, C, tough-pitch copper, 99.9% Cu; ●, G, copper-nickel-zinc alloy, 74.45% Cu; 4.99% Zn, 20.04% Ni; ◓, F, red 85.18% Cu, 14.80% Zn; ◒, H, Admiralty metal, 71.28% Cu, 27.39% Zn, 1.30% Sn, 0.01% Pb; △, K, leaded-silicon brass, 67.08% Cu, 31.07% Zn, 0.81% J, yellow brass, 66.50% Cu, 33.06% Zn, 0.42% Pb; □, L, Muntz metal, 62.37% Cu, 37.54% Zn, 0.36% Pb. ■, B, Muntz metal with arsenic, 62.37% Cu, Zn, 0.065% Pb, 0.08% As.

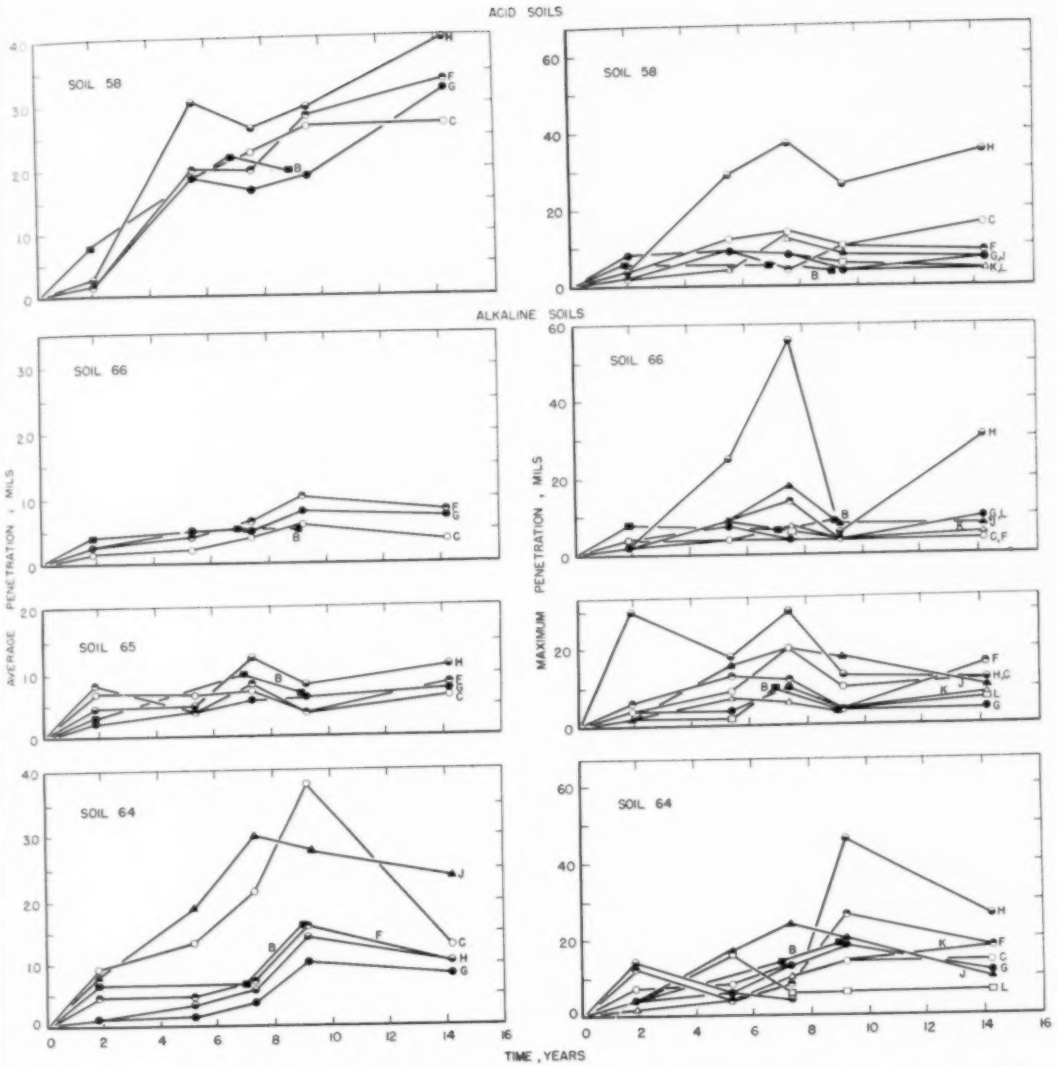

FIGURE 5—Continued. *Average and maximum penetration-time curves of copper-zinc alloys and copper-nickel-zinc.*

Each point is the average of 2 specimens. The average penetration-time curves for the specimens whose weight loss was appreciably affected by dezincification were not plotted (see text). ○, C, tough-pitch copper, 99.9% Cu; ●, G, copper-nickel-zinc alloy, 74.45% Cu; 4.99% Zn, 20.04% Ni; ◓, F, red brass 83.18% Cu, 14.80% Zn; ◒, H, Admiralty metal, 71.28% Cu, 27.39% Zn, 1.30% Sn, 0.01% Pb; △, K, leaded-silicon brass, 67.08% Cu, 31.07% Zn, 0.84% Pb; ▲, J, yellow brass, 66.50% Cu, 33.06% Zn, 0.42% Pb; □, L, Muntz metal, 62.37% Cu, 37.54% Zn, 0.06% Pb, 0.08% As.

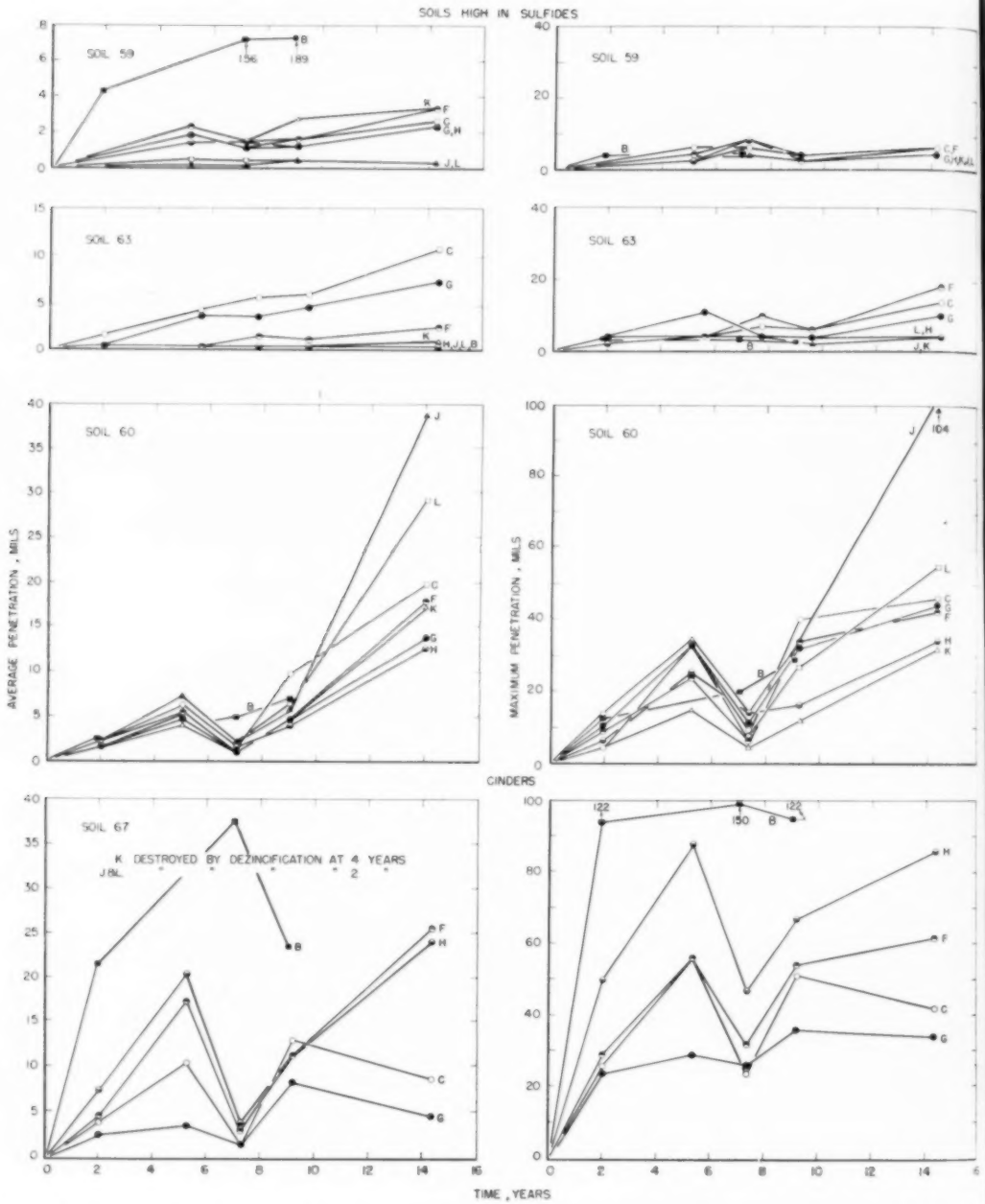

FIGURE 5—Continued. *Average and maximum penetration-time curves of copper-zinc alloys and copper-nickel-zinc.*

Each point is the average of 2 specimens. The average penetration-time curves for the specimens whose weight loss was appreciably affected by dezincification were not plotted (see text). ○, C, Through-pitch copper, 99.9% Cu; ●, G, copper-nickel-zinc alloy, 74.45% Cu, 4.99% Zn, 20.04% Ni; ◓, F, red brass, 85.18% Cu, 14.80% Zn; ◒, H, Admiralty metal, 71.28% Cu, 27.39% Zn, 1.30% Sn, 0.01% Pb; △, K, leaded-silicon brass, 67.08% Cu, 31.02% Zn, 0.84% Pb; ▲, yellow brass, 66.50% Cu, 33.06% Zn, 0.42% Pb; □, L, Muntz metal, 62.37% Cu, 37.54% Zn, 0.36% Pb; ■, B, Muntz metal with arsenic, 62.37% Cu, 37.56% Zn, 0.003% Pb, 0.08% As.

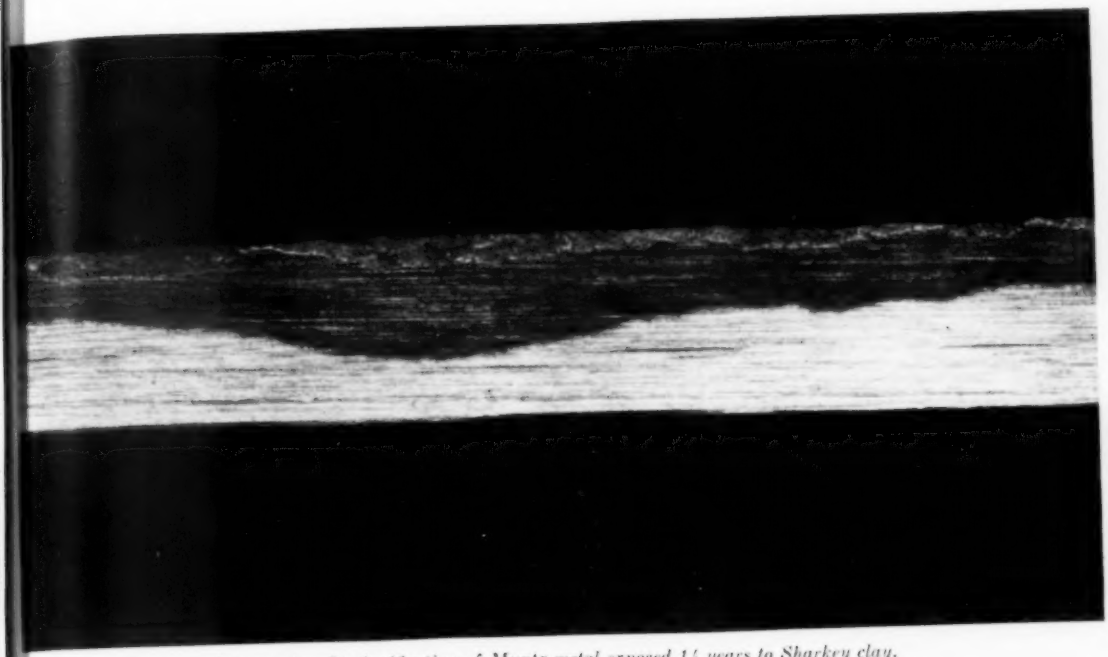

FIGURE 6. *Dezincification of Muntz metal exposed 14 years to Sharkey clay.*

Transverse section showing transition from uncorroded metal to the uniformly dezincified layer, ×15.

FIGURE 7. *Leaded silicon brass (K) exposed 9.5 years to Sharkey clay (soil 61).*

Transverse section showing partial dezincification. The dezincification is more severe at the left, as indicated by the dark, spongy-like areas with irregular boundaries. Light grains of the alpha phase in dezincified areas show that the grains of the beta phase are dezincified first. ×250.

FIGURE 8. *Microstructure of Muntz metal containing 0.08% arsenic.*

Transverse section of specimen exposed 7 years to cinders (site 67) showing intergranular corrosion. ×100.

871926—50——6

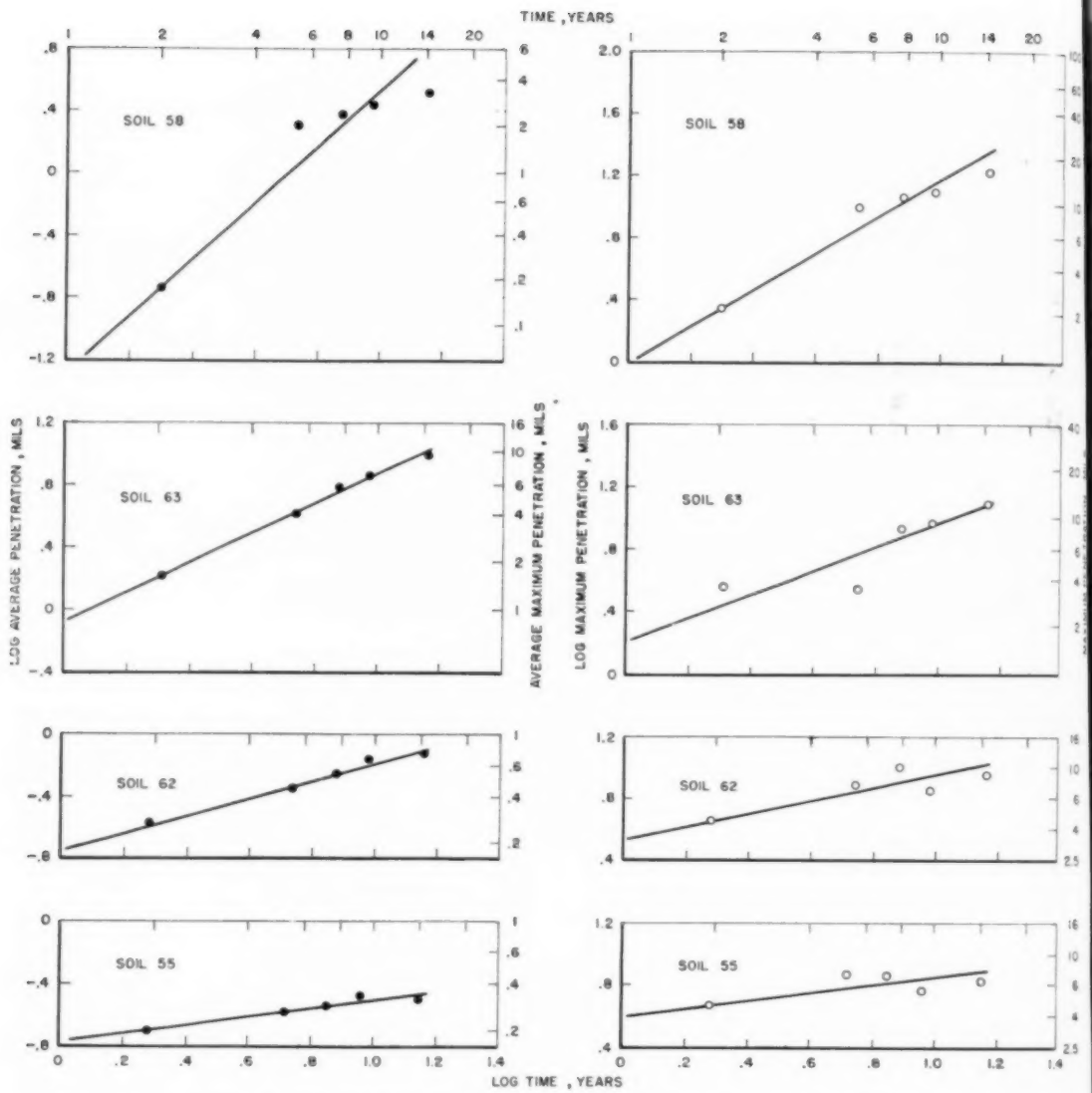

FIGURE 9. *Average and maximum penetration-time curves of copper in typical soils on logarithmic coordinates.*

●, Log average penetration; ○, log maximum penetration.

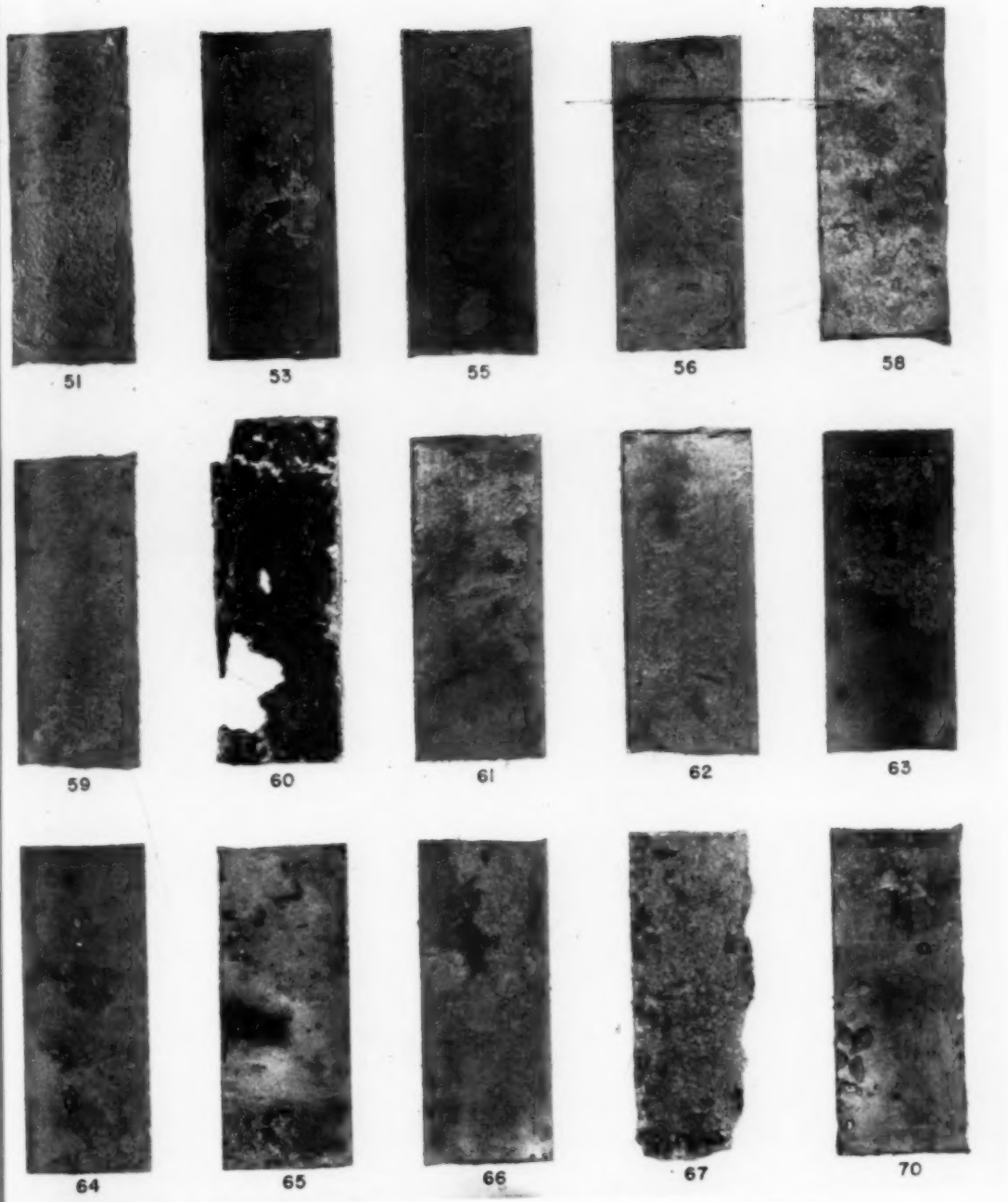

FIGURE 10. *Condition of specimens of rolled zinc (Z) exposed 9 years to 15 soils*

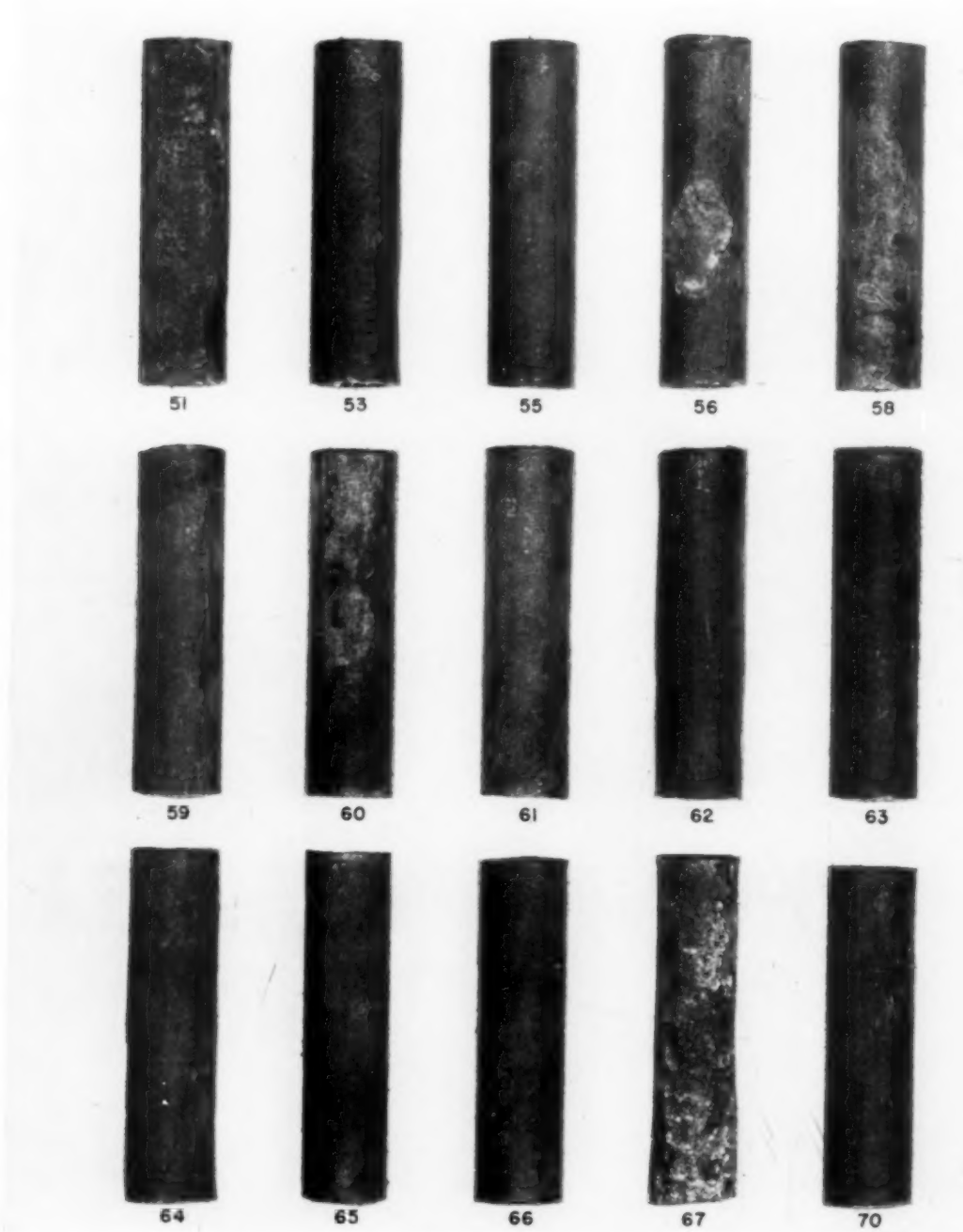

FIGURE 11. *Condition of chemical lead (O) exposed 9 years to 15 soils.*

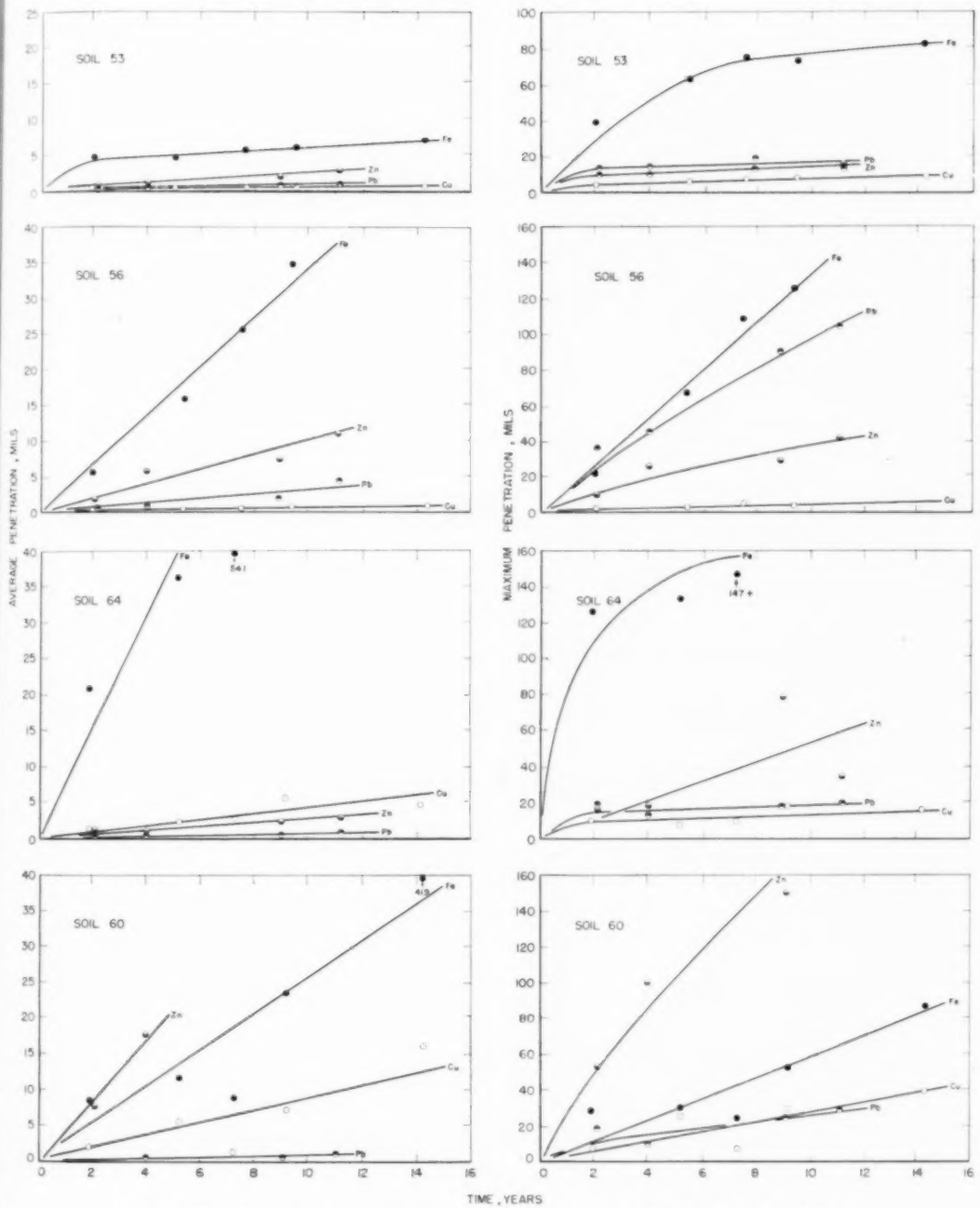

FIGURE 12. *Average and maximum penetration-time curves of steel, copper, lead, and zinc in representative soil environments.*

●, Steel; ○, copper; ◓, lead; ◒, zinc.

WASHINGTON, October 7, 1949.

U. S. Department of Commerce
National Bureau of Standards

Research Paper RP2078
Volume 44, March 1950

Part of the Journal of Research of the National Bureau of Standards

Mass Spectra of Nonanes

By Fred L. Mohler, Laura Williamson, C. Edward Wise, Edmund J. Wells, Helen M. Dean, and Evelyn G. Bloom

Mass spectra of the 35 nonanes have been measured with a Consolidated mass spectrometer. Sensitivity (current per unit pressure) at the maximum peak relative to *n*-butane and total ionization relative to *n*-butane are given, as well as relative intensities for 18 mass peaks.

Relations between molecular structure and mass spectra are similar to those found in lighter saturated hydrocarbons. Some general relations between mass spectra and molecular structure of saturated hydrocarbons are given, but these are not sufficient to deduce the structure uniquely from the spectrum. The analysis of mixtures of nonanes will, in general, be impossible unless the sample is a cut containing comparatively few components.

I. Introduction

Mass spectra of the 35 nonanes have been measured by the Mass Spectrometry Section of this Bureau as part of the program of measuring mass spectra of pure hydrocarbons. All but one of the spectra have been published in detail in the API Catalog of Mass Spectral Data [1].[1] This paper is a summary of the main features of the nonane spectra, and some empirical relations between the mass spectrum and molecular structure are pointed out. A previous paper has described the mass spectra of the octanes [2]. The nonane isomers give, with few exceptions, quite distinctive mass spectra, so that the mass spectrum affords a valuable method of chemical identification.

II. Experimental Procedure

Mass spectra have been obtained with a 180° Consolidated mass spectrometer equipped with automatic control of the electron current and of the temperature of the ionization chamber. Standard procedures have been followed, except for the method of measuring the vapor pressure in the gas reservoir used to compute the sensitivity (current per unit pressure). This pressure was measured by a diaphragm-type of micromanometer in which the diaphragm displacement was measured electrically [3]. API tables of serial numbers less than 250 gave sensitivities measured by the conventional method of measuring pressure in a small volume by a mercury manometer and then expanding the vapor into the reservoir. This leads to large errors for compounds like the nonanes, which have low vapor pressures. A correction page has been published in the API Catalog [1].

Thirteen of the nonanes are NBS Standard Samples of purity 99.8 percent or better. We are indebted to several laboratories for samples of the other nonanes. Sixteen were prepared under the direction of Newell C. Cook of Pennsylvania State College, three were prepared by Frank L. Howard of the Engine Fuel Section of the National Bureau of Standards, and three were supplied by F. D. Rossini of the Thermochemistry and Hydrocarbon Section of the Bureau. Most of these samples were considered to be pure compounds of purity estimated to be about 99 percent. In most cases, the mass spectrometer showed no detectable impurities other than nonanes. A few showed insignificant traces of olefins and one compound, 2,2-dimethylheptane, contained a rather large amount of *n*-octane. Data for this compound are considered inaccurate and provisional.

Mass spectra have been measured with both 50-v and 70-v ionizing voltage, but only measurements at 70-v are given in this paper. Intensities

[1] Figures in brackets indicate the literature references at the end of this paper.

are given relative to the maximum peak equal to 100, and the limit of sensitivity is about 0.01 on this scale. The sensitivity at the maximum peak is measured in terms of current in arbitrary units per unit pressure in the reservoir. On the same day the sensitivity to *n*-butane at mass 43 is measured. The ratio of the sensitivity at the maximum peak to the *n*-butane sensitivity is a molecular property independent of the arbitrary units used.

These spectra have been obtained over a period of about a year, and during most of the time the ionization chamber was thermostated at 245° C. For a few months it was at 275° C. Nine spectra were measured at the higher temperature [1].

III. Results

Table 1 gives the sensitivity relative to *n*-butane and the total ionization relative to *n*-butane for the nonanes. Column 1 gives an index number for cross reference to table 2. Column 2 is the name of the compound, column 3 gives the *m/e* value of the maximum peak, column 4 gives the sensitivity relative to *n*-butane, column 5 is the sum of all the mass peaks in the spectrum, column 6 is the product of column 4 and column 5 divided by 312 (the sum of the peaks in *n*-butane). The last column gives the serial number of the mass spectrum in the API Catalog.

About half of the nonanes have the maximum peak at mass 43 and the other half have the maximum at 57. Values for the sensitivity and for the sum of the mass peaks cover about a two-fold range of values with high sensitivity associated with a small value for the sum and vice versa. The product of the two is not constant but has a much smaller range of values. The mean value of total ionization relative to *n*-butane is 1.94 $\pm$0.13. This is to be compared with values 1.82 $\pm$0.05 for the octanes and 1.68 $\pm$0.04 for the heptanes. The values for octanes and heptanes have been remeasured using a micromanometer, and published values for the octanes [2] are seriously in error.

Table 2 lists the peak heights of 18 mass peaks in the spectra of the 35 nonanes. It includes all the peaks that are large or distinctive in all the spectra. Asterisks mark peaks that cannot be obtained by simple dissociation and involve a rearrangement of atoms in the ionization process.

TABLE 1. *Sensitivity and total ionization relative to n-butane in nonane mass spectra*

Reference	Compound	Maximum Peak	Sensitivity relative to n-butane	Sum of mass peaks	Total ionization relative to n-butane
1	*n*-Nonane	43	1.41	437	1.98
2	2-Methyloctane	43	1.31	389	1.64
3	3-Methyloctane	57	1.84	302	1.78
4	4-Methyloctane	43	1.60	358	1.84
5	3-Ethylheptane	57	1.67	378	2.02
6	4-Ethylheptane	43	1.60	403	2.07
7	2,2-Dimethylheptane	57			
8	2,3-Dimethylheptane	43	1.95	315	1.87
9	2,4-Dimethylheptane	43	1.92	341	2.09
10	2,5-Dimethylheptane	57	1.88	346	2.08
11	2,6-Dimethylheptane	43	1.61	366	1.89
12	3,3-Dimethylheptane	43	1.18	554	2.09
13	3,4-Dimethylheptane	43	1.11	522	1.86
14	3,5-Dimethylheptane	57	2.04	320	2.09
15	4,4-Dimethylheptane	43	1.61	363	1.87
16	2-Methyl-3-ethylhexane	43	1.94	357	2.21
17	2-Methyl-4-ethylhexane	57	1.68	399	2.14
18	3-Methyl-3-ethylhexane	57	1.57	377	1.89
19	3-Methyl-4-ethylhexane	57	1.03	567	1.88
20	2,2,3-Trimethylhexane	57	2.05	312	2.05
21	2,2,4-Trimethylhexane	57	2.50	266	2.13
22	2,2,5-Trimethylhexane	57	2.36	271	2.05
23	2,3,3-Trimethylhexane	43	1.74	364	2.03
24	2,3,4-Trimethylhexane	43	1.79	373	2.15
25	2,3,5-Trimethylhexane	43	1.81	324	1.88
26	2,4,4-Trimethylhexane	57	1.20	508	1.96
27	3,3,4-Trimethylhexane	43	1.13	563	2.04
28	3,3-Diethylpentane	57	2.33	261	1.95
29	2,2-Dimethyl-3-ethylpentane	57	1.96	310	1.94
30	2,3-Dimethyl-3-ethylpentane	57	1.28	452	1.86
31	2,4-Dimethyl-3-ethylpentane	43	1.79	310	1.78
32	2,2,3,3-Tetramethylpentane	57	1.28	389	1.60
33	2,2,3,4-Tetramethylpentane	57	1.29	381	1.58
34	2,2,4,4-Tetramethylpentane	57	2.49	219	1.75
35	2,3,3,4-Tetramethylpentane	43	1.74	333	1.85

Compounds are indicated by a skeleton structur
formula in which all hydrogen atoms are omitte
The reference number corresponds to table
which gives the names of the compounds.
compound 12 the peak 57^+ is given as 101
This is to conform to a formal rule that in the A
tables the maximum peak at 50 v is 100, and
happens that in this case 57^+ is less than 100
50 v.

Values of the parent ion peak at 128^+ range fro
6.4 to 0 with 16 values 0.05 or less. The norm
compound has by far the largest parent ion, as
always true in the paraffin series. Sixteen of th
17 compounds with two side chains on a carb
atom account for all the values of 0.05 or les

TABLE 2. *Mass spectra of nonanes at 70 volts ionizing voltage*

[Values preceded by an asterisk refer to ions that involve a rearrangement of atoms in the ionization process]

Number	Compound	Relative intensities at m/e values—																	
		27	29	41	43	55	56	57	69	70	71	83	84	85	97	98	99	113	128
1	CCCCCCCCC	29.1	36.7	40.5	100	12.1	16.7	67.0	2.34	11.8	19.7	0.20	6.36	23.3	0.47	2.66	4.53	0.14	6.38
2	CCCCCCCC C	21.1	23.1	34.2	100	8.89	14.8	51.2	3.34	1.76	26.6	.31	13.5	16.7	.06	0.32	0.82	7.34	2.08
3	CCCCCCCC C	17.8	27.8	30.7	37.6	8.88	23.9	100	2.63	5.03	8.05	.55	1.84	1.85	.28	12.7	8.84	0.79	1.65
4	CCCCCCCC C	20.4	21.5	25.7	100	11.8	7.96	25.4	2.62	20.9	27.5	.20	18.2	28.2	.03	3.06	1.42	.82	2.46
5	CCCCCCC C C	23.8	28.8	31.2	60.9	13.3	8.60	100	3.50	15.2	14.5	.45	1.50	1.97	.11	20.9	8.84	.04	1.17
6	CCCCCCC C C C	26.8	24.8	33.0	100	13.0	10.3	*71.4	4.71	3.32	*2.63	.42	20.2	26.8	.09	13.1	4.96	.03	1.27
7	CCCCCCC C	16.5	25	33.2	21.4	7.9	38.8	100	5.0	2.5	13.5	1.48	0.55	0.82	.22	0.03	0.05	2.5	0.74
8	CCCCCCC CC	20.1	16.8	25.0	100	10.7	9.81	17.1	4.53	3.67	13.4	0.22	28.1	24.1	.02	.12	.33	0.16	1.03
9	CCCCCCC C C	22.6	18.8	28.9	100	9.04	10.00	25.8	4.02	11.5	21.2	.40	9.51	33.9	.05	.14	.34	.62	0.66
10	CCCCCCC C C	22.0	29.0	35.1	49.3	8.52	23.1	100	2.44	5.46	10.8	.41	0.77	1.37	.03	3.76	10.5	.61	1.07
11	CCCCCCC C C C	24.0	*19.5	34.3	100	6.57	13.7	46.4	2.96	1.45	24.3	.12	3.67	13.2	.08	0.09	*0.20	8.01	2.80
12	CCCCCCC C	31.5	40.1	44.6	100	20.7	7.28	101.5	3.71	29.4	89.0	.61	0.12	0.44	.12	3.85	15.7	3.65	0.00
13	CCCCCCC CC	32.8	45.2	48.1	100	22.2	42.2	66.3	3.43	47.3	29.8	.41	2.77	11.00	.10	1.72	6.81	0.18	1.28
14	CCCCCCC C C C	19.0	34.5	31.8	*32.4	9.98	15.9	100	2.74	7.89	13.3	.45	0.11	0.36	.13	3.73	10.4	.32	0.65
15	CCCCCCC C	23.1	19.3	31.1	100	7.20	10.2	*28.1	5.70	0.56	*10.6	.21	14.7	70.1	.05	0.10	0.31	2.39	.00
16	CCCCCC CC C	24.1	17.8	30.2	100	13.1	11.6	*35.0	6.98	1.64	*4.10	.44	31.6	27.0	.06	1.05	2.44	0.06	.69
17	CCCCCC C C C C	26.6	26.1	34.9	75.2	13.8	10.9	100	4.95	13.2	14.6	1.11	2.64	4.15	.21	8.75	12.2	.08	.89
18	CCCCCC C C	21.5	25.4	31.0	61.7	11.6	2.55	*100	6.59	3.48	*6.77	0.72	7.94	28.5	.10	8.05	19.1	1.45	.02
19	CCCCCC CC C	32.5	50.5	50.2	*85.1	28.3	34.3	100	4.42	64.2	30.1	.64	0.34	*1.28	.20	4.16	13.0	0.05	1.51

TABLE 2. *Mass spectra of nonanes at 70 volts ionizing voltage*—Continued

[Values preceded by an asterisk refer to ions that involve a rearrangement of atoms in the ionization process]

Reference	Compound	Relative intensities at m/e values—																
		27	29	41	43	55	56	57	69	70	71	83	84	85	97	98	99	113
20	C CCCCCC CC	13.3	19.2	31.3	23.6	7.37	65.8	100	2.17	5.30	11.2	0.41	0.22	1.67	0.06	0	0.02	1.79
21	C CCCCCC C C	11.2	21.9	27.1	*13.6	4.81	36.9	100	1.56	4.58	15.2	.59	.12	*0.14	.07	0.04	.11	2.97
22	C CCCCCC C C	11.6	*16.6	26.3	18.9	5.12	37.3	100	1.30	4.32	17.5	.08	.04	.15	.06	0	0	4.31
23	C CCCCCC CC	18.8	13.2	30.5	100	6.83	*14.2	*30.8	10.2	0.92	*9.22	.52	26.4	65.2	.07	0	0	2.10
24	CCCCCC CCC	23.6	24.8	31.6	100	13.1	10.8	29.7	5.14	19.0	31.1	.84	13.2	28.9	.13	.11	.45	0.03
25	CCCCCC CC C	17.0	*12.0	25.1	100	7.18	9.29	23.1	9.19	3.97	14.3	.34	24.0	40.0	.03	.03	*.12	20
26	C CCCCCC C C	26.3	25.2	38.8	95.8	15.5	6.59	100	2.51	3.13	83.7	2.60	0.38	0.62	.16	4.38	17.8	3.41
27	C CCCCCC CC	26.9	36.2	39.6	*100	26.0	5.82	89.3	3.27	72.5	90.1	1.84	.34	*.28	.27	1.54	10.7	2.28
28	C C CCCCC C C	14.3	20.5	24.2	*24.9	8.39	1.64	*100	4.50	1.31	*1.84	0.74	.17	*.12	.05	11.2	19.3	0.04
29	C CCCCC CC C	12.4	20.7	29.2	*23.0	8.91	62.8	100	2.18	8.79	10.9	.72	.29	*.14	.13	0.11	0.59	.98
30	C CCCCC CC C	24.9	22.8	36.2	98.3	13.2	4.01	*100	10.7	3.14	*9.54	2.78	24.8	35.8	.14	4.27	14.5	99
31	CCCCC CCC C	16.0	10.3	24.2	100	6.87	7.78	*25.9	13.1	1.72	*4.01	0.73	25.0	43.2	.09	0.05	0.35	.04
32	CC CCCCC CC	15.8	21.8	32.4	*63.6	13.2	9.25	100	3.31	28.9	41.8	2.01	1.53	*2.47	.23	.92	9.24	2.07
33	C CCCCC CCC	16.7	*19.2	33.7	62.1	10.5	55.3	100	4.09	13.5	14.3	0.28	1.92	11.8	.45	.05	*.08	0.87
34	C C CCCCC C C	8.21	*16.2	23.2	*7.66	4.01	30.5	100	0.43	0.65	1.90	.15	*.02	*0.03	.11	.11	*.17	2.06
35	C CCCCC CCC	16.3	*8.44	29.0	100	6.35	*1.79	*32.2	14.9	1.58	*2.94	.33	27.1	58.3	.34	.04	.00	0.81

Compound No. 7, 2,2-dimethylheptane, is an apparent exception, but this is probably not significant as it was impure.

The 113^+ peak has values ranging from 8 to 0.03 with about half of the values less than 0.8. There is no obvious correlation with structure except that 10 compounds with ethyl side chains have small 113^+ peaks with an average value of 0.38 percent.

The 99^+ peak has a range of values from 19.1 to 0 with about half the values less than 1. As in the case of the 85^+ peak of the octanes, this peak tends to be large when there is an ethyl side chain or an ethyl terminal radical attached to a carbon atom with a side chain. In 14 compounds without terminal ethyl radicals (excluding *n*-nonane), values range from 1.42 to 0 with an average value of 0.28. In six of these cases production of 99^+ involves a rearrangement of atoms, and the values of 99^+ range from 0.2 to 0. Of the 20 compounds with ethyl radicals, four (21, 24, 29, and 31) have small values of 99^+, and other values are in the range 2.4 to 19.1.

In saturated hydrocarbons, ionization with breaking of a carbon bond and without further dissociation usually gives the largest peaks, and exceptions afford a distinctive feature that is useful in the identification of compounds. Nonanes 3, 4, 5, 6, and 35 have a 98^+ peak, which is larger than the 99^+ peak. In the last case both peaks are very small, but in the first four compounds this peak is a distinctive feature.

The complementary process to loss of an ethyl radical to give 99^+ is the production of the ethyl ion, 29^+. The 29 peak has a range of values from 50.5 to 8.44, and there is a rough correlation between the height of 29^+ and 99^+. Seventeen compounds with 99^+ less than 1 give a 29^+ peak ranging from 8.4 to 25 with a mean value of 18. In 18 compounds in which 99^+ is greater than 1 percent, 29^+ ranges from 17.8 to 50.5 with a mean value of 30.

The 85^+ peak has a range of values from 70 to 0.03 with about half of the values less than 2.5. As in the case of the 71^+ peak of the octanes, the height of the 85 peak depends on whether or not there are isopropyl terminal radicals or *n*-propyl terminal radicals attached to carbon atoms with side chains. Of the 13 compounds without terminal propyl radicals, all except *n*-nonane have peaks less than 2.5. This includes seven compounds in which production of 85^+ involves a rearrangement of atoms. Of the 22 compounds with terminal propyl radicals, four have small 85 peaks, and the others have peaks ranging from 4 to 70 percent.

In five compounds 84^+ is larger than 85^+, but in two of these the peaks are very small. 84^+ is distinctive in 2,3-dimethylheptane and in 2-methyl-3-ethylhexane. It is of interest that in the octanes the compounds 2,3-dimethylhexane and 2-methyl-3-ethylpentane have a 70 peak larger than 71^+. Also, the heptane, 2,3-dimethylpentane has 56^+ larger than 57^+. As all these molecules lose mass 44 in preference to 43, it is evident that the terminal isopropyl radical (the only common structural unit) must be removed with an additional hydrogen atom.

The complementary process to production of 85^+ is the production of 43^+. There is a correlation between the size of the two peaks, but there are many exceptions. 43^+ is the maximum peak in half of the nonanes, and the smallest value is 7.66. It is 100 in 14 of the compounds with terminal propyl radicals and in three other compounds. In one of these, No. 27, production of 43^+ and 85^+ involves a rearrangement of atoms.

71^+ has a range of values from 90 to 1.84 with about half of the values less than 14. In nine cases rearrangement of atoms is required to give 71^+, and these values range from 10.6 to 1.84 with a mean value of 5.7. In 26 cases where 71^+ is permitted, only two, No. 3 and No. 34, have values less than 10.6, and the mean value of 71^+ for the 26 compounds is 26.5. Four molecules with the terminal radical,

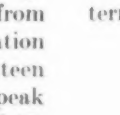

give the four largest 71^+ peaks.

70^+ is larger than 71^+ in four compounds, 3-ethylheptane, 4-ethylheptane, 3,4-dimethylheptane, and 3-methyl-4-ethylhexane, and in the last two cases it is large and distinctive. The octane, 3,4-dimethylhexane, gives a maximum peak at 56^+ in an ionization process similar to production of 70^+ in 3,4-dimethylheptane.

The ion 57^+ is the maximum peak in 18 of the nonanes, and in three of these, 18, 28, and 30, it requires a rearrangement to give 57^+. There seems to be no correlation in size between 57^+

and the complementary peak 71^+. Thus, for molecules with a tertiary butyl radical, 57^+ is by far the largest peak, and 71^+ is in most cases less than the average height.

Grouping of similar spectra is important in any attempt to analyze mixtures of nonanes. Eight compounds (No. 7, 20, 21, 22, 29, 32, 33, and 34) with terminal tertiary butyl radicals give similar spectra. These spectra closely resemble the octanes with tertiary butyl radicals. There are some differences to distinguish these nonanes. Compounds 20 and 29 have larger 56^+ peaks, and in compound 33, 43^+, 56^+, and 85^+ are larger, while in compound 32, 43^+, 71^+, and 99^+ are larger.

Seven compounds—No. 9, 15, 16, 23, 25, 31, and 35—with terminal propyl radicals at both ends, give similar spectra characterized by a large 85^+ peak with all heavier ions small. Another of these compounds, No. 11, differs by having a large 113^+ peak and a small 85^+ peak.

Compounds 12, 26, and 27 have similar spectra with peaks 43^+, 57^+, and 71^+ all of nearly maximum intensity. These are molecules with a terminal radical

$$\begin{matrix} & & \mathrm{C} & & \\ \mathrm{CCC}. & & & & \\ & & \mathrm{C} & & \end{matrix}$$

One other molecule, 2,2,3,3-tetramethylpentane, consists of this radical and a tertiary butyl radical, and the spectrum combines characteristics of both radicals with 71^+ of intermediate height.

It is to be emphasized that compounds in these groups have spectra that are similar but far from identical, and, with a few possible exceptions, each spectrum has distinctive characteristics that would serve to identify the compound when it is nearly pure.

IV. Conclusions

Mass spectra have been published for all isomers of paraffins with nine or less carbon atoms, and it is of interest to summarize some general rules relating spectra of paraffins to molecular structure.

1. The normal molecule gives the largest parent peak.

2. All compounds with two side chains on a carbon atom give very small parent peaks (0.05 or less).

3. The most probable dissociation processes commonly involve breaking a carbon bond without further dissociation, but there are a numbe[r] exceptions. Often these exceptions occur [in] molecules with a common structural unit.

Thus, molecules containing a terminal radi[cal]

$$\begin{matrix} \mathrm{CCC}, \\ \mathrm{CC} \end{matrix}$$

lose mass 44 in preference to mass 43.

4. Nonanes and octanes with a terminal [ter]tiary butyl radical have similar spectra with [57^+] by far the largest peak.

5. In molecules with terminal ethyl or pro[pyl] radicals, loss of these radicals is relatively pro[b]able.

6. Peaks involving rearrangements are, in ge[n]eral, small with many exceptions for 43^+ and [57^+] but not for other peaks.

7. Either 43^+ or 57^+ is the maximum peak [in] paraffins with more than three carbon atom[s]. The only clear exception is the octane 3,4-[di]methylhexane, which has a maximum peak at [57^+] but in 2,3-dimethylpentane, 56^+ and 43^+ [are] essentially equal.

8. The total ionization relative to *n*-butane [is] roughly constant for isomers and increases wi[th] increasing molecular weight.

Rules 4 and 5 often conflict, for if there is [a] terminal butyl radical the rest of the structu[re] does not influence the spectrum appreciabl[y]. This accounts for some of the instances not[ed] above where nonanes with terminal ethyl an[d] propyl radicals have small 99^+ and 85^+ peak[s]. There are other unrecognized factors that in[-]fluence the spectrum, and the rules are not suf[fi]cient to deduce the structure from the observe[d] spectrum.

It will be a long time before mass spectra of a[ll] the decanes have been measured, but spectra [of] paraffins with 10 or more carbon atoms can [be] measured, and such spectra can give incomplet[e] information about the structure of pure com[-]pounds of doubtful structure.

The analysis of mixtures of nonanes will, [in] general, be difficult or impossible unless the sample is a narrow cut containing comparatively few com[-]pounds. The practical experience in analyzing mixtures of octanes [4] will be directly applicable to nonane analysis. In a complicated mixture it would be necessary to analyze for groups with similar spectra as a group using an average pat[-]

tern. Comparable difficulties will be encountered in any method of analysis because of the great number of isomers.

V. References

[1] Catalog of mass spectral data, API Project 44, National Bureau of Standards.

[2] E. G. Bloom, F. L. Mohler, J. H. Lengel, and C. E. Wise, J. Research NBS **41,** 129 (1948) RP1912.

[3] Papers on the micromanometer by Maurice Greenough, William E. Williams, Vernon H. Dibeler, and F. Cordero. Publication pending.

[4] R. A. Brown, R. C. Taylor, F. W. Melpolder, and W. S. Taylor, Anal. Chem. **20,** 5 (1948).

Washington, October 5, 1949.

U. S. Department of Commerce
National Bureau of Standards

Research Paper RP2079
Volume 44, March 1950

Part of the Journal of Research of the National Bureau of Standards

Syntheses and Properties of Two Olefins, Six Paraffins, and Their Intermediates

By Thomas W. Mears, Abraham Fookson, Philip Pomerantz, Edwin H. Rich, Cecil S. Dussinger, and Frank L. Howard

As a part of a study of the desirability of certain hydrocarbon types as jet fuel components, eight aliphatic hydrocarbons have been prepared and purified. This report describes their syntheses and those of several intermediates. Physical constants were measured on the high purity products.

I. Introduction

During the last few years, the advent of reaction engines has presented new fuel problems; one attack on these problems has been the study of the properties of fuel components. The work described herein is part of a project sponsored by the National Advisory Committee for Aeronautics at the National Bureau of Standards, in which certain hydrocarbons are prepared in high purity for tests at the NACA Flight Propulsion Research Laboratory (Cleveland). The tests were selected primarily to provide data regarding the desirability of certain hydrocarbon structures in jet engine fuels. This report describes the preparation and purification of eight hydrocarbons. Common physical constants are given for these hydrocarbons and for several intermediate compounds synthesized for use in their preparation. The methods used for determination of physical constants are given in an appendix at the end of the paper.

II. Apparatus

1. Reaction Vessels

The majority of the reactions were carried out in two 50-gal commercial kettles, one constructed of stainless steel and the other of glass-lined steel. These kettles were double-walled and arranged so that steam or water could be circulated between the walls to maintain the reaction at any temperature from 5° to 150° C. The kettles were fitted with glass-lined steel condensers and arranged so that the jacket water temperature could be regulated. In this manner the condenser could be made to act as a reflux condenser, a dephlegmating column, or a "goose neck" for distillation. Reagents were added to the kettles by means of 5-gal glass-lined steel addition vessels and the rate of addition controlled by means of a neoprene compression valve. The reactions were stirred by means of either a slow-speed anchor type stirrer or by a high-speed Hastelloy propeller stirrer. The kettles were arranged so that reaction products could be distilled either from one to the other or into a 15-gal double-walled copper receiving vessel. Small-scale reactions were carried out in 5-liter glass flasks or 14-liter brass kettles.

2. Dehydration Apparatus

The dehydrations of the carbinols were carried out in the vapor phase, using aluminum oxide catalyst, at 400° C in the case of primary alcohols, and at 300° C in the case of secondary and tertiary alcohols. The aluminum oxide was contained in a stainless steel tube, 2 in. in diameter and 3.75 ft long. This tube was placed in a furnace made by winding 35 ft of nichrome wire (1 ohm/ft) around a 3.25 ft length of 2-in. pipe. The temperature was regulated by means of a variable transformer and measured by means of a thermocouple in a well embedded in the alumina. The products of reaction were condensed in a copper tube condenser after leaving the reaction zone. Flow of material to the apparatus was governed by use of a modified automobile carburetor as a

TABLE 1. *Distillation columns* [a]

Still no.	Type	Size	Packing	Pot capacity
		cm		*ml*
11	Total reflux intermittent take-off	600 × 5.1	35-in. ½-in. carbon raschig rings, then 200-in. 3/32-in stainless steel helices from 0.010-in. wire	
18	Podbielniak Hypercal	127 × 2.5	Heli-grid	250 to 5
19 to 20	do	250 × 2.5	do	250 to 5
21	Total reflux variable take-off	120 × 3.5	3/16-in. glass helices	2
22 to 24	do	183 × 2.5	3/32-in. stainless steel helices from 0.010-in. wire	1
25 to 27	do	183 × 2.5	3/16-in. glass helices	1

[a] Columns 19 and 20 have been equipped with a device for taking a sample in the middle of the night, thereby giving three equal samples in a 24-hr period. Both of these columns operate continuously with only occasional checking.

constant level device. To construct this apparatus, the carburetor was disassembled and all openings for special jets and pumps closed. Then a copper tube line was installed between the float-operated needle valve and a reservoir placed about 12 in. above the carburetor. A large separatory funnel (1-liter or 3-liter) served well as a reservoir. The float chamber cover contained a hole for pressure equalization (breather hole), which was retained in the final set up. Product delivery to the furnace was effected by means of a copper tube from the float bowl outlet to the furnace tube. A small, brass needle valve was installed in this line to regulate rate of flow. By means of this apparatus a constant-rate flow has been maintained for periods of several days during which no adjustments were necessary.

This same apparatus has been found to work well in reduced pressure experiments. In this case a line connected the top of the reservoir, the float bowl cover (breather hole), and the furnace tube. This line served to equalize the pressure in the three units of the system.

3. Hydrogenators

Hydrogenation of olefins was accomplished in high-pressure hydrogenators of the type described by Adkins [1].[1] Bombs of 3- and 20-liter capacity were used. Use of commercial nickel-on-kieselguhr catalyst gave no difficulty in any of the hydrogenations, the extreme conditions being 1,500 lb/in.^{2} pressure and a temperature of 160° C.

4. Stills

All the stills used in these preparations have been previously described [6]. For convenience the salient features of each are listed in table 1.

[1] Figures in brackets indicate the literature references at the end of this paper.

III. Methods and Technique

1. Preparation of Grignard Reagents

The preparation of Grignard reagents in large quantities (up to 300 moles) has been previously reported [6]. In the present syntheses a more or less general procedure for the preparation, coupling, and hydrolysis of the Grignard reagent was used. This general synthesis is given below using the *n*-butyl magnesium chloride synthesis of 5-nonanol as an example (see sec. IV, 1).

2. Determination of Physical Properties

The apparatus and technique for the determination of the freezing point, boiling point, refractive index, and density are described in the appendix. The final products (paraffin hydrocarbons) were filtered through silica gel before measurement of physical properties. The physical properties of the best sample are given in table 2.

The method for determining the quality of each distilled sample and the criteria for the grouping of these samples has been to plot the boiling point and refractive index against the volume distilled and to regard fractions comprising the flat "plateaus" as pure substances. Freezing points spotted at intervals along these plateaus aided in finding the purest sample for physical properties. Recently this method has been supplemented by the use of the difference in refractive index of each sample in relation to an arbitrarily selected reference sample. This property has been measured by means of a Rayleigh interferometer and has been found to be as sensitive to the purity of the sample as the freezing point and in some cases more sensitive. This method takes considerably less time than the freezing point determination and therefore can be applied to every fraction

is not only helps to find the best fraction but o identifies certain isolated "poor" fractions t occasional freezing points might overlook. nother advantage of the interferometer is that it rmits a critical study of the distillation of subnces that freeze with difficulty or not at all.

IV. Preparation of Materials

1. *n*-Nonane

n-Nonane was prepared in three steps: (a) thyl formate was reacted with *n*-butylmagnesm chloride to yield 5-nonanol; (b) 5-nonanol s dehydrated to give a mixture of nonenes; (c) e mixed nonenes were hydrogenated to *n*-nonane.

5-Nonanol. 5-nonanol was prepared by means a modification of the preparation given in rganic Syntheses [8].

Magnesium turnings (6.08 kg, 250 g atoms) re placed in the reactor and covered with 16 rs of ether To this was added about a liter of butyl chloride and a few crystals of iodine. The ixture was allowed to stand without stirring for out ½ hr, while the reaction started. During next 2 hr approximately 6 kg of *n*-butyl chlole was added while the reaction mixture was rred and cooled. The reaction was then diluted with 48 liters of ether and the remainder of the *n*-butyl chloride added. A total of 25.8 kg (278 moles) of *n*-butyl chloride was added over a period of 6½ hr. The apparent excess of *n*-butyl chloride was to compensate for material lost through the condenser during the initial stages of the reaction.

To the Grignard reagent was added 7.5 kg (125 moles) of methyl formate in 16 liters of ether. The rate of addition was rapid enough to maintain a brisk reflux and addition was completed in 5 hr. The reaction mixture became so thick that it was necessary to add 30 liters of ether and work the reaction mixture with a wooden paddle in order to loosen the stirrer.

The mixture was hydrolyzed with 18 liters of water followed by 75 liters of 18-percent sulfuric acid. During this time any ether that volatilized was allowed to distill off and was collected. A large quantity of magnesium sulfate settled out, and the major portion of the aqueous layer saturated with magnesium sulfate was siphoned off. An additional 35 liters of water was added to the mixture in the original kettle to bring the magnesium sulfate into solution and 50 liters of ether removed by distillation. The magnesium sulfate solution was siphoned off leaving the crude

TABLE 2. *Physical properties of compounds prepared*

Compound	Freezing point	Boiling point at 760 mm Hg	dt/dp at 760 mm Hg	Boiling range, 20 to 80% distilled	Density			Refractive index		
					at 20° C	at 25° C	dD/dt	at 20° C	at 25° C	dn/dt
	°C	°C	°C/mm	°C	g/ml	g/ml	(g/ml)/°C	n_D^{20}	n_D^{25}	per °C
Nonane	−53.528	150.770	0.0483	0.008	0.71758	0.71367	−0.000781	1.40541	1.40305	−0.000472
Methyloctane	−80.396	143.263	.0480	.014	.71346	.70961	−.000771	1.40307	1.40079	−.000456
Dimethylheptane	(a)	137.012	.0489	.007	.72560	.72163	−.000793	1.40878	1.40631	−.000494
Decane	−29.669	174.119	.0514	.013	.72987	.72608	−.000758	1.41184	1.40943	−.000484
Methylnonane	−74.65	167.00	.052	.023	.72636	.72250	−.000772	1.41000	1.40752	−.000496
Dimethyloctane	(a)	164.31	.051	.027	.73793	.73414	−.000757	1.41491	1.41266	−.000450
Hexene	−139.9	63.49	.042	.007	.6732	.6684	−.00096	1.3879	1.3850	−.00057
Methyl-1-pentene	−153.95	53.89	.042	.025	.6638	.6589	−.00098	1.3826	1.3797	−.00058
Methyl-1-octene	−77.86	144.85	.048	.12	.7343	.7303	−.00081	1.4184	1.4160	−.00048
Decene	−66.64	170.60	.053	.097	.7410	.7371	−.00077	1.4216	1.4190	−.00051
Methyl-2-nonene	----------	171	.06	----------	.7487	.7447	−.00078	1.4288	1.4264	−.00048
Methyl-3-nonene	----------	161.0	.05	----------	.7340	.7302	−.00076	1.4202	1.4178	−.00048
Dimethyl-3-octene	----------	161.5	.05	----------	.7690	.7651	−.00080	1.4267	1.4242	−.00049
5-Nonanol	+5.6	195.09 b 145	.046 c .18	.007	.8220	.8183	−.00074	1.4295	1.4267	−.00055
5-Methyl-3-nonanol	----------	208.4 b 154	.05 c .20	----------	.8281	.8245	−.00073	1.4343	1.4320	−.00045
5,5-Dimethyl-3-octanol	----------	189.1 b 138	.05 c .19	----------	.8293	.8249	−.00089	1.4375	1.4351	−.00049
3-Methyl-2-butanone	−94.4	94.2	.046	.93	.8100	.8061	−.00078	1.3887	1.3861	−.00053

a Did not freeze, glassy at low temperatures.
b Boiling point at 150 mm Hg.
c dt/dp at 150 mm Hg.

carbinol. The magnesium sulfate solutions were combined and extracted with 24 liters of distilled ether to recover any dissolved carbinol. The ether extract was added to the bulk of the crude carbinol in the original kettle and the ether removed by distillation. The crude carbinol was refluxed with 130 liters of 15-percent potassium hydroxide and finally removed by steam distillation. A total of 18.5 liters of crude carbinol was obtained.

The crude organic material was fractionated at 130 mm Hg in column 25. From this distillation there was isolated methyl valerate, bp 74° to 79° C, n_D^{20} 1.4003, 0.78 kg; *n*-amyl alcohol, bp 92° to 94° C, n_D^{20} 1.4101, 0.24 kg; and 5-nonanol, bp 133° to 138° C, 10.82 kg. This represents a 60-percent yield of 5-nonanol. A charge of the crude organic material was fractionated in column 8, and the results of this distillation are shown in figure 1. Cut A represents the methyl valerate, Cut B, *n*-amyl alcohol, and Cut C, 5-nonanol.

Nonenes. The dehydration of 5-nonanol was accomplished using aluminum oxide catalyst at 285° to 325° C. From 6.54 kg (45.3 moles) of 5-nonanol there was obtained 656 ml of water (80%) and about 7.75 liters of organic material. The organic material was distilled in column 22 to give 5.06 kg (40.2 moles) of nonenes, bp 140° to 150° C. This represents 88 percent dehydration on the basis of carbinol used.

A charge of 2,350 ml of nonene was fractionated in column 20 in an attempt to obtain high-purity samples for physical properties. The greater part of the olefin boiled at 148° to 149° C (uncorrected) but the refractive index (n_D^{20}) dropped steadily from

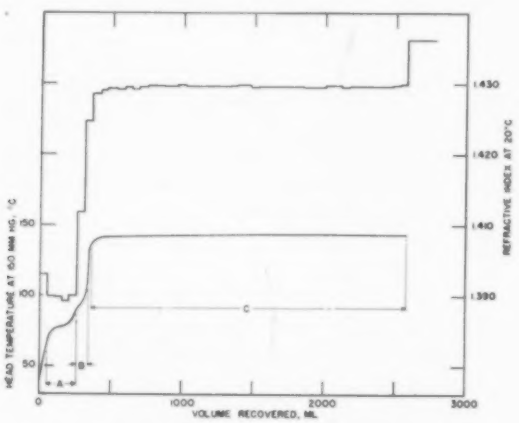

FIGURE 1. *Distillation of 5-nonanol.*

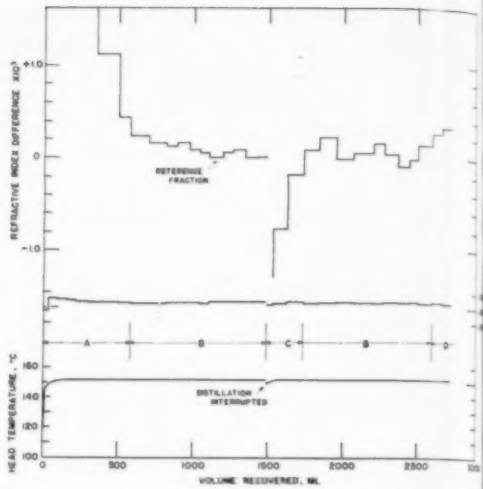

FIGURE 2. *Distillation of n-nonane.*

1.4207 to 1.4199. This is to be expected since the boiling points of the geometric isomers of 4-nonene and 3-nonene are very close together.

n-Nonane. The mixed nonenes (4.40 kg, 35 moles) were hydrogenated in the 20-liter hydrogenator using nickel-on-kieselguhr catalyst at 150 to 160° C. The initial pressure was 1,350 lb. From this operation there was obtained 4.06 kg (31.8 moles) of *n*-nonane. This corresponds to a 91-percent yield.

The crude *n*-nonane was distilled in two separate charges in column 19. The results for one charge are shown in figure 2. Here the usefulness of the interferometer is apparent, showing the low purity of the samples immediately following the point at which the still was accidently turned off. Portion B was collected as *n*-nonane, bp 151°, n_D^{20} 1.4052–53. The purified material from both runs was combined to give 2.38 kg of *n*-nonane, fp −53.528° C. This corresponds to a purity of approximately 99.9 mole percent [5, 11]. In addition, a sample of the purest material was reserved for the measurement of physical constants.

2. 2-Methyloctane

This nonane was prepared by the coupling of *n*-amylmagnesium chloride and methallyl chloride followed by hydrogenation of the resulting 2-methyl-1-octene.

2-Methyl-1-octene. *n*-Amylmagnesium chloride was prepared from 20 kg (188 moles) of *n*-amyl

loride and 4.52 kg (188 g atom) of magnesium ing 56 liters of ether as solvent in the same anner as described in the preparation of 5- nanol. The methallyl chloride was added in her solution over a period of 4 days and the re- tion mixture allowed to stand for 3 weeks. At end of this time the Gilman test [4] was gative for Grignard reagent.

The reaction mixture was hydrolyzed in the ual manner and the ether distilled from the re- tion kettle. There remained 32 liters of crude ganic product. This material was roughly ctionated in columns 25, 26, and 27 into three actions: bp 35° to 55° C, 4,890 ml; bp 55° to 0° C, 11,330 ml; and bp 140° to 150° C, 9,830 . The latter two fractions were redistilled and o major fractions collected, boiling at 110° to 4° C and 140° to 150° C. The fraction boiling 140° to 150° C contained the 2-methyl-1-octene, .7 kg, 84.5 moles, 45-percent yield. The other ajor fraction, boiling 110° to 114° C, was ap- rently a coupling product of two molecules of thallyl chloride. In order to obtain a sample r measurement of physical constants, 3,720 ml crude 2-methyl-1-octene was distilled in column . From this distillation there was obtained 400 ml of 2-methyl-1-octene, bp 143.5° to 145.0° (uncorrected), n_D^{20} 1.4185–86, in addition to the mple for physical properties.

2-Methyloctane. The 2-methyl-1-octene (4.7 kg, moles) was hydrogenated at 140° to 150° C ing nickel-on-kieselguhr catalyst. The initial ressure was 1,000 lb/in.^{2} at 25° C. The result- g 2-methyloctane (6,320 ml, 4.49 kg, 35 moles) as distilled in column 20 in two charges. From ese two distillations there was obtained 3.68 kg purified 2-methyloctane, bp 142.5° to 144° C ncorrected), n_D^{20} 1.4031 to 1.4034. These mples were further classified by means of the fferential refractive index in order to obtain the rest material for shipment. In this manner 53 kg of purified 2-methyloctane, fp −80.42° , was obtained. This corresponds to a purity of pproximately 99.8 percent [5]. In addition, a mple of the purest material was reserved for ysical constants.

3. 3,3-Dimethylheptane

This hydrocarbon was prepared by the coupling n-butylmagnesium chloride with tert-amyl loride.

The *n*-butylmagnesium chloride was prepared from 23.1 kg (250 moles) of *n*-butyl chloride and 6.08 kg (250 g atom) of magnesium using 75 liters of ether as solvent.

The solution of Grignard reagent was cooled to 10° C and tert-amyl chloride was added at the rate of 4.5 kg per day with constant stirring. A total of 23.9 kg (225 moles) of tert-amyl chloride was added over a period of 6 days. A heavy, white precipitate developed but the mixture remained fluid. The reaction mixture stood for 1 month before a negative Gilman test [4] was obtained. During this time the reaction was warmed to room temperature during the day and cooled at night. The mixture in the reaction kettle was worked up in the usual manner and some of the ether stripped off. From these operations there was obtained approximately 30 liters of crude organic material. This material was distilled in columns 22, 23, and 24, and the following fractions were obtained: bp less than 70° C, 16 liters (mostly ether); bp 70° to 130° C, 3.6 liters; bp 130° to 145° C, 7.2 liters (crude 3,3-dimethylheptane); and heavy residue 1.5 liters.

The crude 3,3-dimethylheptane gave a positive test for halogen [3]. Therefore the crude paraffin was divided into two parts, one of which was treated with alcoholic potassium hydroxide, while the other was treated with sodium in liquid ammonia. Both treated samples proved to be free from halogen and were distilled in two charges of 3,400 ml each in column 20. The distillation curve for one charge is shown in figure 3.

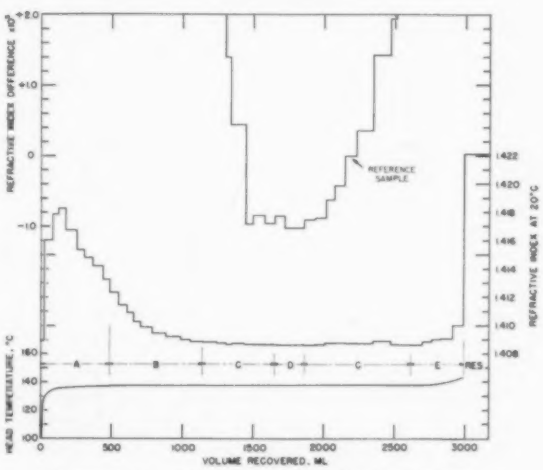

FIGURE 3. *Distillation of 3,3-dimethylheptane.*

From the distillation curve it is apparent that there is some compound of higher refractive index boiling only slightly lower than 3,3-dimethylheptane. Portion C was taken as the purified 3,3-dimethylheptane. Portion D was reserved for the measurement of physical properties.

From these two distillations there was obtained 2,710 ml (1.91 kg) of material for shipment, bp 137.01° C, boiling range (20 to 80 percent) 0.007° C, n_D^{20} 1.40872, in addition to a sample for physical properties.

4. *n*-Decane

n-Decane was prepared by the hydrogenation of 1-decene.

1-Decene. The 1-decene (9.1 kg) was obtained from commercial sources. A trial charge of this material (3,600 ml) was fractionated in column 18 in order to obtain a sample for physical properties and also to determine the amount of impurities in the crude decene. From the data obtained it was decided to distill the remaining crude 1-decene in columns 25 to 27 and to discard the first and last 10 percent. The forerun and residue from these runs were combined and refractionated and it was found that 1,195 ml of this material was satisfactory for hydrogenation. A total of 10.1 liters of 1-decene was obtained for hydrogenation in addition to a sample for physical properties.

n-Decane. Hydrogenation of the 1-decene (4.65 kg) was carried out at 170° C using nickel-on-kieselguhr catalyst. The reaction proceeded so rapidly that 500 lb/in.^{2} hydrogen pressure was quite sufficient. From this hydrogenation 4.62 kg (97 percent) of *n*-decane was obtained. The *n*-decane was fractionated in column 20. In two runs, 4.62 kg of *n*-decane was fractionated to yield 3.43 kg of *n*-decane, fp −29.678° C. This corresponds to a purity of 99.9 mole percent [5, 12]. In addition, a sample of the purest material was reserved for the measurement of physical constants.

5. 2-Methylnonane

This hydrocarbon was prepared by the dehydration of 2-methyl-3-nonanol followed by the hydrogenation of the mixture of olefins.

2-Methyl-3-nonanol. This carbinol was prepared by the reaction of isopropylmagnesium chloride with *n*-heptaldehyde. Isopropylmagnesium chloride was prepared from 6.08 kg (250 g atom) of magnesium and 19.6 kg (250 moles) isopropyl chloride over a period of 4 hr followed by 2 hr of stirring. To the Grignard reagent was added 26.5 kg (250 moles) of *n*-heptaldehyde. The initial reaction was quite vigorous and because this the addition of the heptaldehyde took 12 The reaction mixture was allowed to stand overnight, after which it was worked up in the usual manner and most of the ether stripped off in the reaction kettle. From this reaction there was obtained 42 liters of crude 2-methyl-3-nonanol.

The remaining ether was removed by distillation in column 21. A charge of 3,400 ml of the crude carbinol was fractionated in column 18 at 1 mm Hg. The principal products of this distillation were: fractions 6 to 10, bp 127° to 143° n_D^{20} 1.4263–53, 223 g; and fractions 25 to 57, bp 154° to 155° C, n_D^{20} 1.4341–48, 1,321 g. The first cut (fractions 6 to 10) was principally 1-heptanol from the reduction of the heptaldehyde. The second cut (fractions 25 to 57) was the 2-methyl-3-nonanol fraction. A high boiling residue remained, which was probably an aldol of heptaldehyde, and was not investigated.

The remaining carbinol was fractionated at 170 mm Hg in columns 25 to 27. The two principal products of all distillations were: 1-heptanol, 2.24 kg (19.3 moles, 7.7 %); 2-methyl-3-nonanol, 21.7 kg (137.2 moles, 54.9 %); and residue, probably an aldol, 3.25 kg (14.2 moles, 11.4 %).

2-Methylnonenes. An attempt was made to dehydrate the 2-methyl-3-nonanol using the oxalic acid method of Mulliken, Wakeman, and Gerry [7]. However, no 2-methylnonene was obtained, and the first drop from the ASTM distillation of the product boiled at 170° C and the 40-percent point was 220° C. It is apparent that there was very extensive polymerization, therefore this method of dehydration was rejected.

The large scale dehydration made use of alumina at 300° to 325° C. In the course of 6 hr 7.26 kg (45.9 moles) of 2-methyl-3-nonanol was passed through the dehydrator and 630 g (35.0 moles, 76.5 %) of water and 5.45 kg (38 moles) of organic material were recovered.

A charge (4,000 ml 2.97 kg) of the olefins was distilled in column 19. Data obtained on the distillation are shown in figure 4.

The dehydration of 2-methyl-3-nonanol might be expected to yield four decenes. The princi

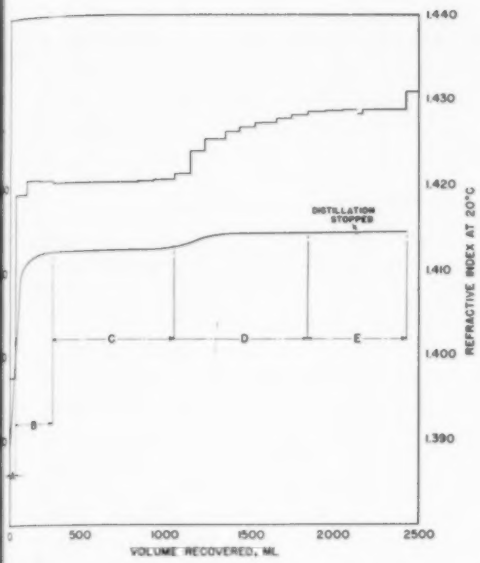

RE 4. *Distillation of olefins from the dehydration of 2-methyl-3-nonanol.*

s are 2-methyl-3-nonene, bp 163° C, n_D^{20} 1.420, 2-methyl-2-nonene, bp 169.9° C, n_D^{20} 1.4289. e two expected in smaller quantities are ethyl-1-nonene, bp 168.2° C, n_D^{20} 1.4241, and ethyl-4-nonene, bp 163° C, n_D^{20} 1.422. Since re are no data available on the properties of se compounds they were calculated by the thod of Francis [2]. These calculations seem to valid qualitatively in figure 4. The major flats *C* and *E* represent 2-methyl-3-nonene and ethyl-2-nonene, respectively. Cut *B*, which s slightly lower than the 2-methyl-3-nonene yet has a slightly higher refractive index, may either 2-methyl-4-nonene or else the minor metric isomer of 2-methyl-3-nonene. The upt rise of refractive index from *C* coupled with slow drifting into the flat at *E* indicates the sence of a compound of slightly lower boiling nt than 2-methyl-2-nonene with a refractive ex considerably lower. This is probably the ethyl-1-nonene. The low-boiling cut *A* is unubtedly heptenes from the dehydration of eptanol. The residue is the undehydrated binol.

The remaining 3,570 ml (2.48 kg) was distilled column 23 and the fraction boiling at 155° to ° C was collected as the methylnonenes. om both distillations, 3.43 kg (24.5 moles) of olefin was obtained for hydrogenation. The recovery of 1.05 kg of 2-methyl-3-nonanol indicated an efficiency of about 65 percent in the dehydration step instead of 76 percent as indicated by the recovered water.

2-Methylnonane. The mixed 2-methylnonenes were hydrogenated at 140° C using nickel-on-kieselguhr catalyst. The starting hydrogen pressure was 600 lb/in.^{2} The hydrogenation proceeded rapidly and was completed in 6 hr to yield 3.29 kg (23.1 moles, 94%) of 2-methylnonane.

The 2-methylnonane (4,200 ml, 3.08 kg) was distilled in column 19 and from this distillation there was obtained 3,580 ml of 2-methylnonane, mp −74.82° C. This corresponds to a purity of 99 mole percent [5, 10]. In addition, a sample of the purest material was reserved for the determination of physical constants.

6. 2,3-Dimethyloctane

This hydrocarbon was prepared by the dehydration of 2,3-dimethyl-3-octanol and hydrogenating the resulting olefins. The 2,3-dimethyl-3-octanol was prepared by the reaction of *n*-amylmagnesium chloride and 3-methyl-2-butanone.

3-Methyl-2-butanone. Methylisopropyl ketone was prepared by a modification of the method given in Organic Syntheses [9]. Tertiary amyl alcohol (10.6 kg 119 moles) was heated to 52° to 53° C and 19.1 kg (119 moles) of bromine was added over a period of 5 hr. The resulting mixture was orange-red in color, and this color persisted upon the addition of another 1.4 kg of tert.-amyl alcohol. Water (32 liters) was added and the reaction mixture refluxed for 24 hours after which the organic material was steam distilled. The distillate was saturated with soda ash, the aqueous layer withdrawn and extracted with 3 liters of ether. The ether was stripped off and the residue added to the crude methylisopropyl ketone. This was distilled in columns 22 and 23 to give 6.76 kg (78.6 moles, 66%) of methylisopropyl ketone, bp 92° to 95° C.

2,3-Dimethyl-3-octanol. *n*-Amylmagnesium chloride was prepared from 9.6 kg of *n*-amyl chloride (90 moles) and 6.95 kg of magnesium (90 g atom) in the same manner as described in the preparation of *n*-butylmagnesium chloride in the synthesis of 5-nonanol. To the Grignard reagent was added 6.76 kg (78.6 moles) of methylisopropyl ketone over a period of 2 hr. The

reaction mixture was stirred for the rest of the day and then worked up in the usual manner. The ether was stripped off and the crude carbinol distilled in column 22 at 130 mm Hg pressure. The fraction boiling at 130° to 135° C was collected as 2,3-dimethyl-3-octanol. From two distillations, 6 kg (37.9 moles, 48%) of 2,3-dimethyl-3-octanol was obtained. A 3,400-ml charge was redistilled in column 18 in order to obtain a sample for physical properties.

2,3-Dimethyloctenes. The 2,3-dimethyl-3-octanol was dehydrated over alumina at 300° C. A total of 5.85 kg (37 moles) of 2,3-dimethyl-3-octanol was passed through the reactor to yield 555 ml of water (30.8 moles, 83.5%) and 5.38 kg of organic material. A charge of this material was fractionated in column 20 in order to obtain pure olefin samples. Of the three most probable olefins, only one was obtained pure enough for physical constants. The properties of this olefin agreed with those previously reported [13] for 2,3-dimethyl-3-octene.

2,3-Dimethyloctane. The 2,3-dimethyloctenes (4 kg, 28.6 moles) was hydrogenated using nickel-on-kieselguhr catalyst at 140° C. The initial hydrogen pressure was 1,300 lb./in.^{2} Fractionation of the crude 2,3-dimethyloctane in two charges in column 20 gave 2.26 kg of 2,3-dimethyloctene bp 163.3° to 164.8° C (uncorrected), n_D^{20} 1.4146–47, as well as a sample for the determination of physical properties. The purest material for shipment was selected by means of interferometer examination, and amounted to 1.55 kg of purified 2,3-dimethyloctane, bp 163.95° C, boiling range (20 to 80 percent) 0.015° C, n_D^{20} 1.41493.

7. 1-Hexene

This hydrocarbon was prepared by the dehydration of 1-hexanol.

Commercial 1-hexanol (32 liters) was distilled in columns 25 to 27 in eight runs. The composite data of these runs were as follows: bp less than 146° C, 52 ml; bp 146° to 153° C, 2,525 ml; bp 153° to 155° C, 1,066 ml; bp 155° to 158° C, 26,900 ml; and residue 180 ml. The purpose of this distillation was to remove the 2-ethylbutanol (bp 146° to 153° C) from the 1-hexanol (bp 155° to 158° C). This carbinol would dehydrate to give hexenes boiling close to 1-hexene and therefore difficult to separate.

The distilled 1-hexanol (11.5 kg, 114 moles) was dehydrated over alumina at 400° C. From t dehydration there were obtained 1,985 ml (1 moles) of water and 13 liters of crude hexe This represented 98 percent dehydration on basis of water recovered. The crude olefin dried and distilled in column 21 to yield the foll ing fractions: bp less than 60° C, 50 ml; bp to 64° C, 3,970 ml (1-hexene); bp 64° to 65° 3,820 ml; bp 65° to 67° C, 3,200 ml (2-hexene bp 67° to 88° C, 950 ml; and residue 1,400 This distillation was very rough and no atte was made to obtain pure samples.

The stripped hexenes were redistilled in runs of approximately 4 liters each in columns and 20. From this distillation there was obtai 3.2 kg (4.2 liters) of purified 1-hexene, bp 63.47° boiling range (20 to 80%) 0.006° C, n_D^{20} 1.387 in addition to a sample for physical properties.

In order to determine the ratio of 1-hexene the 2-hexenes a small charge (1,500 ml) of cr dehydrated 1-hexanol was distilled in column This distillation gave the following fracti Fraction 1, bp 37° to 60° C, n_D^{20} 1.386, 15 fractions 2 to 9, bp 60° to 65.7° C, n_D^{20} 1.3880- 455 g; fractions 10 to 11 bp 65.7° to 68.0° n_D^{20} 1.3899 to 1.3934, 120 g; fractions 12 to 14 68.0° to 69.0° C, n_D^{20} 1.3955–71, 148 g; Fract 15, bp 69° to 107° C, n_D^{20} 1.4026, 37 g; and resi 120 g. This distillation indicated the ratio 1-hexene to the 2-hexenes to be 2 to 1.

8. 4-Methyl-1-pentene

This hydrocarbon was prepared from the c densation of isopropylmagnesium chloride and a chloride.

Isopropylmagnesium chloride was prepa from 3.15 kg (131 g atom) of magnesium and kg (140 moles) of isopropyl chloride in the s manner as described for *n*-butylmagnesium c ride in the preparation of 5-nonanol.

Allyl chloride, 10 kg (131 moles) was mixed w 10 liters of ether and the solution was added to Grignard reagent over a period of 3 days. D ing this time the temperature of the reaction m ture was held at 5° C. The reaction mixture worked up in the usual manner and the ether so tion of 4-methyl-1-pentene was dried over potas um carbonate. The ether was stripped off column 21 in several charges and all the resid from the stripping runs were combined and re

d in column 21. From this distillation there obtained 6.3 kg (75 moles, 57 percent) of ethyl-1-pentene, bp 50° to 56° C. About 1 of diallyl remained as residue.

A charge of 4 liters of crude 4-methyl-1-pentene was distilled in column 19 to yield 2.5 liters (1.5 kg) of purified 4-methyl-1-pentene, fp −153.95° C, and a sample for physical properties.

V. Appendix

1. Determination of Physical Constants

amples of *n*-heptane and 2,2,4-trimethylpentane are mitted to this Bureau, through the American Society Testing Materials, for certification as standard refer- fuels for knock rating work. Certification of these ples, representative of lots of material of over 100,000 is based, in part, on the determination of selected ical constants and the comparison of these physical tants with those measured on high-purity material. e constants are: boiling point, boiling range (20 to 80% illed), freezing point, density, and refractive index. other hydrocarbons and intermediates synthesized in Hydrocarbons Research Laboratory of the Engine Section are characterized by measurement of these erties, supplemented by measurement of: change in ng point with pressure near 760 mm Hg, change in sity with temperature, and change in refractive index temperature.

escriptions of the methods used have been published time to time [6, 16, 18], but it is considered advisa- to present the latest improvements used as part of a plete description. This appendix is such a description.

2. Freezing Point in Air

(a) Apparatus

he apparatus used for the determination of freezing ts in these laboratories contains features adopted from apparatus of Mair [14], Roper [15], Brooks, Howard, Crafton [16], at .l Glasgow, Streiff, and Rossini [5]. apparatus is shown in figure 5.

he sample is placed in tube *C*, which is 26 mm outside meter and 273 mm in length. It is rounded at the om, and the throat is reinforced with heavy glass so the tube may be gripped tightly with a clamp in r to hold it in place when the freezing substance mes viscous.

he electrically heated tube is shown in detail in figure 6. constructed from a pair of glass tubes (*K* and *L*), 41 36 mm in outside diameter and 240 mm in length. e tubes are closed at the base and fit within each other. ut the inner tube, *L*, is wound 49 turns of No. 32 do wire. This possesses a resistance of 185 ohms at m temperature. The resistance wire is secured in e with scotch tape and the annular space filled with affin wax. This wax was found necessary in order to ect the wire from corrosion from atmospheric con- ation. At the top of the tube the resistance wire is r soldered to copper leads *M*. The rates of cooling warming are controlled with high sensitivity by ns of a 1-amp variable transformer. Within the r heating element tube is placed a brass tube *D* closed

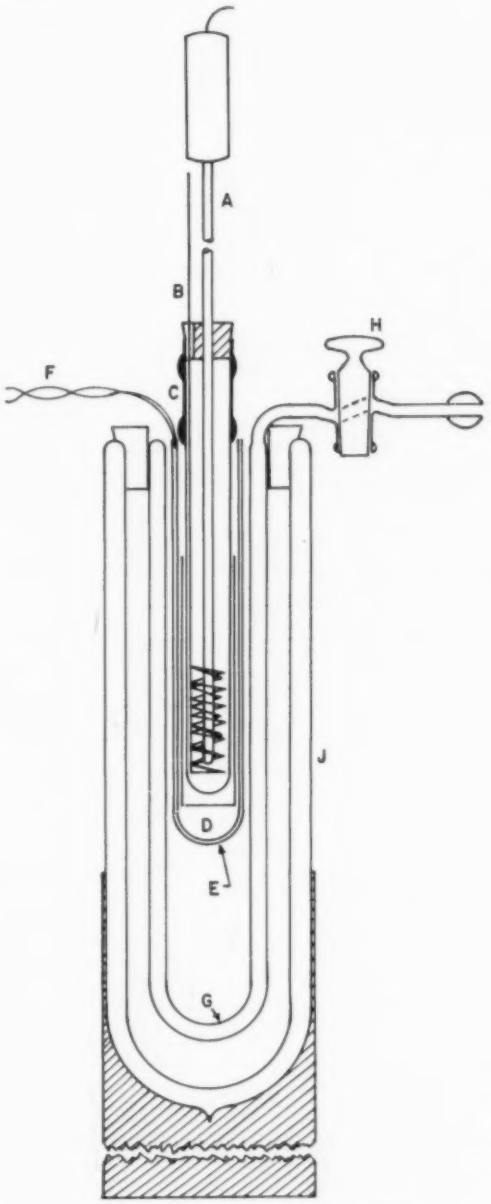

FIGURE 5. *Freezing-point apparatus.*

at the base and having a diameter of 30 mm and a length of 150 mm. This tube is covered with smooth aluminum foil. The purpose of this tube is to equalize the heat transfer over the entire sample and to shield the thermometer from outside radiations.

The cooling rate is roughly controlled by means of an unsilvered Dewar (*G*) (fig. 5) in which the degree of evacuation may be varied. This Dewar is 50 mm diameter, 69 mm outside diameter, and 38 cm in and is evacuated through a high vacuum stopcoc For this purpose a mechanical oil pump has adequate. A number 18 spherical joint connec Dewar to the pump line. Glass wool is placed bottom of this tube to help support the heating tub

The coolant reservoir is a silvered Dewar 95 mm diameter and deep enough to carry the rest of the ens Liquid nitrogen is used as the coolant for ma freezing below −50° C, and dry ice in carbon tetrac and chlorofrom for higher-freezing materials.

The sample is stirred by stirrer *B* (fig. 5). Tw of this double helical stirrer are shown in figure 7 first (A) is made to fit the tube snugly and the edg machined flat in order to scrape the walls of the tub second (*B*) is a loose-fitting double helical stirrer is the turns, except the bottom one, are held rigid vertical rod. This second stirrer was found to b more satisfactory and has since been used for all minations. It is made of 0.078-in. nichrome wir outer helix is 19 mm in diameter, the inner 14 mm the helical length is about 6 cm. The stirrer is by means of a crank operated by a direct current m the speed of which may be varied with a rheostat. length of the stroke is 4.5 cm. With this stirrer, n culty has been encountered in obtaining equili freezing point curves, even for very high purity *n*-he and 2,2,4-trimethylpentane.

The temperature is measured by means of a pla resistance-thermometer held in place by a cork wi

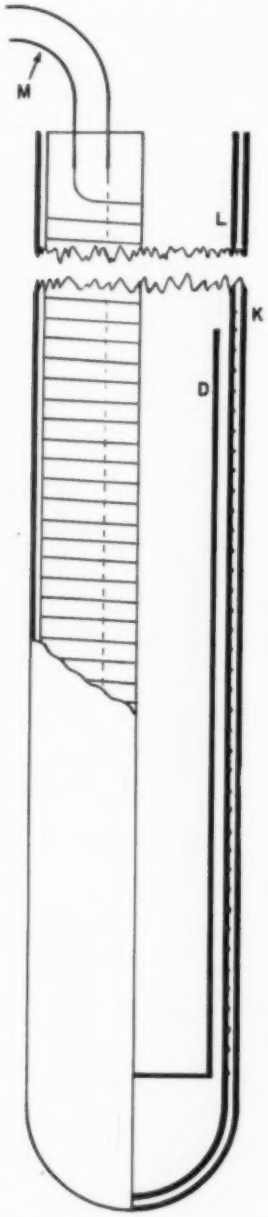

FIGURE 6. *Heating tube of the freezing-point apparatus.*

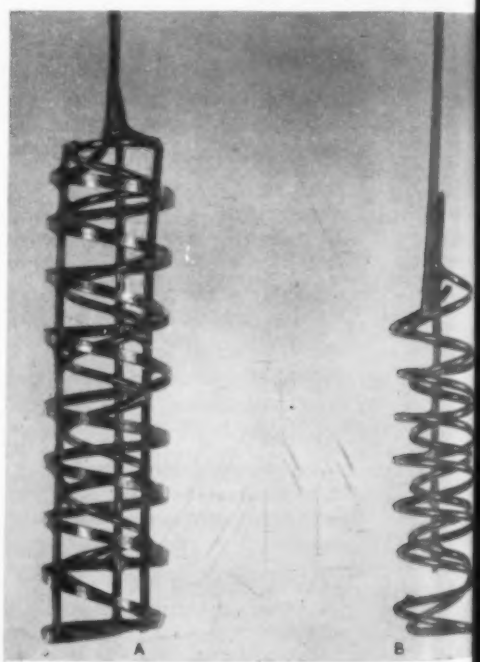

FIGURE 7. *Freezing-point stirrer.*

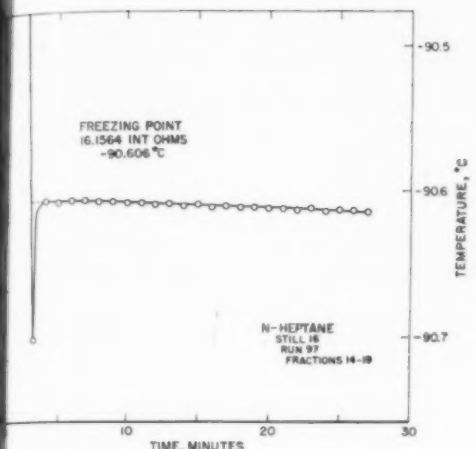

FIGURE 8. *Freezing curve of n-heptane.*

d to provide room for the stirrer. The resistance asured by means of a G–2 Mueller bridge with the accessories.

(b) Determination of the Freezing Point

apparatus is assembled as shown in figure 5 with ent sample in the freezing tube to cover the stirrer top of the stroke. The outer Dewar is filled with nitrogen to within about ½ in. of the top and kept at vel. The stirrer is run at a rate of about 60 strokes inute.

en the temperature reaches 20 to 30 degrees above xpected freezing point, the vacuum pump is started he pumping continued until the temperature has to 3 to 5 degrees above the expected freezing point, ich time the stopcock is closed and the pump stopped. lectric heater is started 10 to 15 degrees above the ng point and set to control the cooling at the desired Near the expected freezing point this rate is 0.25 40 degree per minute. The voltage setting on the ble transformer is based on previous determinations of g rates at various voltages and temperatures.

adings are begun at 1.0 to 1.5 degrees above the cted freezing point. At this time the cooling rate d be 0.25 to 0.40 degree per minute. Readings are each minute and when the material supercools more 0.2 degree below the expected freezing point it is d with a cold rod. At least 30 readings should be at 1-minute intervals after the curve reaches a peak ving supercooling. The curve is plotted and inter- d according to the method of Taylor and Rossini [17]. pical freezing curve is shown in figure 8.

a melting curve is desired the heater is set at a pre- mined voltage to give a warming rate of 0.4 deg C e liquid phase. The other experimental and cal- ive details are the same as with a freezing point.

is freezing point apparatus has been found to give: Rapid cooling with substances that freeze at low erature. By maintaining the air at atmospheric ure within the unsilvered Dewar, it is possible to reach the neighborhood of the freezing point much more quickly than can be done with a fixed vacuum Dewar. It is not necessary to start evacuating the Dewar until 20 to 30 degrees above the expected freezing point.

2. Accurate control of the cooling and warming rates. With the electric heater it is possible to control the cooling or warming rate quite accurately from 0.5 degree per minute cooling to 0.5 degree per minute warming.

3. Efficient stirring, which prevents excessive supercooling and aids quick recovery to the equilibrium state, only 3 to 5 minutes being necessary for recovery.

4. Equilibrium freezing curves, presumably obtained because packing of frozen material in the bottom of the tube is retarded by the new stirrer.

5. A precision of measurement of freezing points of about 0.003 deg C.

3. Boiling Point

The equipment for determining the distillation curves on *n*-heptane, 2,2,4-trimethylpentane, and other compounds as used now has been modified from the apparatus described in reference [19] and is similar to the apparatus designed by Mair [14].

(a) Apparatus

The apparatus used in the determination of boiling points is shown in figure 9.—The pot and column assembly is made by sealing a length of 25-mm tubing to a 125-ml round bottom flask taken from an ordinary distilling flask so that the over-all length is 52 cm. A side arm of

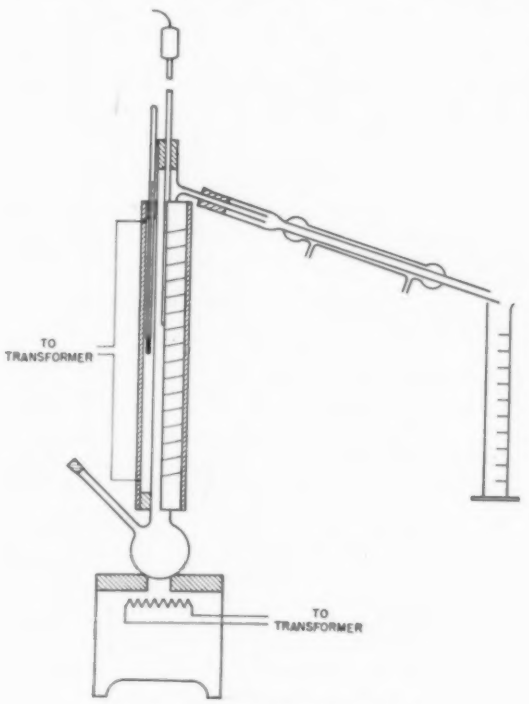

FIGURE 9. *Boiling-point apparatus.*

10-mm tubing is sealed onto the flask at a 45-degree angle to the column. A length of 56-mm tubing 37 cm long, which has two glass knobs sealed 1 cm from the top and bottom, is slipped over the column and an upper side arm is sealed into place. The latter is made of 8-mm tubing sealed to the column 5.5 cm below the top at an angle of about 18 deg below the horizontal. The jacket is separated from the column by two No. 30 corks, which are first bored and then split across the middle to facilitate placing. In one of the top halves is bored a small hole to carry the thermometer (0° to 360° C) for determining the temperature of the jacket. These corks are put in place so that they fit tightly. The jacket is wound with No. 22 (B & S) chromel wire spaced 2 cm apart, and anchored to the glass knobs at the end of the jacket. The jacket and wire are wrapped with one layer of 1/8-in. asbestos and finally covered with smooth tin foil. Corks are used for closing the charging tube and for carrying the resistance thermometer and for connecting the side arm into the condenser. The current input into the jacket heating wire is regulated by a variable transformer.

The pot is heated by a 660-watt laboratory heater, controlled by a 6-ampere variable transformer. The material distilled through the apparatus is condensed in a 300-mm West type condenser and caught in a 100-ml graduate.

The thermometric system used in the determinations consists of a Mueller resistance bridge, a platinum resistance thermometer, and a precision galvanometer. The galvanometer is adjusted so that a change of 0.0001 ohm on the bridge causes a deflection of about 4 mm on the galvanometer scale. The resistance thermometer is the standard four-lead type having a resistance of about 25.5 ohms at the ice point. This thermometer is calibrated every two years by measuring the resistance at the melting point of ice and the boiling points of oxygen, water, and sulfur.

(b) Method

The apparatus is assembled so that the end of the resistance thermometer extends about 6 in. below the side arm. Care must be taken that the bulb of the thermometer does not touch the walls of the column as this makes for erratic readings. The jacket thermometer is adjusted so that the scale readings are visible above the jacket beginning at about 25 deg C below the boiling point of the liquid. The receiver, a, 100-ml, graduate is adjusted so that the distillate from the condenser runs down the inner side of it.

While the sample is being heated in the pot, the jacket temperature is adjusted to 2 to 5 deg C below the boiling point of the material being distilled. When the liquid begins to simmer, the barometer reading, barometer temperature, and the time are taken. This procedure is repeated after 10, 25, 40, 55, 70, 80, and 90 ml have been distilled. The first drop to leave the sidearm after the vapor ring comes up is taken as the zero reading. At this point the resistance of the thermometer and the time are recorded. This is repeated at 2, 4, 6, 8, and 10 ml and every 5 ml thereafter until 90 ml. The rate of distillation is maintained at 5 ml per 1.0 to 1.25 min.

It has been advisable to take all readings with the commutator of the bridge in the normal position. T correction for the reverse reading is made by determi the resistance of the thermometer with the commutato the reverse position after the 30, 35, 45, and 50 ml read

Immediately after the distillation is completed, barometer should be calibrated by boiling distilled w in the apparatus. This corrects not only for the erro the instrument but also the personal error of the oper and, for compounds boiling near 100° C, for thermom error also.

The temperatures are calculated from the resistance the usual manner. The barometer is corrected for te perature and for the difference between the obser barometric pressure and the true pressure as determi by the water. The time furnishes the common ground comparison between temperature and pressure.

4. Refractive Index

Refractive indices are measured on a precision refractometer. This instrument is an Abbe-type refr tometer with the prisms movable in a near-horizontal pla rather than in a vertical plane. The scale is calibra linearly in arbitrary units, and readings are converted refractive index by use of a set of conversion tables fu nished with the instrument. The instrument is readable about 0.002 unit in the arbitrary scale, which, in the nei borhood of n_D^{20} 1.39, is equivalent to about 0.000012 uni refractive index. The reproducibility of readings by skilled operator is about 0.00002 unit of refractive ind Temperature is controlled by circulation of water from constant-temperature bath through a chamber arou the prisms. The constant-temperature bath is of standa design, equipped with two mercury thermostats, one at near 20° C and the other near 25° C. The light sou is a sodium vapor lamp.

The technique used in measuring the refractive index Ten readings are taken on a sample of 2,2,4-trimeth pentane (a working standard), five while approaching t demarcation line from one direction, and five from t opposite direction. The temperature (at the prism) measured to 0.01° C by a mercury thermometer for ea reading. These values are averaged. Immediately the after a sample of the material to be tested is put into t instrument and ten readings are taken in the same manne A comparison of the average of these readings with th obtained on the working standard gives the difference refractive index between the working standard and t compound under test. In this way, instrumental erro are practically eliminated. The refractive index of th working standard is measured periodically by comparis with the standard sample of 2,2,4-trimethylpentane (N Standard Sample 217), the refractive index of which h been accurately measured (to ±0.00002) by the Optic Instruments Section.

Recently, refractive indices of certain compounds ha been measured by comparison with a standard in a Re leigh interferometer. This instrument measures the diffe ence in refractive index between two samples with a great precision (about ±0.000004 with a 1-cm cell in the nei borhood of n_D 1.39 to 1.40) than the refractometer does

5. Density

thin-walled, glass-stoppered picnometer of about 50-ml rity is used in the determination of density (see fig. Measurements are generally made at temperatures 20° and 25° C.

he sample is placed in the picnometer, filling it nearly he cap. The picnometer and sample are immersed in nstant-temperature bath and allowed to remain for 1 At the end of this time the sample is drawn from the of the picnometer with a capillary tube connected vacuum line. The liquid is first drawn out until the is just above the mark, the end of the capillary run nd the walls to dry them, and finally the liquid level djusted so that the bottom of the meniscus is level with line. The picnometer is then stoppered and the bath erature observed.

he picnometer is dried, immersed in acetone, dried n, and weighed. After weighing, the picnometer is tied, washed with acetone, and dried. The empty flask is then dipped in acetone, dried, and weighed. Finally, the barometer and barometer temperature are read and the psychrometer reading taken. By suitable calculations, the mass in vacuo is obtained.

FIGURE 10. *Picnometer used for measuring density.*

The volume of the flask is determined by distilling water into the picnometer and then proceeding as outlined above to obtain the mass of water in vacuo. The density of water at that temperature is taken from tables and the volume of the flask calculated. The flask is calibrated at both temperatures.

From these data, the density of the sample at temperatures near 20° and 25° C is calculated and corrected to 20° and 25° C.

VI. References

[1] H. Adkins, Reactions of hydrogen, chapter III (Univ. Wisconsin Press, 1937).

[2] A. W. Francis, Ind. Eng. Chem. **35,** 442 (1943).

[3] L. Gatterman and H. Wieland, Laboratory methods of organic chemistry, p. 45 (MacMillan & Co., Ltd., London, 1941).

[4] H. Gilman and F. Schulze, J. Am. Chem. Soc. **47,** 2002 (1925).

[5] A. R. Glasgow, Jr., A. J. Streiff, and F. D. Rossini, J. Research NBS **35,** 355 (1945) RP1676.

[6] F. L. Howard, T. W. Mears, A. Fookson, P. Pomerantz, and D. B. Brooks, J. Research NBS **38,** 365 (1947) RP1779.

[7] S. P. Mullekin, R. L. Wakeman, and H. T. Gerry, J. Am. Chem. Soc. **57,** 1605 (1935).

[8] Organic syntheses, second collective volume, p. 179 (John Wiley & Sons, Inc., New York, N. Y., 1943).

[9] Organic syntheses, second collective volume, p. 408 (John Wiley & Sons, Inc., New York, N. Y., 1943).

[10] G. S. Parks, T. J. West, and G. R. Moore, J. Am. Chem. Soc. **63,** 1133 (1941).

[11] A. J. Streiff, E. T. Murphy, J. C. Cahill, H. F. Flanagan, V. A. Sedlak, C. B. Willingham, and F. D. Rossini, J. Research NBS **38,** 53 (1947) RP1760.

[12] A. J. Streiff, E. T. Murphy, J. C. Zimmerman, L. F. Soule, V. A. Sedlak, C. B. Willingham, and F. D. Rossini, J. Research NBS **39,** 321 (1947) RP1833.

[13] F. C. Whitmore and W. L. Evers, J. Am. Chem. Soc. **55,** 812 (1933).

[14] B. J. Mair, J. Research NBS **9,** 457 (1932) RP482.

[15] E. E. Roper, J. Am. Chem. Soc. **60,** 1693 (1938).

[16] D. B. Brooks, F. L. Howard, and H. C. Crafton, Jr., J. Research NBS **23,** 637 (1939) RP1259.

[17] W. J. Taylor and F. D. Rossini, J. Research NBS **32,** 197 (1944) RP1585.

[18] D. B. Brooks, R. B. Cleaton, and F. R. Carter, J. Research NBS **19,** 319 (1937) RP1027.

[19] C. W. Kanolt, BS Sci. Pap. **20,** 619 (1925) S520.

WASHINGTON, July 27, 1949.

S. Department of Commerce
tional Bureau of Standards

Research Paper RP2080
Volume 44, March 1950

Part of the Journal of Research of the National Bureau of Standards

ffect of Deuteration, Oxidation, and Hydrogen-Bonding on the Infrared Spectrum of Cellulose

By John W. Rowen and Earle K. Plyler

Regenerated cellulose films were immersed in heavy water (99.58% D_2O) at temperatures up to 52° C for as long as 100 hours in an attempt to effect a substitution of D for the H in the OH groups of the cellulose. The intensity of the OH vibration in the 3-micron region of the spectrum of the films decreased very little. A weak OD vibration appeared in the 4-micron region. The results indicate that only a small fraction of the OH groups of the cellulose participated in an exchange under the conditions of the experiments.

The infrared spectra from 2 to 16 microns of cellulose nitrate, nitrogen dioxide oxidized cellulose, alginic acid, and sodium alginate are recorded. A comparison of the spectra of these polysaccharides indicates that the strong band at 5.75 microns in the spectrum of the oxidized cellulose is due to the C=O vibration of the carboxyl group, and that the bands at 6.07 and 7.01 microns are due to nitrogen-oxygen vibrations.

The intense bands in the 3-micron region of the spectra of a number of cellulose derivatives, attributed to hydroxyl groups, were examined with the aid of the high-dispersion lithium fluoride prism. The minima of the bands were exactly at or close to 2.86 microns (3,500 cm^{-1}). The possibility of the existence of a common type of hydrogen bond in the cellulose derivatives is discussed.

I. Introduction

A continuation of work previously reported [1][1] s led to further observations on the structure cellulose. The infrared spectrophotometric asurements reported here pertain to three sepate aspects of cellulose chemistry. The experints and spectral measurements represent an empt to answer questions relating to (a) the change reaction between regenerated cellulose d deuterium oxide, (b) the spectrum of cellulose ntaining carboxyl groups, and (c) the nature of drogen bonding in cellulose and its derivatives. e experiments bearing on the exchange reaction ll be discussed first. The work on the exchange ction should be considered as a progress report. is presented in such detail because the results pear to be in somewhat surprising contrast to her findings.

[1] Figures in brackets indicate the literature references at the end of this per.

II. Deuteration of Cellulose

Champetier and Viallard [2] reported that native cellulose undergoes the heterogeneous exchange reaction represented as follows:

$$C_6H_7O_2(OH)_3+3D_2O\rightarrow C_6H_7O_2(OD)_3+3H_2O,$$

and that the reaction goes to completion in 36 hr at 30° C. This implies that all of the hydroxyl groups are accessible to the D_2O molecules and hence available for the exchange. On the other hand, Frilette, Hanle, and Mark [3] studied the reaction, employing both native and regenerated cellulose and concluded that the hydroxyls were not equally accessible. Only 64 percent of the hydroxyl groups of the native cellulose and 66 to 89 percent of the hydroxyls in viscose rayon were found to participate in the exchange in their experiments in 168 hr at 25° C.

Whether all or only a part of the hydroxyls in cellulose are available for the exchange reaction

has an important bearing upon the present-day concept of the structure of this natural polymer. Cellulose is generally believed to consist of a network of long chain molecules arranged in more highly ordered (crystalline) regions and less well-ordered (amorphous) regions. Hydroxyl groups buried inside the crystalline regions would not be expected to be as accessible, and hence as free, to participate in the exchange with deuterium oxide as hydroxyl groups elsewhere in the cellulose.

The extent of the exchange reaction in the studies referred to above was deduced from the change in density of the heavy water. However, in this work infrared spectrophotometry was used in detecting the replacement of hydroxyl hydrogen by deuterium. This method has been applied successfully to the evaluation of the exchange between D_2O and β-methyl glucoside, β-methyl xyloside, α-methyl mannoside, L-rhamnose, and L-sorbose.[2] It was found using the spectroscopic method that the hydroxyl hydrogens of these water soluble compounds are completely exchanged for deuterium in a few hours at 25° C. The exchange is noted in the infrared spectra by the appearance of intense absorption at about 4 μ with simultaneous disappearance of the intense absorption at 3 μ. The absorption at 3 μ is known to be characteristic of hydroxyl hydrogens bonded through a hydrogen bridge to another oxygen atom, and that at 4 μ to hydroxyl deuterium similarly bonded.

Two types of regenerated cellulose films were used in the work to be reported. There was no essential difference in results. The first was prepared by deacetylation of cellulose acetate [1], and the second was commercial cellophane sheeting obtained from the Sylvania Division of the American Viscose Co. The films were 3 to 13 μ thick and were mounted in a stainless steel frame to facilitate handling. The mounted films were dried in an oven for 16 hr at 105° C in a special glass chamber (capacity 10 ml) with its ground glass cover ajar. Liquid heavy water, 99.56-percent D_2O, was run into the chamber from a sealed storage bottle, completely filling it, and the cover was put in place and sealed with a thin film of silicone grease. The cellulose was kept in contact with the D_2O for periods of time ranging from 25 to 100 hr at temperatures from 25° to 52° C. The film was removed and either dried immediately placed in the beam of the infra spectrophotometer [4] in room air at 40-perc relative humidity. Thus the transmission of film in the 2- to 4-μ region could be measu within a few minutes with little opportunity moisture from the air to enter the film and rev the reaction.

The absorption at 3 μ of the film prepa according to the procedure just described wo represent OH groups in the cellulose that had exchanged with D_2O and OH in water in the cel lose that had not been eliminated by the drying by diffusion into the D_2O. The contribution this ordinary water to the absorption at 3 μ wo be small, at least at the time the film was remov from the D_2O.

In order to find out whether there was a reve of the deuteration reaction and removal of deuterium from the cellulose during the measu ments, deuterium-treated films were dried un two conditions, in an oven at 105° C and o anhydrous calcium sulfate at room temperatu The films were removed periodically, and t transmittance at 4 μ relative to that of the u deuterated cellulose was computed. As may b seen from the lower curve in figure 1, the rate loss of the deuterium, as evidenced by decre in the 4-μ band, was so slow at room temperatu as to be insignificant for the first several hours.

In the first experiment designed to observe t extent of reaction, the regenerated cellulose fi

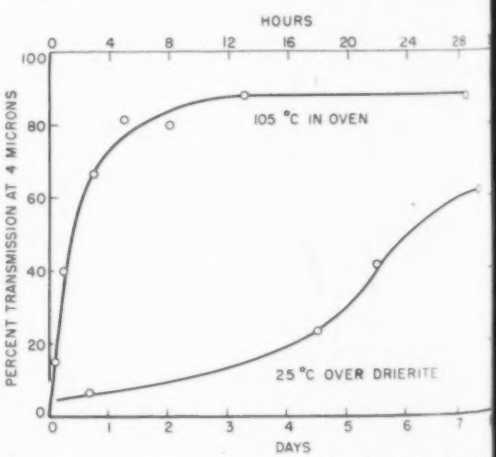

FIGURE 1. *Comparative rates of loss of deuterium fr cellulose under two conditions of drying.*

[2] Unpublished experiments carried out in collaboration with Lester Kuhn of the Ballistics Research Laboratory, Aberdeen Proving Ground, Aberdeen, Md.

as exposed to 99.56-percent D_2O as outlined ove for 72 hr at 25° C. Following the treatment e film was dried over anhydrous calcium sulfate 25° C for 48 hr, and its spectrum was then corded with the Perkin Elmer [5] infrared spectometer. The spectrum of the treated film had extremely weak band at approximately 4 μ th no apparent change in intensity of the band 3 μ.

This attempt to deuterate the cellulose was llowed by seven other experiments in which the me of exposure was varied from 25 to 100 hr nd the temperature from 25° to 52° C. In no se was more than a barely perceptible diminuon of intensity of the 3-μ band observed. This egative result is in sharp contrast to the complete isappearance of the 3-μ band in the spectra of the arbohydrates mentioned above.

In the final experiment, the dried film of reenerated cellulose was exposed for 100 hr at 52° to the D_2O. The recording of the spectrum by he Baird spectrophotometer was started under oom conditions of 40-percent relative humidity 1 in after the film was removed from the reaction essel, and the recording was completed in 4 min. The spectrum of this treated film was recorded at 0-min intervals during the first 3 hr of its approach to equilibrium with the 40-percent relative umidity of the room. The spectrum of the dried, ndeuterated, regenerated cellulose, figure 2, A, is ompared with that of the same specimen 60 min fter removal from the liquid D_2O, figure 2, B, nd 100 minutes after removal, figure 2, C. The pectrum of the treated film immediately after emoval from the D_2O is not shown because of the partial overlapping of the 4-μ band into the 3-μ band.

The absorption at 3.47 μ, attributable to the C−H stretching vibration, serves as an internal standard to which the variations in intensity of the other bands may be referred. A comparison of the intensity of the 3-μ band before and after exposure to the D_2O reveals little change in the intensity of this band. Assuming the Lambert-Beer law to be applicable to this system and further assuming the contribution of any sorbed H_2O to be low, one would have expected a 50-percent deuterium exchange to increase the percentage transmittance from the observed value of 17 percent (fig. 2, A) to about 40 percent.

The spectrum in figure 2, C was recorded 40

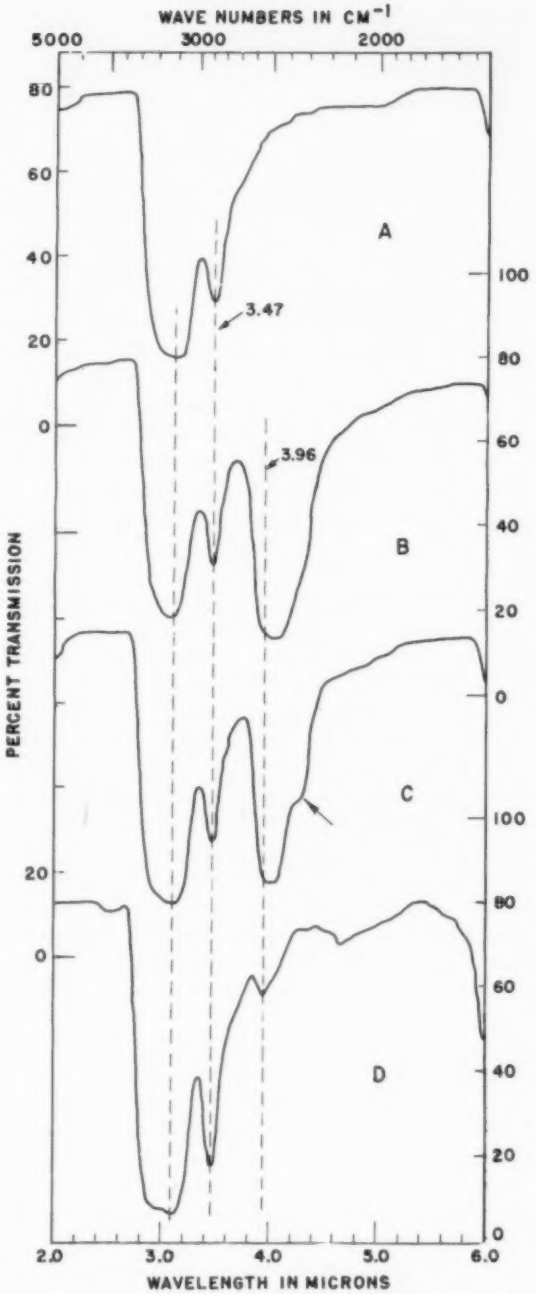

FIGURE 2. *Effect of deuteration on the infrared absorption spectrum of a film of regenerated cellulose.*

A, Cellulose before exposure to heavy water; *B*, cellulose 60 min after exposure to heavy water for 100 hr at 52° C; *C*, same as *B*, but 40 min later; *D*, same as *C* after attempts to remove O−D band by drying for 5 days at 25° C over anhydrous calcium sulfate, drying in oven at 105° C, immersion in water at 25° C for 6 hr, and drying.

min after obtaining that in B. During this time the OD band at 4 μ had decreased in intensity and showed the shoulder or secondary peak indicated by the arrow. This vibration at 4.3 μ was present in the spectra for most of the eight experiments and suggests that the OD band may be made up of at least two bands representing two vibrational frequencies. The absorption in the region of 4 μ for the deuterated carbohydrates mentioned above was usually found to consist of two or three separate and distinct vibrations. An attempt was made to eliminate the OD absorption from the film giving the spectrum shown in figure 2, C by drying it over anhydrous calcium sulfate in a desiccator at 25° C for 18 hr. A fairly strong OD band was still present. The film was then immersed in ordinary water at 25° C for 6 hr and dried. The spectrum of the film, figure 2, D, still showed a small but significant absorption band at 4 μ. Evidently the removal of the last trace of deuterium from the film is difficult.

The relative decrease in intensity of the band at 3 μ in figure 2, B and the residual absorption at 4 μ in figure 2, D indicate that some deuteration has taken place. However, it appears that the extent of reaction was either small, or that the HOH formed as a result of the reaction remained in the cellulose film and did not migrate into the surrounding D_2O in the time and at the temperature of these experiments. Since such extremely slow diffusion of normal H_2O from the film into the D_2O seems unlikely, it must be concluded that the extent of deuteration of the regenerated cellulose film under the above conditions was much less than 50 percent, contrary to the findings of previous workers.

III. Carboxyl Group in Oxidized Cellulose

Earlier work showed that cellulose oxidized with nitrogen dioxide had three main new absorption bands [1] located at 5.75, 6.07, and 7.81 μ. Nitrogen dioxide is said to be specific and to oxidize the primary alcohol group on the number six carbon atom to a carboxyl group [7, 8].

Many organic acids containing carboxyl groups have absorption bands at approximately 5.75, 6.07, and 7.81 μ [9, 10]. It was, therefore, tentatively concluded at that time that the three absorption bands at 5.75, 6.07, and 7.81 μ were in some way connected with the carboxyl grou However, our attention was called to the fa that the two intense bands at 6.07 and 7.8 were also present in the spectrum of cellul nitrate. Although the amounts of cellulose trate formed in the reaction with nitrogen diox are said to be relatively small [7, 8], it is possi that under the conditions of our experime appreciable amounts of cellulose nitrate w formed. The cellulose nitrate and adsorb nitrogen dioxide might possibly give rise to t strong bands at 6.07 and 7.81 μ. Any adsorb water in the film would make a small contribut to the 6.07-μ band, as possibly would carbo groups. In view of the above it was, the fore, desirable that the spectrum of the N oxidized cellulose be compared with the spe trum of cellulose nitrate and with a closely relat polysaccharide molecule containing carbo groups.

The polysaccharide alginic acid is a polym of D-mannopyrano-uronic acid. The stereois meric difference between NO_2 oxidized cellul (celluronic acid) and alginic acid may be se from the following structural formulas. T units in alginic acid are linked through the nu

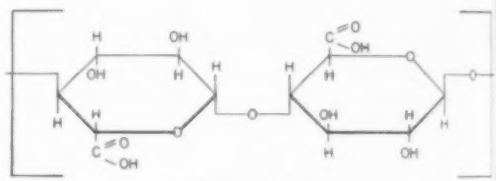

CELLURONIC ACID

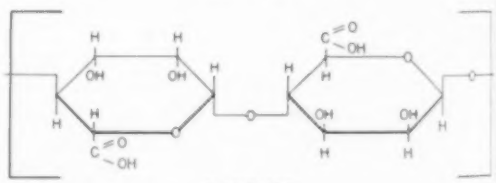

ALGINIC ACID

ber one and number four carbon atoms, a like NO_2 oxidized cellulose they have carboxy groups in the number six position. The algin acid films used in this work were prepared fro sodium alginate. One-half gram of the latte obtained from the Algin Corporation of Ame ica, was dissolved in 30 ml of distilled water co

ining 0.3 ml of a 5-percent stock solution Aerosol O. T. (The Aerosol O. T. facilitated pping of the film and had no effect on the ectrum of the polymer). The solution was st on a chromium-plated surface using a blade h a 0.04-in. clearance. This yielded a film μ thick. The film so obtained was then verted into alginic acid by treatment with N hydrochloric acid. The resulting alginic d film was found to be gelatinous and quite ong after washing in cold water. The films re dried in air for 24 hr and then over anhydrous cium sulfate for 48 hr before recording the ectrum. The cellulose nitrate was prepared by method of Davidson [6]. One-half gram of ed nitrated cotton was dissolved in 100 ml of rm ethyl acetate. A film 6.9 μ thick was n prepared with the aid of a 0.04-in. Bird m applicator. The NO_2 oxidized cellulose film s prepared from regenerated cellulose obtained deacetylation of cellulose acetate [1]. The llulose film so obtained was suspended at room mperature in a glass chamber that was evacu- ed. Dry nitrogen dioxide was then passed into e chamber. The films were left in the nitrogen oxide atmosphere for 2 hr and then soaked for nother 2 hr in distilled water with three changes water. The spectrum of the three polysaccharides prepared in the above manner are shown figure 3.

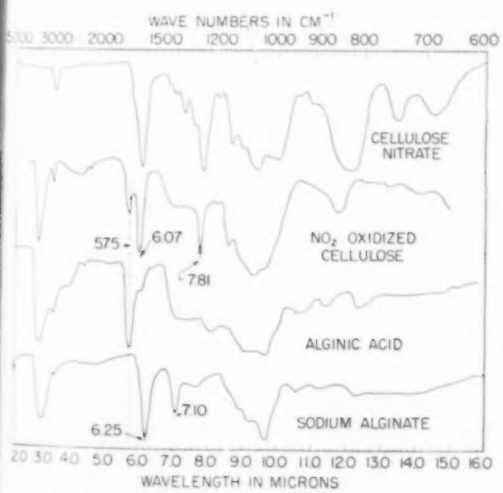

FIGURE 3. *Comparison of spectra of cellulose nitrate, oxidized cellulose, and alginic acid.*

It is noted in figure 3 that the two questionable bands (6.07 and 7.81 μ, measured to the second decimal place in order to compare their positions in the two spectra) are absent in alginic acid, but present in cellulose nitrate. The intense absorption at 5.75 μ in the spectrum of alginic acid is undoubtedly due to the C=O vibration of the carboxyl group. The shift in band from 5.75 to 6.25 μ, which occurs in the neutralization of the alginic acid, is noted in figure 3. This behavior is apparently characteristic of the carboxyl group when it is converted to the ionized carboxylate group. It has been observed [10, 11] when the acid group is converted to the sodium salt. It then appears, at this point, that although the band at 5.75 μ in the NO_2 oxidized cellulose is certainly due to a C=O vibration in the chain molecules, it is highly probable that the other two bands (the one at 6.07 and 7.81 μ) are related to nitrogen-oxygen vibrations [12].

IV. Hydrogen Bonding in Cellulose

In the earlier work [1] the regeneration of the cellulose from cellulose acetate was accompanied by a shift in the minimum of the OH band to slightly longer wavelengths. The minimum appeared at approximately 3,500 cm^{-1} (2.86 μ) in cellulose acetate and at approximately 3,400 cm^{-1} (2.94 μ) in regenerated cellulose. This fact suggested that the hydrogen bridges between the unacetylated OH groups in cellulose acetate were relatively weaker [13] than the hydrogen bridges between the OH groups in regenerated cellulose. The apparent difference in positions of the minima is shown in figure 4, in which the spectra of three different cellulose acetates and one sample of methyl cellulose may be seen. The cellulose triacetate used in obtaining the spectrum in figure 4 was obtained from the Eastman Kodak Co. It was insoluble in acetone and, therefore, cast from a 10-percent chloroform solution. In preparing the 10-percent solution, five parts of alcohol were added to 100 parts of the chloroform to facilitate dispersion of the cellulose triacetate. The film made with a 0.04-in. Bird film applicator was 7.6 μ in thickness. The cellulose acetate had an acetyl content of approximately 54 percent (as acetic acid); it was prepared and partially deacetylated as previously described [1]. The

871926—50——8

methyl cellulose (4,000 centipoises) used in this work was obtained from the Dow Chemical Co. A 2½-percent water solution was spread with a blade having a clearance of 0.006 in. The resulting film (4.6 μ) was then removed from the glass plate with the aid of a razor blade and a pair of tweezers.

It is noted in figure 4 that the commercial cellulose triacetate and methyl cellulose have OH bands (due to a few unreacted hydroxyl groups) whose minima are at approximately 2.87 μ. On the other hand, the partially deacetylated acetates had OH bands whose minima are at 3.0 μ.

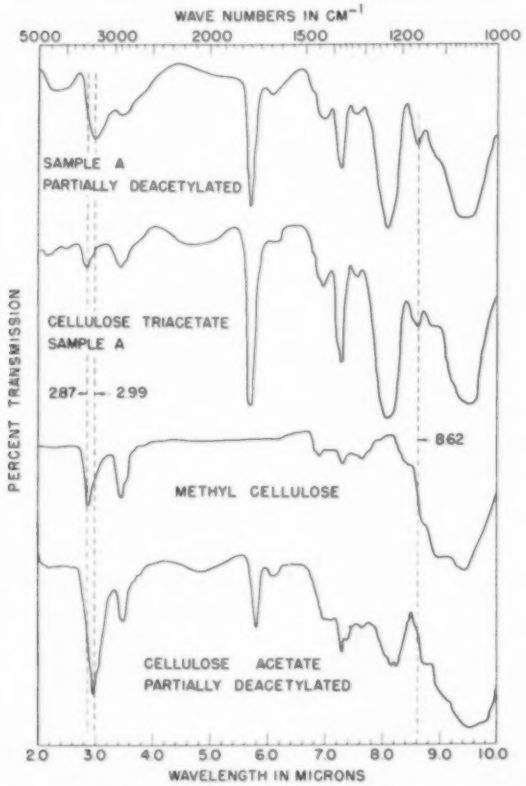

FIGURE 4. *Comparison of the infrared absorption spectra of some cellulose derivatives.*

In view of the above difference in the position of the minimum of the OH band, it was of interest to examine the band with the aid of the wide dispersion lithium fluoride prism in an additional experiment designed to detect, in a qualitative manner, the effect of water molecules and the band intensities upon the position of the mini-

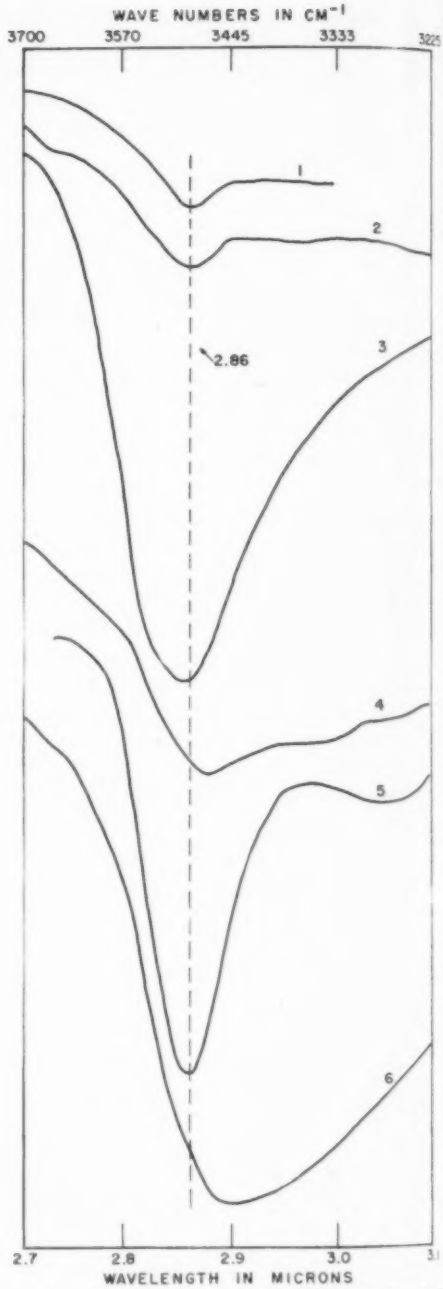

FIGURE 5. *Infrared absorption spectra in the hydr region for several cellulose derivatives.*

1, Cellulose acetate butyrate (0.03 equivalent) film thickness 13 μ; 2, cellulose acetate butyrate (0.52 equivalent) film thickness 14 μ; 3, cellulose acetate butyrate (0.94 equivalent) film thickness 12 μ; 4, benzyl cellulose, film thickness 3 μ; 5, ethyl cellulose, film thickness 12 μ; 6, regenerated cellulose, film thickness 2 μ.

um. For this preliminary experiment, the tensity of the band could be varied by changing e hydroxyl content. The change in intensity the band was made possible by means of a ries of cellulose acetate butyrate esters available the Bureau. It would have been more desira- e to use a cellulose acetate series to study the fect of varying hydroxyl content for this experi- ent; however, such a series was not immedi- ely available. For the study, three samples of e mixed ester having three different hydroxyl ntents, 0.03 equivalent, 0.52, and 0.94 were osen. (One equivalent of OH here means that ere is one hydroxyl group in each anhydro- cose unit). In addition, the following three aterials were also examined at the same time: hyl cellulose, benzyl cellulose, and regenerated llulose. In order to minimize any possible effect water on the positions of the OH bands, the ove six samples were compared after drying er anhydrous calcium sulfate for 24 hr in a ecially constructed cell having rock-salt win- ws. It was thus possible to obtain the spectra these dry films with the aid of this cell and a hium fluoride prism.

The spectra of the six derivatives of cellulose e shown in figure 5. It is noted that the first, cond, third, and fifth spectra all have minima 3,500 cm^{-1} (2.86 μ). The minima of the benzyl pectrum 4) and regenerated cellulose (spectrum appear to be shifted to slightly longer wave- ngths. It is apparent that the position of the inimum in the dried mixed ester (spectra 1, 2, nd 3) is at 2.86 μ and that the difference, 0.12 μ, reviously observed in figure 4, is an effect that is ost likely due to additional hydrogen bonding the deacetylated cellulose acetate.

An absorption band in the region of 3,500 m^{-1} (2.86 μ) has been observed in dilute carbon trachloride solutions of alcohols. The position this band has been attributed [14, 15] to the pe of hydrogen bonding between the two alcohol olecules, which are associated in some manner, hich leads to the formation of a dimer alcohol olecule. The presence of this vibration in fferent dried cellulose derivatives suggests that e mechanism by which the cellulose chains are ound together may possibly be of the "dimer" pe and common to many cellulose derivatives. his association may be imagined as follows:

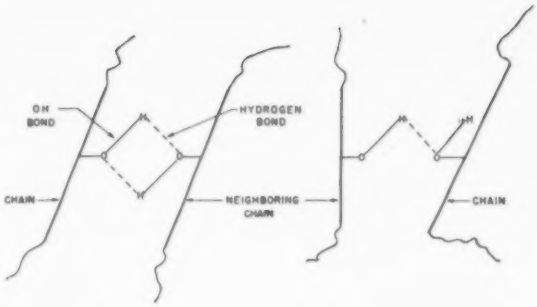

Although these bridges may exist in ordered (crystalline) regions of cellulose, they would not be present in large numbers in the disordered (amorphous) regions.

In the disordered regions many of the OH groups on neighboring chains are not close enough to each other to enter into a hydrogen bonding arrangement. This inability of some of the OH groups in cellulose to undergo hydrogen bonding in the amorphous regions should give rise to frequencies characteristic of free OH vibrations. The frequencies reported for free OH groups in alcohols in solutions [16, 17, 18] are found to be in the region of 2.72 to 2.75 μ. Small inflections in the region of the spectra of cellulose acetate butyrate (0.52 equiv.—spectrum 2 in fig. 5) and in regenerated cellulose (spectrum 6) suggest the presence of a few free OH groups in these derivatives. However, additional work will have to be done on thicker films before the presence of free OH groups in cellulose and its derivatives is definitely established.

The preliminary work described here suggests the advisability of examining the short wavelength region, under high dispersion, of samples of dried and undried cellulose and its derivatives, both deuterated and nondeuterated, having varying tensile strengths and different degrees of crystallinity.

The authors are indebted to Charles M. Hunt and Sara L. Roser for valuable assistance in preparing some of the derivatives and films used in this work.

V. References

[1] J. W. Rowen, C. M. Hunt, and E. K. Plyler, J. Research NBS **39,** 133 (1947) RP1816.

[2] G. Champetier and R. Viallard, Bull. soc. chim. [5] **33,** 1042 (1938).

[3] V. J. Frilette, J. Hanle, and H. Mark, J. Am. Chem. Soc. **70,** 1107 (1948).

[4] W. S. Baird, H. M. O'Bryan, G. Ogden, and D. See, J. Opt. Soc. Am. **37,** 754 (1947).

[5] R. B. Barnes, R. S. McDonald, V. Z. Williams, and R. F. Kinnaird, J. Applied Phys. **16,** 77 (1945).

[6] G. F. Davidson, J. Textile Inst. **29,** T197 (1938).

[7] C. C. Unruh and W. O. Kenyon, Textile Research J. **16,** p. 1 to 12 (1946).

[8] E. C. Yackel and W. O. Kenyon, J. Am. Chem. Soc. **64,** 121 (1942).

[9] R. B. Barnes, R. C. Gore, U. Liddel, and V. Z. Williams, Infrared spectroscopy (Reinhold Publishing Co., New York, N. Y., 1944).

[10] I. M. Klotz and O. M. Gruen, J. Phys. & C... Chem. **52,** 961 (1948).

[11] M. M. Davies and G. B. B. M. Sutherland, J. Ch... Phys. **6,** 755 (1939).

[12] J. Lecomte and J. P. Mathieu, J. Chim. Phys. **39,** ... (1942).

[13] R. Barnes, R. C. Gore, R. W. Stafford, and V. ... Williams, Anal. Chem. **20,** 405 (1948).

[14] J. Errera, R. Gaspart, and H. S. Sack, J. Ch... Phys. **8,** 63 (1940).

[15] S. C. Stanford and W. Gordy, J. Am. Chem. Soc. ... 1247 (1940).

[16] W. Gordy, J. Am. Chem. Soc. **60,** 605 (1938).

[17] N. Coggeshall, J. Am. Chem. Soc. **69,** 1620 (194...

[18] J. J. Fox and A. E. Martin, Proc. Royal Soc. (Lon... [A] **162,** 419 (1937).

Washington, December 12, 1949.

U. S. Department of Commerce
National Bureau of Standards

Research Paper RP2081
Volume 44, March 1950

Part of the Journal of Research of the National Bureau of Standards

Vapor Pressure and Fixed Points of Oxygen and Heat Capacity in the Critical Region

By Harold J. Hoge

Vapor-pressure measurements on oxygen covering the entire range from the triple point to the critical point are reported. By measuring short sections of isotherms, the critical temperature and pressure were found to be 154.78° K and 50.14 atm, respectively. The triple point temperature and pressure were found to be 54.363° K and 1.14 mm Hg respectively. The two solid-solid transitions were found to be at 43.80$_6$° and 23.886° K respectively. Measurements were made of the heat capacity of oxygen in the critical region at six different filling densities. A comparison of the temperature scales of three different laboratories is made, based upon reported values of the fixed points of hydrogen, nitrogen, and oxygen.

I. Introduction

This Bureau has maintained since 1939 a provisional temperature scale [1][1] covering the range 1° to 90° K. This scale was based on a group of seven resistance thermometers, two of which have since suffered accidents that caused them to be removed from the group.[2] The initial impetus for the work now being reported was a desire to relate this provisional temperature scale (PTS) to the properties of pure materials such as oxygen, so that the scale could be maintained without reference to the preservation of the original group of thermometers. Oxygen was chosen because its boiling point defines the lower limit of the International Temperature Scale (ITS) [2], and because the triple point and the two solid-solid transitions have promise of being usable fixed points.

We have for some time been aware that the ITS and the PTS maintained by this Bureau do not join as smoothly (at 90.19° K) as would be desirable. It seems likely that the two scales cannot be brought into agreement with the thermodynamic scale without modifications of both. The vapor pressure data above 90.19° K will be useful when the time for modification of the two scales arrives. The vapor pressure of oxygen above 1 atm was not as well known as that of many other common gases. The last major investigation was by Dodge and Davis [3] in 1927 and went only to 21.47 atm. Prior to that the best values were probably those reported by Onnes, Dorsman, and Holst [4] in 1914. The ITS was not employed in either investigation. Hence it was decided to extend the present measurements all the way to the critical point, using a modern high-purity platinum resistance thermometer calibrated on the ITS. Some high-pressure heat-capacity measurements were made to test the value of calorimetry in mapping the critical region and determining the critical temperature. The critical point was located by measurement of short sections of isotherms (p versus V).

The work now being reported was begun in 1942. It was laid aside during the war and has been completed since the war. The primary purpose of defining the provisional temperature scale covering the range 11° to 90° K in terms of the vapor pressures and fixed points of pure materials is only partially accomplished by the present work. Additional fixed points are needed, especially below 40° K. Work on nitrogen and perhaps neon would help to complete the picture, and it is

[1] Figures in brackets indicate the literature references at the end of this paper.

[2] This group has recently been supplemented by 6 new thermometers carefully compared with members of the original group. The new thermometers belong to a large group of thermometers recently made by the Leeds and Northrup Co. from the same piece of wire, at the suggestion of the Conference on Low Temperature Calorimetry of the American Chemical Society.

hoped that this can be carried out in the not too distant future.

II. Apparatus

The apparatus used in the 1942 measurements was a small adiabatic calorimeter originally used by Brickwedde and Scott in their investigations of HD. This calorimeter was similar in general design to the one described by Scott et al [5] except that it was much smaller. The vapor pressure was transmitted to the manometer through a small filling tube. The determinations of solid-solid transition temperatures were made in this apparatus; also some triple-point measurements and most of the vapor-pressure measurements below 1/10 atm. With this apparatus both oil and mercury manometers were used.

The apparatus used in the measurements made since the war is shown schematically in figure 1. The low-pressure apparatus (upper half of fig. 1) was of glass, with a conventional mercury-in-glass manometer, which was read on a mirror-backed glass scale. Pressures up to about 1 m Hg were read directly on this scale, and higher pressures up to about 1.7 atm were read by opening the stop cock to the atmosphere, and adding the reading of the barometer to the reading of the manometer. A flask of approximately 3-liter capacity marked *calibrated volume* was used for measuring the quantity of O_2 admitted to the apparatus. One of the condensing tubes was used to collect the O_2 as it was prepared by decomposition of $KMnO_4$. The other

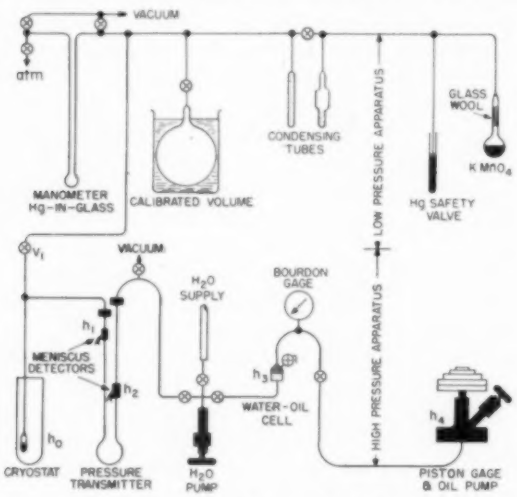

FIGURE 1. *Apparatus used in most of the measurements.*

was useful in certain cases where oxygen was to be transferred from one part of the apparatus to another.

The apparatus capable of withstanding high pressure (lower half of fig. 1) consisted of a cryostat, a pressure transmitter, a water pump, a water-oil cell, a Bourdon pressure gage, and finally a piston gage. Pressure exerted by O_2 in the cryostat was communicated by vapor of the sample itself to mercury contained in the pressure transmitter. Thence it was transmitted through mercury from the first meniscus to the second, then thru water to the water-oil cell, and finally thru oil to the piston gage.

Cryostat. Some details of the equilibrium chamber and its immediate surroundings are shown in figure 2. The equilibrium chamber was made by boring out a short section of pure nickel rod (⅝ in. outside diameter) closing the lower end with a nickel cap and connecting the upper end to a heavy-wall nickel tube (⅛ in. by 1/16 in.) which transmitted the vapor pressure to the measuring system. After assembly with silver solder the equilibrium chamber was inserted into a well in the heavy copper block and soft-soldered in place. The heavy copper block contained also a well for the resistance thermometer. Thermal contact between the thermometer and the block was obtained with stopcock grease. Actually there were two equilibrium chambers and two thermometer wells spaced alternately at 90° intervals about the axis of the block, but only one thermometer and one well were used in the present experiments. For convenience in representation figure 2 shows a thermometer in the position actually occupied by the second equilibrium chamber. The copper block was held firmly in place by a short length of ½-in. monel tubing. The vapor-pressure tubes passed through slots in this tube. All three of the tubes were soldered to a copper bushing, which fit snugly into a sleeve that formed part of the shield. In figure 2 the sleeve and bushing appear as a single piece of metal. Stopcock grease was placed in the joint between them to improve thermal contact. The weight of the copper-block assembly was carried by the two vapor-pressure tubes. For the insertion or removal of thermometers, the container and the thermal shield could be removed and the vapor-pressure tubes unsoldered from another sleeve and bushing above the cryostat

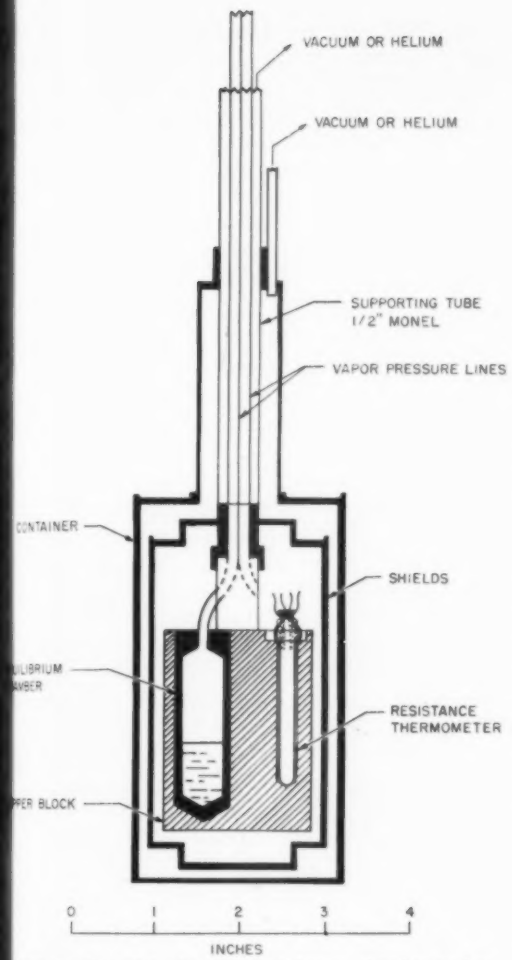

URE 2. *Cryostat, showing equilibrium chamber and resistance thermometer.*

Drawn to scale.

fier which the block assembly could be lowered veral inches.

The shield system was rather heavy (1/16-in. all) and was vacuum tight. This permitted e space between the shield and the container be evacuated while a small amount of helium as left inside the shield and in the supporting be that contained the vapor pressure lines. y varying the helium pressure, the temperature the heavy vapor pressure lines could be conlled without the use of unduly large heaters. e system worked satisfactorily but was less nvenient to adjust than a system involving only ctrical heaters. No advantage was anticipated from having helium around the block itself, but this simplified the problem of getting the leads to the block. However, when the measurements were about three-fourths completed a leak developed in the resistance thermometer. This would have prevented further measurements had it not been possible to operate with the block in an atmosphere of helium. The helium was of course a disadvantage in heat-capacity measurements.

The supporting tube carried the shield at its lower end. For a distance of about 2.5 in.[3] above the shield it was protected from the refrigerating bath by a 1-in. tube that was essentially a continuation of the container. A heater was wound on the outside of the protected section of the supporting tube. Two thermel (thermel=thermocouple or thermopile) junctions were placed on the vapor pressure lines, but no heater was wound on them. In addition a six-power difference thermel was used in controlling the temperature of the tubes and shield. Two junctions were on the tubes, one on the top of the shield, two on the side, and one on the bottom. They could be used as a single pile; also certain junctions and subgroups could be observed separately The bottom, top, side, and tube heaters were all in series. The first three were controlled as a unit, with only occasional adjustment of shunts across the bottom and top heaters. It was found impractical to include the tube heater in the group.

To permit rough heat-capacity measurements, a heater was wrapped on the outside of the block. One of the potential terminals for power measurement was located where the current lead reached the block; the other was located near the top of the short section of thin monel tubing that helped to support the copper block.

Meniscus detectors. The pressure transmitter used during the latter part of the measurements was a ½-in. stainless steel tube partially filled with mercury. Since the positions of the menisci could not be observed visually, a method was employed that involved the detection of the positions of nickel floats by means of an inductance bridge. The scheme and detecting circuit were designed for us by Maurice L. Greenough. The floats were pure nickel cylinders (5/16-in. inside diameter, 0 012-

[3] A length 25% greater would have been better.

in. wall) machined from larger stock so as to leave four projections at each end to keep the floats centered inside the stainless steel tube. When placed on a mercury surface the floats did not sink, but were held entirely above the mercury by surface tension. Mercury tended to wet them on prolonged contact. This was controlled by oxidizing the floats in an oxygen flame before use.

Each detecting unit was a center-tapped inductance coil of AWG38 enameled copper magnet wire. The two halves were wound on a common lucite form, which slid freely up and down the stainless steel tube. Each half had an inductance of about 0.495 henry and a resistance of about 825 ohms, and occupied a space ½ in. long, with inside and outside diameters of $^{21}/_{32}$ and 1⅛ in., respectively. The output of a beat-frequency oscillator was applied across either detecting unit with the center taps of the oscillator and the detecting unit connected together through a microammeter and a germanium rectifier so as to form an inductance bridge. The bridge was balanced by moving the detector until the float was midway between the two halves of the detector coil. Accuracy of the detection is discussed later.

Diaphragm cell. The pressure transmitter just described was used only in the later measurements. In the earlier measurements a diaphragm cell was used that was similar to the one described by Osborne, Stimson, Fiock, and Ginnings [6]. The diaphragm was of pure nickel 0.003 in. thick, clamped between two cylindrical blocks of monel metal about 4 in. in diameter. The adjacent surfaces of the blocks were hollowed out to a maximum depth of 0.005 in., so that the center of the diaphragm was free to move through a distance of 0.010 in. The dished-out areas had a diameter of 2.36 in. This was larger than the cell used by Osborne et al., for the purpose of obtaining higher sensitivity, but the larger size seemed to be more difficult to assemble vacuum tight. It was clamped by twelve ¼-in. bolts. Larger bolts, and a working diameter of perhaps 1¾ in. would have reduced the troubles encountered. The cell was assembled in such a way as to stretch the diaphragm slightly just before it was permanently clamped between the cell blocks. This was done by making the diaphragm larger than would otherwise have been necessary and first clamping it at its periphery so as to hold it in a plane slightly above the lower cell block. When the upper cell block was placed in position it pushed the central portion of the diaphragm out of its original plane before clamping it against the lower block. At the center of each block a 0.014-in. hole was drilled. Through one of these the pressure of oxygen vapor was applied to the lower side of the diaphragm. The upper side of the cell was connected to a line leading to the piston gage. This line contained two glass tubes, one immediately above the diaphragm in which the position of a water meniscus was observed; and another where the position of the oil meniscus was observed. The line connecting the tops of the two glass tubes contained a tee for admitting helium gas to the appropriate pressure. Water filled the space above the diaphragm and the line leading from it, so that the position of the diaphragm was registered by the height of the water column in the glass tube. The diaphragm cell worked satisfactorily for a period of months. After this it received very little use while the heat-capacity measurements were in progress. When vapor-pressure measurements were resumed the diaphragm was found to be unusable, presumably because its position of equilibrium was no longer in the middle of the cell. The pressure transmitter shown in figure 1 was then substituted for it, with the addition of the water pump and water-oil cell. When both apparatuses were working properly they gave results of comparable accuracy. The one shown in figure 1 was easier to use, however, and had the advantage that at higher pressures the quantity of O_2 in the cryostat could be varied over a large range. This was accomplished by changing the positions of the menisci and thus varying the volume in the transmitter that was occupied by O_2 gas at high pressure.

Water pump and water-oil cell. The water pump was introduced between the oil and the mercury for reasons of safety. It could be omitted from apparatus where the possibility of O_2-oil explosion was not present. The water pump was constructed much like an ordinary packed needle valve with a ⅝-in. polished bronze plunger replacing the needle. The plunger had a travel of 2½ in. The thread on the stem was ½ in.-13, and the 4½-in. hand wheel was reasonably easy to turn up to pressures of 50 atm. The water-oil cell contained a valve for bleeding the line and thus making sure of the position of the water-oil meniscus.

Piston gage. The piston gage used was numbe

A-30213, previously described by Meyers and Jessup [7]. It had a range of about 100 atm. The effective area of the piston was 1.0065$_3$ cm^2 according to data furnished by Meyers. Since it is known that pistons occasionally suffer appreciable changes in diameter, the gage was checked by comparing it with another gage of the group described by Meyers and Jessup (number D-30778). The two gages agreed to better than 1 part in 5,000.

III. Preparation and Purity of Samples

Three different samples of O_2 were used. The first sample was used in all the 1942 measurements, the second in all subsequent measurements prior to July 1, 1947, and the last sample in all later measurements. All were prepared from $KMnO_4$. The first sample was fractionally distilled and tested by comparison of the vapor pressures of various fractions. No improvement in purity was noted. The last two samples were not distilled, but at the time of preparation the first and last portions of the oxygen generated were discarded. The possibility that the concentration of O^{18} in the samples would be affected by the distillation or the method of preparation was considered. Stedman [8] was able to increase the concentration of O^{18} from the normal 1 part in 500 to 1 part in 400 by running a 16-ft distillation column for 27 hr. The vapor pressure of the pure heavy isotope is probably only 1.5 percent less than that of the normal mixture. Hence it seems very unlikely that changes in isotopic composition could have any appreciable effect on the present measurements.

As some have had difficulty in preparing pure oxygen from $KMnO_4$, a few of the details of the technique used will be described. Except for minor modifications the procedures are those described by Scott [9]. A mass of $KMnO_4$ equal to about ten times [4] the required mass of oxygen is placed in a glass bulb, confined with a plug of glass wool and sealed to the system. The bulb should be only about half full as the crystals swell and turn to powder during the reaction. The glass wool prevents powder from contaminating the rest of the system. A furnace is placed around the bulb, and the system is evacuated overnight or longer with the temperature slightly above 100° C. The temperature is then raised fairly rapidly to, say, 160° C and then more slowly until a noticeable evolution of O_2 is registered by the pressure gage of the vacuum system. This will occur at about 200° C. The vacuum pump is left running, and the temperature is slowly raised until the reaction chamber is thoroughly flushed. The rate of generation of O_2 is estimated by closing the line to the pump temporarily and noting the rate of rise of pressure. After it is judged that 5 or 10 percent of the material has reacted, the pump line is closed and collection of the sample is begun. The reaction accelerates as it proceeds, and is accompanied by decrepitation of the $KMnO_4$ crystals. It seems plausible that any adsorbed gases will be gotten rid of more completely if a small amount of decrepitation occurs before collection of the sample is started. The furnace temperature should be rather carefully controlled as the reaction gets under way. Generally the furnace temperature need not be raised above 230° C. Collection of the sample is observed in one of the condensing tubes, and when the reaction is judged to be about 80 percent complete the remainder of the O_2 is either discarded or collected in the other tube.

There was no indication in the vapor-pressure data of any difference in the purity of the three samples. Melting-point data were taken on the first and last samples. The equilibrium temperature was plotted versus the reciprocal of F, the fraction of the sample melted, and the slope of a straight line drawn through the points was measured. This slope is the coefficient of $1/F$ in the usual formula for freezing point depression: $T_f - T = (xRT_f^2/L_f)(1/F)$. Using Giauque and Johnston's [10] value for L_f(106.3 cal mole^{-1}) and 54.363° K for T_f, values of x, the mole fraction of impurity, were computed. For the first sample x was found to be 2×10^{-7}, with an uncertainty in x of about 50 percent. The graph for the third sample gave the same value of x, but the uncertainty was larger—of the order of 100 percent. No melting-point data were taken on the second sample, but it is thought to have been of the same purity as the other two.

IV. Vapor Pressure

Measurements. The vapor-pressure data are given in table 1. One column of this table gives the type of pressure-measuring system employed.

[4] According to the reaction $2KMnO_4 + \text{heat} \rightarrow MnO_2 + K_2MnO_4 + O_2$, it takes 0.8 g of $KMnO_4$ to make 1 g of O_2 or 11.3 g to make 1 cm^3(1.14 g) of liquid O_2.

This was either a simple oil manometer (oil), a simple mercury manometer (Hg), a mercury manometer reading the excess above barometric pressure (HgB), a piston gage with pressure transmitted to it through a diaphragm cell (PGD), or a piston gage with pressure transmitted to it through the mercury-filled U-tube shown in figure 1 (PGHg). The method used at each point is indicated in one of the columns of table 1.

TABLE 1. *Observations of the vapor pressure of* O_2

The column headed Δp contains deviations of the observed values from table 2

Date	Pressure measuring system [a]	T	p Observed	Δp Observed—calculated
		°K	mm Hg	mm Hg
Mar. 16, 1942 [b]	Oil	[c] 51.286	0.47	
		[c] 52.176	.53	
		[c] 53.082	.76	
		[d] 54.363	1.12	−0.02
		[d] 54.363	1.13	−.01
Mar. 17, 1942 [b]	Oil	[d] 54.363	1.12	−.02
		[d] 54.363	1.13	−.01
		56.788	2.28	−.04
Mar. 24, 1942	Hg	89.677	720.0	.0
		89.914	738.4	.1
		90.068	750.1	−.2
		90.231	763.2	.0
		90.387	775.5	−.3
		90.637	796.3	.1
		90.788	808.6	−.1
		90.604	793.0	−.5
Mar. 25, 1942	Oil	54.823	1.30	−.01
		60.070	5.53	−.03
		64.991	17.4	.0
Mar. 25, 1942	Hg	70.141	47.9	−.1
		75.150	111.0	−.2
		80.171	230.3	−.2
		82.692	320.5	.1
		86.419	502.2	−.1
		90.182	759.2	−.2
Mar. 26, 1942	Oil	[d] 54.363	1.14	.00
Aug. 15, 1946	Hg	84.417	596.6	.0
		84.950	623.1	.2
		85.639	658.8	.0
		86.384	700.3	−.1
		87.134	744.7	−.3
		88.030	802.3	−.1
		88.951	866.3	.1
		89.867	934.6	.0
		90.827	1011.8	−.2
		91.728	1080.1	.0
		92.599	1171.1	.1
		92.727	1183.3	−.1
Sept. 9, 1946	Hg	56.538	2.2	.0
		58.024	3.2	−.1
		64.407	15.2	−.2
		70.995	56.0	.0
		79.918	222.8	.0
		89.386	698.0	.0

TABLE 1. *Observations of the vapor pressure of* O_2—

Date	Pressure measuring system [a]	T	p Observed	Δp Observed—calculated
		°K	mm Hg	mm Hg
Sept. 12, 1946	Hg	71.890	65.2	
		73.082	79.8	
		73.929	91.7	
		75.030	109.2	
		75.989	126.5	
		76.996	147.1	
		78.026	170.7	
		79.042	197.6	
		80.009	225.6	
		81.045	259.0	
		82.106	297.5	
		83.019	333.8	
		87.447	564.3	
Sept. 19, 1946	Hg	61.042	7.0	
		62.119	9.1	
		63.099	11.6	
		64.048	13.9	
		65.002	17.6	
		66.025	21.8	
		66.978	26.0	
		67.956	31.9	
		68.989	38.9	
		69.988	46.9	
		70.974	55.7	
		72.470	72.1	
		73.491	85.4	
		74.487	100.2	
		76.534	137.9	
		78.524	183.8	
		85.277	439.8	
Sept. 24, 1946	Hg	87.747	584.0	
		90.597	793.0	
		92.606	971.9	
Sept. 24, 1946	HgB	93.153	1025.4	
		94.632	1181.9	
		95.757	1312.0	
		96.648	1423.6	
Jan. 20, 1947	Hg	92.615	972.8	
Jan. 20, 1947	HgB	93.145	1024.3	
		93.146	1024.8	
Jan. 23, 1947	HgB	94.893	1200.8	
		94.894	1201.4	
Jan. 27, 1947	HgB	92.861	995.9	
		92.862	995.7	
		94.472	1164.1	
		94.473	1164.2	
		96.193	1366.2	
Jan. 27, 1947	PGD	97.518	1538.4	
Jan. 28, 1947	HgB	92.477	959.2	
Jan. 28, 1947	PGD	97.596	1549.1	
		100.163	1931.4	
		100.164	1931.6	
		102.581	2352.4	
		104.354	2702.3	
		106.083	3078.6	
		107.290	3363.3	
		108.665	3710.7	
Feb. 4, 1947	HgB	92.290	941.8	
		92.289	941.8	

See footnotes at end of table.

TABLE 1. *Observations of the vapor pressure of* O_2—Con.

Date	Pressure measuring system [a]	T	p Observed	Δp Observed−calculated
		°K	*mm* Hg	*mm* Hg
		99.998	1904.0	−.7
		99.998	1904.5	−.2
	PGD	101.969	2239.1	−.5
		103.962	2620.6	−.7
		106.291	3124.3	−1.9
		110.568	4231.7	−2.9
	Hg	92.460	957.8	0.0
		101.055	2078.8	−.4
		107.172	3333.0	−1.5
	PGD	111.268	4438.8	−1.5
		113.708	5214.9	0.6
		115.654	5898.6	.3
		118.095	6846.8	.8
	Hg	92.547	966.0	.0
		100.116	1924.4	.8
		107.392	3388.7	.7
		109.311	3883.1	.3
		110.142	4113.5	.6
		111.082	4385.3	.4
		112.028	4672.4	.6
	PGD	112.974	4972.6	.6
		114.493	5483.4	.6
		116.110	6068.8	.9
		118.313	6936.3	.6
		119.398	7394.7	.0
		120.996	8110.4	.6
		122.503	8829.0	.4
		124.687	9951.3	.2
		127.357	11459	2
	Hg	92.079	922.4	0.3
		112.895	4945.7	−.6
		113.628	5186.9	−.4
		121.762	8468.4	−1.1
		122.480	8816.6	−1.2
		127.261	11400	0
		128.066	11883	0
	PGD	129.635	12866	0
		131.794	14312	0
		135.048	16709	1
		139.403	20351	0
		143.062	23833	1
		146.530	27521	2
		149.575	31103	0
	Hg	92.451	956.4	−0.5
		99.897	1888.1	−.4
		117.174	6475.3	−1.2
	PGD	125.957	10646	−2
		130.703	13566	−1
		137.611	18789	−1
		145.120	25973	1
	Hg	92.321	944.8	0.1

TABLE 1. *Observations of the vapor pressure of* O_2—Con.

Date	Pressure measuring system [a]	T	p Observed	p Observed-calculated
		°K	*mm* Hg	*mm* Hg
		99.044	1756.5	−.3
		133.317	15399	−1
		141.429	22227	−1
		144.241	25039	−2
		146.000	26929	−1
		147.566	28700	−1
		148.681	30015	0
Mar. 20, 1947	PGD	150.163	31834	−1
		150.740	32567	0
		151.299	33287	−3
		151.866	34036	1
		152.394	34742	0
		152.948	35499	2
		153.467	36221	3
		153.984	36952	2
		154.482	37674	4
Mar. 24, 1948	HgB	92.362	948.6	0.1
Mar. 26, 1948	HgB	92.368	949.3	.2
Apr. 2, 1948	HgB	92.280	941.0	.2
		96.297	1378.9	.1
		82.522	313.6	.0
Nov. 9, 1948	Hg	83.359	348.2	−.1
		84.148	383.8	−.1
		82.581	316.1	.2
		82.748	322.8	.1
		83.215	342.0	−.1
		83.641	360.6	−.1
Nov. 12, 1948	Hg	84.113	381.9	−.3
		84.760	413.1	−.2
		85.210	435.9	−.3
		85.913	473.3	−.5
		85.914	473.6	−.2
		88.045	603.2	−.2
		89.558	710.9	.0
		90.506	785.3	−.2
		91.490	869.1	.1
Nov. 12, 1948	HgB	92.647	975.3	−.4
		93.530	1063.3	−.4
		94.266	1141.1	−.4
		94.298	1144.4	−.6
Nov. 18, 1948	HgB	91.386	859.9	.0
		93.756	1087.2	.1
		96.976	1465.9	.1
Nov. 18, 1948	PG Hg	100.029	1910.1	.3
		104.684	2770.8	.0
		104.694	2773.1	.2
Nov. 23, 1948	Hg	89.950	741.1	.0
	PG Hg	104.417	2715.0	.1
Nov. 30, 1948	Hg	88.700	648.3	.0
		88.700	648.4	.1

See footnotes at end of table.

TABLE 1. *Observations of the vapor pressure of* O_2—Con.

Date	Pressure measuring system [a]	T	p Observed	p Observed-calculated
		°K	*mm* Hg	*mm* H
Dec. 17, 1948	PG Hg	131.540	14140	4
		141.159	21973	2
		146.974	28022	1
		150.294	31999	−1
		151.301	33291	−1
		152.574	34986	1
		153.553	36339	−1
Dec. 21, 1948	Hg B	87.887	593.1	0.2
		91.526	872.3	.2
		93.770	1089.0	.4
		93.769	1088.5	.0
Dec. 21, 1948	PG Hg	109.930	4053.1	−.3
		124.725	9971.3	−.2
		140.329	21196	2
Dec. 29, 1948	PG Hg	135.592	17133	−1
		140.615	21458	−1
		144.396	25203	−1
		148.029	29239	−2
		151.145	33086	−3
		154.188	37240	−3
		154.580	37816	1
		154.760	38079	0

[a] Pressure-measuring systems are identified as follows: Oil=oil manometer; Hg=mercury manometer, one side evacuated; HgB=mercury manometer, one side open to atmosphere, reading added to barometer reading; PGD=piston gage, with pressure transmitted through diaphragm cell; PG Hg=piston gage with pressure transmitted through mercury as shown in figure 1.

[b] Data taken on March 16 and 17, 1942 are less reliable than later data because of possibility of condensation in tube leading to manometer.

[c] Oxygen was solid at this temperature.

[d] Triple point.

The oil manometer contained apiezon-B oil with a density $\rho(\text{g cm}^{-3}) = 0.86022 - 0.00063(t-25)$ as determined from measurements at 20°, 25°, and 30° C by the Capacity, Density, and Fluid Meters section of this Bureau. However, when the same pressure was read simultaneously on the oil manometer and the Hg manometer the pressures did not agree exactly, possibly due to solution of O_2 in the oil. Densities given by the above equation were accordingly multiplied by 0.997 to bring the oil- and mercury-manometer data into agreement. The rate of diffusion of oxygen through the oil in the manometer appeared to be very slow; however, the vacuum side of the manometer was reevacuated frequently as a precautionary measure. All pressure measurements were reduced to standard mm Hg ($g = 980.665$, $t = 0°$ C) assuming local gravity to be 980.10.

Temperatures were measured by a capsule-type platinum resistance thermometer. Thermometer L3 was used in the 1942 measurements and L14 in all subsequent work. Thermometer L3 was one of the original group used to define the temperature scale below 90° K, which this Bureau now maintains. Its calibration is discussed in reference [1]. Thermometer L14 was calibrated below 90° K by comparison with thermometers of this original group, and above 90° on the ITS. Resistances were measured on a Mueller resistance bridge.

Both the oil and the Hg manometers were read on mirror-backed calibrated glass scales. When several observations were made at the same point the vertical position of the scale was shifted slightly after each pair of readings. This has been found to increase the accuracy of the observations. In general an experimental point consisted of three manometer readings alternated with two resistance readings. Where the pressure was too high to be read on the Hg manometer alone it was necessary to read the barometer. Barometer readings are also required when the piston gage is used. Rather than read the instruments simultaneously it was found better to make barometer readings at more convenient times and to record the times of all readings. The barometer height was then plotted as a function of time, and appropriate values were read from the curve to add to the readings of the other instruments.

The procedure for taking data with the piston gage was different when the diaphragm cell was used than when the apparatus was employed as shown in figure 1. With the diaphragm cell, the first step was to calibrate the diaphragm by finding the height of the water column in the glass tube above it as a function of the pressure difference across the diaphragm. This was done before almost every run, although the change in calibration was small and monotonic over the period of most of the measurements involving the diaphragm cell. To calibrate, a pressure near the lower limit of the piston gage (~900 mm Hg) was measured simultaneously by the manometer (Hg or HgB) and by the piston gage (PGD). The two results were set equal to each other, with the pressure supported by the diaphragm appearing as an unknown quantity to be determined from the equation. After an observation the weight on the piston gage was changed by a few grams and conditions readjusted so that the diaphragm

d moved slightly. A calibration consisted of e or ten such observations. Over a range of out 70 mm in the height of the water column the libration was linear, with a change in water ight of 1 mm corresponding to a pressure change 0.95 mm Hg. To make measurements the mperature of the cryostat was raised to the sired value, helium was admitted to the line tween the diaphragm and the piston gage until e diaphragm was near its equilibrium position. hen the valve to the piston gage was opened ghtly and the weights adjusted until balance as obtained. The weights were then recorded d also the heights of the menisci in the water d oil sight glasses. Room temperature was corded for use in computing the densities of the l and water columns. After a pressure balance d been obtained, the weight on the piston gage as changed by 5 or 10 g and balance restored changing the amount of oil or helium in the stem. This caused the diaphragm to take up a w position, still in the linear range covered by e calibration. Another set of readings was then ade. An experimental determination consisted three sets of readings of the piston gage and aphragm, alternated with four readings of the sistance thermometer.

The diaphragm worked satisfactorily in all easurements made in 1947. When it was first ed in 1948, however, the data did not agree mong themselves or with the earlier data. The aphragm cell was found to be unusable and was placed by the pressure transmitter shown in gure 1. The cell could have been put back in rvice by replacing the diaphragm, but it was ought preferable to replace it with a different echanism and thus obtain an independent check n the reliability of the data. The pressure trans- itter shown in figure 1 was therefore used. The ethod of observing mercury meniscus positions described in the section on apparatus. After e piston gage had been balanced and the weights corded, a series of observations of thermometer sistance was begun. While one operator re- rded resistances at 1-min intervals, the second erator simultaneously observed the heights of e mercury columns in each arm of the pressure ansmitter. Temperatures were recorded for use computing the density of the mercury, water, d oil through which the pressure was trans- itted. The water-oil cell was bled occasionally to establish the position of the water-oil boundary in this cell. The valves were manipulated in such a way as to keep this position constant except for the compressibility of the oil and the leakage of oil past the piston. The density of the oil was not greatly different from the density of water. A 64-mm uncertainty in the height of the water-oil boundary would have been required to cause an error in pressure of 1 mm Hg.

The computation of pressures from piston-gage data requires a number of corrections to be made. The desired pressure P is that at the liquid-vapor interface in the equilibrium chamber. This pressure is equal to the hydrostatic pressure due to all fluids in the transmitting line, plus the pressure exerted by the piston gage, plus the barometric pressure. That is

$$P(\text{dyne cm}^{-2}) = \int \rho g \, dh + (m_0 + m)(g/a) + b,$$

where g is the acceleration of gravity, m_0 is the fixed mass of the piston, weight-carrier etc., m is the mass of the weights added, a is the effective area of the piston, and b is the barometric pressure. The integral can be divided into several parts. Starting at the liquid-vapor surface we have first a column of O_2 vapor. We integrate along the transmitting line, taking dh positive upward. Referring now to figure 1 there is next a section of the line filled with mercury, then one filled with water and finally oil. Let h_0, h_1, h_2, h_3, h_4 be the respective heights of the phase boundaries between O_2-liquid and O_2-vapor, O_2-vapor and Hg, Hg and water, water and oil, oil and the base of the piston. Then the integral can be broken into the following parts

$$\int \rho g \, dh = \int_{h_0}^{h_1} \rho(O_2) g \, dh + \rho(Hg) g (h_2 - h_1)$$

$$+ \rho \text{ (water)} g (h_3 - h_2) + \rho(\text{oil}) g (h_4 - h_3).$$

All heights remain constant except h_1 and h_2, provided the apparatus remains undisturbed and the water-oil cell is properly bled. In the above formula, heights must be in centimeters if densities are in grams per cubic centimeter.

The correction for the hydrostatic pressure of oxygen vapor is quite small and was applied only at pressures above 1 m Hg. Many of the quantities entering into the correction had to be esti-

mated—particularly the temperature distribution along the tube leading out of the cryostat. Other data were taken from the Mollier chart of Millar and Sullivan [11]. The correction ranged from about 0.1 mm Hg at 1 m Hg to about 6.5 mm Hg at the critical point. Except near the latter point it was nearly proportional to the pressure. The correction was applied by increasing $\log_{10}P$ by values ranging from 0.00005 to 0.00007, in the case of the PG Hg measurements.

For the diaphragm cell (PGD) apparatus the correction for oxygen vapor was only slightly different. The equation for P given above was modified, however, to take into account the changed arrangement of fluids in the transmitting line, and included a term for the pressure supported by the diaphragm.

To reduce piston-gage readings to std mm Hg ρ(Hg, 0°C) was taken to be 13.59504 g cm^{-3} [12], and the values of local and standard gravity given earlier were used. The piston-gage oil had a density of 0.8680 g cm^{-3} at 20° C. Variations in the density of water and oil with temperature were taken into account, although they were nearly negligible. Effect of pressure on the density of the oil was neglected. At 50 atm, the density would probably be from 4 to 6 per mille greater than at 1 atm [13]. This would cause an error of only 0.1 mm Hg in the PGD data, and would have still less effect on the PGHg measurements. The mercury column height h_2–h_1 was of course reduced to standard conditions.

Analysis of the data. A number of vapor-pressure equations were used at various stages of the work. The procedure finally adopted, however, is the only one that will be described in detail. This procedure led to the preparation of table 2, which gives $\log_{10}p$ at uniform intervals of $1/T$(or $2/T$). It is thought that interpolation in this table will be more rapid and convenient than evaluating any equation that might represent the data with comparable accuracy. The table gives logarithms of pressures in mm Hg, in atmospheres, and in pounds per square inch absolute. Since a change in units changes logarithms by a constant amount, a single column of differences suffices for all three columns of $\log_{10}p$. Values of all negative logarithms have been increased by 10 to keep the mantissa positive. The value of T corresponding to each value of $1/T$ is given in the table. However, interpolations in the table should be made in terms of the argument $1/T$ (or $2/T$) rather than in terms of T if maximum accuracy is desired. For convenience of those who prefer engineering units, the argument in table 2 is given in units based on Rankine (Fahrenheit absolute) temperatures, as well as Kelvin temperatures.

The scattering of the experimental data, as well as the accuracy with which table 2 represents the data, may be seen in figure 3. Here the deviations (p observed $-p$ calculated) in mm Hg are plotted versus T, the calculated values being found by interpolation in table 2. Numerical values of the plotted data are given in table 1. In figure 3, points belonging to the same run have been joined by straight lines where this could be done without impairing the clarity of the figure.

The procedure used in preparing table 2 was as follows: For each observed point, T log p was computed and plotted versus T. Over limited ranges ($\sim$ 20° to 30°) the curves obtained were very nearly straight lines. Accordingly five linear equations of the form T log $p=AT+B$ were derived and the deviations of the observations from them computed and plotted. Smooth curves were drawn through the points. From these, values were read off at 1° intervals and added to the corresponding values of the equations. The ranges covered by each equation overlapped the range of the next higher equation. In the region of overlap both equations were used, and the results adjusted if necessary to join smoothly near the middle of the range. This procedure led to a table of values of T log P at 1° intervals. This table was smoothed with a 7-point smoothing formula applied by an Underwood-Sundstrand automatic accounting machine. Deviations of the observations from the smoothed table were plotted, after which the table was adjusted and resmoothed where the data required it. Next, table 2 was computed from the table of T log p. As a final check the deviations of the observations from table 2 were computed and plotted. These are given in table 1 and figure 3. Table 3 contains values of the vapor pressure at 5° temperature intervals. It is more convenient than table 2 when rough values are adequate, but table 2 should be used whenever accurate values are to be found by interpolation.

TABLE 2. *Vapor pressure of liquid oxygen*

Interpolation with $1/T$ (or $2/T$) as argument is more accurate and also more convenient than with T as argument. Linear interpolation introduces no significant errors below about 140° K ($2/T°K=3.6/T°R=0.0142$). At higher temperatures linear interpolation can introduce slight errors, which however do not exceed 4 mm Hg and reach this value only in the immediate neighborhood of the critical point

$\frac{2}{T}$	T	$\log_{10} p$				T	$\frac{3.6}{T}$	$\frac{1}{T}$	T	$\log_{10} p$				T	$\frac{1.8}{T}$
°K⁻¹	°K	*mm* Hg	*atm*	*psia*	Δ	°R	°R⁻¹	°K⁻¹	°K	*mm* Hg	*atm*	*psia*	Δ	°R	°R⁻¹
0.037	54.054	*(0.014)	(7.133)	(8.300)	197	97.297	0.037	0.0100	100.000	3.27989	0.39908	1.56627	3641	180.000	0.0100
.036	55.556	.211	[1]7.330	[1]8.497	197	100.000	.036	.0099	101.010	3.31630	.43549	1.60268	3639	181.818	.0099
.035	57.143	.408	7.527	8.694	197	102.857	.035	.0098	102.041	3.35269	.47188	1.63907	3636	183.763	.0098
.034	58.824	.605	7.724	8.891	197	105.882	.034	.0097	103.093	3.38905	.50824	1.67543	3634	185.567	.0097
.033	60.606	.802	7.921	9.088	197	109.091	.033	.0096	104.167	3.42539	.54458	1.71177	3630	187.500	.0096
.032	62.500	.999	8.118	9.285	197	112.500	.032	.0095	105.263	3.46169	.58088	1.74807	3627	189.474	.0095
.031	64.516	1.196	8.315	9.482	196	116.129	.031	.0094	106.383	3.49796	.61715	1.78434	3623	191.489	.0094
.030	66.667	1.392	8.511	9.678	195	120.000	.030	.0093	107.527	3.53419	.65338	1.82057	3622	193.548	.0093
.029	68.966	1.587	8.706	9.873	194	124.138	.029	.0092	108.696	3.57041	.68960	1.85679	3620	195.652	.0092
.028	71.429	1.781	8.900	0.067		128.571	.028	.0091	109.890	3.60661	.72580	1.89299	3620	197.802	.0091
								.0090	111.111	3.64281	.76200	1.92919	3619	200.000	.0090
								.0089	112.360	3.67900	.79819	1.96538	3618	202.247	.0089
$\frac{1}{T}$							$\frac{1.8}{T}$	.0088	113.636	3.71518	.83437	2.00156	3619	204.545	.0088
								.0087	114.943	3.75137	.87056	2.03775	3619	206.896	.0087
0.0140	71.429	1.7807	8.8999	0.0671	385	128.571	0.0140	.0086	116.279	3.78756	.90675	2.07394	3621	209.302	.0086
.0139	71.942	1.8192	8.9384	.1056	384	129.496	.0139	.0085	117.647	3.82377	.94296	2.11015	3622	211.765	.0085
.0138	72.464	1.8576	8.9768	.1440	383	130.435	.0138	.0084	119.048	3.85999	.97918	2.14637	3624	214.286	.0084
.0137	72.993	1.8959	9.0151	.1823	383	131.387	.0137	.0083	120.482	3.89621	1.01542	2.18261	3626	216.867	.0083
.0136	73.529	1.9342	9.0534	.2206	382	132.353	.0136	.0082	121.951	3.93249	1.05168	2.21887	3631	219.512	.0082
								.0081	123.457	3.96880	1.08799	2.25518	3636	222.222	.0081
.0135	74.074	1.9724	9.0916	.2588	382	133.333	.0135								
.0134	74.627	2.0106	9.1298	.2970	382	134.328	.0134	.0080	125.000	4.00516	1.12435	2.29154	3640	225.000	.0080
.0133	75.188	2.0488	9.1680	.3352	381	135.338	.0133	.0079	126.582	4.04156	1.16075	2.32794	3646	227.848	.0079
.0132	75.758	2.0869	9.2061	.3733	381	136.364	.0132	.0078	128.205	4.07802	1.19721	2.36440		230.769	.0078
.0131	76.336	2.1250	9.2442	.4114	381	137.404	.0131								
.0130	76.923	2.1631	9.2823	.4495	381	138.462	.0130								
.0129	77.519	2.2012	9.3204	.4876	380	139.535	.0129								
.0128	78.125	2.2392	9.3584	.5256	380	140.625	.0128								
.0127	78.740	2.2772	9.3964	.5636	378	141.732	.0127	$\frac{2}{T}$							$\frac{3.6}{T}$
.0126	79.365	2.3150	9.4342	.6014	377	142.857	.0126								
.0125	80.000	2.3527	9.4719	.6391	377	144.000	.0125	0.0156	128.2051	4.07802	1.19721	2.36440	1826	230.769	0.0156
.0124	80.645	2.3904	9.5096	.6768	376	145.161	.0124	.0155	129.0323	4.09628	1.21547	2.38266	1826	232.258	.0155
.0123	81.301	2.4280	9.5472	.7144	376	146.341	.0123	.0154	129.8701	4.11454	1.23373	2.40092	1829	233.766	.0154
.0122	81.967	2.4656	9.5848	.7520	375	147.541	.0122	.0153	130.7190	4.13283	1.25202	2.41921	1832	235.294	.0153
.0121	82.645	2.5031	9.6223	.7895	375	148.760	.0121	.0152	131.5789	4.15115	1.27034	2.43753	1834	236.842	.0152
.0120	83.333	2.5406	9.6598	.8270	375	150.000	.0120	.0151	132.4503	4.16949	1.28868	2.45587	1836	238.410	.0151
.0119	84.034	2.5781	9.6973	.8645	375	151.260	.0119	.0150	133.3333	4.18785	1.30704	2.47423	1840	240.000	.0150
.0118	84.746	2.6155	9.7348	.9020	374	152.542	.0118	.0149	134.2282	4.20625	1.32544	2.49263	1842	241.611	.0149
.0117	85.470	2.6530	9.7722	.9394	374	153.846	.0117	.0148	135.1351	4.22467	1.34386	2.51105	1846	243.243	.0148
.0116	86.207	2.6904	9.8096	.9768	373	155.172	.0116	.0147	136.0544	4.24313	1.36232	2.52951	1849	244.898	.0147
.0115	86.957	2.7277	9.8469	1.0141		156.522	.0115	.0146	136.9863	4.26162	1.38081	2.54800	1853	246.575	.0146
								.0145	137.9310	4.28015	1.39934	2.56653	1856	248.276	.0145
								.0144	138.8889	4.29871	1.41790	2.58509	1860	250.000	.0144
.0115	86.957	2.72767	9.84686	1.01405	3725	156.522	.0115	.0143	139.8601	4.31731	1.43650	2.60369	1864	251.748	.0143
.0114	87.719	2.76492	9.88411	1.05130	3718	157.895	.0114	.0142	140.8451	4.33595	1.45514	2.62233	1869	253.521	.0142
.0113	88.496	2.80210	9.92129	1.08848	3712	159.292	.0113								
.0112	89.286	2.83922	9.95841	1.12560	3704	160.714	.0112	.0141	141.8440	4.35464	1.47383	2.64102	1875	255.319	.0141
.0111	90.090	2.87626	9.99545	1.16264	3697	162.162	.0111	.0140	142.8571	4.37339	1.49258	2.65977	1880	257.143	.0140
								.0139	143.8849	4.39219	1.51138	2.67857	1886	258.993	.0139
.0110	90.909	2.91323	0.03242	1.19961	3690	163.636	.0110	.0138	144.9275	4.41105	1.53024	2.69743	1893	260.870	.0138
.0109	91.743	2.95013	0.06932	1.23651	3685	165.138	.0109	.0137	145.9854	4.42998	1.54917	2.71636	1900	262.774	.0137
.0108	92.593	2.98698	0.10617	1.27336	3679	166.667	.0108								
.0107	93.458	3.02377	0.14296	1.31015	3674	168.224	.0107	.0136	147.0588	4.44898	1.56817	2.73536	1909	264.706	.0136
.0106	94.340	3.06051	0.17970	1.34689	3669	169.811	.0106	.0135	148.1481	4.46807	1.58726	2.75445	1919	266.667	.0135
								.0134	149.2537	4.48726	1.60645	2.77364	1930	268.657	.0134
.0105	95.238	3.09720	0.21639	1.38358	3663	171.428	.0105	.0133	150.3759	4.50656	1.62575	2.79294	1942	270.677	.0133
.0104	96.154	3.13383	0.25302	1.42021	3659	173.077	.0104	.0132	151.5152	4.52598	1.64517	2.81236	1956	272.727	.0132
.0103	97.087	3.17042	0.28961	1.45680	3654	174.757	.0103								
.0102	98.039	3.20696	0.32615	1.49334	3649	176.470	.0102	.0131	152.6718	4.54554	1.66473	2.83192	1977	274.809	.0131
.0101	99.010	3.24345	0.36264	1.52983	3644	178.218	.0101	.0130	153.8462	4.56531	1.68450	2.85169	2008	276.923	.0130
								.0129	155.0388	(4.58539)	(1.70458)	(2.87177)	2050	279.070	.0129
.0100	100.000	3.27989	0.39908	1.56627		180.000	.0100	.0128	156.2500	(4.60589)	(1.72508)	(2.89227)		281.250	.0128

* Parentheses indicate extrapolated values, outside normal liquid range.

[1] Logarithms have been increased by 10 wherever necessary to avoid negative mantissas.

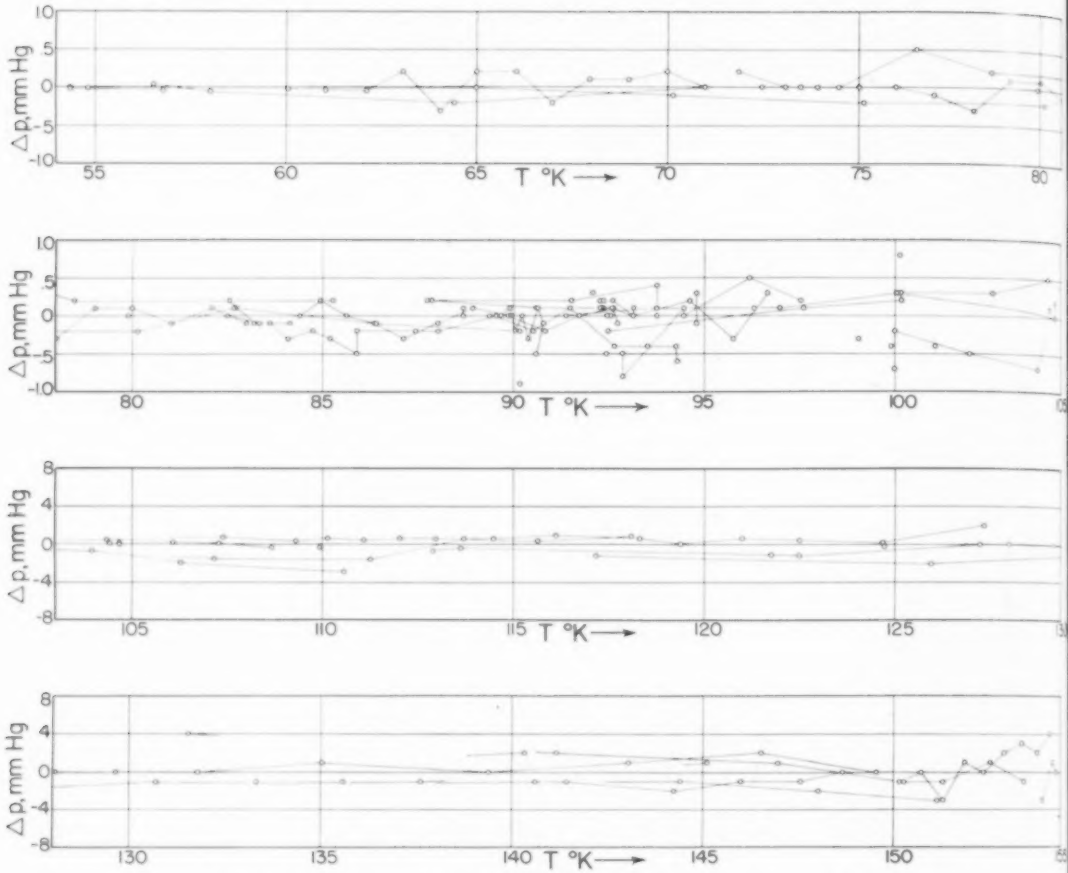

FIGURE 3. *Deviations (observed—calculated) of the observed vapor-pressure data from table 2.*

TABLE 3. *Vapor pressure of oxygen at uniform temperature intervals; also triple-point, boiling-point, and critical-point temperatures and pressures*

T	p	p	p	T	p	p	p
° K	*mm* Hg	*atm*	*psia*	° K	*mm* Hg	*atm*	*psia*
[a] 54.363	1.14	0.00150	0.022	95	1223.3	1.6086	23.65
[b] 90.190	760.0	1.	14.696	100	1905.0	2.5066	36.84
[c] 154.780	38,109	50.14	736.9	105	2838.2	3.7345	54.88
				110	4072.9	5.3591	78.76
55	1.38	0.00182	0.027	115	5661.6	7.4495	109.48
60	5.44	.00716	.105	120	7658.6	10.077	148.09
65	17.4	.0229	.34	125	10,120	13.316	195.7
70	46.8	.0616	.90	130	13,102	17.239	253.4
75	108.7	.1430	2.10	135	16,670	21.934	322.3
80	225.3	.2964	4.36	140	20,892	27.489	404.0
85	425.4	.5597	8.23	145	25,843	34.004	499.7
90	745.0	.9803	14.41	150	31,631	41.620	611.6

[a] Triple point.
[b] Boiling point.
[c] Critical point.

Accuracy of the results. The average deviation om table 2 of the points measured with the oil anometer is 0.014 mm Hg. Where the mercury anometer was used alone, the average deviation s 0.13 mm Hg. Where mercury manometer d barometer were both read, the corresponding ure was 0.22 mm Hg. For piston gage readings ere the diaphragm cell was employed, the erage deviation was 0.84 mm Hg, and where e pressure transmitter shown in figure 1 was d the deviation was 1.13 mm Hg.

The first two runs (March 16 and 17, 1942) re made under rather unfavorable conditions. that time the tube heater was so controlled at the tube thermel indicated a temperature ual to that of the calorimeter. Later it was nd that a somewhat higher temperature was quired to avoid all danger of a cold spot on the be. The values are probably correct, at least thin the limits of their agreement with the later ta. They are included because of the scarcity data at the lowest pressures. They contain the ee measurements made on solid oxygen. As ntioned earlier, leakage of helium from the sistance thermometer caused trouble at one stage the measurements. This was eliminated by erating with a small amount of helium in the ace inside the shield. All data subject to error om loss of helium from the thermometer were carded.

Three possible sources of error must be conered: impurity in the material; the pressure asurements; and the temperature measureents. Effect of impurity is believed to be all compared to other errors. Between the iple point and 95° K, which is about the upper it of the HgB measurements, pressures are ought to be accurate to 0.1 or 0.2 mm Hg. This fers to the smoothed values given by table 2 ther than to individual measurements. Above e range of mercury manometry the uncertainty reases to 1 or 2 mm Hg, and then gradually reases still more as the pressure rises. The certainty near the critical point may be 10 mm g, which is about 1 part in 4,000. Each of the st three values in table 1 is an average obtained om the isotherm data of table 5, and hence is mewhat more accurate than other values in e neighborhood.

Errors associated with temperature measureents are more difficult to estimate. The reproducibility of temperature measurements with a given thermometer was easily ½ mdeg. The triple-point determinations made with thermometers L3 and L14 agreed to better than 1 mdeg, which indicates that the accuracy of our calibrations on the PTS is of the order of 1 or 2 mdeg. It is hoped that the PTS does not deviate from the thermodynamic scale by more than 20 mdeg [1]. Above the oxygen boiling point the ITS was used. The reproducibility of this scale depends on the distances to the nearest calibration points, which in this case were 90.19° and 273.16° K. At the critical point (154.78° K) the uncertainty in the ITS may be as large as 5 mdeg. This does not include any allowance for deviations of the ITS from the thermodynamic scale, which may be as large as 50 mdeg. A few comparisons of temperature scales are made later in this paper.

Comparison with previous work. The more important previous investigations of the vapor pressure of liquid O_2 are listed in table 4. This table gives the range covered by each set of observations and the number of experimental points. A number of isolated values of the vapor pressure of oxygen have been reported, most of them in the neighborhood of the boiling point. These have been omitted from table 4, as have some of the earlier investigations covering more extended ranges. Stull's [21] references give a very complete coverage of both the older and the more recent work on the vapor pressure of oxygen. Additional references are also given in reference [22].

TABLE 4. *Some previous investigations of the vapor pressure of liquid oxygen*

Some additional data, which cover only the neighborhood of the normal boiling point, are referred to in table 6

Year	Reference	Range covered	Number of observations
1913	Siemens [14]	2.68 to 766.8 mm Hg	10
1914	Onnes, Dorsman, and Holst [4].	9.696 to 23.59 atm	13
1918	Cath [15]	0.01262 to 1.0350 atm	10
1924	Henning and Heuse [16]	35.1 to 773.2 mm Hg	26
1927	Giauque, Johnston, and Kelley [17].	60.46 to 757.15 mm Hg	5
1927	Dodge and Davis (also Dunbar) [3].	0.208 to 21.47 atm	64
1935	Aoyama and Kanda [18]	2.04 to 17.85 mm Hg	3
1935	Aston, Willihnganz, and Messerly [19].	11.28 to 746.70 mm Hg	8
1936	Henning and Otto [20]	25.17 to 739.90 mm Hg	19

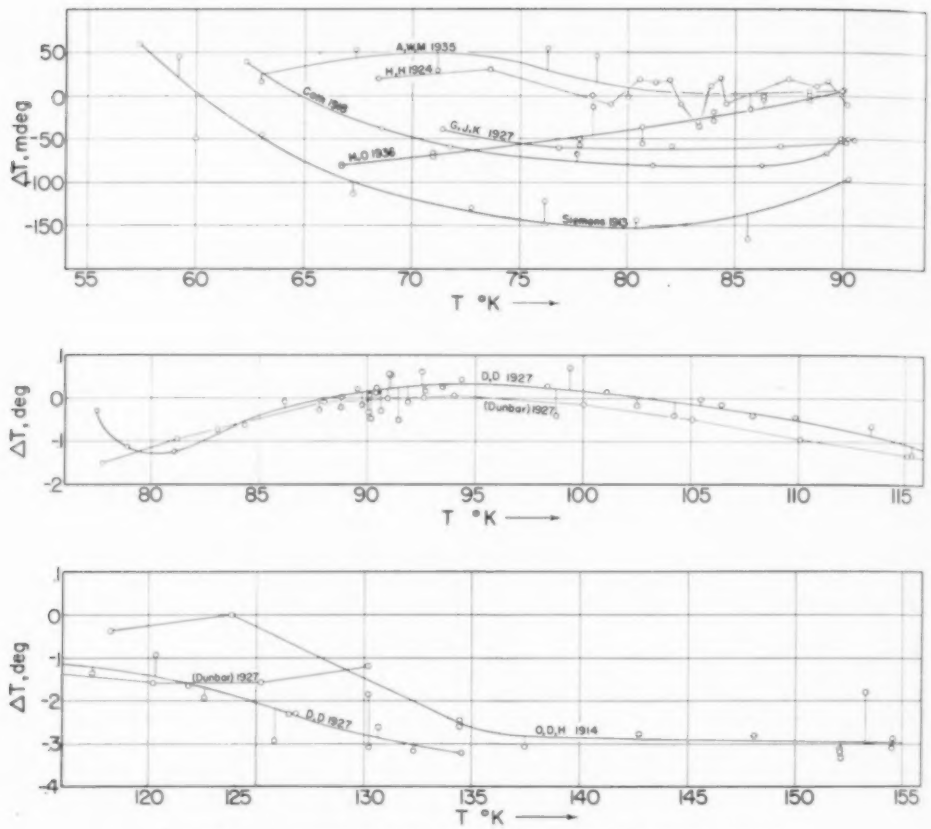

FIGURE 4. *Comparison of the vapor-pressure data of various observers.*

The ordinate is the temperature reported by the observer minus the temperature calculated from table 2.

For all of the data referred to in table 4, deviations from table 2 were computed. These are plotted in figure 4, with the exception of the three points in the paper of Aoyama and Kanda [18]. These had negative deviations of more than half a degree and so are beyond the range of the graph. It is the writer's belief that figure 4 is more instructive as a comparison of various temperature scales than as a comparison of accuracy in pressure measurement, and for this reason the deviations in Figure 4 are in terms of temperature rather than in terms of pressure as in figure 3. The data of Aoyama and Kanda just referred to are probably in error because of unsatisfactory pressure measurements, and this may be true of the data of Onnes, et al.; but most of the differences between the rest of the data and table 2 are probably associated with the temperature. The temperatures of Henning and Heuse [16] were converted from the centigrade to the Kelvin scale w $T_0=273.20$.

In the range below 90° K the negative dev tions considerably outweigh the positive o If however the older data of Siemens [14] a Cath [15] are excluded, there is not a great p ponderance of deviations of either sign. Abo 90° K the data plotted are those of Dodge a Davis [3] (including those of Dodge and Dun in the same reference) and those of Onnes, D man, and Holst [4]. The former show good agr ment with table 2 at 90° but fall more and m below it at higher temperatures, reaching an e treme of about −0.3° at 134° K. Dodge a Davis calibrated their thermocouple at the boil points of N_2, O_2, and CH_4 using for the temp ture of the last 111.52° K. A currently accep [23] value for the boiling point of CH_4 is 111.67 which is 0.15 higher. Dodge and Davis obtai

mperatures above this point by extrapolating
eir calibration, which could easily have intro-
ced the remainder of the −0.3° discrepancy.
he two lowest points of Onnes et al. agree fairly
ell with table 2. The higher points are nearly
about 0.3° below it. It may be significant
at the first two points were measured with a
ultiple-column mercury manometer and the rest
ith a closed-end hydrogen-filled manometer.

V. Isotherms

Measurements of isotherms (p versus v) were
ade to determine the critical temperature and
essure and also vapor pressures immediately be-
w the critical point. The measurement of an
otherm was similar to a series of vapor-pressure
easurements all at the same temperature, except
at after each measurement the amount of water
the pressure-transmitting line (see fig. 1) was
anged. This varied the height h_1 of the first
eniscus and caused O_2 to flow out of the cryo-
at into the transmitting line or vice versa.
hange in h_1 made it necessary of course to rebal-
ce the piston gage even when the change in h_1
d not change the pressure in the equilibrium
amber. Table 5 contains the results of the iso-
erm measurements, after adjustment of each
ies to a common temperature. The adjust-
nts were made in log p, using values of d log p/dT derived from table 2. The largest adjustment was less than 4 mdeg.

Knowing h_1 it was possible to compute the specific volume v of the O_2 remaining in the equilibrium chamber. Some of the data entering into this calculation were not well known, and so the values of v are not very accurate, but this has no effect on the observations of pressure and temperature. In figure 5, the isotherm data of table 5 are plotted versus v. The three isotherms are all below the critical temperature. The highest (154.760° K) has a short horizontal portion.[5]

To help in estimating the temperature of the critical isotherm from figure 5, the shapes of the isotherms in this figure were compared with the accurate isotherms covering the critical region of CO_2 published by Michels, Blaisse, and Michels [25]. From the comparison it was estimated that the critical temperature of O_2 is 154.78°±0.03° K. This is 0.02° above the highest isotherm in figure 5. Accepting this value of T_c, the critical

TABLE 5. *Isotherm data*

[Mean specific volume, v, of material in equilibrium chamber was varied by changing the height of the mercury column in contact with O_2 vapor]

Date	T	v	p
	°K	cm^3g^{-1}	*mm* Hg
Dec. 21 and 29, 1948	154.187	2.72	37,239
		3.02	37,239
		2.33	37,247
		2.57	37,241
		2.73	37,239
		2.93	37,237
		3.22	37,233
Dec. 23, 1948	154.580	1.97	38,586
		2.07	38,114
		2.18	37,895
		2.31	37,829
		2.44	37,817
		2.59	37,816
		2.77	37,814
		2.97	37,804
		3.21	37,742
		3.49	37,592
		2.78	37,818
Dec. 27, 1948	154.759	2.79	38,060
		2.88	38,047
		3.06	38,006
		2.72	38,071
		2.58	38,078
		2.46	38,090
		2.32	38,115
		2.64	38,078

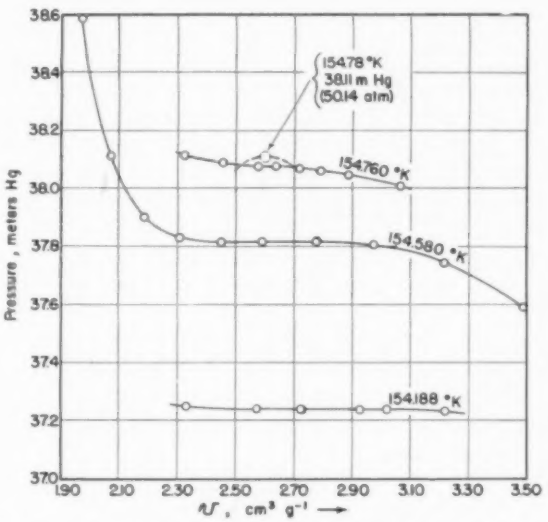

FIGURE 5. *Isotherms of oxygen, showing pressure as a function of specific volume.*

The estimated position of the critical point is shown by the dotted circle.

[5] When the correction for hydrostatic pressure of O_2 vapor is computed from the middle of the equilibrium chamber as was done in the present case, the critical isotherm will not appear to be exactly flat. The exact critical condition progresses from the bottom of the chamber to the top as the material is compressed, so that the hydrostatic correction should strictly be varied along the length of an isotherm. The equilibrium chamber was about 47 mm high. A 47-mm column of O_2 at the critical density of 0.43 g cm^{-3} [24] exerts a hydrostatic pressure of about 1.5 mm Hg. Hence an isotherm that was in truth flat should show a variation of this amount when computed and plotted as in figure 5.

pressure is found from table 2 to be $p_c = 38{,}109 \pm 50$ mm Hg (50.14 atm).

The method by which v was computed from h_1 will be briefly explained. It was necessary to know the mass of O_2 in the equilibrium chamber and the connecting tubes extending to the valve V_1 and the mercury surface h_1. It was also necessary to know the volumes and temperatures of the various parts of this volume. This permitted the mass of O_2 outside the equilibrium chamber to be computed from the known properties of oxygen gas. The mass of O_2 in the equilibrium chamber could then be determined by difference. Division of the volume of the equilibrium chamber by this mass gives v. That is, v is the mean specific volume for the entire chamber, without regard for the fact that two phases were sometimes present.

The volume V containing the known mass of O_2 can be expressed as $V = V_0 - ah_1$, where a is the known inside cross section of the pressure transmitter (0.96_8 cm^2). The volume V was known approximately from the dimensions of the apparatus, but was measured accurately as follows: With all parts of V near room temperature, gas was admitted to a pressure of about 1 atm, which pressure was measured by the height $h_2 - h_1$. The space above h_2 (later filled with water) had been previously evacuated. Next the space above h_2 was opened to the atmosphere, and after time for thermal equilibrium the new pressure in V ($= h_2 - h_1 +$ barometer) was observed. Two or more pairs of values of p and h_1 plus the ideal gas law permit V to be determined as a function of h_1. If necessary V may be treated as a sum of subvolumes each at a different temperature. Several measurements of the type just described gave the following equation, which was accepted for V

$$V(\text{cm}^3) = 84.45 - 0.0968\, h_1\ (\text{mm}). \qquad (1)$$

When this value was checked by computing V from the dimensions of the apparatus, a value 1.15 cm^3 smaller was found. For this reason the specific volumes given in table 5 and figure 5 are rather uncertain.

Computed volumes of various parts of V were adjusted to give agreement with the observed total volume (eq 1). Then from the known pressure, the mass of O_2 at room temperature (assumed to be 300° K) was computed, using compressibility factors from reference [26]. The temperature change from equilibrium chamber to room temperature occurred in a vertical section of tube. Hence the mass of O_2 in this tube could be readily obtained from the integral computed for the hydrostatic pressure corrections to the vapor pressure measurements.

The total mass of O_2 in V was obtained by noting the fall of pressure in the calibrated volume and connecting lines when the mass was transferred to the cryostat. The temperatures of the calibrated volume and the connecting lines were observed. The volumes of the connecting lines including the Hg-in-glass manometer were found by means similar to those used in determining V.

From figure 5 the critical density of O_2 is about $1/2.6 = 0.38$ g cm^{-3}. By making the most extreme assumptions in distributing the 1.15-cm^3 discrepancy previously referred to among the various parts of V, the computed critical density can be raised from 0.38 to about 0.44 g cm^{-3}. Comparison of earlier values of T_c, p_c, and ρ_c with those given in this paper is deferred until after presentation of the calorimetric measurements in the critical region.

VI. Heat Capacities in the Critical Region

Heat-capacity measurements were undertaken to investigate the nature of the changes that take place near the critical point and also to determine whether or not calorimetric methods of determining the critical constants could compete with conventional methods. The apparatus was primarily designed for vapor-pressure work and has several drawbacks as a calorimeter. Hence the results are only indicative of what could be done with a calorimeter properly designed for high-pressure work.

Measurements. All of the heat-capacity measurements were made in the PGD (piston gage-diaphragm cell) apparatus. A known quantity of O_2 was introduced into the volume V, which comprised the equilibrium chamber and the lines extending from it to the valve V_1 and to the diaphragm cell. The quantity of O_2 introduced into V was determined from the fall in pressure in the calibrated volume, as in the case of the isotherm measurements. With the diaphragm cell, eq (1) for V does not apply. Except for motion of the

aphragm, V remains constant. Direct measurement of V by gas-law methods similar to those scribed in the section on isotherms again showed to be more than 1 cm³ larger than the value mputed from available dimensions.

With a known mass of O_2 in V, heat-capacity easurements were made in the usual way by easurement of E, I, and the heating time, t. he shields were kept at the temperature of the alorimeter at all times. The chief weakness of e apparatus as a calorimeter was the rather ort path for heat flow between the copper block g. 2) and the shield, along the two pressure-ansmitting tubes and the larger supporting tube. eat leak here might be expected to affect the oss and tare heat capacities about equally, owever. The latter were measured with V acuated. Owing to the small size of the sample O_2 in V (1.63 to 4.00 g) the net heat capacity as a rather small fraction of the gross heat apacity ($\sim$ 5 to 10% except near the maxima).

Because the conditions under which the heat apacity was measured are somewhat unusual, it ill be worth while to enumerate the various pro-sses taking place in the calorimetric system as easurements are made. Most of the energy pplied is absorbed by the calorimeter (tare heat apacity). The rest is absorbed by the sample. the calorimeter contains both liquid and vapor, rt of the energy will go to raise the temperature each phase, and in addition some material will general pass from one phase to the other, sulting in the absorption or liberation of heat of porization. Besides these processes, the rise temperature increases the vapor pressure of the aterial. This causes vapor to flow out of the alorimeter into the pressure-transmitting tube here its heat capacity is no longer measured. he measurements yield a quantity that is not ry closely related to the familiar C_{sat}, C_v, or C_p a single phase, although these heat capacities n be computed from the measurements if certain uxiliary data are known with adequate accuracy. Although the heat capacities of the individual hases have not in general been computed from e present measurements, the significance of the sults is perhaps most easily grasped by giving e relation between them and the heat capacities the individual phases. The quantity reported also rather simply related to the slopes of certain es on the entropy-temperature diagram. In a previous publication the author [27] derived relations between the heat capacity, c_c, of saturated condensed phase and that of a two-phase system consisting of saturated condensed phase and vapor in equilibrium. Although these were developed primarily to permit correcting for the presence of vapor, they can easily be modified for use in the case under discussion. The present experiments were of type 4 according to the classification of the paper referred to (gross charge, M; tare charge, O; filling tube, yes). For this type of experiment the net observed heat capacity (gross minus tare) of the two phases in the calorimeter is

$$C_{net}=(M-M_t)c_c+T\frac{dS'}{dT}+l\frac{dM_t}{dT} \qquad (2)$$

where M_t is the mass of material in the tube (outside the calorimeter proper), S' is the "excess entropy" of the material in the calorimeter proper, and l is the heat of vaporization per gram. The "excess entropy" is the excess above the entropy of the same mass of saturated condensed phase and may be computed either from latent heat or vapor-pressure data when these and certain other auxiliary data are known. The term $l\ (dM_t/dT)$ is the contribution to the heat capacity of the heat of vaporization of that material which is forced out of the calorimeter by the rising pressure.

In analyzing the present results, the mass M_t was computed by the methods outlined in the section on isotherms, *using the same values* as were used there for the various subvolumes of V. The term $l(dM_t/dT)$ was then computed and subtracted from C_{net} for all points where two phases were actually present in the calorimeter. Division by $M-M_t$, the mass of material present in the calorimeter, and multiplication by W, the molecular weight, gave the molar heat capacity under the conditions of the experiment, which is

$$C(j\ \text{mole}^{-1})=C_c+\frac{WT}{M-M_t}\frac{dS'}{dT} \qquad (3)$$

This quantity has been plotted in figure 6. Except in one isolated case mentioned later, the two terms on the right were not separately evaluated. Each of the six curves in the figure was taken with a different mass of material in the calorimeter so that data would be obtained at volumes both above and below the critical. All but the top curve have pronounced maxima corresponding to

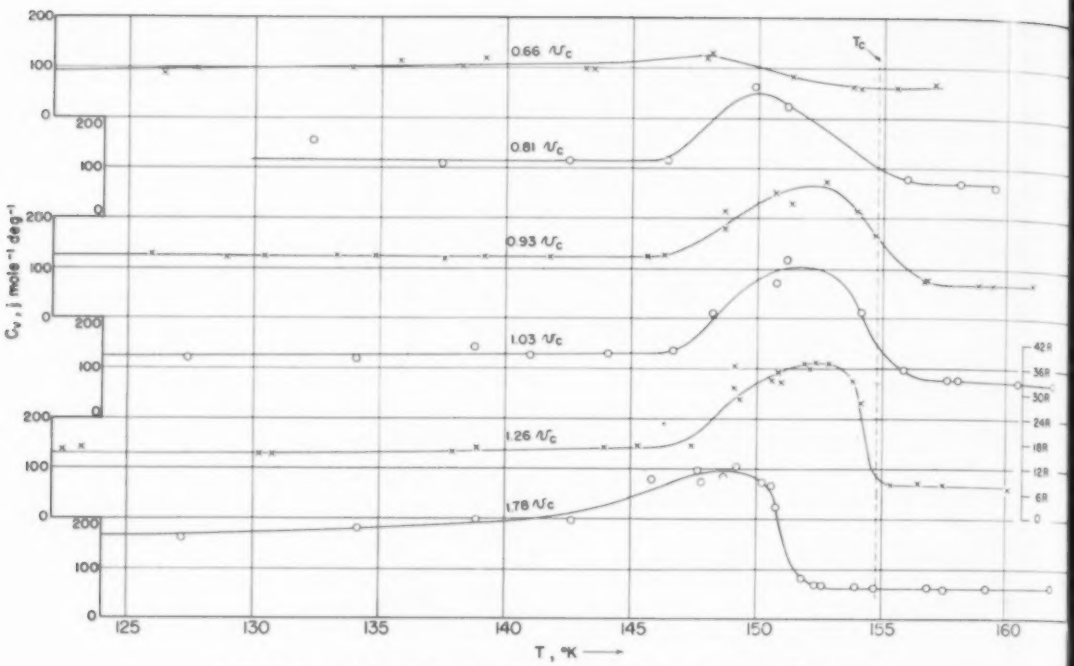

FIGURE 6. *Molar heat capacity, C_v, of oxygen at various specific volumes.*

Maxima in the curves are caused by the rapid absorption of the heat of vaporization.

a much more rapid absorption of heat as the critical temperature is approached. The quantity plotted is a property of the material, but as the figure shows, it also depends on volume. Owing to the gradual increase in M_l, the curve obtained with any one filling does not correspond to a constant volume line, although it approximates rather closely to such a line at temperatures well below the critical. The mass of material present in the calorimeter falls by 10 or 20 percent as the pressure rises, so the over-all specific volume of the material being measured increases by this amount. The molar volumes given in figure 6 for each curve were computed for the temperatures at which the respective maxima occurred.

On the entropy-temperature diagram the paths followed are at first approximately constant-volume lines in the two-phase region, but as the temperature rises the paths deviate more and more in the direction of higher volumes. Figure 7 is an S-T diagram, drawn somewhat schematically. Along any path in such a diagram, $C_{path}=T(dS/dT)_{path}$, because of the fundamental relation $dS=\delta Q/T$. Hence the slope of a constant-volume line is T/C_v, and the slope of any path is T/C_{path}. The maxima in the heat-capacity curve of figure 6 correspond therefore to the portions of the paths having the least slopes. Three constant volume lines (solid curves) are drawn in figure 7 about as they usually appear in S-T diagrams. These lines have a slowly decreasing slope in the two-phase region, with an abrupt increase in slope at the boundary. This corresponds to slowly increasing heat capacity while two phases are present, with an abrupt drop to a lower heat capacity on crossing the boundary of the liquid-vapor dome.

The two lowest heat-capacity curves of figure 6 ($v=1.78\ v_c$ and $v=1.26\ v_c$) show that a rather abrupt drop does occur at the dome boundary when the volume is considerably greater than the critical volume. At the critical and all lower volumes, however, the drop is gradual rather than abrupt, but there is a region of high heat capacity several degrees wide before the dome boundary is crossed. The paths followed on the S-T diagram therefore look more like the two dotted curves than like the solid curves. It would seem that the differences in the two sets of curves are a little too large to be entirely accounted for by the

dual increase in molar volume of the material. this is the case, the constant-volume lines in *S-T* diagram should be drawn with short tions of high curvature at the dome boundary her than sharp breaks, at least for v less than v_c. Accurate calorimetric data would permit the nstruction of an *S-T* diagram, and those antities most difficult to determine from *-T* data would be most easily found by orimetry. The present data were not con- ered accurate enough to warrant the con- uction of such a diagram, but they indicate at might be done with a calorimeter containing arger sample, with better thermal isolation, and referably without the complication of a filling e permanently in communication with the uilibrium chamber.[6]

The curves of figure 6 show that the heat pacity of a sample always drops when the orimeter is entirely filled with one phase, ardless of whether this phase is liquid or vapor. the lowest filling ($v=1.78\ v_c$) both liquid and por were present up to about 151° K, at which mperature all the liquid had evaporated. the highest filling ($v=0.66\ v_c$) the liquid ex- panded until at about 148° K it entirely filled the calorimeter.

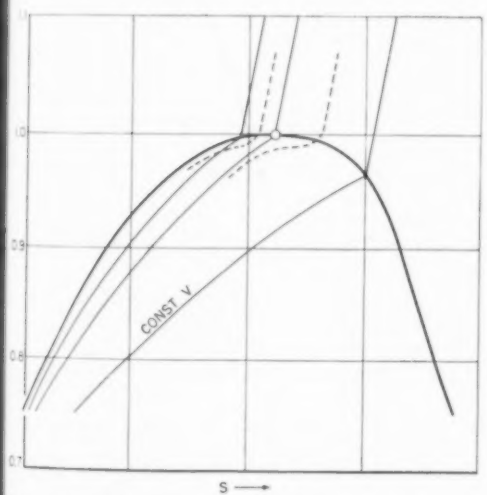

FIGURE 7. *Schematic entropy-temperature diagram.*

he heat-capacity curves of figure 6 correspond more closely to the dotted ant-volume lines than to the solid lines with sharp breaks in them.

rofessor A. Michels (private communication) states that the Van Der ls Laboratory will shortly publish measurements of the heat capacity y extending through the critical region. These give promise of furnish- a more conclusive demonstration of the value of high-pressure calorimetry the present results.

A few somewhat puzzling facts regarding figure 6 should be pointed out. At temperatures above their respective maxima all the curves drop to values lying between 60 and 70 j mole^{-1} deg^{-1}. Only one phase is present in the calorimeter and (at least for the three lower curves) material is not being forced out of the calorimeter as rapidly as it was at the maxima. Hence the heat capacity, which must lie somewhere between C_v and C_p, should in fact be rather close to C_v. For molecular oxygen in this temperature range the heat capacities in the ideal gas state are $C^\circ_p=29.12$ and $C^\circ_v=20.81$ j mole^{-1} deg^{-1} [28]. The observed values are therefore about $65-25=40$ j mole^{-1} deg^{-1} or about $5R$ higher than the ideal gas value. This seems rather high in comparison with similar data for other substances. For example, Bennewitz and Splittgerber [29] measured C_v for CO_2 through the critical region, at one volume slightly below and another slightly above the critical volume. The two values of C_v that they obtained at 40° C (about 9 deg above T_c) differ by less than 2 percent, the average being 56.0 j mole^{-1} deg^{-1}. This value is in fairly good agreement with the results of Michels and de Groot [30], who computed heat capacities from *P–V–T* data. At 40° C and approximately the critical volume, the latter give $C_v=53.7$. The ideal gas value at 40° C is about 29.3 [31], so $C_v-C^\circ_v \doteq 55-29.3=25.7$ j mole^{-1} deg^{-1}, or 3.1 R. Data are also available for ethylene. Pall, Broughton, and Maass [32] measured C_v for ethylene at a volume slightly less than the critical. At 22° C (about 12.5 deg above T_c) they found 47.5 j mole^{-1} deg^{-1}, whereas the ideal gas value [33] is about 34.9. Hence $C_v-C^\circ_v=12.6$, or 1.5 R.

The excess of the heat capacity of a fluid above the value in the ideal gas state may be computed from an equation of state. Unfortunately, there does not appear to be any such equation that represents the behavior of oxygen in the critical region. Using the Beattie-Bridgeman equation, with constants that fit the *P–V–T* data for oxygen at somewhat lower densities, a calculated value of $C_v-C^\circ_v=1.2\ R$ is obtained at the critical density and slightly above the critical temperature. A similar calculation for CO_2 gave $C_v-C^\circ_v=1.8\ R$. W. S. Benedict made calculations using the Kellogg equation in a reduced form that gives a very good

representation of the behavior of hydrocarbons, and also using Su and Chang's reduced form of the Beattie-Bridgeman equation. At the critical density and temperature the result with the Kellogg equation was $C_v - C_v^\circ = 1.3\ R$, and with the reduced Beattie-Bridgeman, $C_v - C_v^\circ = 1.5\ R$. So far as experimental data are available for checking, values of $C_v - C_v^\circ$ calculated from these equations of state appear to be too low, and we may expect that when better equations of state are found they will lead to higher values.

The value of $C_v - C_v^\circ$ found for oxygen from figure 6 is $5\ R$, as compared with experimental values of $3.1\ R$ for CO_2 and $1.5\ R$ for ethylene. Although the value of $5\ R$ is not so far out of line as to be impossible, it is considerably larger than might be expected. The heat capacities well below the maxima in the curves are also rather higher than was expected, as is discussed in the following paragraph. Such results could be explained by assuming that the tare heat capacity was incorrectly determined, or that the heat leak changed between the gross and the tare measurements. However, the error required is larger than would be anticipated.

As previously pointed out, the heat capacities plotted in figure 6 are given by eq 3. By evaluating and subtracting the last term in this equation, the molar heat capacity C_c of saturated liquid can be obtained. This was done for each of the curves at 130° K, using for the excess entropy the expression $S' = (dP/dT)[V - (M - M_l)v_c]$ from reference [27]. Molar volumes of saturated liquid were taken from reference [11], and values of dP/dT were calculated from table 2. The values of C read from the six curves of figure 6 at 130° K are (from bottom to top) 172, 130, 126, 123, 115, 100 j mole^{-1} deg^{-1}. The corresponding values of C_c found from eq 3 are in the same order 135, 108, 111, 111, 107, 96 j mole^{-1} deg^{-1}. In the absence of error all these values should agree. Giving most weight to the values for which the correction was small, the data give a value of at least 100 j mole^{-1} deg^{-1} for saturated liquid at 130° K. There are no other measurements at this temperature, but Giauque and Johnston [10] have reported heat capacities up to the boiling point (90.19° K). At this temperature C_c is about 54 j mole^{-1} deg^{-1}, and the curve is gradually rising. Compared with this, a value of 100 at 130° K seems rather high. One could of course postulate some cause of high heat capacity throughout the en critical region, such as the existence of a la proportion of O_4 molecules. Rather than draw a such conclusion, it seems wiser simply to pres the data as a qualitative picture of the depende of heat capacity on volume in the critical reg It is planned, when time permits, to perfo similar experiments in an apparatus capable normal calorimetric accuracy. The loss of heli from the resistance thermometer, which made necessary to operate the apparatus with the sp inside the shields filled with helium, also makes seem unwise to repeat any of the calorimet measurements with the present apparatus.

As a method of determining the critical te perature and volume, the calorimetric meth appears to be comparable in ease of applicati with the isotherm method. It may be slight inferior in accuracy with equal expenditure effort. Before it can be practically applied better knowledge of the relation between he capacity curves and isotherms is needed. present the exact point on the critical he capacity curve to associate with the point on t critical isotherm having a horizontal tangent not known. From figure 6 one would say th at the critical temperature C_v has fallen somewh more than half way from its maximum to i limiting value.

VII. The Critical Constants

The critical constants derived from the isother data (fig. 5) are $T_c = 154.78° \pm 0.03°$ K, p_c 50.14 ± 0.07 atm, and $\rho_c = 0.38$ g cm^{-3}. Of the T_c and p_c are probably better values than a previously available. The value of ρ_c is mu less accurate. There do not appear to be a reported measurements of the critical constan of O_2 since the survey of Pickering [34] in 19 which summarized the results of 11 differe investigations in which one or more of the criti constants was determined. Pickering selected best values: $t_c = -118.8°$ C, $p_c = 49.7$ atm, a $\rho_c = 0.430$ g cm^{-3}. These are also the valu contributed by Germann and Pickering to th International Critical Tables [24]. They a essentially the values of Onnes, Dorsman, a Holst [4] for T_c and p_c, and the value of Mathi and Onnes [35] for ρ_c. In the original pap Onnes, Dorsman, and Holst give T_c both centigrade and Kelvin units ($-118.82°$ C

4.27° K). They determined the critical temperature by observing the formation of a meniscus when the sample was suddenly expanded by a small amount. If the meniscus remained permanently the temperature was considered to be below T_c. At the accepted value of T_c the meniscus appeared in the middle of the tube; then slowly disappeared at the same level. The critical density was found by Mathias and Onnes by extrapolation of the rectilinear diameter of the density parabola.

The critical pressure now being reported is 43 atm higher than the value of Onnes et al. (49.713 atm). The critical temperature is 0.51 deg higher. One may ask whether this is simply the result of using different methods of identifying the critical point, as it is common experience that the meniscus disappears somewhat below the highest temperature for which $(\partial p/\partial v)_T=0$. If this were the case the values 154.27° K and 49.713 atm would satisfy table 2, being simply a slightly lower point on the vapor-pressure curve than the critical point now being reported. Figure 4 shows that less than half the discrepancy can be explained in this way. The highest plotted point in figure 4 is the critical point of Onnes, Dorsman, and Holst. It is about 0.29 deg lower than the table. This discrepancy must be due either to actual differences in temperature or pressure measurements or to the purity of the sample.

The value of the critical density deduced from the isotherm measurements (0.38 g cm^{-3}) is probably less accurate than the value of Mathias and Onnes (0.4299).[7]

VIII. The Two Solid-Solid Transitions

One heat-capacity run extending from 20.4° K to above the triple point of O_2 was made in 1942, with the small conventional adiabatic calorimeter. No tare run was made, and the mass of O_2 was only approximately known, so no specific heats or heats of transition are reported. The shape of the heat-capacity curve at the lower transition is shown in figure 8. The upper curve was obtained first, proceeding from lower to higher temperatures as indicated by the arrows. Then the apparatus was left for about an hour, with the shields cold so that the O_2 cooled partially through the transition again. On resuming measurements from this condition a much lower heat capacity curve was obtained in the transition region. This is presumably due to hysteresis in the transition and would not have been observed if the second cooling had proceeded to 20.4° K like the first. The maximum in the first heat-capacity curve is at 23.886° ±0.005° K.

Table 6 contains the previously reported values for the temperature of this transition and also for the temperature of the transition at 43.8° K. The table also contains the more recent reported

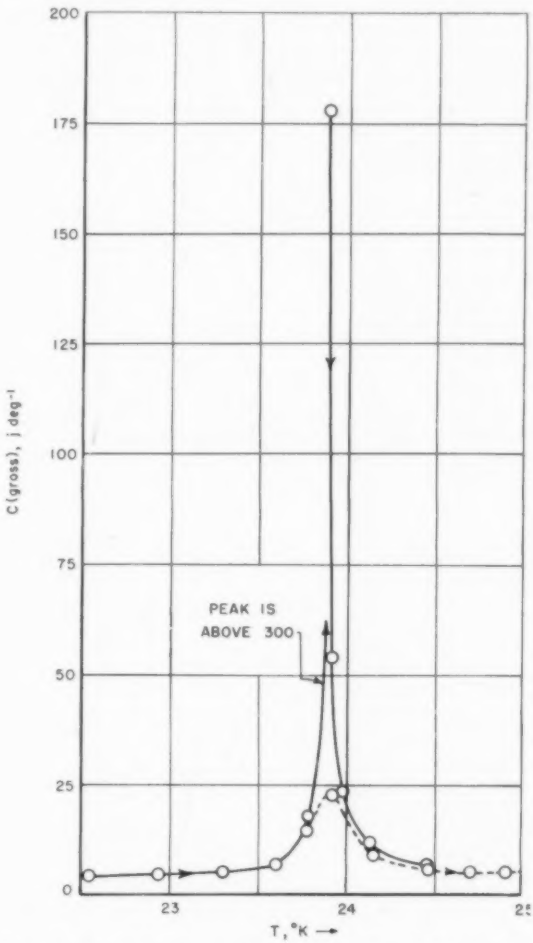

FIGURE 8. *Heat capacity of oxygen in the neighborhood of 23.9° K.*

Solid curve obtained in the usual way; dotted curve obtained after cooling only part way through the transition.

[7] Since completing this paper, the apparatus has been used on another project. The measurements of volumes occupied by fluid at high pressure, discussed on p. 336, have been repeated and extended. The redeterminations confirm the value $\rho_c=0.38$ g cm^{-3}, and it is now thought that this value should receive equal weight with that of Mathias and Onnes.

871926—50——9

TABLE 6. *Some previously reported values of the transition temperatures, the triple-point temperature and pressure, and the normal boiling point of oxygen*

Year	Reference	T	p	Thermometer
	TRANSITION AT 23.9° K			
		° K	*mm Hg*	
1916	Eucken [36]	23.5	...	Pb resistance
1929	Clusius [37]	23.8	...	Pb resistance
1929	Giauque and Johnston [10]	23.66	...	Cu-const thermel
1949	This research	23.886	...	Pt resistance
	TRANSITION AT 43.8°K			
1916	Eucken [36]	42.5	...	Pb resistance
1929	Clusius [37]	43.5	...	Pb resistance
1929	Giauque and Johnston [10]	43.76	...	Cu-const thermel
1935	Aoyama and Kanda [18]	43.70	...	Cu-const thermel
1949	This research	43.80_0	...	Pt resistance
	TRIPLE POINT			
1911	Onnes and Crommelin [38]	[a] 54.7	...	Pt resistance
1911	Dewar [39]	54	1.12	H_2 gas
1916	Eucken [36]	54.1	...	Pb resistance
1929	Clusius [37]	54.1	...	Pb resistance
1929	Giauque and Johnston [10]	54.39	...	Cu-const thermel
1931	Justi [40]	54.24	1.20	Resistance
1935	Aoyama and Kanda [18]	54.4_0	...	Cu-const thermel
1935	Lisman and Keesom [41]	54.32_5	...	Pt resistance
1936	Henning and Otto [20]	54.33	...	He gas const volume
1949	This research	54.363	1.14	Pt resistance
	BOILING POINT			
1918	Cath [15]	90.14	.....	He gas const volume
1924	Henning and Heuse [16]	[b] 90.196	.....	He gas const volume
1927	Henning [42]	[b] 90.21	.....	Pt resistance
1929	Giauque and Johnston [10]	90.13	.....	Cu-const thermel
1929	Keesom, Van der Horst, and Jansen [43]	[c] 90.143	.....	He gas const volume
1931	Heuse and Otto [44]	[d] 90.198	.....	He gas const volume
1932	Heuse and Otto [45]	[d] 90.195	.....	He gas const volume
1935	Aoyama and Kanda [46]	[d] 90.18	.....	H_2 gas const volume
1935	Keesom and Dammers [47]	[e] 90.159	.....	Pt resistance
1937	Blue and Hicks [48]	90.20	.....	He gas const volume

[a] Using $T_0 = 273.09$.
[b] Using $T_0 = 273.20$.
[c] Using $T_0 = 273.12$.
[d] Using $T_0 = 273.16$.
[e] Using $T_0 = 273.144$.

values of the triple point temperature and pressure and the boiling point. Most of the references in table 6 are from a previous survey made by the author [22], which also contains some additional references published prior to 1915. Eucken [36] states that the 23.9° K transition showed time lags that made it difficult to measure the he transition accurately. Clusius [37] says transition is sharp, but Giauque and Johnston found temperature variations of 0.1 deg while transition varied from 15 to 65 percent comp In the present experiments the transition found to be rather broad, but no very notic tendency for the temperature to drift after he periods was observed. This was in contra the behavior at the 43.8° K transition, where tendency to drift was extreme.

The transition at 43.8° K is more satisfact represented by a temperature versus energy c than by a heat-capacity curve. Figure 9 sh the gradual rise in temperature as successive tions of the sample were transformed. After addition of energy the temperature drifted d rapidly at first and then more and more slo The temperature was plotted versus time for t drifts, to see whether the limiting value was i pendent of the amount of material conver This was quite definitely not the case. The w ing periods were not all the same length. The points in figure 9 correspond to short wa periods and the low points to long waiting per The line drawn through the points corresp roughly to an average drift period of 10 min. waiting longer the whole curve would have b lowered and might have lost some of its upw slope, but could certainly not have been made Figure 9 gives 43.81_0° K as the temperature w the transition is half completed. With m longer drift periods this value might have b lowered to about 43.80_0° K. The latter valu included in table 6 as the best value of the tra

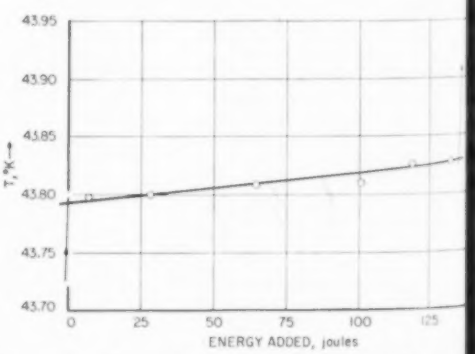

FIGURE 9. *Temperature versus energy curve for oxyg the neighborhood of 43.8° K, showing that the trans covers a temperature interval of more than 0.03 deg.*

temperature derivable from the present work. is of interest that the heat of transition at ° K is larger than the heat of fusion (at 54.363° in the ratio of 5 to 3. This transition is gen- y assumed to be due to a change in crystal cture. The heat of the transition at 23.9° K out one-fifth of the heat of fusion. It has been gested that this transition is of magnetic origin. curve in figure 8 bears some resemblance to e that are commonly attributed to the onset otation of the molecules of a crystal lattice, is somewhat more symmetrical than the typ- curve of this type. Perrier and Onnes [49] d that on cooling from 33° to 20° K, the mag- susceptibility of O_2 suddenly drops to about its original value. Although they thought change occurred near 33° K it is more likely it took place at the 23.9° K transition.

The Triple Point and the Boiling Point

he plotting of melting-point data versus the procal of F, the fraction of the sample melted, discussed in the section on preparation and ty of the samples. The intercept of the ight line drawn gives the triple point of pure erial. Measurements on the first sample, e with platinum resistance thermometer L3, a triple point temperature of 54.363° K. lar measurements on the third sample, made thermometer L14 gave a value less than 1 g lower. Such close agreement is fortuitous, L14 was calibrated by comparison with some he group of standard thermometers of which was a member, and the comparison could be cted to introduce uncertainties of 2 or 3 mdeg. veral observations of the triple-point pressure given in table 1. The last of these is the t reliable. Earlier points may possibly be in r because of condensation in the tube lead- to the manometer. For previously reported es of triple-point temperatures and pressure, e 6 should be consulted.

he temperature of the normal boiling point of was taken to be 90.19° K. This is the value ined when the accepted value on the ITS 82.97° C) is converted to the Kelvin scale T_0=273.16° K. The calibration of the stance thermometers was based on this value hence the present data yield no information its correctness. This value has been used in all our work since and including the establishment of the NBS provisional temperature scale below 90° K. Some of the more recent reported values of the boiling point are given in table 6.

X. Remarks on Temperature Scales

No correlation of vapor-pressure data with latent heat data is presented at this time. It is known that the ITS and the provisional scale below 90.19° K on which these measurements are reported (PTS) are not in exact agreement with the thermodynamic scale. This is particularly true near the point where the PTS and the ITS join. The quantity $d(\log_{10}p)/d(1/T)$ was computed from table 2 by numerical differentiation. It exhibited noticeable irregularities that are undoubtedly due to irregularities in the temperature scale. Our temperature scale could undoubtedly be improved simply by smoothing the curve of $d(\log_{10}p)/d(1/T)$ and computing the corresponding changes in temperatures, but it seems best not to include such an investigation in the present paper. By use of Clapeyron's equation it is easily shown that

$$-\frac{d\ (\log_{10}p)}{d(1/T)}=\frac{L}{2.303R(Z_g-Z_l)}$$

where L is the heat of vaporization, and the Z's are compressibility factors ($Z=PV/RT$) for the gas and the liquid phases, respectively. Experimental determination of L *on the same temperature scale* as the vapor pressure measurements would permit a much more significant correlation of vapor pressures and latent heats than is now possible, and would permit our temperature scale to be more accurately smoothed. It is planned to undertake measurements of the heat of vaporization as soon as time permits.

TABLE 7. *Fixed-point temperatures reported by three different laboratories, selected for a comparison of temperature scales*

Values in parentheses are accepted values rather than original determinations

Fixed point	PTR	NBS	California	PTR −Calif.	NBS −Calif.
	° K	° K	° K	mdeg	mdeg
n-H_2 triple point	13.96 [20]	13.96 [1]	13.92	40	40
n-H_2 boiling point	(2.380)[20]	20.39 [1]	20.36	20	30
O_2 upper trans		43.80a	43.76 [10]		40
O_2 triple point	54.33 [20]	54.363	54.39 [10]	−60	−27
N_2 triple point	63.14 [20]		63.14 [50]	0	
N_2 boiling point	77.352 [20]		77.32 [50]	32	
O_2 boiling point	a 90.195 [45]	(90.19)	90.13 [10]	65	60

aUsing T_0=273.16° K.

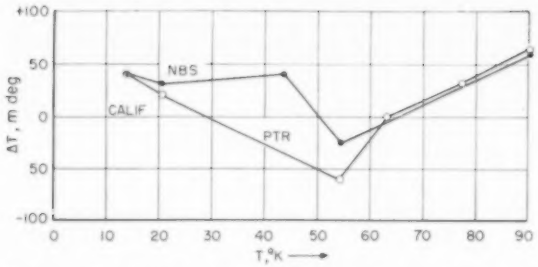

FIGURE 10. *A comparison of the temperature scales of three different laboratories by means of the fixed-point data of table 7.*

Certain laboratories, such as the Leiden Laboratory, the Physikalisch-Technische Reichsanstalt (PTR), the cryogenic laboratory of Professor Giauque at the University of California, and the National Bureau of Standards, have maintained and used more or less well defined temperature scales over periods of years. As the temperatures of various fixed points on these scales are published it becomes possible to compare them. Table 7 contains a few data of this sort from three of the laboratories mentioned. Differences in the reported values for each fixed point are plotted in figure 10, using the California scale as a base line because it contains all of the fixed points included. The figure shows that the PTR and NBS values are in somewhat better agreement with each other than with the California data. The comparison of vapor-pressure data given in figure 4 is, as previously pointed out, essentially a comparison of temperature scales. Judging from this figure, temperatures between 60° and 90° K are uncertain by at least 30 mdeg; and slopes, which determine the accuracy of heat capacity measurements, may be uncertain by a part in 300.

Russell B. Scott collaborated in all the measurements made in 1942. Thanks are due also to a number of persons who have assisted in the subsequent work, particularly Ruth (Cheney) Suits, Robert E. McCoskey, and Martin T. Wechsler. The drawings and graphs were prepared by W. L. Cross, Jr.

XI. References

[1] Harold J. Hoge and Ferdinand G. Brickwedde, Establishment of a temperature scale for the calibration of thermometers between 14° and 83° K, J. Research NBS **22,** 351 (1939) RP1188.

[2] H. F. Stimson, The International Temperature Sc... of 1948, J. Research NBS **42,** 209 (1949) RP19...

[3] Barnett F. Dodge and Harvey N. Davis, Vapor pr... sure of liquid oxygen and nitrogen, J. Am. Ch... Soc. **49,** 610 (1927).

[4] H. Kamerlingh Onnes, C. Dorsman, and G. Ho... Vapor pressures of oxygen and critical point ... oxygen and nitrogen, Commun. Phys. Lab. Un... Leiden **145b** (1914).

[5] Russell B. Scott, Cyril H. Meyers, Robert D. Ra... Jr., Ferdinand G. Brickwedde, and Nor... Bekkedahl, Thermodynamic properties of ... butadiene in the solid, liquid, and vapor sta... J. Research NBS, **35,** 39 (1945) RP1661.

[6] N. S. Osborne, H. F. Stimson, E. F. Fiock, and D. ... Ginnings, The pressure of saturated water va... in the range 100° to 374° C, BS J. Research ... 155 (1933) RP523.

[7] C. H. Meyers and R. S. Jessup, A multiple manom... and piston gages for precision measurements, BS ... Research **6,** 1061 (1931) RP324.

[8] D. F. Stedman, Preliminary survey of the fracti... tion of isotopic isomers by distillation, Can. ... Research [B] **13,** 114 (1935).

[9] Russell B. Scott, *The calibration of thermocouples ... low temperatures.* Temperature—its measureme... and control in science and industry, p. 206 to ... (Reinhold Pub. Corp., New York, N. Y., 1941).

[10] W. F. Giauque and H. L. Johnston, The heat capac... of oxygen from 12° K to its boiling point and ... heat of vaporization. The entropy from spect... scopic data, J. Am. Chem. Soc. **51,** 2300 (1929).

[11] Russell W. Millar and John D. Sullivan, Therm... dynamic properties of oxygen and nitrogen, U. ... Bureau of Mines Technical Paper 424 (1928).

[12] Raymond T. Birge, The general physical consta... Reports on Progress in Physics **8,** 90 (1941).

[13] R. S. Jessup, Compressibility and thermal expans... of petroleum oils in the range 0° to 300° C, BS ... Research **5,** 985 (1930) RP244.

[14] H. v. Siemens, On vapor pressure measurements a... thermometry at low temperatures, Ann. Phys. ... **42,** 871 (1913).

[15] P. G. Cath, Vapor pressures of oxygen and nitrog... for obtaining fixed points on the temperature sc... below 0° C, Commun. Phys. Lab. Univ. Le... **152d** (1918).

[16] F. Henning and W. Heuse, A new determination ... the normal boiling points of oxygen, nitrogen, a... hydrogen, Zeit. Physik. **23** 105 (1924).

[17] W. F. Giauque, H. L. Johnston, and K. K. Kel... Hydrogen gas thermometer compared with ... oxygen and hydrogen vapor-pressure thermo... eters by means of a copper-constantan therm... couple, J. Am. Chem. Soc. **49,** 2367 (1927).

[18] Shinichi Aoyama and Eizo Kanda, The vap... tensions of oxygen and nitrogen in the solid sta... Sci. Repts. Tohoku Imp. Univ. Sendai **24,** ... (1935).

[1] J. G. Aston, Eugene Willihnganz, and George H. Messerly, A thermodynamic temperature scale in terms of the copper-constantan thermocouple from 12° to 273° K, J. Am. Chem. Soc. **57,** 1642 (1935).

[2] F. Henning and J. Otto, Vapor-pressure curves and triple points in the temperature range from 14° to 90° abs., Phys. Zeit. **37,** 633 (1936).

[3] Daniel R. Stull, Vapor pressures of pure substances, Ind. Eng. Chem. **39,** 517 (1947).

[4] Harold J. Hoge, *A practical temperature scale below the oxygen point and a survey of fixed points in this range.* Temperature—its measurement and control in science and industry, p. 141 to 156 (Reinhold Pub. Corp., New York, 1941).

[5] American Petroleum Institute Research Project 44 at the National Bureau of Standards. Selected Values of Properties of Hydrocarbons. Table No. 1a-Paraffins, C_1 to C_5. Boiling point, dt/dp, refractive index, density and freezing point. (June 30, 1945; June 30, 1948).

[6] International Critical Tables **3,** 248 (1928).

[7] A. Michels, B. Blaisse, and C. Michels, The isotherms of CO_2 in the neighborhood of the critical point and round the coexistence line, Proc. Roy. Soc. London [A]**160,** 358 (1937).

[8] Harold J. Hoge, Cyril H. Meyers, and Robert E. McCoskey, Charts of compressibility factors and charts showing quantities delivered by commercial cylinders for hydrogen, nitrogen, and oxygen, NBS Misc. Pub. **M191** (1948).

[9] Harold J. Hoge, Heat capacity of a two-phase system, with applications to vapor corrections in calorimetry, J. Research NBS **36,** 111 (1946) RP1693.

[10] Harold W. Woolley, Thermodynamic functions for molecular oxygen in the ideal gas state, J. Research NBS **40,** 163 (1948).

[11] K. Bennewitz and E. Splittgerber, Specific heat of carbon dioxide at the critical point, Zeit. physikal. Chem. **124,** 49 (1926).

[12] A. Michels and S. R. de Groot, Thermodynamical properties of carbon dioxide as function of density and temperature, Appl. Sci. Research **A1,** 94 (1948).

[13] Serge Gratch, Zero-pressure thermodynamic properties of carbon dioxide. Presented at the annual meeting of the Am. Soc. Mech. Engrs. (New York, N. Y., Nov. 28 to Dec. 3, 1948).

[14] D. B. Pall, J. W. Broughton, and O. Maass, The heat capacity at constant volume of the system ethylene near the critical temperature and pressure, Can. J. Research **B16,** 230 (1938).

[15] American Petroleum Institute Research Project 44 at the National Bureau of Standards. Selected Values of the Properties of Hydrocarbons. Table No. 8v (Part 1) Monoolefins, C_2 to C_4, Heat Capacity, C_p^0, for the ideal gas state, at 0° to 1500° K (Dec. 31, 1944; April 30, 1946).

[16] S. F. Pickering, A review of the literature relating to the critical constants of various gases, BS Sci. Pap. **21,** 597 (1926) S541.

[35] E. Mathias and H. Kamerlingh Onnes, The rectilinear diameter for oxygen, Commun. Phys. Lab. Univ. Leiden **117** (1911).

[36] A. Eucken, On the thermal behavior of some compressed and condensed gases at low temperatures, Verhandl. deut. physik. Ges. **18,** 4 (1916).

[37] Klaus Clusius, On the specific heats of some condensed gases between 10° abs. and their triple points, Zeit. physikal. Chem. **B3,** 41 (1929).

[38] H. Kamerlingh Onnes and C. A. Crommelin, Remarks upon the critical temperature of neon and upon the melting point of oxygen, Commun. Phys. Lab. Univ. Leiden 121c (1911).

[39] James Dewar, Production of solid oxygen by the evaporation of the liquid, Proc. Roy. Soc. London [A] **85,** 589 (1911).

[40] E. Justi, On the triple points of nitrogen and oxygen as fixed points of the temperature scale, Ann. Physik **10,** 983 (1931).

[41] J. H. C. Lisman and W. H. Keesom, The melting curve of oxygen to 170 kg/cm², Commun. Kamerling Onnes Lab. Univ. Leiden **239a** (1935).

[42] F. Henning, Vapor pressure and resistance thermometers in the temperature regions of liquid nitrogen and hydrogen, Zeit. Physik **40,** 775 (1927).

[43] W. H. Keesom, H. van der Horst, and A. F. J. Jansen, New determination of the normal boiling point of oxygen, Commun. Phys. Lab. Univ. Leiden **203b** (1929).

[44] W. Heuse and J. Otto, A new gas-thermometric determination of fixed points below 0° in connection with vapor-pressure and resistance thermometers, Ann. Physik. **9,** 486 (1931).

[45] W. Heuse and J. Otto, Gas thermometric determination of some fixed points below 0°, with vapor-pressure and resistance thermometers. II, Ann. Physik **14,** 185 (1932).

[46] Shinichi Aoyama and Eizo Kanda, Determination of fixed points in the low termperature with a hydrogen thermometer, Bull. Chem. Soc. Japan **10,** 472 (1935).

[47] W. H. Keesom and B. G. Dammers, On the construction of platinum resistance thermometers and the determination of their basic points, Commun. Kamerlingh Onnes Lab. Univ. Leiden **239d** (1935).

[48] R. W. Blue and J. F. G. Hicks, Jr., Comparison of platinum-rhodium resistance thermometers with the helium gas thermometer from 11° to 300° K. An improved cryostat, J. Am. Chem. Soc. **59,** 1962 (1937).

[49] Albert Perrier and H. Kamerlingh Onnes, The susceptibility of liquid mixtures of oxygen and nitrogen, and the influence of the mutual distances of the molecules upon paramagnetism, Commun. Phys. Lab. Univ. Leiden **139d** (1914).

[50] W. F. Giauque and J. O. Clayton, Heat capacity and entropy of nitrogen. Heat of vaporization. Vapor pressures of solid and liquid. The reaction $1/2N_2 + 1/2\ 0_2 = NO$ from spectroscopic data, J. Am. Chem. Soc. **55,** 4875 (1933).

WASHINGTON, September 26, 1949.